

DISS. ETH NO. 22561

**DECENTRALISED URINE TREATMENT WITH THE  
NITRITATION/ANAMMOX PROCESS**

A thesis submitted to attain the degree of  
DOCTOR OF SCIENCES of ETH ZURICH  
(Dr. sc. ETH Zurich)

presented by

SARINA SCHIELKE-JENNI

Dipl. Umwelt.-Ing. ETH

born on 19.01.1983

citizen of Eggwil BE and Uster ZH

accepted on the recommendation of

Prof. Dr. Eberhard Morgenroth, examiner

Prof. Dr. Ir. Nico Boon, co-examiner

Dr. Kai M. Udert, co-examiner

2015



## ACKNOWLEDGEMENTS

I thank the Swiss National Science Foundation for the financial support of this PhD thesis (grant 200021\_125133 and 200020\_144498).

Many people have contributed to this PhD thesis with their work, advice and support:

I would like to start by expressing my gratitude to my advisor Kai Udert for his valuable support, inspiring ideas, fruitful discussion and continuous enthusiasm for the project. I am also very grateful to my supervisor Eberhard Morgenroth who always kept an overview and ensured that I stayed on track. Furthermore, I would like to thank my co-examiner Nico Boon for his willingness to co-examine my thesis and the invitation to his lab where I learned all the important details about FISH.

Many thanks to Helmut Bürgmann, Francisco Vazquez, Lukas Emmenegger, Joachim Mohn, Siegfried Vlaeminck and Kris Villez for the pleasant and productive collaboration.

Thank you Johanna Obrecht, Marc d'Engrement and Kangning Xu for the support of this work with either a master thesis or internship work. Special thanks to Alexandra Fumasoli and Hanspeter Zöllig for the great care of my reactors whenever I was away and the pleasant working atmosphere in the urine lab.

I would also like to thank all other persons at Eawag who supported me with their knowledge, equipment and analyses, especially Adriano Joss, Michele Laurenzi, Jack Eugster, Thomas Fleischmann, Nele Schuwirth, Brian Sinnet, Ilona Szivak, Jacqueline Traber and the AuA lab team. Special thanks to Claudia Bänninger and Karin Rottermann for the analysis of the 1342 samples I took during this thesis and their patience to deal with all the problems arising from the complex urine matrix.

Finally, I am very grateful to all my colleagues from both the ENG and SWW departments at Eawag for the nice working atmosphere. Special thanks to all my former office mates: Markus Gresch, David Dürrenmatt, Pascal Wunderlin, Christoph Egger, Dario Del Guidice, Rahel Künzle, Alexandra Florin and Alexander Flück.



## TABLE OF CONTENTS

ACKNOWLEDGEMENTS .....	III
SUMMARY .....	VII
ZUSAMMENFASSUNG .....	XI
<b>General Introduction .....</b>	<b>1</b>
<b>Chapter 1</b> Regime shift and microbial dynamics in a sequencing batch reactor for nitrification and anammox treatment of urine .....	11
Supporting Information for Chapter 1 .....	37
<b>Chapter 2</b> Observability of anammox activity in single-stage nitritation/anammox reactors using mass balances .....	43
Supporting Information for Chapter 2 .....	65
<b>Chapter 3</b> Successful application of nitritation/anammox to wastewater with elevated organic carbon to ammonia ratios .....	85
Supporting Information for Chapter 3 .....	107
<b>Chapter 4</b> Temperature dependence and interferences of NO and N <sub>2</sub> O microelectrodes used in wastewater treatment .....	115
Supporting Information for Chapter 4 .....	137
<b>Chapter 5</b> Evaluation of critical factors for the operation of a nitritation/anammox process with urine .....	149
Supporting Information for Chapter 5 .....	179
<b>General Conclusions and Outlook .....</b>	<b>191</b>
REFERENCES .....	195
CURRICULUM VITAE .....	211



## SUMMARY

Urine contains over 80% of the total nitrogen but accounts for less than 1% of the total wastewater volume. Due to higher concentrations, nitrogen removal from source-separated urine is potentially much cheaper and less energy intensive than from wastewater. For many cities, removing nitrogen in small decentralized reactors could be more efficient and affordable than in large treatment plants situated at the end of extensive sewer networks. However, due to a lack of personnel and expensive instruments, process control of small on-site reactors is potentially critical. In addition, process stability and resilience tend to be low due to a lower microbial diversity. Therefore, the main goal of this thesis is to contribute to the development of a reliable and simple process configuration for decentralised nitrogen removal from urine.

Urine does not contain enough biodegradable organic substrate for conventional nitrogen removal via autotrophic nitrification and heterotrophic denitrification. Therefore, if no organic substrate is added, anaerobic ammonium-oxidising bacteria (AMX) are required for nearly complete nitrogen removal from urine. The combination of aerobic ammonium oxidation (nitrification) and anaerobic ammonium oxidation (anammox) has frequently been applied for nitrogen removal from wastewater with very low organic substrate content, as e.g. digester supernatant. The composition of urine is though very different from the one of digester supernatant. Both the higher organic substrate content and the much higher total salinity of urine could hinder nitrogen removal from urine with the nitrification/anammox process. Urine also contains high concentrations of individual salts, and potentially also pharmaceuticals, which could inhibit the activity of the involved bacteria.

This thesis consists of two main experimental series, one with diluted urine and one with undiluted urine. The experimental series with diluted urine showed that nitrification/anammox with diluted urine is possible, however, prone to process instabilities. The initially successful operation was followed by an extended period of process degradation. Multiple lines of evidence, e.g. cluster and ordination analysis of the microbial community, indicated that an ecological regime shift had occurred. The system shifted to a new stable state that was characterised by inferior process performance and low AMX activity, and could not be reversed during the remaining observation period.

A simple and fast tool that allows the detection of decreasing AMX activity in time, and thus taking appropriate measures to omit impending regime shifts, would therefore be crucial for a successful operation. Mass balances are a common tool to determine the bacterial activities of ammonium-oxidising bacteria, nitrite-oxidising bacteria and AMX in a nitrification/anammox process. However, if the influent contains elevated amounts of biodegradable organic substrate, as in the case of urine, heterotrophic growth on oxygen, nitrite and nitrate must also be included

in the mass balances. While all six bacterial activities are theoretically observable with mass balances, the calculated reaction rates are practically coupled to very high uncertainties. Therefore, mass balances are not suitable for a fast and reliable assessment of the bacterial activities in a nitrification/anammox reactor with high heterotrophic activity.

Because the detection of impending regime shifts is difficult, more knowledge is required about the factors which cause them. One factor that correlated with the observed regime shift was the ratio of biodegradable organic carbon to ammonia nitrogen (COD/N) in the influent. To test if heterotrophic bacteria (HET), which grow on organic substrate, are able to outcompete AMX when the influent COD/N ratio exceeds a certain threshold value, increasing amounts of acetate were dosed to digester supernatant. This experiment showed that, provided the sludge retention time is high enough, AMX are able to coexist with HET up to the influent COD/N ratio of urine. AMX activity though decreases with increasing influent COD/N ratio because HET take over part of the nitrogen removal.

Another factor that correlated with the observed regime shift was the increase of the oxygen sensor baseline signal, which indicates an accumulation of nitric oxide (NO) and/or nitrous oxide (N<sub>2</sub>O). Both gases are obligate intermediates of heterotrophic denitrification and the elevated organic substrate content of urine might lead to an increased production of the two gases. To allow a further characterisation of the influence of NO and N<sub>2</sub>O on a nitrification/anammox process, microelectrodes for the measurement of NO and N<sub>2</sub>O in the liquid phase were tested with respect to an application in a wastewater treatment process. These experiments showed that the temperature dependency and the interference of NO on the N<sub>2</sub>O sensor must be considered, while the interference of ammonia, nitrous acid, hydroxylamine and hydrazine on the NO sensor is not relevant in most applications.

The experimental series with undiluted urine was conducted in three different process configurations: (1) a single-stage nitrification/anammox reactor, (2) a reactor for pre-oxidation of organic substances followed by a single-stage nitrification/anammox reactor, and (3) a two reactor setup with an oxic step for nitrification and oxidation of organic substances and an anoxic step for anammox. However, none of the three tested configurations was suitable for stable and reliable nitrogen removal from urine.

A detailed evaluation of all possible influence factors, including urine compounds, nitrogen intermediates and operating parameters, revealed three potentially critical factors: first, a strong decrease of the biomass content caused by a floc destabilisation due to the high ratio of monovalent to divalent cations in urine, second, a direct inhibition of AMX by non-biodegradable organic substances and third, a direct inhibition of AMX by pharmaceuticals. Further research is required to evaluate whether all three factors or only one or two of them are critical. While a strong influence from the non-biodegradable organic compounds or the pharmaceutical could



be reduced with dilution of the urine, additional divalent cations would be necessary to decrease the high ratio of monovalent to divalent cations in urine. Higher biomass retention could also be achieved with a biofilm system.

To conclude, this thesis contributes many new insights and directs the way of further research for the development of a reliable and simple process configuration for nitrogen removal from urine. The operation of a single-stage nitritation/anammox reactor with urine remains challenging, but proved itself to be the best option for biological nitrogen removal from urine.



## ZUSAMMENFASSUNG

Urin beinhaltet über 80% des gesamten Stickstoffs und macht aber nur etwas weniger als 1% des gesamten Abwasservolumens aus. Aufgrund der höheren Konzentrationen ist Stickstoffentfernung aus separat gesammeltem Urin potentiell günstiger und verbraucht weniger Energie als Stickstoffentfernung aus dem gesamten Abwasser. Stickstoffentfernung in kleinen dezentralen Reaktoren könnte deshalb für viele Städte effizienter und erschwinglicher sein als in grossen Reinigungsanlagen am Ende von weitläufigen Kanalisationsnetzen. Da aber kein Personal und keine teuren Instrumente zur Verfügung stehen, kann die Prozesskontrolle von kleinen, dezentralen Reaktoren kritisch sein. Aufgrund der niedrigeren mikrobiellen Diversität, ist in kleinen Systemen tendenziell auch mit einer geringeren Stabilität und Belastbarkeit der Prozesse zu rechnen. Das Hauptziel dieser Arbeit war deshalb, einen Beitrag zur Entwicklung eines einfachen und robusten Prozesses zur dezentralen Stickstoffentfernung aus Urin zu leisten.

Urin enthält nicht genügend biologisch abbaubares organisches Substrat für konventionelle Stickstoffentfernung via autotrophe Nitrifikation und heterotrophe Denitrifikation. Falls kein zusätzliches organisches Substrat dosiert wird, braucht es deshalb anaerobe Ammoniumoxidierende Bakterien (AMX) um den Stickstoff nahezu vollständig aus dem Urin zu entfernen. Die Kombination aus aerober Ammonium-Oxidation (Nitritation) und anoxischer Ammonium-Oxidation (Anammox) wird häufig für Stickstoffentfernung aus Abwasser mit wenig organischem Substrat, wie beispielsweise Faulwasser, angewendet. Die Zusammensetzung von Urin unterscheidet sich aber wesentlich von derjenigen von Faulwasser. Sowohl der höhere Anteil an organischem Substrat als auch der massiv höhere Salzgehalt könnte eine Stickstoffentfernung aus Urin via Nitritation/Anammox erschweren. Urin enthält auch höhere Konzentrationen einzelner Salze, und potentiell auch Pharmazeutika, welche die Aktivität der beteiligten Bakterien hemmen können.

Diese Doktorarbeit besteht aus zwei praktischen Versuchsreihen: eine mit verdünntem Urin und eine mit unverdünntem Urin. Die Versuchsreihe mit verdünntem Urin hat gezeigt, dass Nitritation/Anammox mit verdünntem Urin zwar möglich ist, aber zu Prozessinstabilitäten neigt. Auf den anfänglich erfolgreichen Betrieb folgte eine ausgedehnte Phase der Prozessverschlechterung. Mehrere Beweisketten, unter anderem eine Cluster- und Ordinations-Analyse der mikrobiologischen Gemeinschaft, deuten an, dass eine ökologische Populationsverschiebung stattgefunden hat. Das System wechselte in einen neuen stabilen Zustand, der durch verminderte Leistung und eine niedrige AMX Aktivität charakterisiert werden kann, und während der verbleibenden Beobachtungszeit nicht reversibel war.

Für einen erfolgreichen Betrieb wäre es äusserst hilfreich, eine einfache und schnelle Methode zu haben, mit der man abnehmende AMX-Aktivität erkennen und dadurch rechtzeitig Mass-

nahmen ergreifen kann, um drohende Populationsverschiebungen abzuwenden. Massenbilanzen werden häufig verwendet, um die Aktivität von Ammonium-oxidierenden Bakterien, Nitrit-oxidierenden Bakterien sowie AMX in einem Nitritation/Anammox-Prozess zu bestimmen. Falls das Abwasser aber, wie im Fall von Urin, erhöhte Mengen an biologisch-abbaubarem organischem Substrat enthält, muss auch heterotrophes Wachstum mit Sauerstoff, Nitrit und Nitrat berücksichtigt werden. Während theoretisch alle sechs bakteriellen Aktivitäten mit Massenbilanzen identifizierbar sind, sind die berechneten Reaktionsraten an hohe Unsicherheiten gekoppelt. Massenbilanzen sind deshalb nicht geeignet für eine schnelle und zuverlässige Beurteilung der bakteriellen Aktivitäten in einem Nitritation/Anammox Prozess mit hoher heterotropher Aktivität.

Da die Erkennung von möglichen Populationsverschiebungen also schwierig ist, braucht es mehr Wissen über die Faktoren, welche Populationsverschiebungen auslösen können. Ein Faktor, der mit der beobachteten Populationsverschiebung korreliert hat, ist das Verhältnis von biologisch abbaubarem organischem Substrat zu Ammonium-Stickstoff (CSB/N) im Zulauf. Um zu testen, ob sich heterotrophe Bakterien, die organisches Substrat verwerten, ab einem bestimmten CSB/N Verhältnis gegenüber AMX durchsetzen können, wurden zunehmende Mengen Azetat zu Faulwasser hinzugegeben. Dieses Experiment hat gezeigt, dass AMX bis zum CSB/N-Verhältnis von Urin mit heterotrophen Bakterien koexistieren können, sofern das Schlammalter genügend hoch ist. Da heterotrophe Bakterien einen Teil der Stickstoffentfernung übernehmen, nimmt die AMX Aktivität aber mit zunehmendem CSB/N Verhältnis im Zulauf ab.

Ein weiterer Faktor, der mit der beobachteten Populationsverschiebung korrelierte, war der Anstieg des Grundsignals der Sauerstoffelektrode, welcher eine Akkumulation von Stickstoffmonoxid (NO) und/oder Lachgas (N<sub>2</sub>O) anzeigt. Da beide Gase obligate Zwischenprodukte der heterotrophen Denitrifikation sind, könnte der erhöhte Anteil an organischem Substrat im Urin zu einer erhöhten Produktion der beiden Gase führen. Um den Einfluss der beiden Gase auf einen Nitritation/Anammox-Prozess charakterisieren zu können, wurden Mikroelektroden für die Messung von NO und N<sub>2</sub>O in der Flüssigphase, mit einem speziellen Augenmerk auf die Anwendung in einem Abwasserbehandlungsprozess, getestet. Diese Versuche haben gezeigt, dass die Temperaturabhängigkeit sowie die Querempfindlichkeit der N<sub>2</sub>O Elektrode auf NO berücksichtigt werden müssen, wohingegen die Interferenz von Ammoniak, salpetriger Säure, Hydroxylamin und Hydrazin auf die NO-Elektrode für die meisten Anwendungen nicht relevant ist.

Die Versuchsreihe mit unverdünntem Urin umfasste drei verschiedene Prozess-Anordnungen: (1) ein einstufiger Nitritation/Anammox Reaktor, (2) ein Reaktor für die Vor-Oxidation organischer Substanzen gefolgt von einem einstufigen Nitritation/Anammox Reaktor, und (3) eine

zweistufige Anordnung mit einem aeroben Reaktor für die Nitritation und die Oxidation organischer Substanzen gefolgt von einem anoxischen Reaktor für Anammox. Allerdings war keine der drei Prozess-Anordnungen für eine stabile und zuverlässige Stickstoffentfernung aus Urin geeignet.

Anhand einer detaillierten Evaluierung aller möglicher Einflussfaktoren, wie Urinkomponenten, Zwischenprodukte des Stickstoffabbaus, und Betriebsparameter, konnten drei potentiell kritische Faktoren identifiziert werden: Erstens eine starke Abnahme der Biomasse aufgrund von Flockenzerfall, der durch das hohe Verhältnis von einwertigen zu zweiwertigen Kationen im Urin verursacht wird, zweitens eine direkte Hemmung der AMX durch nicht-abbaubare organische Substanzen und drittens eine direkte Hemmung der AMX durch Pharmazeutika. Weitere Forschung muss noch zeigen, ob alle drei Faktoren oder nur einer oder zwei der drei Faktoren wirklich kritisch sind. Während eine direkte Hemmung der AMX durch biologisch nicht-abbaubare organische Substanzen oder durch Pharmazeutika mit einer Verdünnung des Urins reduziert werden könnte, müssten zusätzliche zweiwertige Kationen dosiert werden, um das hohe Verhältnis an einwertigen zu zweiwertigen Kationen im Urin zu senken. Ein höherer Biomasserückhalt könnte auch mit einem Biofilmsystem erreicht werden.

Zusammenfassend bringt diese Doktorarbeit viele neue Erkenntnisse und gibt den Weg für die weitere Forschung zur Entwicklung eines stabilen und einfachen Prozesses für die Stickstoffentfernung aus Urin vor. Der Betrieb eines einstufigen Nitritation/Anammox Reaktors mit Urin ist zwar anspruchsvoll, aber die beste Option für eine biologische Stickstoffentfernung aus Urin.



## **General Introduction**

## **General Introduction**

### **Decentralised treatment of source-separated urine**

Sewers and centralized wastewater treatment plants are today the preferred approach for urban wastewater management. Although this system has itself proven to be successful, it has drawbacks in industrialized as well as in low-income countries (Lienert and Larsen 2007). First of all, apart from the fact that waterborne sewerage would be a waste in regions suffering from water scarcity, the dilution of pollutants makes their elimination less efficient and requires larger treatment facilities. Furthermore, while extensive sewer systems and complex central treatment plants are hardly affordable for low-income countries, their treatment efficiency with respect to nitrogen is usually less than 80 percent, even with the best available technology. The main reasons for this inefficiency are sewer leaks and discharge of untreated wastewater during rain events (Larsen and Gujer 2001). Consequently an increasing number of research groups worldwide pursue a paradigm shift towards decentralized treatment of source separated wastewater streams (Larsen et al. 2013).

A separate collection and treatment of urine is the most promising version of source separation in wastewater treatment, because this relatively small change in resources management would lead to large environmental advantages. Today, only few countries have denitrifying wastewater treatment plants (50% to 75% nitrogen removal without additional organic carbon) and many have no facilities at all (Lienert and Larsen 2007). Van Drecht et al. (2009) estimated that only about 10% of the total nitrogen in domestic wastewater is removed in the currently existing wastewater treatment plants. Urine contains over 80% of the total nitrogen in wastewater and thus, even if the remaining wastewater is discharged untreated, a separate collection and treatment of urine as the only measure could equal or surpass the nitrogen removal of conventional wastewater treatment plants and rapidly improve water quality of the receiving waters. Furthermore, the high nitrogen concentration in urine makes nitrogen removal from urine less cost- and energy-intensive than from wastewater (Maurer et al. 2003, Wilsenach and van Loosdrecht 2006).

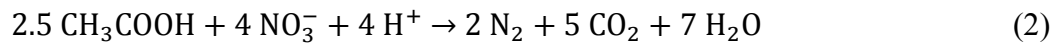
Decentralised treatment of source separated urine in small on-site reactors offers the significant advantage that no transport system to a centralised treatment plant is required. Reliable operation of small on-site treatment reactors has to face a number of challenges. In contrast to large centralised facilities, no personnel and expensive instruments are available to monitor and control the treatment process. Furthermore, due to the potentially lower microbial diversity, small biological reactors are even more prone to process failures than large wastewater treatment plants (Curtis et al. 2003). So far, a reliable and simple process configuration for decentralised



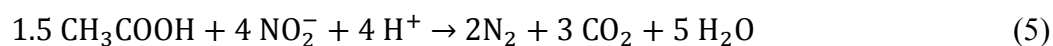
nitrogen removal from source-separated urine is still missing and therefore, a contribution to its development is the main goal of this doctoral thesis.

### Biological nitrogen removal processes

In general, biological processes for nitrogen removal from wastewater are more economical than the available chemical and physical processes (van Kempen et al. 2001). All known process combinations for biological nitrogen removal involve an aerobic reaction in which nitrogen oxides are produced followed by an anoxic reaction in which the nitrogen oxides are reduced to gaseous dinitrogen. The most conventional process combination for nitrogen removal from wastewater is autotrophic nitrification (Equation 1) followed by heterotrophic denitrification (Equation 2).



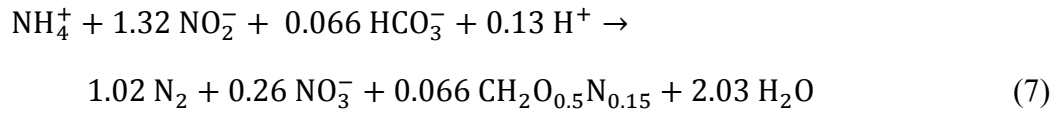
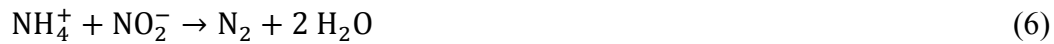
Autotrophic nitrification is a two-step process: ammonium oxidizing bacteria (AOB) oxidize ammonium to nitrite (Equation 3), which nitrite oxidizing bacteria (NOB) further oxidize to nitrate (Equation 4). If ammonium oxidation is stopped at nitrite (Equation 3) and combined with a subsequent reduction of the nitrite to gaseous dinitrogen by heterotrophic bacteria (HET; Equation 5), 25% oxygen and up to 40% organic substrate can be saved compared to conventional nitrification/denitrification (Equation 1 and 2).



Nevertheless, nitritation/denitritation still requires a biodegradable organic carbon to ammonia nitrogen (COD/N) ratio of at least 1.71 g COD·g N<sup>-1</sup> for complete nitrogen removal. Several types of wastewater, including urine, have COD/N ratios below 1.71 g COD·g N<sup>-1</sup> and thus, if no additional organic substrate should be dosed, another process combination is required for nitrogen removal from these types of wastewater.

In the 1990s, the anaerobic ammonium oxidation, also named anammox, was independently detected in different wastewater treatment systems by several research groups (Mulder et al. 1995, Hippen et al. 1997, Siegrist et al. 1998). Anammox bacteria (AMX) are able to oxidize ammonium with nitrite as the electron acceptor and can produce gaseous dinitrogen without organic substrate (Equation 6). AMX growth is always associated with nitrate production, as

AMX oxidise additional nitrite to generate reducing equivalents for CO<sub>2</sub> fixation (Kartal et al. 2013). The overall AMX reaction is given in Equation 7 (Strous et al. 1998).



In combination with nitrification (Equation 3), anammox is a cost saving alternative for all wastewaters with low organic substrate content and saves up to 58% oxygen compared to conventional nitrification/denitrification (Siegrist et al. 2008, Vlaeminck et al. 2012).

### **Operation of a nitritation/anammox process**

The operation of a nitritation/anammox process has some challenges. AMX are, for example, highly sensitive to oxygen (Strous et al. 1997a), while AOB require oxygen for aerobic ammonium oxidation. In order to stop nitrification at nitrite, the growth of NOB must be suppressed. Furthermore, due to the very low growth rate of AMX (doubling time 11 d at 32 °C; Strous et al. 1998), efficient biomass retention is required.

In general, there are two different strategies for the operation of a nitritation/anammox process, namely a two reactor setup, where nitritation and anammox each take place in a separate reactor, and a single-stage reactor, where one reactor contains both AOB and AMX. For a better control of the two reactions, early implementations used two-stage reactor configurations as, e.g., the SHARON<sup>®</sup>-Anammox<sup>®</sup> process (van Dongen et al. 2011). In the nitritation step, NOB can be selectively washed-out by adjusting the solids retention time (SRT) to a minimum level, because AOB usually have higher growth rates than NOB at temperatures around 30 °C (Hellinga et al. 1998). At the same time, a high SRT can be maintained in the anammox step. However, in order to generate a suitable influent for the anammox step, high nitrite concentrations must be maintained in the nitritation step. High nitrite concentrations though pose a high risk for process instabilities. Nitrite is a known bacterial inhibitor (Philips et al. 2002) and high nitrite levels are also known to increase the emission of NO and N<sub>2</sub>O from nitrifying systems (Kampschreur et al. 2008a).

The obvious advantage of single-stage reactors is that only one reactor and its associated equipment is required. Operational costs are potentially also lower, because only one reactor has to be maintained. Single-stage reactors though involve the challenge to maintain both aerobic and anoxic conditions in one reactor. Spatial niches can be provided by using stratified reactors as, e.g., the case with biofilm (Pynaert et al. 2003) or with granular biomass (Vlaeminck et al. 2008) while temporal niches can be established with intermittent aeration (Joss et al. 2009).

Because the low growth rate of AMX requires high biomass retention, reactor operation under oxygen limited conditions, which favours AOB due to their higher oxygen affinity compared to NOB, is considered to be the best strategy to limit NOB growth (Blackburne et al. 2008, Wyffels et al. 2004).

To date, more than 100 full-scale nitrification/anammox processes are running and many operation strategies have been successfully developed, implemented and optimised for nitrogen removal from high-strength nitrogen wastewaters with low biodegradable organic substrate (Lackner et al. 2014). With a share of 88%, the prevailing operation strategy is a single-stage reactor (Lackner et al. 2014).

### **Nitrification/anammox with urine**

Urine is a highly concentrated solution and contains numerous different substances, many of which could hinder a stable operation of a nitrification/anammox process. For one thing, stored urine has an elevated COD/N ratio of up to 1.8 g COD·g N<sup>-1</sup> (Bürgmann et al. 2011). Biodegradable organic substrate fosters the growth of HET, which compete with AOB for oxygen and with AMX for nitrite. Additionally, more heterotrophic growth will lead to a higher sludge production, which in turn often leads to a higher sludge loss, and thus to a decrease in the sludge retention time (SRT). A low SRT is particularly critical for the slowly growing AMX. Several studies reported decreasing AMX and AOB activities with high COD/N ratios in the influent. Chamchoi et al. (2008) for instance, reported that AMX were outcompeted by HET when the COD/N ratio in the influent of a complete anoxic system was higher than 2.0 g COD·g N<sup>-1</sup>. Zhu and Chen (2001) observed a 70% reduction of AOB activity when the influent COD/N ratio of a nitrification reactor was between 1.8 and 3.5 g COD·g N<sup>-1</sup>. Specific organic compounds can also be directly toxic for AOB and AMX. Complete inhibition of AOB was for instance observed in the presence of 3.7 mg·L<sup>-1</sup> phenol or 1.3 mg·L<sup>-1</sup> cresol (Dyreborg and Arvin 1995). For AMX, Güven et al. (2005) observed a complete loss of activity in the presence of 23 mg·L<sup>-1</sup> methanol.

Furthermore, urine has an electric conductivity in the range of 27 to 32 mS·cm<sup>-1</sup> which corresponds to a total salinity in the range of 13.6 to 16.2 g NaCl·L<sup>-1</sup>. Both the total salinity (Dapena-Mora et al. 2010, Moussa et al. 2006) and high concentrations of single ions (Dapena-Mora et al. 2007, Mosquera-Corral et al. 2005) could inhibit the bacteria. Moreover, it is likely that the anaerobic conditions in collection and storage tanks allow growth of sulphate-reducing bacteria. Due to the much higher sulphate concentration compared to digester supernatant, this most likely results in much higher sulphide concentrations. Sulphide is another potential inhibitor for the bacteria (Dapena-Mora et al. 2007, Sears et al. 2004). Finally, many pharmaceuticals are

excreted via urine (Lienert et al. 2007) and could also have a toxic effect on the bacteria (Fernández et al. 2009, van de Graaf et al. 1995).

Udert et al. (2003) tried to operate a nitrification/anammox process with undiluted urine. In this case, the system was operated as a two-stage process. Nitrification was successfully operated for 35 d. The second stage, anammox, was though only tested in a batch experiment. The results were promising, however, due to dilution with the anammox sludge, the concentration of the urine compounds were much lower than in undiluted urine and the experiment only lasted for 90 min. The operation of a nitrification/anammox process with diluted urine was tested by Udert et al. (2008). On one hand, this study showed that nitrification/anammox could be suitable for nitrogen removal from urine. On the other hand, it also indicated that process instabilities due to increased HET activity are likely to occur.

### **Microbial diversity and process stability**

Small decentralised reactors potentially have lower biodiversity and are less stable than large centralised wastewater treatment plants because large systems tend to offer more diverse niches than small systems (Curtis et al. 2003). The influent fluctuations of small decentralised systems in terms of loading and composition over time might though lead to a higher diversity, but are also likely to cause process instabilities. In any case, a good understanding of the conditions for process stability is required in order to develop successful and simple process control strategies for decentralised reactors.

The complex interactions between the different bacterial groups and the potential for system instabilities make nitrification/anammox with urine an ideal subject with which to explore the use of microbial community analysis and ecological theory for the development of stable processes. Microbial community fingerprints such as denaturing gradient gel electrophoresis (DGGE) and automated ribosomal intergenic spacer analysis (ARISA) can be useful tools to assess the influences of process operation on the overall microbial community structure without knowing the abundance or identity of individual species (Gilbride et al. 2006, Wittebolle et al. 2008). Statistical tools then allow elucidating the interdependencies of microbial populations and the environmental conditions. Approaches such as canonical ordination that are frequently used in ecology can be applied to identify driving forces of the microbial community structure in the studied system.

In addition to such gradient analysis, community fingerprints can also be analysed for evidence for ecological regime shifts. The theory of ecological regime shifts suggests that ecological systems may have a tendency for rapid and potentially catastrophic change in ecosystem species composition and function, interpreted as a switch to an alternate stable state as certain variables cross a threshold or in response to stress events (Scheffer and Carpenter 2003). The fact that

regime shifts tend to be irreversible as their definition includes the resilience of the system against a return to the previous state, implies that their prevention is crucial for a successful and stable operation and thus, more knowledge is required about the factors which might lead to a regime shift.

### **Gaseous nitrogen emissions**

Among other factors, high ammonium ( $\text{NH}_4^+$ ) and nitrite ( $\text{NO}_2^-$ ) concentrations can cause imbalances in the microbial processes and lead to the accumulation of nitric oxide (NO) and nitrous oxide ( $\text{N}_2\text{O}$ ; Wunderlin et al. 2012a). Therefore, all nutrient removal processes from high-strength nitrogen wastewaters bear the risk to displace the environmental problem from water bodies to the atmosphere (Kampschreur et al. 2009a). Both gases are critical atmospheric pollutants:  $\text{N}_2\text{O}$  is a potent contributor to global warming (Solomon et al. 2007) and the most important ozone-depleting substance in the stratosphere (Ravishankara et al. 2009). NO is rapidly oxidised in the troposphere. Its product, nitrogen dioxide ( $\text{NO}_2$ ) is a precursor of ozone and is, together with sulphur dioxide ( $\text{SO}_2$ ), responsible for acid rain.

Further research is required to identify the main production pathways and to develop operation strategies that limit the production of the two gases in the different nitrogen removal processes. Both gases are usually analysed in the off-gas. NO and  $\text{N}_2\text{O}$  analysis in the liquid phase with Clark-type microsensors could though be an attractive alternative. The most important advantages of liquid phase measurements are that they allow differentiating between production and emission of the two gases (Ahn et al. 2010) as well as measuring concentration gradients in stratified (e.g. biofilm) reactors. Electrodes for NO and  $\text{N}_2\text{O}$  measurement have been on the market for some time, but have not yet been tested for an application in wastewater treatment processes.

### **Goals and general research questions**

The general goal of this thesis was to contribute to the development of a reliable and simple process configuration for decentralised nitrogen removal from urine. It is hypothesised that a nitrification/anammox process is the best choice for nitrogen removal from urine. Therefore, the following research questions were addressed to assess the challenges and possibilities of nitrogen removal from urine via nitrification/anammox:

- Is nitrification/anammox suitable for stable and nearly complete nitrogen removal from urine (Chapter 1 and 5)?
- Do microbial community analysis and ecological theory provide some useful information for the development of stable and simple processes (Chapter 1)?

- Is there a simple and reliable method to detect changing bacterial activities in time, in order to prevent impending regime shifts and increase process stability (Chapter 2)?
- Is the nitrification/anammox process suitable for nitrogen removal from wastewaters that contain elevated amounts of biodegradable organic matter (Chapter 3)?
- Do microsensors allow reliable NO and N<sub>2</sub>O measurement in nutrient removal processes from high-strength nitrogen wastewaters (Chapter 4)?
- Which are the main influence factors on AMX activity in a nitrification/anammox process with urine (Chapter 5)?

## Thesis outline

**Chapter 1** describes the operation of a nitrification/anammox process with diluted urine. One goal of this experiment was to gain first long-term experiences with nitrogen removal from urine via nitrification/anammox. Furthermore, microbial community fingerprints such as denaturing gradient gel electrophoresis (DGGE) and automated ribosomal intergenic spacer analysis (ARISA) were used to evaluate if microbial community analysis and ecological theory can provide some useful information for the development of stable and simple processes. Regime-shift analysis of chemical and physical parameters and cluster and ordination analysis of the microbial community indicated that the system had experienced a rapid and irreversible shift to a new stable state with inferior process rates and low AMX activity.

A simple and fast tool that allows the detection of changing bacterial activities in time, and thus taking appropriate measures to omit impending regime shifts, would be crucial for a stable operation of a nitrification/anammox process with urine. A common approach to determine bacterial activities is based on mass balances of dissolved compounds such as ammonium, nitrite and nitrate. In **Chapter 2**, the applicability of mass balancing for the determination of bacterial activities in a nitrification/anammox process was tested by setting up and solving mass balances of different degrees of complexity. In contrast to previous studies, heterotrophic activity with oxygen, nitrite and nitrate was also included in the mass balances, because even in wastewater with low amounts of organic substrate, heterotrophic denitrification can contribute substantially to nitrogen removal.

Because the detection of impending regime shifts is difficult, more knowledge is required about the factors which cause them. One factor that correlated with the observed regime shift was the ratio of biodegradable organic carbon to ammonia nitrogen (COD/N) in the influent. Therefore, the goal of **Chapter 3** was to characterise the influence of elevated COD/N ratios on a nitrification/anammox process. In order to minimise influences from other potentially toxic influent compounds, increasing amounts of acetate were added to digester supernatant, which is a typical substrate for a nitrification/anammox process. Bacterial activities were followed with batch

activity measurements, and fluorescent in-situ hybridisation was used to identify the involved types of AMX.

Another factor that correlated with the observed regime shift was the increase of the oxygen sensor baseline signal, which indicates an accumulation of nitric oxide (NO) and/or nitrous oxide (N<sub>2</sub>O). Both gases are obligate intermediates of heterotrophic denitrification and the elevated organic substrate content of urine might lead to an increased production of NO and N<sub>2</sub>O. The goal of **Chapter 4** was to test the suitability of microelectrodes for nitric oxide (NO) and nitrous oxide (N<sub>2</sub>O) measurements in nutrient removal processes from high-strength nitrogen wastewaters. Both electrodes were assessed with respect to their linear or non-linear response, temperature dependence and potential cross sensitivity to dissolved compounds, which are present and highly dynamic in nitrogen conversion processes.

High AMX activity is a crucial factor for the stable nitrogen removal from urine. In **Chapter 5**, potential influence factors on AMX activity in a nitrification/anammox process with urine are evaluated. This involved a comparison of three different process configurations: (1) a single-stage nitrification/anammox reactor, (2) a reactor for pre-oxidation of organic substances followed by a single-stage nitrification/anammox reactor, and (3) a two reactor setup with an oxic step for nitrification and oxidation of organic substances and an anoxic step for anammox. During all three experiments, bacterial activities were followed with batch activity measurements. Furthermore, additional batch experiments were performed to characterise the influence of selected urine compounds on AMX.





## CHAPTER 1

### **Regime shift and microbial dynamics in a sequencing batch reactor for nitrification and anammox treatment of urine**

Helmut Bürgmann, Sarina Jenni, Francisco Vazquez, Kai M. Udert  
*Applied and Environmental Microbiology*, 2011, 77(17), 5897-5907

# **Regime shift and microbial dynamics in a sequencing batch reactor for nitrification and anammox treatment of urine**

Helmut Bürgmann<sup>1</sup>, Sarina Jenni<sup>2</sup>, Francisco Vazquez<sup>1</sup>, Kai M. Udert<sup>2</sup>

*1: Eawag, Swiss Federal Institute for Aquatic Science and Technology, 6047 Kastanienbaum, Switzerland*

*2: Eawag, Swiss Federal Institute for Aquatic Science and Technology, 8600 Dübendorf, Switzerland*

## **ABSTRACT**

The microbial population and physicochemical process parameters of a sequencing batch reactor for nitrogen removal from urine were monitored over a 1.5-year period. Microbial community fingerprinting (automated ribosomal intergenic spacer analysis), 16S rRNA gene sequencing, and quantitative PCR on nitrogen cycle functional groups were used to characterize the microbial population. The reactor combined nitrification (ammonium oxidation)/anammox with organoheterotrophic denitrification. The nitrogen elimination rate initially increased by 400%, followed by an extended period of performance degradation. This phase was characterized by accumulation of nitrite and nitrous oxide, reduced anammox activity, and a different but stable microbial community. Outwashing of anammox bacteria or their inhibition by oxygen or nitrite was insufficient to explain reactor behaviour. Multiple lines of evidence, e.g., regime-shift analysis of chemical and physical parameters and cluster and ordination analysis of the microbial community, indicated that the system had experienced a rapid transition to a new stable state that led to the observed inferior process rates. The events in the reactor can thus be interpreted to be an ecological regime shift. Constrained ordination indicated that the pH set point controlling cycle duration, temperature, airflow rate, and the release of nitric and nitrous oxides controlled the primarily heterotrophic microbial community. We show that by combining chemical and physical measurements, microbial community analysis and ecological theory allowed extraction of useful information about the causes and dynamics of the observed process instability.

## **INTRODUCTION**

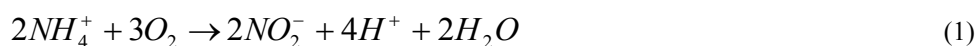
The ever-increasing arsenal of molecular and biochemical methods for microbial ecology has shaped our appreciation of biotechnological systems, e.g., in wastewater treatment, as complex, diverse, and dynamic microbial ecosystems. With the understanding that these systems can rival

classic aquatic or terrestrial ecosystems in complexity came the realization that their effective design and operation may benefit from or even require an understanding of ecological theory (McMahon et al. 2007).

The microbial ecosystem in many biotechnological systems consists of diverse microbial populations linked through a multitude of enzymatic processes. While understanding the structure, functions, and dynamics of the microbial communities is of fundamental concern for process optimization, such systems are so complex that determining all interactions is very challenging, if not impossible (McMahon et al. 2007). Microbial community fingerprints such as denaturing gradient gel electrophoresis (DGGE) and automated ribosomal intergenic spacer analysis (ARISA) can be useful tools to assess the influences of process operation on the overall microbial community structure without knowing the abundance or identity of individual species (Gilbride et al. 2006, Wittebolle et al. 2008). While microbial community fingerprinting allows fast and simple qualitative characterization of microbial communities, statistical tools are required to elucidate the interdependencies of microbial populations and the environmental conditions. In wastewater treatment, microbial processes have usually been described with mechanistic models focusing on known mechanisms of limitation and inhibition of the most important microbial groups. This approach has its limitations for complex systems, because too many kinetic parameters have to be known to accurately model the microbial dynamics (Gujer 2006). Alternatively, statistical approaches such as canonical ordination that are frequently used in ecology can be applied to identify driving forces of the microbial community structure in the studied system. In addition to such gradient analysis, the rapid and often step-like changes in system parameters led us to analyse our data for evidence for ecological regime shifts. The theory of ecological regime shifts suggests that (some) ecological systems may have a tendency for rapid (catastrophic) change in ecosystem species composition and function, interpreted as a switch to an alternate stable state as certain variables cross a threshold or in response to stress events (Scheffer and Carpenter 2003). This property thus arises from the interaction of internal processes and external forcing (Collie et al. 2004). The concept of regime shifts has been explored in general ecology to a considerable extent (Collie et al. 2004, Folke et al. 2004, Scheffer and Carpenter 2003). In microbial ecology, biotechnology, and wastewater engineering, this is not the case, and indeed, evidence for regime shifts in purely microbial communities is currently missing (Botton et al. 2006). The prevailing view is still that microbial communities are flexible systems that adjust mostly deterministically to the external environmental conditions (Finlay et al. 1997). The idea that “everything is everywhere, the environment selects” (Baas-Becking 1934) was long considered one of the foundations of microbial ecology (Finlay et al. 1997), although this view is increasingly being questioned (Logue et al. 2008, Whitaker et al. 2003). The traditional perspective thus predicts that microbial communities along temporal or spatial

gradients of environmental parameters will be determined exclusively by these gradients and not by history or a specific local microbial community. Also, disturbances are seen as temporal phenomena according to this perspective, because high dispersal and a large local seed bank are thought to result in resilient communities that will eventually return to an optimal state. There is increasing evidence that this may not always be the case and that disturbance can directly affect microbially mediated ecosystem processes (Allison and Martiny 2008). The importance of a comprehensive understanding of the role of microbial community composition and the need to apply ecological theory not only to microbial ecology in general (Prosser et al. 2007) but also to engineered microbial reactors have consequently become increasingly evident (Briones and Raskin 2003, McMahon et al. 2007).

In this study, a combined nitrification/anammox reactor for urine treatment is used as an example. The process consists of two basic steps: first, aerobic ammonium-oxidizing bacteria (AOB) oxidize about 50% of the ammonium ( $\text{NH}_4^+$ ) to nitrite ( $\text{NO}_2^-$ ; Equation. 1), and then anammox bacteria (AMX) oxidize the  $\text{NH}_4^+$  with  $\text{NO}_2^-$  to molecular nitrogen ( $\text{N}_2$ ; Equation 2).



Combined nitrification/anammox in a single reactor has proven to be simple and stable, if the oxygen ( $\text{O}_2$ ) concentration is controlled well (Joss et al. 2009, Vlaeminck et al. 2009).

Nitrification/anammox processes are particularly interesting for  $\text{NH}_4^+$ -rich wastewaters that do not contain sufficient biodegradable organic substrate for organoheterotrophic denitrification. The source-separated urine used in this study had an average biodegradable organic substrate content of 1.5 g chemical oxygen demand (COD)/g  $\text{NH}_4^+$ -N, which is too low for complete organoheterotrophic denitrification (1.71 g COD/g  $\text{NH}_4^+$ -N) but still sufficiently high to support considerable growth of denitrifying bacteria (DNB) and aerobic organoheterotrophic bacteria (AHB).

Figure 1 shows a simplified scheme of the main bacterial groups and their nitrogen and organic matter conversion patterns. The bacterial groups potentially involved in the nitrogen conversion are AOB, AMX, DNB, and, if process control is insufficient, nitrite-oxidizing bacteria (NOB). AMX convert about 11% of their total nitrogen substrate ( $\text{NH}_4^+$  and  $\text{NO}_2^-$ ) into nitrate ( $\text{NO}_3^-$ ) (Strous et al. 1998) as a result of reverse electron flow. This  $\text{NO}_3^-$  as well as  $\text{NO}_2^-$  can be reduced by DNB. Environmental conditions and the kinetic properties of the bacterial groups determine their relative abundance.  $\text{O}_2$ , nitrite/nitrous acid ( $\text{NO}_2^-/\text{HNO}_2$ ), and ammonium/ammonia ( $\text{NH}_4^+/\text{NH}_3$ ) are of special importance for inhibition and limitation effects. Table 1 summarizes some typical literature values for relevant kinetic parameters. The data show that NOB growth can be suppressed if  $\text{O}_2$  concentrations are very low, because NOB have a lower affinity to  $\text{O}_2$

than AOB and AHB. The data also illustrate that AMX have strong kinetic disadvantages. Their growth rate is very low, and they are (reversibly) inhibited by traces of  $O_2$  (Egli et al. 2001, Strous et al. 1997a). AHB and DNB grow about 100 times faster than AMX, and their yield (with respect to electrons transferred) is 10 times higher. Previous studies reported that in solutions with high COD/  $NH_4^+$  ratios, anammox activity can be suppressed by heterotrophic bacteria (Van Hulle et al. 2010). Imbalances in the microbial community or substrate limitations can result in the accumulation of the denitrification intermediates  $NO_2^-$ , nitric oxide (NO), and nitrous oxide ( $N_2O$ ). While  $N_2O$  is mainly of environmental concern, NO is toxic for microorganisms (Mancinelli and McKay 1983).

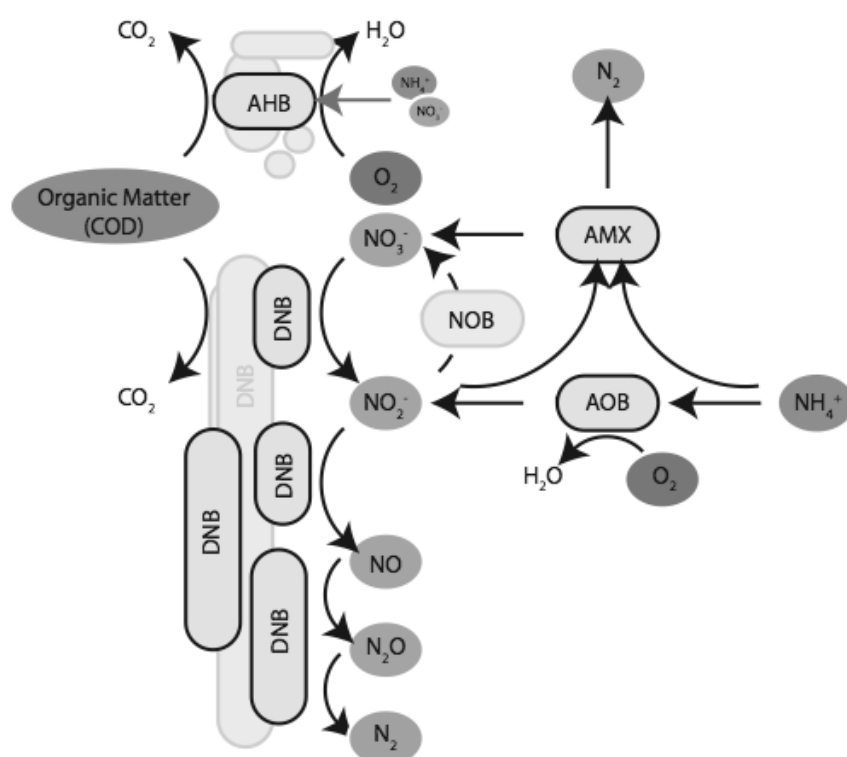


**Figure 1** Microbial functional groups and processes that dominate the nitrogen cycle and the  $O_2$  consumption in a combined nitrification/anammox reactor with a high COD/ $NH_4^+$ -N ratio. AHB primarily live by aerobic respiration and utilize organic matter as an electron donor and carbon source. Inorganic nitrogen ( $NO_3^-$ ,  $NH_4^+$ ) may be taken up as a nutrient but is not involved in catabolic processes. DNB live mostly or exclusively by anaerobic respiration using nitrate or one, several, or all of the intermediates of the denitrification pathway as electron acceptors. NOB are suppressed by low  $O_2$  in the study system.

The complex interactions between the different bacterial groups, the competition for nitrite between AMX and DNB, and the potential for system instabilities due to accumulation of toxic intermediates make the nitrification/anammox treatment of urine an ideal subject with which to explore the use of microbial community analysis and ecological theory. In the present study, we analysed a comprehensive data set for indications of regime shift behaviour in the microbial ecosystem of a bioreactor and discuss possible implications of regime shifts in microbial systems.

**Table 1** Kinetic parameters of bacteria potentially involved in nitrogen removal from urine<sup>a</sup>

Bacterial group	Growth rate [d <sup>-1</sup> ]	Yield [g COD·mol <sup>-1</sup> ·e <sup>-</sup> ]	O <sub>2</sub> half saturation constant (Monod kinetics) [mg·L <sup>-1</sup> ]	Concn for 50% HNO <sub>2</sub> inhibition [mg·L <sup>-1</sup> ]	NH <sub>3</sub> concn [mg L <sup>-1</sup> ]
AMX <sup>b</sup>	0.065	0.40	0.04 <sup>d</sup>	100 <sup>e</sup>	770 <sup>g</sup>
AOB <sup>c</sup>	0.77	0.34	0.3	0.21 <sup>f</sup>	540
NOB <sup>c</sup>	1.08	0.29	1.1	0.26	-- <sup>h</sup>
AHB (aerobic) <sup>c</sup>	7.1	3.4	0.08	ND <sup>i</sup>	ND
DNB (nitrate reduction) <sup>c</sup>	2.6	3.2		ND	ND
DNB (nitrite reduction) <sup>c</sup>	1.5	3.2		ND	ND

<sup>a</sup> These are typical parameters from a wide range of literature values

<sup>b</sup> Strous et al. (1998), 32°C

<sup>c</sup> Wiesmann (1994), 20°C, assuming 1 g COD/g organic dry matter

<sup>d</sup> Complete inhibition at 0.04 mg·L<sup>-1</sup>, Strous et al. (1997a)

<sup>e</sup> Inhibition at NO<sub>2</sub><sup>-</sup> concentration of >100 mg·L<sup>-1</sup>

<sup>f</sup> Lochtmann (1995) in Hellinga et al. (1999)

<sup>g</sup> Dapena-Mora et al. (2007)

<sup>h</sup> Stüven et al. (1992). In mixed systems, NH<sub>2</sub>OH rather than NH<sub>3</sub> inhibits NOB

<sup>i</sup> ND, not determined

## MATERIAL AND METHODS

A large number of parameters have been measured or calculated in this work. An overview and additional explanations are given in the Supporting Information S1.

### Reactor operation

The experimental system was a sequencing batch reactor (SBR) designed for treating diluted urine with a combined nitrification/anammox process by alternating between aerobic and anoxic phases. Throughout the duration of the monitoring period, the reactor was operated with the goal of achieving or maintaining a high nitrogen elimination rate (NER). The reactor setup is described in detail by Udert et al. (2008). Briefly, the experiments were conducted in an SBR with a total liquid volume of 6.7 L. A Simatic S5-100 apparatus was used for process control

(Siemens, Munich, Germany). The durations of the aerobic and anoxic phases were operator controlled (times between 15 and 60 min were chosen), with the proportion of the total duration of anoxic phase ( $P_{anox}$ ) versus aerobic phase per cycle varying between 34% and 83%. The airflow ( $Q_{air}$ ) was kept sufficiently low to always keep the  $O_2$  concentration below  $0.2 \text{ mg } O_2 \cdot L^{-1}$ . The number of aerobic and anoxic phases and therefore the total duration of each cycle depended on an operator-controlled pH threshold ( $pH_{set}$ ). In each cycle, following sedimentation, between 1.3 and 1.8 L of liquid ( $V_{Exch}$ ) was replaced with 5-times-diluted anthropogenic urine collected from the NoMix system in the Eawag main building Udert et al. (2008). An overview of the most important changes in operating parameters over the observation period is given in Figure S1 (Supporting Information S2).

## Chemical parameters

### *Continuous measurements*

Electrodes were used to measure pH (HA405-DXK-S8/225; Mettler Toledo, Greifensee, Switzerland),  $O_2$  concentration ( $O_2$ ), and electric conductivity ( $Cond$ ) (TriOxmatic 700 and Tetracon 325, both sensors; WTW, Weilheim, Germany). pH,  $O_2$ , electric conductivity, and temperature ( $Temp$ ) were continuously monitored with a data logger (Memograph S; Endress\_Hauser, Weil am Rhein, Germany). For this chapter, we did not quantify the  $N_2O$  concentrations. It was shown that the increase of the  $O_2$  sensor baseline concentration is linearly correlated with the  $N_2O$  concentration in the reactor (demineralized water was aerated with different mixtures of 100,000 ppm  $N_2O$  in  $N_2$  and pure  $N_2$  gas; unpublished data). We used this to calculate a non-calibrated indicator variable for  $N_2O$  accumulation,  $N_2O_{ind}$ , with the units  $\text{mg } O_2 \cdot L^{-1}$  (value of interference on the  $O_2$  sensor).

### *Sampling-based analyses*

Beginning on 15 February 2008, the reactor was regularly monitored for further chemical parameters: samples were regularly taken from the inflow (on average, every 2.5 d) and analysed for  $NH_4^+$  ( $NH4_{in}$ ) and dissolved COD ( $COD_{in}$ ). The reactor outflow was sampled at the same time and analysed for  $NH_4^+$ ,  $NO_2^-$ , and  $NO_3^-$  ( $NH4_{out}$ ,  $NO2_{out}$ , and  $NO3_{out}$ , respectively). The COD in the outflow was measured on selected dates. COD and  $NH_4^+$  were measured photometrically with vial tests (Hach Lange, Düsseldorf, Germany).  $NO_2^-$  and  $NO_3^-$  were analysed either with vial tests (Hach Lange) or on an ion chromatograph (Metrohm, Herisau, Switzerland). A small systematic deviation of the  $NO_2^-$  and  $NO_3^-$  vial test results was corrected to match the ion chromatograph measurements.  $NO_3^-$  vial tests were corrected for cross-sensitivity to  $NO_2^-$ . All samples were filtered (pore size, 0.7  $\mu\text{m}$ ; GF/F; Whatman, Middlesex, United Kingdom), measured immediately (photometric measurements), or stored for less than 7 d at  $4^\circ\text{C}$  (for analysis on an ion chromatograph). Starting on 22 September 2008, total sus-

pended solids (TSS) were determined in the mixed reactor and in the outflow according to standard methods (American Public Health Association 2005). These values were used to calculate the sludge retention time (SRT). The biodegradable fraction of the dissolved COD in the influent was determined by subtracting the measured dissolved COD in the effluent from the measured dissolved COD in the influent.

## **Microbial community analysis**

### *Sampling*

Eleven samples for microbial community analysis were taken throughout the observation period from 15 April 2008 to 15 April 2009 (samples C to N). Two additional samples taken prior to the beginning of the regular chemical monitoring, on 25 September 2007 and 21 November 2007 (samples A and B), are considered only for microbial community analysis. The sampling dates are given in Table S5 (Supporting Information S3).

### *Nucleic acid extraction*

At each time point, 1 mL samples of suspended biomass were taken from the reactor with a micropipette, mixed with 10% of a nucleic acid preserving solution (95% ethanol, 5% buffered phenol, Bürgmann et al. (2005)), centrifuged, and decanted, and the pellets were frozen at -80°C until further processing. DNA was extracted with a bead-beating method described previously (Kleikemper et al. 2005) with some modifications. Briefly, 0.5 mL sample and 1.5 mL lysis buffer (50 mM Tris [pH 8], 50 mM EDTA, 50 mM sodium chloride) were lysed by bead beating (3 times for 80 s each time at 3,000 rpm using 0.2 g 106- $\mu\text{m}$ - and 0.2 g 150- to 212- $\mu\text{m}$ -diameter beads), followed by chemical and enzymatic lysis with 10 mg·mL<sup>-1</sup> lysozyme (final concentration) for 10 min and with 1% SDS and 3,600 U·mL<sup>-1</sup> proteinase K for 30 min. DNA was purified by phenol-chloroform extraction and precipitation in isopropanol.

### *DNA quantification and quality control*

DNA was quantified by standard measurements of light adsorption at 260- and 280-nm wavelengths using a Nanodrop spectrophotometer (Nanodrop Products, Wilmington, DE) or by detection of fluorescence with a picogreen DNA quantification kit (Invitrogen, Basel, Switzerland) according to the manufacturer's instructions. Fluorescence was determined on a Synergy HT plate reader (Bio-Tek Instruments, Inc., Winooski, VT). DNA integrity was checked by gel electrophoresis in 1% agarose gels. Extracts with poor 260-nm wavelength/280-nm wavelength ratios were cleaned using a QIAquick gel extraction kit (Qiagen, Basel, Switzerland) according to the manufacturer's instructions. Prior to use in PCR, extracted nucleic acids were diluted to 10 or 2 ng· $\mu\text{L}^{-1}$  in nuclease-free water (Qiagen).



*Phylogenetic community characterization*

DGGE band sequencing (short sequence reads) and a nearly full-length amplicon clone library sequencing approach (long reads) were combined to obtain an overview of the microbial community compositions. DGGE was performed using general bacterial primers 341F-GC and 534R as described in reference 6 using a DCode DGGE system (Bio-Rad Laboratories AG, Reinach, Switzerland) for gel electrophoresis. For sequencing, all distinct band types were cut from three different gels containing samples from the period from 25 November 2007 to 15 April 2009. Cut bands were eluted in nuclease-free water and reamplified using the same primers described above but without the GC clamp and following the procedures described previously (Buesing et al. 2009). Successful PCR products were purified using a QIAquick PCR purification kit (Qiagen), and commercial sequencing was performed by Microsynth (Balgach, Switzerland). Out of 17 band types cut for sequencing, 10 sequences were obtained; other bands failed to amplify or sequences were unreadable, possibly indicating comigrating bands. DGGE patterns were analysed using the Quantity One software package (Bio-Rad).

Nearly full-length 16S rRNA gene amplicons from the sample obtained on 25 September 2007 were obtained by PCR using general bacterial primers 27F (3'-AGA GTT TGA TCM TGG CTC AG-5') and 1492R (TAC GGY TAC CTT GTT ACG ACT T) (25). Products were cloned using a pGEM-T Easy vector systems cloning kit (Promega, Madison, WI) according to the manufacturer's instructions, followed by plasmid preparation with a GenElute HP plasmid miniprep kit (Sigma-Aldrich, St. Louis, MO), also according to the manufacturer's instructions. Thirty-eight clones were screened with DGGE as described above. Eight clones representing unique DGGE phlotypes were selected for sequencing.

All PCRs were prepared with *Taq* polymerase and buffer obtained from MP Biomedical (Solon, OH), and primers were synthesized by Microsynth (Balgach, Switzerland).

*Phylogenetic classification*

Sequences were assigned to the taxonomical hierarchy using the Classifier tool on the Ribosomal Database Project 2 website (<http://rdp.cme.msu.edu/classifier/>) (42). Sequences were checked for chimera formation using the Bellerophone (version 3) program ([http://greengenes.lbl.gov/cgi-bin/nph-bel3\\_interface.cgi](http://greengenes.lbl.gov/cgi-bin/nph-bel3_interface.cgi)). One nearly full-length sequence was a suspected chimera and was eliminated from the data set. Where multiple DGGE band sequences were obtained for the same band type or where sequences were highly similar (>97% similarity in overlapping segments), only the sequence of the best quality was deposited in GenBank.

### *Microbial community fingerprinting*

Although we also analysed the DGGE fingerprints, we relied on ARISA as the main microbial community fingerprinting method. ARISA was performed as described previously (Fisher and Triplett 1999, Yannarell et al. 2003), with minor modifications. The ribosomal intergenic spacer was amplified using primers 1406f (labelled with fluorescent dye 6-carboxyfluorescein) and 23S. PCR mixtures (1 or 0.5  $\mu\text{L}$ ) were denatured for 3 min at 95°C with 9  $\mu\text{L}$  HiDi formamide and 0.5  $\mu\text{L}$  LIZ1200 size standard (both from Applied Biosystems, Carlsbad, CA) and placed on ice immediately afterwards. Fragment size analysis was performed on an ABI 3130xl capillary sequencer, using a 50-cm 16-capillary array and POP7 polymer (Applied Biosystems). Fragment analysis was performed with GeneMapper software. Only peaks with sizes between 350 and 1,250 bp were considered for analysis, and the minimum peak area in fluorescence units (FU) was 150 FU.

### *qPCR*

The temporal dynamics of the bacterial functional groups of the nitrogen cycle were analysed using a quantitative real-time PCR (qPCR) approach. The nitrogen cycle functional genes *amoA*, *nirS*, *nirK*, and *nosZ* were analysed using the primers and protocols of Geets et al. (2007), with some changes. Reaction mixtures contained 12.5  $\mu\text{L}$  2x SYBR green master mix (Applied Biosystems), 0.3  $\mu\text{M}$  each primer, and bovine serum albumin at a final concentration of 0.1 mg  $\text{mL}^{-1}$  in a final volume of 25  $\mu\text{L}$ . For *nosZ*, KCl was added to increase the concentration by 25 mM. The thermal cycling program for *amoA*, *nirS*, *nirK*, and *nosZ* was as described in Geets et al. (2007): 50°C for 2 min, 94°C for 10 min, and 40 cycles of 95°C for 60 s and annealing at 50°C for 60 s and 60°C for 60 s.

AMX-specific 16S rRNA gene qPCR was performed using primers Pla46rc and Amx0368aA18 (Schmid et al. 2005). qPCRs were performed as described above, but 2 mM MgCl<sub>2</sub> was added to the reaction mixture. The thermal cycling program was as before, but with an annealing temperature of 56°C.

General bacterium-specific 16S rRNA gene qPCR was performed using primers 519f and 907r (Lane 1991, Stubner 2002). PCRs were as described above for functional genes, but the PCR mixtures contained each primer at a final concentration of 0.8  $\mu\text{M}$ . The thermal cycling program was as before, but with an annealing temperature of 55°C.

All qPCR analyses were performed on an Applied Biosystems 7500 Fast real-time PCR system. Standard curves were prepared from dilutions of reference PCR amplicons cloned into pGEM-T Easy vectors and quantified as described above. Copy numbers of functional group targets are expressed as abundance according to the percentage of the general bacterial 16S rRNA gene copy numbers. Abundance as calculated here is operationally defined and may be distorted by different copy numbers of target genes in bacterial genomes. All samples were tested in dupli-

cate or triplicate on each 96-well plate, and at least two independently prepared plates were analysed per target. The amplification efficiency of all reactions was 95% or higher, except for *nosZ*, where one run had a lower efficiency of 88%.

### Statistical analysis

All errors given are standard deviations. Linear regression analyses (least-squares method) were calculated and plotted in Excel software. Regime-shift analysis was performed using the method described by Rodionov (2004) using the Sequential Regime Shift Detection program (version 2.1; <http://www.beringclimate.noaa.gov/regimes/>).

Heat map cluster analysis (Euclidean distance, average linkage method) of ARISA data was performed using the R program (version 2.9.1; R Development Core Team, 2006) function `heatmap.2` from the `gplots` package (Warnes et al. 2010).

Constrained and unconstrained ordination analysis and Bray similarity matrix calculation were conducted in R with the packages `BiodiversityR` (Kindt and Coe 2005) and `Vegan` (Oksanen et al. 2010).

The environmental data set used in constrained ordination (redundancy analysis [RDA]) was created with samples from the chemical sampling date closest to the DNA sampling date (0 to 6 d offset; 0.7 d, on average). Alternative methods for data set assembly (period averages) were tested but rejected because of their lower predictive power.

Three groups of variables were considered for RDA. (i) Group 1 consists of process control parameters, which are operator-defined parameters used for process control, i.e., the pH value that triggers a new cycle (*pH<sub>set</sub>*), proportion of anoxic conditions (including sedimentation) relative to total duration of the cycle (*P<sub>anox</sub>*), airflow rate (*Q<sub>air</sub>*), and exchange volume (*V<sub>Exch</sub>*). (ii) Group 2 consisted of environmental variables, which comprised variables for the properties of the inflow or the physical environment not directly under operator control: chemical oxygen demand (*COD<sub>in</sub>*), concentration of  $\text{NH}_4^+$  in the inflow (*NH4<sub>in</sub>*), electrical conductivity (*Cond*; using the maximum value per cycle), and temperature (*T*). (iii) Group 3 included response variables, which are parameters that depend on the process control, the environmental variables, and the microbial activity. They include  $\text{NO}_2^-$ ,  $\text{NO}_3^-$ , and  $\text{NH}_4^+$  in the outflow (*NO2<sub>out</sub>*, *NO3<sub>out</sub>*, and *NH4<sub>out</sub>*, respectively), cycle duration (determined by pH set point and proton production in the reactor (*Cycle*)), maximum  $\text{O}_2$  concentration during aerobic phase (*O2*), and the  $\text{N}_2\text{O}$  indicator (*N2O<sub>ind</sub>*). Derived parameters, i.e., parameters that are calculated from one or more of the above-mentioned measured variables (e.g., *NER*) were not considered for RDA, as they would violate the assumption of independent variables. RDA was performed once with the variables in groups 1 and 2 and separately with the variables in group

3. For each environmental data set, we performed forward selection of constraining variables using the ordistep function (Vegan). The statistical model was built from the selected variables. The significance of the model and the contribution of individual constraints were tested by permutation analysis.

Inspired by the moving window analysis described by Wittebolle et al. (2008), an analysis of community similarity over time was conducted using the Bray distance metric ( $B$ ) (equation 3) calculated on the basis of ARISA peak area (FU) data in R.

$$B_{ij} = \frac{\sum_{k=1}^S |x_{ik} - x_{jk}|}{\sum_{k=1}^S (x_{ik} + x_{jk})} \quad (3)$$

where  $x_{ik}$  and  $x_{jk}$  the area of peak  $k$  in samples  $i$  and  $j$ , respectively, and  $S$  is the total number of peaks.

### **Nucleotide sequence accession numbers**

The nearly full-length sequences are available in GenBank under accession numbers HQ917036 to HQ917042. DGGE band sequences were deposited in GenBank under accession numbers HQ917043 to HQ917052.

## **RESULTS**

### **Reactor performance**

At the beginning of the observation period in February 2008, the reactor had been in continuous operation for 10 months (Udert et al. 2008). From the beginning of June to the end of September 2008, the NER (Figure 2A) increased continuously from  $<100$  to  $>430$   $\text{mg N}\cdot\text{L}^{-1}\cdot\text{d}^{-1}$ . Beginning in late October 2008, a marked and sustained decrease in NER to values of  $165 \pm 35$   $\text{mg N}\cdot\text{L}^{-1}\cdot\text{d}^{-1}$  was observed.

Nitrogen elimination efficiency was  $>80\%$  throughout the study period and remained  $>94\%$  between 11 April 2008 and 25 August 2008 (Figure 2B). The highest efficiencies were measured in early August 2008 and decreased continuously after that.

### **Environmental variables**

The concentrations in the influent did not show strong variations:  $\text{NH}_4$ \_ concentrations in the inflow ( $\text{NH}_4$ \_in; Figure 2C) averaged  $590 \pm 90$   $\text{mg NH}_4\text{-N}\cdot\text{L}^{-1}$ , the concentration of dissolved COD was  $960 \pm 110$   $\text{mg O}_2\cdot\text{L}^{-1}$  (proportion of biodegradable COD,  $89\% \pm 16\%$ ), the pH was  $8.7 \pm 0.2$ , and the average electric conductivity was  $6.1 \pm 0.4$   $\text{mS}\cdot\text{cm}^{-1}$  ( $25^\circ\text{C}$ ). However,

$NH_4$ \_in showed a slight seasonal behaviour, with lower concentrations in winter and higher concentrations in summer (Figure 2C). The average temperature in the laboratory varied seasonally, with higher values in summer and lower values in winter, but the temperature variation in the reactor ( $22.8 \pm 1.5^\circ\text{C}$ ) was small.

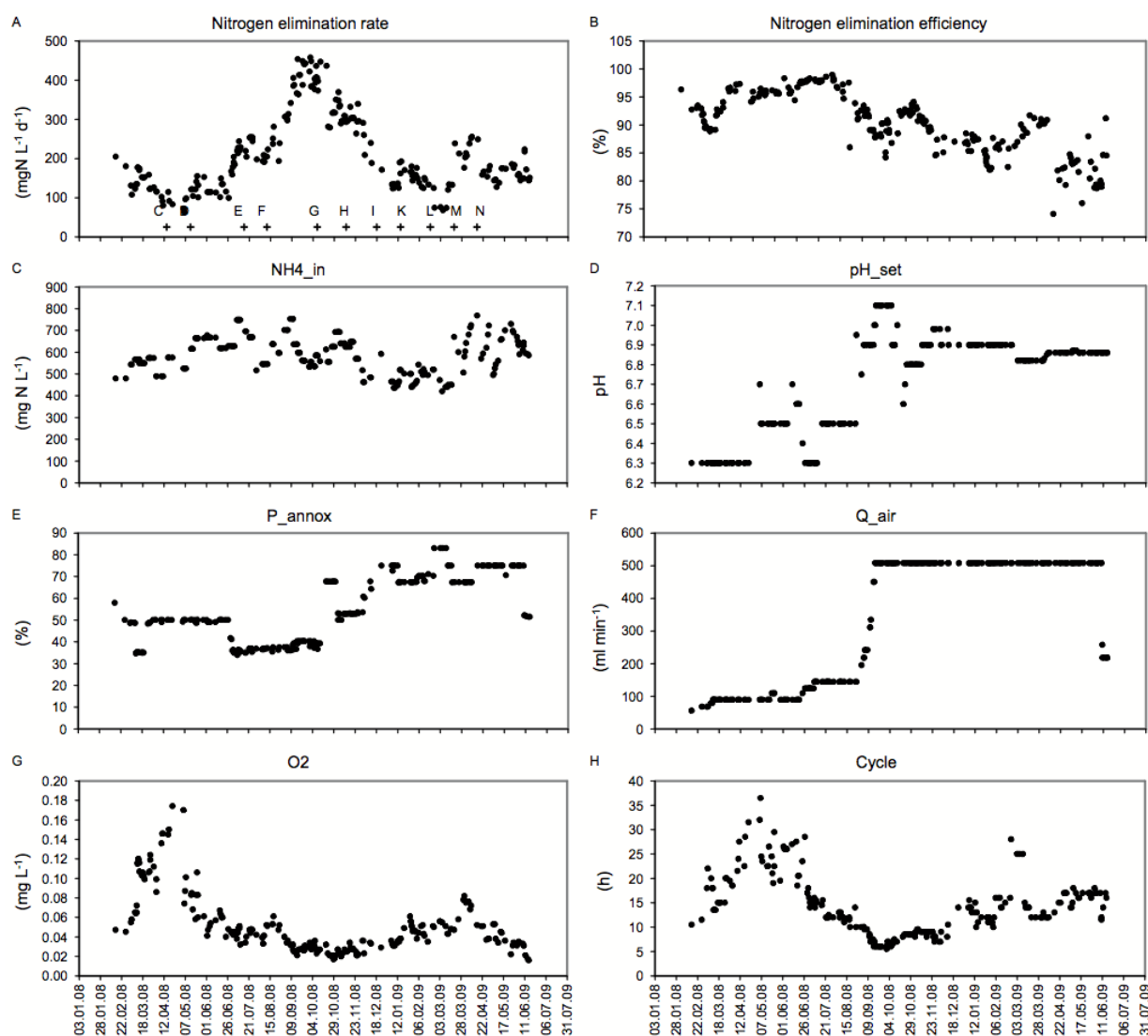


**Figure 2** Time series for several process indicators. Nitrogen elimination rate (A) and nitrogen elimination efficiency (B) are measures for the reactor performance.  $NH_4^+$  in the influent is an independent environmental variable (C).  $pH_{set}$  (D),  $P_{anox}$  (E), and  $Q_{air}$  (F) are independent process parameters controlled by the operator.  $O_2$  (G) and  $Cycle$  (H) are response variables which depend on environmental variables and process parameters. The plus signs in panel A indicate the sampling dates for microbial community analysis, and letters indicate sample designations. Samples A and B (not shown) were taken in 2007.

### Process control parameters

Process control parameters were adjusted at various times to improve the performance of the SBR (Figure S1 in the Supporting Information S2). The increase in NER was achieved mainly by gradually raising the pH set point ( $pH_{set}$ ; Figure 2D) from 6.3 to 7.1, which resulted in shorter cycles and thus higher urine throughput. Maximum NERs were achieved in September and October 2008, with  $pH_{set}$  adjusted to 7.0 and 7.1. During the same time period the airflow rate ( $Q_{air}$ ) was gradually increased from 140 mL·min<sup>-1</sup> to 510 mL·min<sup>-1</sup> (Figure 2F), primarily for the purpose of improving conditions for AOB. The increase in  $Q_{air}$  had little effect on the measured maximum dissolved O<sub>2</sub> concentrations ( $O_2$ ; Figure 2G), which was always below 0.2 mg·L<sup>-1</sup> and decreased from April to the end of October 2008 to values as low as 0.02 mg·L<sup>-1</sup>.  $P_{anox}$  (Figure 2E) was kept at approximately 50% until the end of June 2008 and was then lowered to approximately 35 to 40% until 13 October 2008. Subsequently, higher values up to 83% were used. The exchange volume ( $V_{Exch}$ ; data not shown) increased from 1.3 L to 1.5 L and finally 1.8 L between 22 September 2008 and 20 October 2008 but was reset to 1.3 L on 22 October 2008 and not changed any more. The short period with increased  $V_{Exch}$  had only a limited effect on the SRT, which remained high (>30 d) for most (10 out of 18) of the sampling events during that period as well as for the entire remaining observation period (156 out of 173).

### Response variables

NH<sub>4</sub><sup>+</sup> was the dominant nitrogen species in the outflow (75%, on average). NO<sub>2</sub><sup>-</sup> reached maximum concentrations of 25 mg N·L<sup>-1</sup>. NO<sub>3</sub><sup>-</sup> in the outflow remained below 8 mg N·L<sup>-1</sup> at any time. All outflow concentrations ( $NH4_{out}$ ,  $NO3_{out}$ ,  $NO2_{out}$ ) and the indicator variable for N<sub>2</sub>O ( $N2O_{ind}$ ) were subjected to statistical regime-shift analysis, in order to determine phases of relative stability (Figure 3). The regime-shift analysis of  $NH4_{out}$  (Figure 3A) indicated that after an initial drop, this parameter remained in a stable regime (despite decreasing cycle duration; Figure 2H), extending from mid-April to mid-August 2008. During this period, NH<sub>4</sub><sup>+</sup> concentrations mostly varied between 10 and 20 mg NH<sub>4</sub>-N·L<sup>-1</sup>. This phase ended with a strong regimen shift on 26 August 2008, with a sudden increase to >50 mg NH<sub>4</sub>-N·L<sup>-1</sup>. This is assumed to be due to an increase of the pH set point from 6.5 to 6.95 on 26 August 2008 (Figure 2D). Because AOB lower the pH during ammonia oxidation, a higher  $pH_{set}$  decreases the amount of ammonia oxidized. The higher ammonia level was maintained with some variations until the end of the study period.

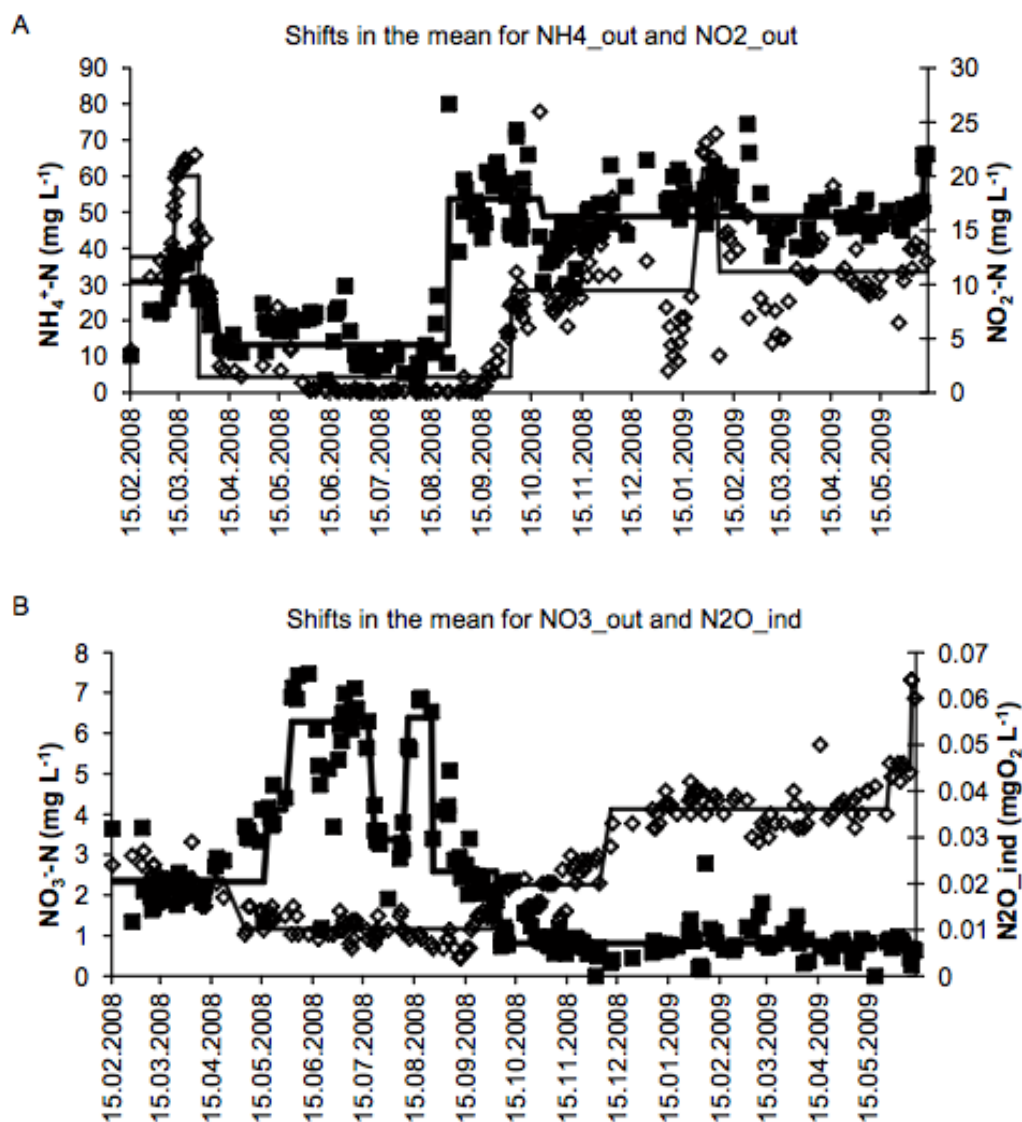


**Figure 3** Regime-shift analysis of the temporal trends in the concentrations of  $\text{NH}_4^+$  ( $\text{NH4\_out}$ ; black squares) and  $\text{NO}_2^-$  ( $\text{NO2\_out}$ ; empty diamonds) in the outflow (A) and  $\text{NO}_3^-$  ( $\text{NO3\_out}$ ; black squares) in the outflow and the maximum  $\text{N}_2\text{O}$  in the reactor extracted from  $\text{O}_2$  sensor data ( $\text{N2O\_ind}$ ; empty diamonds) (B). Solid lines indicate statistically significant regimes determined using sequential regime-shift detection with the parameters probability equal to 0.001, cutoff length equal to 10, and Huber parameter equal to 1.

$\text{NO}_2\text{-out}$  exhibited a similar pattern as  $\text{NH}_4\text{-out}$  (Figure 3A); an early regime of elevated concentrations was followed by a stable phase with low values. From the beginning of June 2008 to mid-September 2008,  $\text{NO}_2\text{-out}$  concentrations were mostly lower than 1 mg  $\text{N}\cdot\text{L}^{-1}$ . Values began to increase in mid-September, and the regime-shift analysis placed the significant shift to a new regime with higher  $\text{NO}_2\text{-out}$  concentrations on 25 September 2008, a month after the shift in  $\text{NH}_4\text{-out}$ .  $\text{NO}_2\text{-out}$  was slightly more variable than  $\text{NH}_4\text{-out}$ , but a similar regime with elevated concentrations became established until the end of the study period. The indicator for

N<sub>2</sub>O accumulation (*N2O\_ind*) also began to increase in mid-September, and the statistically significant shift to increased N<sub>2</sub>O accumulation was detected for 2 October 2008. *N2O\_ind* shifted again to a regime of even higher accumulation on 11 December 2008 (Figure 3B). *NO3\_out* fluctuated strongly during the first 8 months of the observation period. During the period from June to August 2008, several episodes with relatively high NO<sub>3</sub><sup>-</sup> concentrations (6 to 7.4 mg NO<sub>3</sub>-N·L<sup>-1</sup>) occurred. By 26 August 2008, *NO3\_out* had decreased and a stable regime was established with an average concentration of 0.8 mg NO<sub>3</sub>-N·L<sup>-1</sup> that lasted until the end of the study period (Figure 3B).

In summary, all nitrogen-related system response variables showed a statistically significant regime shift between mid-August and the beginning of October 2008.

## **Analysis and dynamics of bacterial community**

### *Phylogenetic characterization*

The sequences retrieved from the clone library and DGGE band sequencing were classified as belonging to the *Flavobacteria*; *Bacteroidia*; *Clostridia*; *Alpha-*, *Beta-*, and *Gammaproteobacteria*; *Sphingobacteria*; *Bacilli*; and *Acidobacteria*. The detected organisms had a wide range of substrate preferences, which ranged from aerobic (e.g., *Flavobacteria*) to facultatively anaerobic (*Burkholderiales*, *Simplicispira*) and strictly anaerobic, mostly fermentative species (*Anaerovorax*, *Bacteroidales*). A number of sequences were similar to those of known nitrate reducers/denitrifiers (*Simplicispira*, *Pleomorphomonas*, *Petrimonas*, *Thauera*). *Haliscomenobacter* is a known filamentous activated sludge bacterium which is associated with O<sub>2</sub>-deficient situations (Gaval and Pernelle 2003). While our sequencing effort was not exhaustive, the analysis revealed that organoheterotrophs were abundant members of the microbial community in the reactor.

### *Dynamics of functional microbial groups*

qPCR revealed a continued presence of all major functional microbial groups involved in the nitrogen cycle that were analysed (Figure 4). AMX were initially present in low numbers (this was also the case for the samples from 2007; data not shown), with a pronounced abundance maximum on 11 August 2008 (Figure 4). The *amoA* gene, representing AOB, did not show a pronounced dynamic. For *nirS* and *nosZ*, representing different process steps of denitrification by DNB, we observed decreases in their abundance of 71 and 79%, respectively, during the period between 15 April 2008 and 15 July 2008. During this period we observed a strong increase in AMX. The abundance of *nirK* was below 1% throughout (data not shown).



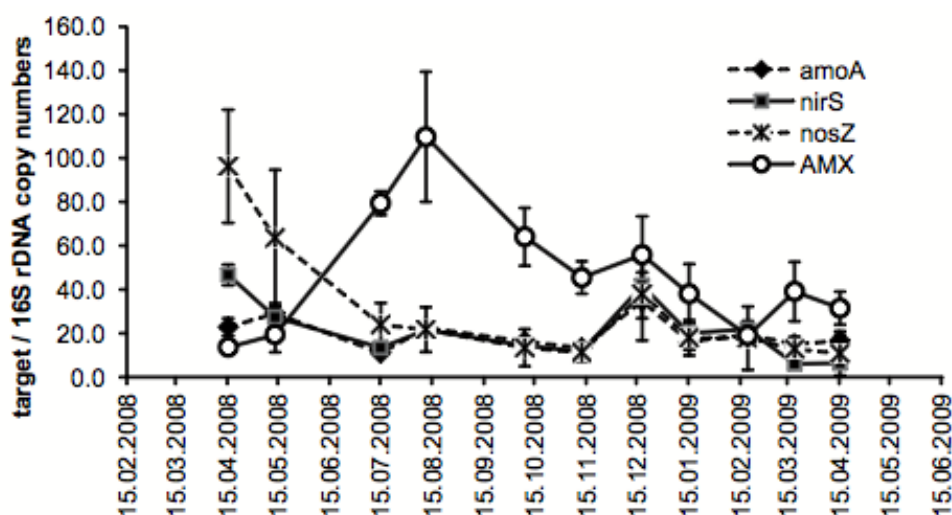


**Figure 4** Quantitative PCR analysis of bacterial functional groups of the nitrogen cycle. AOB are represented by the ammonium monooxygenase gene (*amoA*), DNB are represented by the nitrite reductase gene (*nirS* [*nirK* was present at 1% throughout]) and the nitrous oxide reductase gene (*nosZ*), and AMX were detected using a groupspecific primer set for the AMX 16S rRNA gene. All data were normalized against qPCR using general bacterial 16S rRNA gene primers.

#### Community dissimilarity

Community turnover was visualized by plotting the Bray dissimilarities of ARISA fingerprints for consecutive sampling dates (Figure 5). The analyses based on DGGE (data not shown) agreed remarkably well with those based on ARISA ( $R^2 = 0.62$ ,  $P < 0.01$ ), considering the different principles, genetic targets, and specific biases of each method. Two spikes in dissimilarity indicated a community shift between the August and October 2008 samples and between the February and March 2009 samples, separated by a period of high stability.

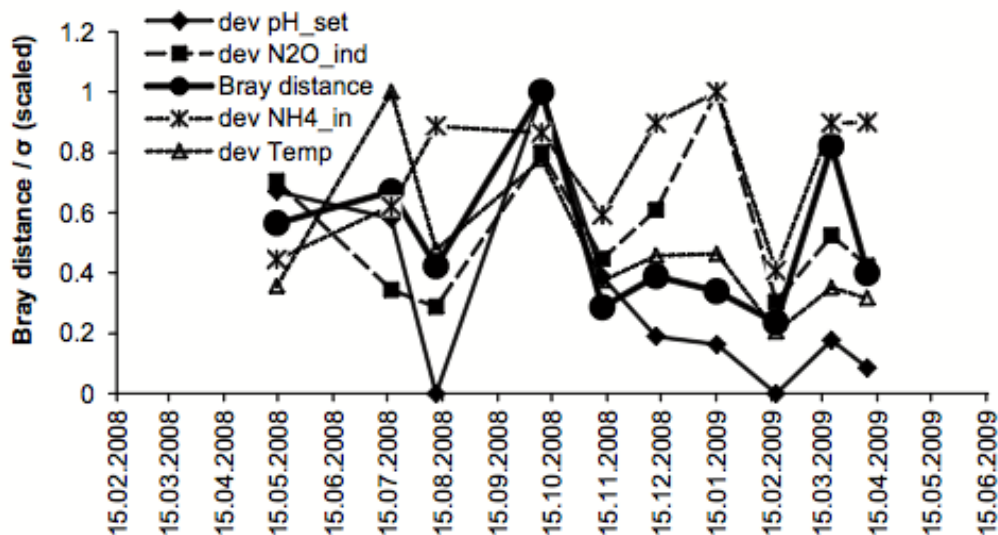


**Figure 5** Time series analysis of Bray distance based on ARISA community fingerprints compared to time series of standard deviations (dev,  $\sigma$ ) plotted for important driving variables according to redundancy analysis. The Bray distance graph plots the Bray dissimilarity metric of each sample to the previous sample. The time series of standard deviation plots the standard deviation of all measurements from the time interval between the date closest to the microbial sampling date and the previous microbial sampling date. All series are scaled to the highest value. Solid lines, significant correlations ( $P < 0.05$ ) with Bray dissimilarity; dashed lines, no significant correlation.

### *Cluster analysis*

The heat map cluster analysis of ARISA profiles (Figure 6) demonstrated the good reproducibility of the analysed technical replicates with 1 and 0.5  $\mu\text{L}$  DNA, as these are largely indistinguishable. Using an arbitrarily set cutoff (Figure 6), we designated 3 main clusters: The samples from 2007 (A and B) form the first cluster, and the 2008 samples up to August 2008 (C to F) form cluster 2. Cluster 3, which consists of all later samples (G to N), is clearly separated from both cluster 1 and cluster 2. The strongest shift in the community thus occurred between the times of collection of samples F (11 August 2008) and G (9 October 2008). The two latest samples (M and N) formed a separate subcluster (cluster 3b). The clustering of the ARISA peaks indicated operational taxonomic units (OTUs) with similar behaviour over the time course (Figure 6). It is evident that the shift between clusters 1 and 2 not only was due to a strong shift in the dominance structure of abundant OTUs (left side of the heat map in Figure 6), including the disappearance of some key OTUs (e.g., peak P54), but also is reflected in the appearance of previously undetected OTUs (right side of the heat map).

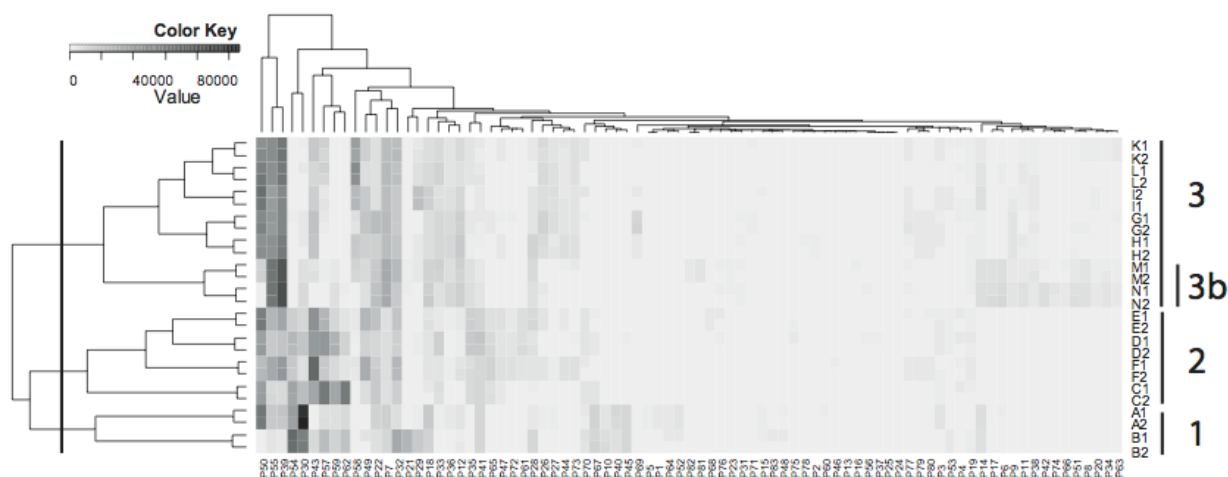


**Figure 6** Heat map representation and hierarchical clustering of ARISA community fingerprints. Row labels indicate the sampling dates (see Figure 2A) and the DNA volume used in ARISA (1 = 1 L, 2 = 0.5 L), and columns correspond to ARISA peaks (phylotypes). Darker shading indicates a higher relative ARISA peak area, an indication of high relative abundance. Numbers on the right are cluster designations.

#### *Drivers of community dynamics*

The effect of key variables on the bacterial community was studied using a constrained ordination, RDA. Ordinations were carried out once with process control parameters and environmental variables (process variables; Figure 7A) and once with response variables (Figure 7B) as the environmental data set. Forward selection of constraints selected *pH\_set*, *NH4\_in*, and *Temp* from the process variables data set. *O2* and *N2O\_ind* were selected from the response variables. However, it should be noted that *N2O\_ind*, *NO2\_out*, and *NH4\_out* had similar vectors in RDA, and the use of any one of these parameters results in a statistically significant model. Forward selection from a combination data set of process and response variables resulted in selection of the same variables selected from the process variables alone. The models using process variables and response variables as constraints explained 69 and 66% of the total variance on the two primary axes, respectively. Permutation analysis ( $n = 1,000$ ) revealed that the ordinations were highly significant ( $P < 0.001$ ). All individual constraints contributed significantly ( $P < 0.05$  to  $P < 0.01$ ). In the process variable ordination (Figure 7A), *pH\_set* was mainly associated with the first ordination axis, and the period of the regime shift (from F to G) was mostly associated with a shift of the community along this axis, while the community dynamics prior to the regime shift may also have been affected by *Temp*. It is noteworthy that the samples taken after the proposed regime shift from October 2008 to February 2009 (G to L) cluster very closely together, indicating high community stability in this phase. *NH4\_in* con-

tributed most strongly to axis 2 and appears to be related to the community development in the last two samplings (N and M).

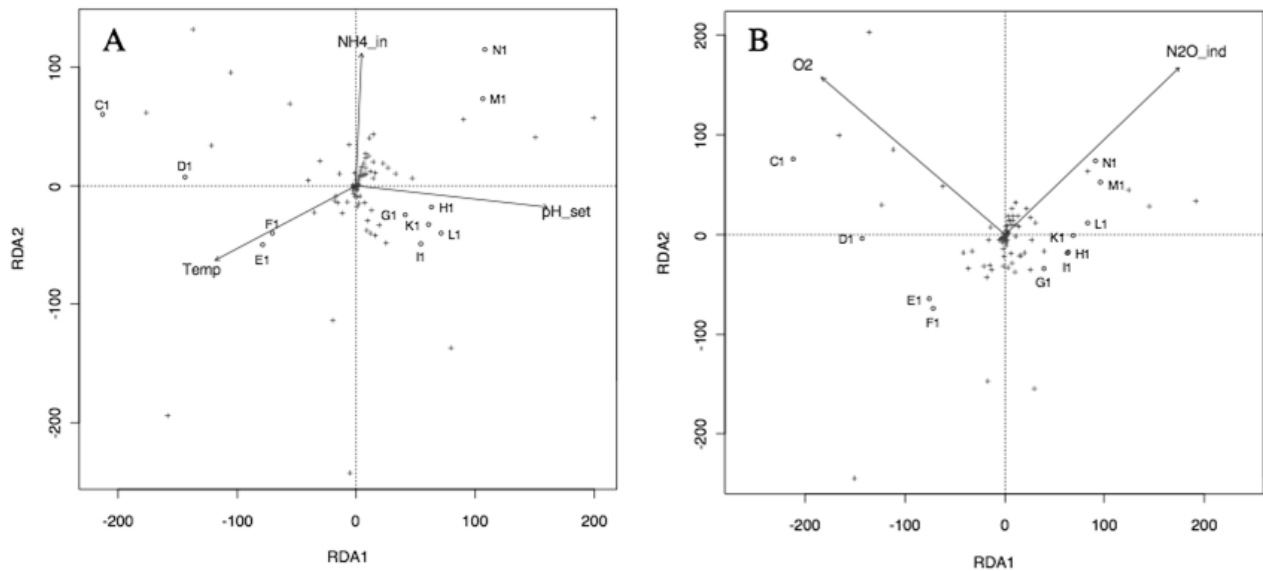


**Figure 7** Triplots of redundancy analysis of ARISA community structure data using operational parameters and independent environmental variables (A) or system response (output) variables as the constraining data set (B). Empty circles, samples labelled according to sampling date; plus signs, ARISA peaks, representing OTUs. Arrows, constraining variables of the environmental data set.

In the RDA with response variables, *N2O\_ind* and *O2* were equally related to both axes. The community development in the pre-regime-shift phase is best explained by *O2*, while the regime shift itself (shift from samplings F to G) and subsequent changes are best explained by *N2O\_ind*.

The influence of the parameters *pH\_set*, *NH4\_in*, *Temp*, and *N2O\_ind* was analysed further by overlaying the analysis of community dissimilarity with plots of the standard deviation calculated for the period between the current and the previous microbial sampling (Figure 5). The result supports the ordination in indicating a key role for *pH\_set*. The variability in *pH\_set* was significantly correlated with the extent of change in the bacterial community ( $R^2 = 0.49$ ,  $P < 0.05$ ), while this was not the case, e.g., for *NH4\_in* or *Temp* ( $P > 0.05$ ). Variability in community composition was also linked to variability in the nitrogen outflow *Ntot\_out* (sum of *NH4\_out*, *NO2\_out*, and *NO3\_out*;  $R^2 = 0.59$  and  $P < 0.01$ ; data not shown). Similar results were obtained with unconstrained ordination (data not shown).

## DISCUSSION

### Evidence for a regime shift

Ecological regime shifts are defined as large and rapid shifts from one stable ecosystem state to another (Scheffer and Carpenter 2003). In theory, such shifts can be attributed to the existence of alternative stable system states for a given set of control factors (Collie et al. 2004, Scheffer and Carpenter 2003). For purely microbial ecosystems, evidence for alternate stable states is still largely missing (Botton et al. 2006). Scheffer and Carpenter (2003) discuss typical indications for ecological regime shifts and possible sources of evidence in field data in their review. Typical observations indicating an ecological regime shift include (i) jumps in time series, (ii) clear differences in species composition or abundance, (iii) a change in the relationship between system control parameters and response variables or between response variables, (iv) the resilience of the system against a return to the previous state, and (v) the absence of strong stress events. Our data provide multiple lines of evidence that an ecological regime shift was observed.

(i) Strong shifts in the response variables *NH4\_out*, *NO2\_out*, *NO3\_out*, and *N2O\_ind* were visible in our data and were confirmed by a statistical analysis (sequential regime-shift detection; Rodionov (2004)). The regimen shifts were statistically highly significant ( $P < 0.001$ ) for each of these parameters during the period from mid-August to mid-October 2008 (Figure 3).

(ii) The bacterial community structure showed dynamic changes throughout most of the observation period, but ordination and cluster analysis (Figure 6 and 7) and time series analysis of community dissimilarity (Figure 5) indicated that the most dramatic shift in the community structure occurred between August and October 2008. This coincides with the period when the reactor reached its peak performance and began to accumulate  $\text{NO}_2^-$ . It also coincides with other observed regime shifts in the nitrogen outflow data. Finally, we observed a strong decrease of the AMX abundance from its peak in August 2008. DNB gene abundance (*nirS*, *nosZ*) had already reached a low level before the shift and continued to decline during this period. According to the phylogenetic analysis, the general bacterial community was dominated by heterotrophs. This indicates that the entire microbial community and not only the functional groups directly involved in nitrogen transformations was affected by the regime shift. The detected heterotrophic genera are well-known to have different physiological properties which correspond well to the SBR environment, with niches created by the fluctuating availability of  $\text{O}_2$  and oxidized nitrogen compounds as external electron acceptors and the availability of various organic carbon substrates in urine. Our data thus point to the potential value of general microbial community analysis as a tool for monitoring engineered microbial systems.

(iii) Correlations between variables were affected by the proposed regime shift: e.g., an analysis of the correlation between  $NO_2\_out$  and  $NH_4\_out$  showed a strong correlation prior to and a complete lack of correlation after the period of regime shifts (Figure 8).

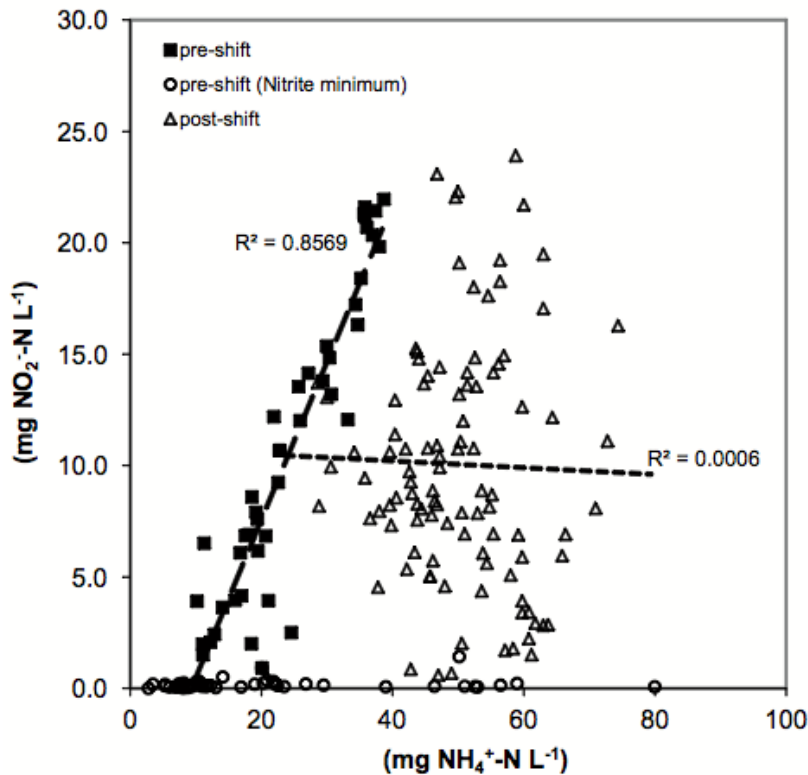


**Figure 8** Correlation between outflow concentrations of  $NH_4^+$  and  $NO_2^-$  before (black squares) and after (white triangles) the observed main regime shifts in nitrite and  $NH_4^+$ . The initially highly significant correlation ( $P < 0.001$ ) breaks down completely after the regime shift. For a period of time before and during the regime shift, nitrite levels were at or below the detection limit; these values are not used in the regression (white circles).

(iv) Both the time series of community dissimilarity (Figure 5) and ordination analysis (Figure 7) clearly showed that following the shift, the community experienced an extended period of high stability from October 2008 to February 2009, despite continued fluctuations in system control parameters, environmental variables, and response variables. Compared to the dynamics during the first half of the observation period, this relative stability was also observed in the qPCR data (Figure 4). This is an indication that the system had settled into a new stable state. However, we did not attempt to move operating parameters back to values from before the performance maximum within the observation period.

(v) Changes in control parameters, such as the nearly simultaneous changes of  $pH\_set$  and  $Q\_air$ , are strongly indicated to be related to the observed shifts in the microbial community.

However, it is not clear to what extent these changes constitute strong stress events: raising  $pH\_set$  represented a reduction of pH-related stress (e.g., for AOB). However, the resulting decrease in cycle duration and sludge age probably represented a stress event for AMX, although these changes were gradual (Figure 2H) and temporary. While the control parameter  $Q\_air$  was increased considerably during the regime-shift period, with the idea of improving conditions for AOB and thus  $NH_4^+$  conversion rates, the  $O_2$  concentrations always remained in the subinhibitory range, showing that the microbial community was capable of absorbing the additional  $O_2$ . In addition, raising  $Q\_air$  did not have a strong effect on the cumulative air volume per cycle ( $V\_air$ ; data not shown), which describes the total amount of the electron acceptor oxygen available per cycle. This parameter showed a roughly linear increase from an initial value of about 20 L to an average of  $96 \pm 22$  L, reached approximately in January 2009, and afterwards fluctuated in that range until the end of the monitoring period. Due to its dependence on  $Cycle$ ,  $P\_anox$ , and  $Q\_air$ , this parameter is dependent on both control and system response parameters and was therefore not included in the ordination analysis, despite its obvious relevance.

### Causes of regime shift

The regime shift between July and October 2008 resulted in an unfavourable system state. NER was greatly reduced from its peak value,  $NO_2^-$  accumulated in the system and was present in the outflow, and an increase of  $N_2O\_ind$  shows that the system started producing the greenhouse gas  $N_2O$  and, possibly, also toxic  $NO$ .  $pH\_set$ ,  $Temp$ , and  $N_2O\_ind$  were indicated by the ordination analysis to be possible drivers of the community dynamics between July and October 2008. In the following, we will discuss why changes of  $pH\_set$ ,  $Temp$ , and  $N_2O\_ind$  might have triggered the strong changes in microbial community structure and function.

#### $pH\_set$

The higher  $pH\_set$  was expected to increase the activity of AOB, which are inhibited at lower pH values. qPCR indicated that AOB did not increase in number in response, but this does not necessarily rule out a higher AOB activity. The higher AOB activity could have caused the increase of the  $NO_2^-$  concentration, which in turn supported the growth of DNB that use  $NO_2^-$  as an electron acceptor. While the new conditions favoured certain DNB, AMX activity decreased due to the higher  $NO_2^-$  and AHB had to compete with DNB for organic substances. This change could largely explain the observations made with ARISA and DGGE, which are mainly due to changes in the heterotrophic community.

By increasing  $pH\_set$ , the cycle duration was significantly reduced (Figure 2D and H). A possible consequence might have been the outwashing of slow-growing organisms such as AMX. However, qPCR analysis revealed that while the abundance of AMX indeed decreased, they

were never lost from the system and their abundance remained above levels present at the beginning of the observation period (Figure 4). Thus, their inability to increase in abundance again was not due to losing them from the system.

### *Temp*

All microbial activity increases with temperature, as long as the temperature does not exceed the physiological range. Between July and October 2008, the temperature steadily decreased from a maximum of 26.6°C to a minimum of 21.9°C. The concomitant decrease of the maximum growth rate can be assumed to have been most critical for slow growing bacteria, especially AMX. As mentioned above, however, AMX were never completely lost.

### *N<sub>2</sub>O<sub>ind</sub>*

Besides N<sub>2</sub>O, another intermediate of denitrification, NO, is also known to interfere with oxygen measurements (Fux et al. 2006) and could have contributed to *N<sub>2</sub>O<sub>ind</sub>*. In contrast to N<sub>2</sub>O, NO production not only is critical for the environment but also affects microorganisms. NO is generally known to be inhibiting or toxic for microorganisms involved in the nitrogen cycle, but it is also an electron acceptor for some denitrifying bacteria (Zumft 1993). The decrease of *nosZ* abundance (Figure 4) during the phase of low NO<sub>2</sub><sup>-</sup> concentrations (June to August 2008) may have contributed to the strong increase in *N<sub>2</sub>O<sub>ind</sub>* after the system switched back to NO<sub>2</sub><sup>-</sup> accumulation. There are only a few studies specifically on the effect of NO on AMX. However, previous studies (Kartal et al. 2010, Schmidt et al. 2002) showed that “*Candidatus Brocadia fulgida*” and “*Candidatus Brocadia anammoxidans*” tolerated NO concentrations of 600 ppm and 3,500 ppm, respectively, and even higher AMX activities in the presence of NO were reported. We therefore assume that AMX might not be negatively affected by NO, but it is very likely that NO influenced other microbial communities involved in nitrogen cycling and thus contributed to the community change.

In summary, we hypothesize that the concomitant change of an important process control parameter (*pH<sub>set</sub>*), a strongly influential environmental parameter (*Temp*), and a reinforcing response parameter (*N<sub>2</sub>O<sub>ind</sub>*) caused a fundamental change of the microbial community and nitrogen cycle processes. This combination of external forcings and internal processes is typical for regime shifts (Collie et al. 2004). A final conclusion about the actual cause of the regime shift cannot be drawn in this chapter, because targeted experiments are required to test the different hypotheses.

## **Implications of regime shifts for microbial reactors**

The occurrence of regime shifts in wastewater treatment systems could have strong implications on the use of models based on microbial kinetics, such as activated sludge model (ASM) 3 (Gujer et al. 1999). In these models, microbial kinetics are modelled on the basis of constant



Monod parameters, such as the half-saturation constant  $K$  and the maximum growth rate  $\mu_{max}$ . Adaptations of the bacteria to new environmental conditions are modelled by using saturation and inhibition terms only. Regime shifts, however, can change the microbial population so significantly that the constant kinetic parameters would not be applicable anymore. To account for regime shifts in Monod parameter-based mechanistic models, the number of bacterial groups would have to be increased, and with them, the number of kinetic parameters would have to be increased. The need for a high number of reliable kinetic parameters, however, limits the applicability of large mechanistic models. Statistical and ecological model approaches might be viable alternatives for complex biological processes such as nitrification/anammox treatment of urine, but further work is required to be able to assess their full potential.

### Conclusions

A 400% increase of NER was achieved in the studied SBR for partial nitrification/anammox over the course of 5 months by raising  $pH_{set}$  and by increasing aeration. However, continued operation resulted in a low NER and  $NO_2^-$  and  $N_2O$  accumulation. Analysis of the chemical and biological data indicated that the system behaviour can be described as an ecological regime shift. This regime shift could not be successfully reversed during the observation period, and the microbial community remained stable over an extended period of time, indicating that the system had shifted to a new stable state marked by reduced AMX and increased DNB activity.

The concept of ecological regime shifts and the existence of alternate stable states in microbial communities have so far received little attention in microbial ecology or environmental engineering. In this chapter, we have, for the first time, presented evidence that complex, purely microbial communities may experience regime shifts with marked effects on ecosystem processes. The concept of regime shifts provides a new perspective on process instabilities in engineered microbial systems. Alternative stable states could underlie other observations in wastewater treatment, such as bulking and foaming. An understanding of the stability landscapes of microbial reactors and the mechanistic consequences associated with them could provide important insights for the development of stable and efficient processes.

### ACKNOWLEDGEMENTS

We gratefully acknowledge funding by Eawag and the Swiss National Science Foundation, project 200021\_125133. We thank M. S. M. Jetten and M. Schmid from Radboud University Nijmegen for providing positive controls for AMX PCR. We express our thanks to Nathanaël Legeard, Ashish Sahu, Anna Kraj, Karin Rottermann, and Claudia Bänninger for support in the laboratory.



## **SUPPORTING INFORMATION**

### **FOR CHAPTER 1**

#### **Regime shift and microbial dynamics in a sequencing batch reactor for nitrification and anammox treatment of urine**

Helmut Bürgmann, Sarina Jenni, Francisco Vazquez, Kai M. Udert

*Applied and Environmental Microbiology*, 2011, 77(17), 5897-5907

## S1 List of variables used in the manuscript

Environmental parameters are properties of the inflow or the environment which are not or only under limited control of the operator (Table S2). Response variables are influenced by active microbial processes in the reactor. They represent the system response, but also influence the microbial community in the reactor (Table S3). Performance indicators are calculated values describing the system performance (Table S4).

**Table S1** Operator-controlled parameters. Variables in italics indicate parameters used in the statistical analysis.

<b>Parameter</b>	<b>Unit</b>	<b>Description</b>
<i>pH<sub>set</sub></i>	-	pH setpoint. Reaching the pH setpoint triggers the end of a cycle. <i>pH<sub>set</sub></i> determines the extent of NH <sub>4</sub> <sup>+</sup> oxidation by AOB, because this process releases protons. Lowering <i>pH<sub>set</sub></i> prolongs the cycle, because AOB have to oxidize more NH <sub>4</sub> <sup>+</sup> , to lower the pH value. Additionally AOB activity slows down at lower pH values.
<i>Q<sub>air</sub></i>	ml·min <sup>-1</sup>	Flux of air supplied during aerobic phases. Higher <i>Q<sub>air</sub></i> supplies more O <sub>2</sub> per unit time and can lead to higher O <sub>2</sub> concentrations ( <i>O<sub>2</sub></i> ) and can provide O <sub>2</sub> to more bacteria (diffusion). Since higher oxygen concentrations also increase the activity of aerobic bacteria, higher <i>Q<sub>air</sub></i> does not necessarily lead to a strong increase of <i>O<sub>2</sub></i> .
<i>V<sub>exch</sub></i>	L <sup>-1</sup>	Exchange volume. The volume of liquid drawn from the reactor after sedimentation and replaced with a fresh batch of inflow. Higher exchange volumina can lead to a higher output of biomass depending on the sedimentation efficiency.
<i>P<sub>anox</sub></i>	%	Proportion of anoxic conditions. The proportion of time the system is in anoxic or anaerobic phases relative to total cycle duration. This is derived from T <sub>anox</sub> and T <sub>aerob</sub> . <i>P<sub>anox</sub></i> shows whether the bacteria are exposed more to anoxic or to aerobic conditions.
<b>T<sub>anox</sub></b>	min	The duration of a single stirred anoxic phase.
<b>T<sub>aerob</sub></b>	min	The duration of a single stirred aerobic phase.

**Table S2** Environmental parameters. Variables in italics indicate parameters used in the statistical analysis.

<b>Parameter</b>	<b>Unit</b>	<b>Description</b>
<i>COD_in</i>	mg·L <sup>-1</sup>	Chemical oxygen demand in the inflow. Supply of organic electron donors for heterotrophic bacteria. The parameter is subject to changes due to COD degradation during storage in the urine collection tank of the toilet system and in the influent tank of the reactor.
<i>NH4_in</i>	mg N·L <sup>-1</sup>	Ammonium concentration in the inflow. Supply of electron donor for AOB and AMX. Changes are mainly due to ammonia volatilization during storage.
<i>Cond</i>	mS·cm <sup>-1</sup>	Electrical conductivity. A measure for the dilution of urine. It depends on the total concentration of ions in urine. Does not change substantially.
<i>Temp</i>	°C	Influenced by the temperature in the lab. Fluctuates seasonally with peaks in summer. The lab was not air-conditioned.
<i>pH_in</i>	pH	Determined by the composition of urine. Influenced by bacterial activity during urine storage, ammonia volatilization and urine dilution. Variations are small.

**Table S3** Response parameters. Variables in italics indicate parameters used in the statistical analysis.

<b>Parameter</b>	<b>Unit</b>	<b>Description</b>
<i>NO2_out</i>	mg N·L <sup>-1</sup>	Nitrite (NO <sub>2</sub> <sup>-</sup> ) in the outflow. NO <sub>2</sub> <sup>-</sup> is produced by AOB and consumed by DNB, AMX or NOB (the later were probably negligible in our system).
<i>NO3_out</i>	mg N·L <sup>-1</sup>	Nitrate (NO <sub>3</sub> <sup>-</sup> ) in the outflow. NO <sub>3</sub> <sup>-</sup> is produced by AMX and NOB and consumed by DNB. It is possibly used by some bacterial groups as nitrogen source.
<i>NH4_out</i>	mg N·L <sup>-1</sup>	Ammonium (NH <sub>4</sub> <sup>+</sup> ) in the outflow. AOB and AMX use NH <sub>4</sub> <sup>+</sup> as electron donors. It is also used by several bacterial groups as nitrogen source.
<i>Ntot_out</i>	mg N·L <sup>-1</sup>	Sum of NH <sub>4_out</sub> , NO <sub>2_out</sub> , NO <sub>3_out</sub>

<i>Cycle</i>	h	Cycle duration. Determined by pH <sub>set</sub> , Q <sub>air</sub> and the rate of nitrification, which lowers the pH value, and the extent of denitrification and anammox activity, which tend to increase the pH value. The faster the AOB work, the shorter the cycle will become.
<i>O<sub>2</sub></i>	mg O·L <sup>-1</sup>	Oxygen concentration in the reactor liquid. A critical parameter for AMX, which are inhibited by high oxygen concentrations. Higher O <sub>2</sub> concentrations foster AOB, AHB and NOB.
<i>N<sub>2</sub>O<sub>ind</sub></i>	mg O·L <sup>-1</sup>	N <sub>2</sub> O indicator. The indicator is derived from the increase of the O <sub>2</sub> baseline over a cycle. The O <sub>2</sub> electrode has a linear cross-sensitivity for N <sub>2</sub> O, and the increase of the baseline (in mgO <sub>2</sub> L <sup>-1</sup> ) is interpreted as an indication of N <sub>2</sub> O accumulation. Since these values have not been calibrated they are given in oxygen concentration equivalents.
<i>V<sub>air</sub></i>	L	Air volume. Total volume of air used for aeration during one cycle. V <sub>air</sub> depends on the oxygen demand of the bacteria and the oxygen transfer from the gas phase into the liquid phase, and the cycle duration. The oxygen transfer is determined by Q <sub>air</sub> .
<i>SA</i>	d	Sludge Age. It is determined as ratio between the suspended solids in the reactor and the outflow of suspended solids. To sustain a certain bacterial population in the reactor, SA has to be as least as high as the inverse of the net growth rate of the slowest bacterial group.

**Table S4** Performance indicators. Variables in italics indicate parameters used in the statistical analysis.

<b>Parameter</b>	<b>Unit</b>	<b>Description</b>
<i>NER</i>	mg N·L <sup>-1</sup> ·d <sup>-1</sup>	The key parameter from an operator point of view is the amount of nitrogen eliminated from the system (mainly as N <sub>2</sub> ) per unit volume and unit time
<i>NEE</i>	%	The proportion of Nitrogen eliminated at the end of a cycle relative to the inflow concentration.

## S2 Time series plot

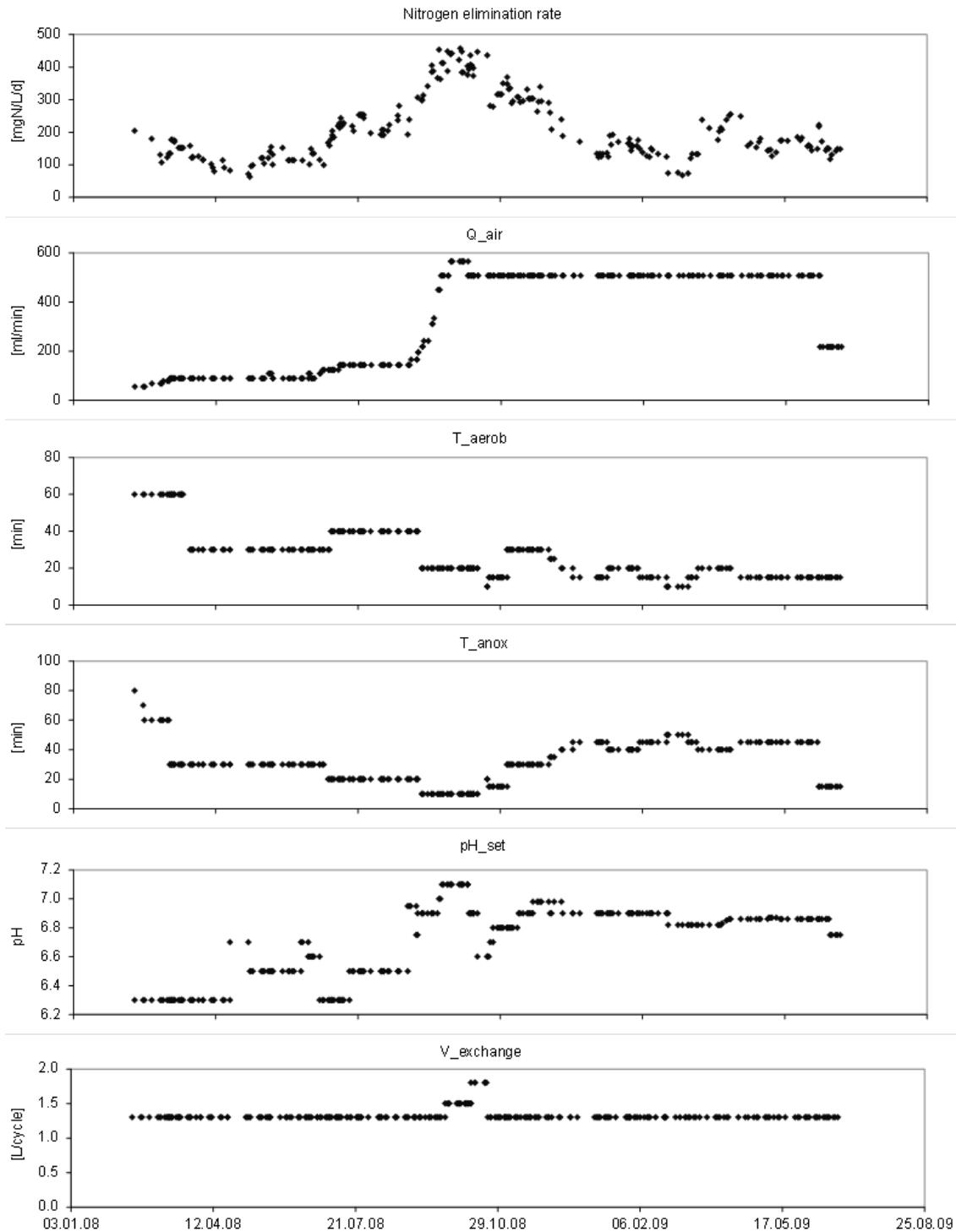


**Figure S1** Time series plots of nitrogen elimination rate (top panel) and changes in operating parameters during the observation period. Q<sub>air</sub>: Flux of air supplied during aerobic phases. T<sub>aerob</sub>, T<sub>anaerob</sub>: duration of aerobic and anaerobic phases, respectively. pH<sub>set</sub>: pH set-point. V<sub>exchange</sub>: exchange volume. Detailed explanations of parameters are given in the Supporting Information S1.

### S3 Sample labels

Table S5 Sample labels.

Sampling date	Sample label
25-09-07	A
21-11-07	B
15-04-08	C
13-05-08	D
15-07-08	E
11-08-08	F
09-10-08	G
12-11-08	H
18-12-08	I
15-01-09	K
19-02-09	L
19-03-09	M
15-04-09	N



## **CHAPTER 2**

### **Observability of anammox activity in single-stage nitritation/anammox reactors using mass balances**

Sarina Schielke-Jenni, Kris Villez, Eberhard Morgenroth, Kai M. Udert

*Submitted*

# Observability of anammox activity in single-stage nitrification/anammox reactors using mass balances

Sarina Schielke-Jenni<sup>1</sup>, Kris Villez<sup>1</sup>, Eberhard Morgenroth<sup>1,2</sup>, Kai M. Udert<sup>1</sup>

*1: Eawag, Swiss Federal Institute for Aquatic Science and Technology, 8600 Dübendorf, Switzerland*

*2: Institute of Environmental Engineering, ETH Zurich, 8093 Zurich, Switzerland*

## ABSTRACT

In nitrification/anammox reactors, several bacterial groups contribute to the overall nitrogen conversion. Knowing the activity of the main bacterial groups, especially of anaerobic ammonium-oxidising bacteria (AMX) is extremely helpful to understand the process and optimize its operation. A common approach to determine bacterial activities is based on mass balances of dissolved compounds such as ammonium, nitrite and nitrate. Besides AMX, aerobic ammonium-oxidising bacteria (AOB) and nitrite-oxidising bacteria (NOB) are considered in such mass balances. The activity of heterotrophic bacteria (HET) is usually neglected, although heterotrophic denitrification can contribute substantially to nitrogen removal, even in wastewater with low contents of organic substrate. To test the applicability of mass balancing for the determination of bacterial activities, we set up and solved mass balances of different degrees of complexity. The linear equation system which consists of catabolic reactions alone is underdetermined and does not allow estimation of any of the considered bacterial reaction rates. The alternative equation system which consists of balances according to the activated sludge model stoichiometry is also under-determined. When kinetic rate expressions are included in the mass balances, it is possible to compute the concentrations of the bacterial groups, but the estimation uncertainty is far too high for practical purposes. The high standard deviations of the calculated bacterial concentrations can be significantly reduced by adding an additional mass balance for the total biomass. The required number of measurements to achieve an acceptable accuracy of the AMX concentration is still far too high though for practical purposes. In our example, about 600 independent conversion rate measurements for each balanced compound will give a 50% standard deviation for the AMX concentration. To conclude, mass balances including kinetics theoretically allow the observation of the bacterial activities in nitrification/anammox reactors with high HET activity. However, the required precision of the calculated conversion rates, the uncertainty of stoichiometric and kinetic parameters and reactor dynamics (unsteady conditions) makes mass balances unsuitable for practical estimation of AMX activity. It is well possible that mass balances will be a suitable tool in the future, thanks to high frequency sensor measurements.

## INTRODUCTION

Nitrogen removal using the nitrification/anammox process is a cost efficient alternative to conventional nitrification/denitrification, thanks to reductions in the requirements for oxygen and organic substrates in comparison to conventional nitrification/denitrification processes. However, maintaining a high activity of anammox bacteria (AMX) can be challenging (Joss et al., 2011). Especially in reactors with high ratios of biodegradable organic carbon to nitrogen (COD/N) decreasing AMX activity might not be noticed in time, because heterotrophic bacteria (HET) take over a considerable part of the nitrogen removal from AMX (Jenni et al., 2014). Several analytical and experimental methods exist for the reliable determination of AMX concentrations or activities as Podmirseg et al. (2015) have shown recently. However, all of these methods require equipment, which is usually not available in conventional wastewater treatment plants. It would be desirable to be able to calculate the activities of the involved bacterial groups from regularly measured variables for performance monitoring such as the concentrations of for example ammonium and nitrite.

Mass balances for nitrogen compounds, i.e., ammonium, nitrite and nitrate, have frequently been used to calculate the activities of aerobic ammonium-oxidising bacteria (AOB), nitrite-oxidising bacteria (NOB) and AMX in nitrification/anammox reactors (for example Daverey et al., 2012; Pellicer-Nàcher et al., 2010). However, as elaborated by Mutlu et al. (2013), the calculation of AOB, NOB and AMX activity with such mass balances is coupled to the assumption that the activity of HET is negligible. Quite frequently, this assumption is incorrect. On one hand, it has been shown experimentally that even in biofilm systems without organic carbon in the influent, up to 50% of the biomass can be heterotrophic, supported by microbial decay products (Kindaichi et al., 2004; Okabe et al., 2005). On the other hand, wastewater almost always contains biodegradable organic matter. Digester supernatant, which is the most common influent for a nitrification/anammox system has biodegradable organic carbon to nitrogen (COD/N) ratios in the range of 0.2 to 0.5 g COD·g N<sup>-1</sup> (Joss et al., 2009; van der Star et al., 2007; Wett 2007). Some wastewaters even have elevated COD/N ratios in the range of 1 to 1.5 g COD·g N<sup>-1</sup>, which is still not high enough for complete nitrogen removal via heterotrophic denitrification. Examples are stored urine with a theoretical COD/N ratio between 1 g COD·g N<sup>-1</sup> (Udert et al., 2006) and 1.5 g COD·g N<sup>-1</sup> (Udert et al., 2008). COD/N ratios of approximately 1 g COD·g N<sup>-1</sup> are also expected in the recently discussed integration of anammox into mainstream wastewater treatment (De Clippeleir et al., 2013; Winkler et al., 2012a).

To our knowledge, only three studies included COD consumption in their mass balances to assess the bacterial activities in a nitrification/anammox process (Jia et al., 2012; Lan et al., 2011; Wang et al., 2010). These three studies used four equations representing the conversion of ammonium, nitrite, nitrate and COD. As only four unknowns can be determined with four inde-

pendent equations, the authors considered only the activities of AOB, NOB, AMX and nitrate reduction by HET. However, in single-stage nitrification/anammox reactors, heterotrophic consumption of oxygen and nitrite is not negligible. For one thing, the yield of HET growth with oxygen is higher than with nitrite and nitrate and therefore, in the presence of all three electron acceptors, HET might prefer oxygen over nitrate and nitrite. Secondly, especially in the presence of high amounts of biodegradable organic matter, HET are able to take over a substantial part of the nitrite removal from AMX (Jenni et al. 2014).

The goal of this study is to test whether mass balances with commonly measured compounds (for example ammonium and nitrite), can be used to observe the six main bacterial activities in a single-stage nitrification/anammox reactor: aerobic ammonium oxidation by AOB, nitrite oxidation by NOB, anaerobic ammonium oxidation by AMX, heterotrophic oxygen reduction, heterotrophic nitrite reduction and heterotrophic nitrate reduction. Mass balances with increasing complexity are analyzed starting with catabolic reactions only and ending with a stoichiometric matrix which accounts for information on both catabolic and anabolic reactions, microbial kinetic rate functions and a balance for biomass. For all resulting mass balances, both structural and practical observability of the bacterial activities are evaluated.

## **MATERIAL AND METHODS**

### **Definitions**

In this chapter, we use the following definitions:

Parameters: Parameters characterize the chemical, physical or biological processes and are assumed to be constant for a given system. Examples for biological processes are stoichiometric and kinetic constants such as the yield or the maximum growth rate. The parameters were taken from literature.

State variables: In this study, state variables are compounds, which are converted in the chemical, physical and biological processes. Examples are the ammonia concentration or the biomass concentration. In theory, state variables can be determined by analytical measurements.

Conversion rates ( $r_{Ci}$ ) describe the conversion of a state variable per time unit. A net conversion rates describe the overall conversion of a state variable by all bacterial processes.

Bacterial reaction rates ( $r_{Ri}$ ) quantify bacterial reactions ( $R_i$ ) such as catabolic or anabolic reactions or, in terms of the activated sludge model (ASM, Henze et al. 2000), growth and decay processes.

Bacterial activities: The activity of a bacterial group is defined as the conversion of a characteristic compound by this bacterial group. The characteristic compound can be a substrate, e.g. ammonia in the case of AMX or the concentration of the respective bacterial group.

**Structural observability:** In a linear equation system, all unknowns are structurally observable if the number of independent equations is equal to or higher than the number of unknowns. An equal number means that the equation system is determined; a larger number means that it is over-determined. Mathematically, the number of unknowns that can be estimated is evaluated by calculating the rank of the balancing matrix  $A$  (see equation 6). This rank will equal the number of unknowns, if they are structural observable.

**Practical observability:** To be practically observable, the unknowns have to fulfil two more conditions besides being structurally observable: first, the set of parameters must allow the calculation of meaningful values for the unknowns (e.g. positive concentrations of biomasses). In extreme cases, empirically determined parameters do not allow the estimation of all unknowns, although the unknowns are structurally identifiable. This can occur for example, if the particular choice for yield parameters causes one balance equation to become a linear combination of two or more of the remaining balancing equations. Second, the precision of the calculated values for the estimates must be sufficiently precise to be of practical use.

### Choice of state variables

The considered mass balances involve seven compounds: ammonium ( $\text{NH}_4^+$ ), nitrite ( $\text{NO}_2^-$ ), nitrate ( $\text{NO}_3^-$ ), oxygen ( $\text{O}_2$ ), dissolved organic substances (measured as chemical oxygen demand, COD), protons ( $\text{H}^+$ ) and total inorganic carbon (TIC). These compounds and their net conversion rates can be determined on large wastewater treatment without highly sophisticated analytical methods. Most of these compounds and their conversion rates are directly accessible with measurements:  $\text{NH}_4^+$ ,  $\text{NO}_2^-$ ,  $\text{NO}_3^-$ ,  $\text{O}_2$ , and organic substances. The  $\text{H}^+$  conversion rate and the concentration and conversion rate of TIC can be calculated from alkalinity measurements, pH values and estimated of the  $\text{CO}_2$  stripping (equation 2). It should be noted that in more highly concentrated wastewaters (for example urine) additional bases such as phosphate species or free ammonia need to be measured and accounted for. To simplify the mass balance for dissolved biodegradable organic substances, we assume that all organic substances are degraded by bacteria. We choose acetate ( $\text{C}_2\text{H}_3\text{O}_2^-$ , abbreviated as Ac) to represent the organic compounds.

### Determining the net conversion rates

We assumed that measurements are taken from an ideally stirred continuous flow reactor with biomass retention in which all state variables are at their steady state values. For dissolved compounds, which have no gas phase exchange the net conversion rate can be calculated as

$$r_{S_i} = \frac{Q}{V} \cdot (S_i - S_{i,in}) \quad (1)$$

where  $Q$  is the flow rate ( $\text{m}^3 \cdot \text{d}^{-1}$ ),  $V$  is the reactor volume ( $\text{m}^3$ ),  $S_i$  is the concentration of the dissolved compound  $i$  ( $\text{g i} \cdot \text{m}^{-3}$ ) in the reactor, and  $S_{i,in}$  is the influent concentration of the dissolved compound  $i$  ( $\text{g i} \cdot \text{m}^{-3}$ ).

Volatile compounds, such as  $\text{O}_2$  and  $\text{CO}_2$ , are influenced by gas exchange processes. In this case, the net conversion rate  $r_{S_i}$  becomes

$$r_{S_i} = \frac{Q}{V} \cdot (S_i - S_{i,in}) - r_{i,gas} \quad (2)$$

with

$$r_{i,gas} = (S_{i,G} - H_i \cdot S_i) \cdot \frac{Q_{air}}{V} \cdot \left( 1 - \exp\left(-\frac{K_L a_i \cdot V}{H_i \cdot Q_{air}}\right) \right) \quad (3)$$

where  $H_i$  is the Henry coefficient of compound  $i$  ( $\text{g i} \cdot \text{m}^{-3}_{\text{gas}} / \text{g i} \cdot \text{m}^{-3}_{\text{liquid}}$ ),  $S_{i,G}$  is the concentration of compound  $i$  in the gas used for aeration ( $\text{g i} \cdot \text{m}^{-3}$ ),  $Q_{air}$  is the aeration rate ( $\text{m}^3 \cdot \text{d}^{-1}$ ) and  $K_L a_i$  is the mass transfer rate constant for compound  $i$  ( $\text{d}^{-1}$ ).

Net conversion rates can also be given for particulate compounds such as bacteria and inert biomass:

$$r_{X_j} = \frac{Q}{V} \cdot (X_{j,eff} - X_{j,in}) \quad (4)$$

where  $X_{j,in}$  is the influent concentration of bacteria type  $j$  ( $\text{g COD} \cdot \text{m}^{-3}$ ), and  $X_{j,eff}$  is the concentration of bacteria type  $j$  in the reactor ( $\text{g COD} \cdot \text{m}^{-3}$ ). In this study, we assumed that no particulate material enters the reactor with the influent, so that  $r_{X_j} = \frac{Q}{V} \cdot X_{j,eff}$  for all bacteria and inert biomass.

### Setting up the mass balances

In general, mass balancing equations for a system with  $n$  compounds and  $m$  relevant bacterial reactions ( $R$ ) result in an equation system with the following structure:

$$\begin{pmatrix} v_{i,j} & \cdots & v_{i,m} \\ \vdots & \ddots & \vdots \\ v_{n,j} & \cdots & v_{n,m} \end{pmatrix} \cdot \begin{pmatrix} r_{Rj} \\ \vdots \\ r_{Rm} \end{pmatrix} = \begin{pmatrix} r_{Ci} \\ \vdots \\ r_{Cn} \end{pmatrix} \quad (5)$$

where  $v_{i,j}$  is the stoichiometric coefficient of compound  $i$  in the bacterial reaction  $Rj$ ,  $r_{Rj}$  is the unknown reaction rate of reaction  $Rj$  and  $r_{Ci}$  is the measured net conversion rate of compound  $i$ . In most cases,  $C_i$  describes a dissolved compound but it can also be used for biomass.

Equation 5 can also be written in matrix notation as

$$\mathbf{A} \cdot \mathbf{r}_R = \mathbf{r}_C \quad (6)$$

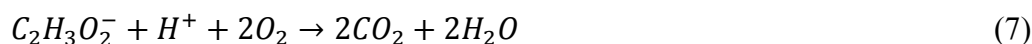
where  $\mathbf{A}$  is the matrix of the stoichiometric coefficients as shown in equation 5,  $\mathbf{r}_R$  is the vector of the biomass reaction rates and  $\mathbf{r}_C$  is the vector of the net conversion rates. Generally,  $\mathbf{A}$  is also called the balancing matrix.

### Mass balances with catabolic reactions only (equation system 1)

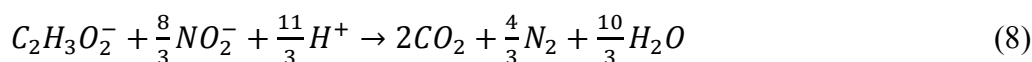
In the first equation system, we assumed that biomass growth and biomass decay are in equilibrium and no inert biomass is produced; this means the net biomass production is zero. For such a system, the net conversion rates are mainly determined by catabolic bacterial reactions. With this approach the stoichiometric coefficients are given by the chemical sum formulae of the catabolic reactions and do not require empirically determined parameters such as yield or nitrogen content of biomass.

The six main catabolic bacterial reactions in a nitrification/anammox reactor with heterotrophic activity are:

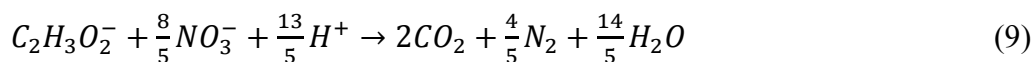
Heterotrophic COD degradation with  $O_2$ :



Heterotrophic COD degradation with  $NO_2^-$ :



Heterotrophic COD degradation with  $NO_3^-$ :



Aerobic ammonium oxidation:



Aerobic nitrite oxidation:



Anaerobic ammonium oxidation:



Nine compounds are produced or consumed in these six reactions, but two of the compounds,  $H_2O$  and  $N_2$ , are not considered in the mass balances, because the produced amounts are too low compared to the background concentration in water and air.

An overview of the equation system is given in Table 5, the complete equation system is given in the Supporting information S1. The unknowns to be calculated are the bacterial reaction rates

$r_{Rj}$  ( $d^{-1}$ ), which could be later used to calculate bacterial activities by multiplying the bacterial reaction rates with the respective stoichiometric coefficients for the substrates.

### Mass balances based on the activated sludge models (equation systems 2 to 4)

According to the activated sludge models (ASM, Henze et al., 2000) biological metabolism can be represented by growth and decay of biomass. Both processes are modelled with empirical stoichiometric coefficients. In ASM, growth inherently includes catabolic and anabolic reactions, whereas decay can be due to anabolic reactions, predation and chemical decomposition (e.g. hydrolysis). In this study, biomass decay was simulated as endogenous respiration. Median values of a literature review were used for the stoichiometric coefficients for growth and decay (Table 1). The biomass composition was assumed to be  $C_5H_7O_2N$  for HET, AOB and NOB, while for AMX, the biomass composition given by Strous et al. (1998) was used ( $CH_2O_{0.5}N_{0.15}$ ).

**Table 1** Median, minimum and maximum values for stoichiometric parameters of the combined catabolic and anabolic reaction equations. The values are compiled from Alpkvist et al. (2006)<sup>1</sup>, Fang et al. (2009)<sup>2</sup>, Gujer et al. (1999)<sup>3</sup>, Henze et al. (2000)<sup>4</sup>, Kampschreur et al. (2007)<sup>5</sup>, Koch et al. (2000a)<sup>6</sup>, Koch et al. (2000b)<sup>7</sup>, Moussa et al. (2005)<sup>8</sup>, Strous et al. (1998)<sup>9</sup>, Vangsgaard et al. (2013)<sup>10</sup>, Wiesmann (1994)<sup>11</sup> and Wyffels et al. (2004).

Symbol	Parameter	Median	Min	Max	Unit
$Y_{HET,O_2}$	Yield for growth of $X_{HET}$ with oxygen	0.630 <sup>3,4</sup>	0.609 <sup>11</sup>	0.800 <sup>7</sup>	g COD·g COD <sup>-1</sup>
$Y_{HET,NO_2}$	Yield for growth of $X_{HET}$ with nitrite	0.540 <sup>3,4</sup>	0.540 <sup>3,4</sup>	0.650 <sup>7</sup>	g COD·g COD <sup>-1</sup>
$Y_{HET,NO_3}$	Yield for growth of $X_{HET}$ with nitrate	0.540 <sup>3,4</sup>	0.540 <sup>3,4</sup>	0.650 <sup>7</sup>	g COD·g COD <sup>-1</sup>
$Y_{AOB}$	Yield for growth of $X_{AOB}$	0.210 <sup>2,6</sup>	0.150 <sup>1</sup>	0.292 <sup>10</sup>	g COD·g N <sup>-1</sup>
$Y_{NOB}$	Yield for growth of $X_{NOB}$	0.046 <sup>1,2</sup>	0.030 <sup>6</sup>	0.059 <sup>11</sup>	g COD·g N <sup>-1</sup>
$Y_{AMX}$	Yield for growth of $X_{AMX}$	0.150 <sup>6</sup>	0.124 <sup>10</sup>	0.159 <sup>9</sup>	g COD·g N <sup>-1</sup>
$i_{N,XI}$	Nitrogen content of inorganic biomass $X_I$	0.04 <sup>7</sup>	0.02 <sup>4</sup>	0.06 <sup>4</sup>	g N·g COD <sup>-1</sup>
$f_{XI}$	Fraction of biomass converted into $X_I$ during endogenous respiration	0.18 <sup>5,6,7,8</sup>	0.08 <sup>4</sup>	0.20 <sup>6,7</sup>	-

Three different equation systems were tested. In equation system 2 (Table 5) only mass balances for dissolved compounds were considered and the mass balances were set up according to equation 6: instead of the bacterial reaction rates  $r_{Rj}$ , bacterial activities ( $\alpha_{Rj}$ ) were used as unknowns



$$\mathbf{A} \cdot \mathbf{a}_R = \mathbf{r}_C \quad (13)$$

with

$$\alpha_{R,j} = r_{R,j} \cdot X_j \quad (14)$$

This approach was used because the stoichiometry of ASM is given per biomass unit. It should be noted that this approach does not require that  $X_j$  are calculated.

In equation systems 3 and 4 (Table 5), balances for the bacterial groups and inert biomass were also included (see equation 4). Most of the previously published models (for example Kaelin et al., 2009) assumed that one type of HET can use all three electron acceptors ( $O_2$ ,  $NO_2^-$ ,  $NO_3^-$ ). In reality, HET biomass will consist of a mixture of heterotrophic bacteria that can use one, two or all three electron acceptors (Van de Pas-Schoonen et al., 2005). In our study, we compared mass balances with one type of HET that can use all three electron acceptors (equation system 3) and three types of HET which specifically use only one of them (equation system 4).

An overview of the equations systems is given in Table 5. The complete equation systems are given in the Supporting information S2.

### Mass balances based on the activated sludge model including kinetics (equation system 5)

In equation system 5 (Table 5) the bacterial reaction rates are described with more detailed kinetic expressions

$$r_{Ri} = \rho_j \cdot X_j \quad (15)$$

where  $\rho_j$  is the process rate, which is the product of saturation and inhibition terms, and the maximum growth rate  $\mu_{max,j}$  ( $d^{-1}$ ) or the maximum endogenous respiration rate  $b_{max,i}$  ( $d^{-1}$ ). When kinetic constants are included, growth and endogenous respiration of each type of bacteria can be combined in one equation and merged with the stoichiometric coefficients. In this equation system, biomass concentrations instead of bacterial rates are the unknowns:

$$\mathbf{A} \cdot \mathbf{X} = \mathbf{r}_C \quad (16)$$

with the balancing matrix  $\mathbf{A}$

$$\mathbf{A} = \begin{pmatrix} v_{i,j} \cdot \rho_j & \cdots & v_{i,m} \cdot \rho_m \\ \vdots & \ddots & \vdots \\ v_{n,j} \cdot \rho_j & \cdots & v_{n,m} \cdot \rho_m \end{pmatrix} \quad (17)$$

and the vector of the biomass concentrations

$$\mathbf{X} = \begin{pmatrix} X_j \\ \vdots \\ X_m \end{pmatrix} \quad (18)$$

**Table 2** Process rates  $\rho_j$  for a nitrification/anammox system with high HET activity based on Kaelin et al. (2009) in case of AOB, NOB and HET, and Lackner et al. (2008) in case of AMX. The parameter values are given in Table 3 and the reference concentrations in Table 4.

	Process	Process rate
HET,O <sub>2</sub>	Growth	$\mu_{max,HET} \cdot \frac{S_{O_2}}{S_{O_2} + K_{O_2,HET}} \cdot \frac{S_{Ac}}{S_{Ac} + K_{Ac,HET}}$
	Endogenous respiration	$b_{max,HET} \cdot \frac{S_{O_2}}{S_{O_2} + K_{O_2,HET}}$
HET,NO <sub>2</sub>	Growth	$\mu_{max,HET} \cdot \eta_{NOX} \cdot \frac{K_{I,O_2,HET}}{K_{I,O_2,HET} + S_{O_2}} \cdot \frac{S_{NO_2}}{S_{NO_2} + K_{NO_2,HET}} \cdot \frac{S_{Ac}}{S_{Ac} + K_{Ac,HET}}$
	Endogenous respiration	$b_{max,HET} \cdot \eta_{NOX} \cdot \frac{K_{I,O_2,HET}}{K_{I,O_2,HET} + S_{O_2}} \cdot \frac{S_{NO_2}}{S_{NO_2} + K_{NO_2,HET}}$
HET,NO <sub>3</sub>	Growth	$\mu_{max,HET} \cdot \eta_{NO_3} \cdot \frac{K_{I,O_2,HET}}{K_{I,O_2,HET} + S_{O_2}} \cdot \frac{S_{NO_3}}{S_{NO_3} + K_{NO_3,HET}} \cdot \frac{S_{Sneg}}{S_{Ac} + K_{Ac,HET}}$
	Endogenous respiration	$b_{max,HET} \cdot \eta_{NOX} \cdot \frac{K_{I,O_2,HET}}{K_{I,O_2,HET} + S_{O_2}} \cdot \frac{S_{NO_3}}{S_{NO_3} + K_{NO_3,HET}}$
AOB	Growth	$\mu_{max,AOB} \cdot \frac{S_{O_2}}{S_{O_2} + K_{O_2,AOB}} \cdot \frac{S_{NH_4}}{S_{NH_4} + K_{NH_4,AOB}}$
	Endogenous respiration	$b_{max,AOB} \cdot \frac{S_{O_2}}{S_{O_2} + K_{O_2,AOB}}$
NOB	Growth	$\mu_{max,NOB} \cdot \frac{S_{O_2}}{S_{O_2} + K_{O_2,NOB}} \cdot \frac{S_{NO_2}}{S_{NO_2} + K_{NO_2,NOB}}$
	Endogenous respiration	$b_{max,NOB} \cdot \frac{S_{O_2}}{S_{O_2} + K_{O_2,NOB}}$
AMX	Growth	$\mu_{max,AMX} \cdot \frac{K_{O_2,AMX}}{K_{O_2,AMX} + S_{O_2}} \cdot \frac{S_{NH_4}}{S_{NH_4} + K_{NH_4,AMX}} \cdot \frac{S_{NO_2}}{S_{NO_2} + K_{NO_2,AMX}}$
	Endogenous respiration	$b_{max,AMX} \cdot \frac{S_{NO_2}}{S_{NO_2} + K_{NO_2,AMX}}$

The relevant process rates for a nitrification/anammox reactor with heterotrophic activity are listed in Table 2. Whenever possible we used median values based on a literature review (Table 3). While the affinity and inhibition constants of AOB, NOB and HET have been documented in several studies, the number of values is sparse for the saturation coefficient of AMX for ammonium ( $K_{NH_4,AMX}$ ) and nitrite ( $K_{NO_2,AMX}$ ) and the inhibition coefficient of AMX for oxygen ( $K_{I,O_2,AMX}$ ). Strous et al. (1999) reported that both, the affinity constants for the substrates ammonium and nitrite, lower than  $0.1 \text{ mg N}\cdot\text{L}^{-1}$ . We assumed that  $K_{NH_4,AMX}$  and  $K_{NO_2,AMX}$  were

0.1 mg N·L<sup>-1</sup> each. Strous et al. (1997a) reported that AMX were completely inhibited at 0.5% air saturation, which equals 0.036 mg O<sub>2</sub>·L<sup>-1</sup> at 30°C. In this study, we assumed that  $K_{I,O_2,AMX}$ , which corresponds to the oxygen concentration at 50%, was 0.1 mg O<sub>2</sub>·L<sup>-1</sup>. For the concentrations of O<sub>2</sub>, NO<sub>2</sub><sup>-</sup>, NO<sub>3</sub><sup>-</sup>, NH<sub>4</sub><sup>+</sup> and Ac we used simulated reference values (Table 4). The complete mass balance for equation system 5 is given in the Supporting information S3.

**Table 3** Median, minimum and maximum values of the parameters that are required for the calculation of the relevant process rates in a nitrification/anammox system with high HET activity (Table 2) at 20°C according Dapena-Mora et al. (2004)<sup>1</sup>, Guisasola et al. (2005)<sup>2</sup>, Gujer et al. (1999)<sup>3</sup>, Hao et al. (2002)<sup>4</sup>, Henze et al. (2000)<sup>5</sup>, Hunik et al. (1994)<sup>6</sup>, Jayamohan et al. (1988)<sup>7</sup>, Kaelin et al. (2009)<sup>8</sup>, Kampschreur et al. (2007)<sup>9</sup>, Koch et al. (2000a)<sup>10</sup>, Koch et al. (2000b)<sup>11</sup>, Manser et al. (2005)<sup>12</sup>, Moussa et al. (2005)<sup>13</sup>, Sánchez et al. (2001)<sup>14</sup>, Vangsgaard et al. (2013)<sup>15</sup>, Wett and Rauch (2003)<sup>16</sup>, Wiesmann (1994)<sup>17</sup> and Wyffels et al. (2004). Temperature dependency was considered as follows:  $\mu(20^\circ\text{C}) = \mu(T) \cdot \exp(\Theta_T \cdot (20-T))$ . The absolute values of the maximum endogenous respiration rates were assumed to be 10% of the maximum growth rates.

Symbol	Parameter	Median	Min	Max	Unit
$\mu_{\max,HET}$	Maximum growth rate of $X_{HET}$	3.0 <sup>11</sup>	2.0 <sup>3,5</sup>	7.2 <sup>17</sup>	d <sup>-1</sup>
$b_{\max,HET}$	Max. endogenous respiration rate of $X_{HET}$	-0.3			d <sup>-1</sup>
$\Theta_{T,HET}$	Temperature dependency of $X_{HET}$ rates	0.07 <sup>5,11</sup>			°C <sup>-1</sup>
$\eta_{NOX}$	Anoxic reduction factor for nitrite and nitrate	0.7 <sup>10</sup>	0.6 <sup>3</sup>	0.8 <sup>5</sup>	-
$K_{Ac,HET}$	Saturation coefficient of $X_{HET}$ for $S_{Ac}$	4.0 <sup>5</sup>	2.0 <sup>3,5</sup>	20 <sup>5</sup>	g COD·m <sup>-3</sup>
$K_{O_2,HET}$	Saturation coefficient of $X_{HET}$ for O <sub>2</sub>	0.20 <sup>3,5,11,16</sup>	0.08 <sup>17</sup>		g O <sub>2</sub> ·m <sup>-3</sup>
$K_{NO_2,HET}$	Saturation coefficient of $X_{HET}$ for nitrite	0.50 <sup>3,11,16</sup>	0.14 <sup>17</sup>	8.0 <sup>9</sup>	g N·m <sup>-3</sup>
$K_{NO_3,HET}$	Saturation coefficient of $X_{HET}$ for nitrate	0.50 <sup>3,5,9,11,16</sup>	0.12 <sup>17</sup>		g N·m <sup>-3</sup>
$K_{I,O_2,HET}$	Inhibition coefficient of $X_{HET}$ for O <sub>2</sub>	2.0 <sup>9</sup>			g O <sub>2</sub> ·m <sup>-3</sup>
$\mu_{\max,AOB}$	Maximum growth rate of $X_{AOB}$	0.770 <sup>17</sup>	0.481 <sup>6</sup>	1.0 <sup>10</sup>	d <sup>-1</sup>
$b_{\max,AOB}$	Max. endogenous respiration rate of $X_{AOB}$	-0.077			d <sup>-1</sup>
$\Theta_{T,AOB}$	Temperature dependency of $X_{AOB}$ rates	0.105 <sup>10</sup>	0.094 <sup>4</sup>	0.120 <sup>8</sup>	°C <sup>-1</sup>
$K_{NH_4,AOB}$	Saturation coefficient of $X_{AOB}$ for ammonium	1.00 <sup>9</sup>	0.14 <sup>12</sup>	5.00 <sup>13</sup>	g N·m <sup>-3</sup>

$K_{O_2,AOB}$	Saturation coefficient of $X_{AOB}$ for $O_2$	0.685 <sup>2,7</sup>	0.300 <sup>17</sup>	1.66 <sup>14</sup>	$g\ O_2 \cdot m^{-3}$
$\mu_{max,NOB}$	Maximum growth rate of $X_{NOB}$	0.720 <sup>4,8</sup>	0.341 <sup>15</sup>	1.338 <sup>16</sup>	$d^{-1}$
$b_{max,NOB}$	Max. endogenous respiration rate of $X_{NOB}$	-0.072			$d^{-1}$
$\Theta_{T,NOB}$	Temperature dependency of $X_{NOB}$ rates	0.070 <sup>10</sup>	0.061 <sup>4</sup>	0.078 <sup>8</sup>	$^{\circ}C^{-1}$
$K_{NO_2,NOB}$	Saturation coefficient of $X_{NOB}$ for nitrite	1.55 <sup>7,17</sup>	0.280 <sup>12</sup>	3.00 <sup>9</sup>	$g\ N \cdot m^{-3}$
$K_{O_2,NOB}$	Saturation coefficient of $X_{NOB}$ for $O_2$	1.05 <sup>9</sup>	0.470 <sup>12</sup>	3.00 <sup>14</sup>	$g\ O_2 \cdot m^{-3}$
$\mu_{max,AMX}$	Maximum growth rate of $X_{AMX}$	0.029 <sup>4,15</sup>	0.020 <sup>1</sup>	0.080 <sup>10</sup>	$d^{-1}$
$b_{max,AMX}$	Max. endogenous respiration rate of $X_{AMX}$	-0.0029			$d^{-1}$
$\Theta_{T,AMX}$	Temperature dependency of $X_{AMX}$ rates	0.093 <sup>4</sup>	0.090 <sup>4</sup>	0.096 <sup>10</sup>	$^{\circ}C^{-1}$

### Mass balances based on the activated sludge model including kinetics and a biomass balance (equation system 6)

Equation system 5 can be extended with with a biomass balance according to

$$\sum_j^m (\rho_{j,growth} + (1 - f_{XI}) \cdot \rho_{j,end\ resp}) \cdot X_j = r_{X_{tot}} \quad (19)$$

$\rho_{j,growth}$  ( $d^{-1}$ ) is the process rate for bacterial growth and  $\rho_{j,end\ resp}$  ( $d^{-1}$ ) is the process rate for endogenous respiration. The kinetic expressions for  $\rho_{j,growth}$  and  $\rho_{j,end\ resp}$  are given in Table 3.  $f_{XI}$  (-) is the fraction of biomass converted into inert biomass  $X_I$  (Table 1).  $r_{X_{tot}}$  ( $gCOD \cdot m^{-3} \cdot d^{-1}$ ) is the conversion rate for the total biomass. The term  $(1 - f_{XI})$  ensures that the production of inert biomass is included in the total production of biomass. An overview of equation system 6 is given in Table 5. The complete mass balances are given in the Supporting information S4.

### Reference data for conversion rates

Computer simulations with the software Aquasim (Reichert 1998) were used to obtain reference data for solving the mass balances. Measurements from a single-stage sequencing batch reactor with five-times diluted urine (Bürgmann et al. (2011); influent COD/N ratio 1.27  $g\ COD \cdot g\ N^{-1}$ ) were used as influent concentrations and as initial conditions (Supporting information S5). All compounds included in the model are listed in the Supporting information S6. The stoichiometric constants and the kinetic constants were the same as given in Table 1 and Table 3. Three groups of HET were introduced to represent the heterotrophic activity with oxygen, nitrite and nitrate as electron acceptors. The simulation of pH equilibria and aeration effects is described in the Supporting information S7. Long-term simulations with constant influent rates were used to

approximate concentrations at steady state. The net conversion rates and the biomass concentrations at steady state are listed in Table 4.

**Table 4** Simulated net conversion rates, biomass concentrations and compound concentrations in the reactor at steady state.

Net conversion rates			Biomass conc. [g COD·m <sup>-3</sup> ]		Comp. conc. in reactor		
$r_{S,O_2}$	[g O <sub>2</sub> ·m <sup>-3</sup> ·d <sup>-1</sup> ]	-507	$X_{HET,O_2}$	3550	$S_{NH_4}$	[g N·m <sup>-3</sup> ]	1.18
$r_{S,Ac}$	[g COD·m <sup>-3</sup> ·d <sup>-1</sup> ]	-266	$X_{HET,NO_3}$	1340	$S_{NO_2}$	[g N·m <sup>-3</sup> ]	$2.19 \cdot 10^{-2}$
$r_{S,NH_4}$	[g N·m <sup>-3</sup> ·d <sup>-1</sup> ]	-209	$X_{HET,NO_2}$	334	$S_{NO_3}$	[g N·m <sup>-3</sup> ]	$2.59 \cdot 10^{-2}$
$r_{S,NO_3}$	[g N·m <sup>-3</sup> ·d <sup>-1</sup> ]	$7.76 \cdot 10^{-3}$	$X_{AOB}$	2030	$S_{O_2}$	[g O <sub>2</sub> ·m <sup>-3</sup> ]	$7.11 \cdot 10^{-3}$
$r_{S,NO_2}$	[g N·m <sup>-3</sup> ·d <sup>-1</sup> ]	$6.58 \cdot 10^{-3}$	$X_{NOB}$	0	$S_{Ac}$	[g COD·m <sup>-3</sup> ]	$6.99 \cdot 10^{-1}$
$r_{S,H}$	[g H·m <sup>-3</sup> ·d <sup>-1</sup> ]	10.8	$X_{AMX}$	1100			
$r_{S,TIC}$	[g C·m <sup>-3</sup> ·d <sup>-1</sup> ]	61.6					
$r_{X,tot}$	[g COD·m <sup>-3</sup> ·d <sup>-1</sup> ]	104					

### Evaluating structural observability

To solve a linear equation system we need at least as many independent equations (mass balances) as unknown variables (bacterial reaction rates, bacterial activities or biomass concentrations). Independent means that none of the equations can be linearly combined and transformed to another of the available equations. Practically, the classification of the considered equation systems and observability of the unknowns is based on the evaluation of the rank of the linear equation system: the rank must be equal to the number of unknowns otherwise the linear equation system is under-determined.

When empirically determined stoichiometric parameters are used, some equations might be dependent due to a particular choice of parameter values and not due to an under-determination of the equation system for any feasible parameter value choice. In this case, the lack of observability would not be structural but only practical. To test whether the lack of observability is not only practical but also structural, we performed Monte Carlo simulations: 10,000 simulations were done with uniformly and randomly distributed parameter values in a range of  $\pm 50\%$  of the default values (median values from literature according to Table 1 and Table 3). If this test does not provide any parameter sets, which make the equation system observable, it is very likely that the lack of observability is structural. A stringent test of the structural observability would be considerably more complex (Ponzoni et al., 1999) and was considered to be unnecessary for this study. All computations were executed by means of MATLAB (R2013b, The MathWorks Inc., Natick MA, USA). The Matlab codes are given in the Supporting information S8 and S9.

### Evaluating practical observability

If the test for structural observability was successful, we tested the practical observability by estimating the theoretical standard deviations of the estimates. To this end, we assumed that the net conversion rates  $r_{Ci}$  have a standard deviation of 5 % of their steady-state value. In practice these standard deviations are due to measurement errors and can be higher than 5% so that the computed standard deviations are rather optimistic (i.e., low). In real systems, the variation is probably even larger due to imprecise parameter values. Furthermore, parameter values and analytical measurements of variables can be systematically wrong, leading to systematic estimation errors (bias). Assuming that measurement errors for the rate measurements,  $r_{Ci}$ , are drawn independently from a normal distribution with zero mean and a given standard deviation ( $\sigma_{r_{Ci}}$ ), one can compute the expected value for the bacterial concentrations  $X_j$  in equation systems 5 and 6 (Table 5) as follows (Narasimhan and Jordache, 1999):

$$\mathbf{A} \cdot \mathbf{X} = \mathbf{r}_C \quad (20)$$

$$\mathbf{X} = (\mathbf{A}^T \cdot \Sigma_{r_C}^{-1} \cdot \mathbf{A})^{-1} \cdot \mathbf{A}^T \cdot \Sigma_{r_C}^{-1} \cdot \mathbf{r}_C = \mathbf{P} \cdot \mathbf{r}_C \quad (21)$$

$$\forall k, l : k = l \Rightarrow \Sigma_{r_C}(k, l) = \sigma_{r_C}^2 \quad (22)$$

$$\forall k, l : k \neq l \Rightarrow \Sigma_{r_C}(k, l) = 0 \quad (23)$$

The variance-covariance matrix for the rate estimates is then:

$$\Sigma_{X_j} = \mathbf{P} \cdot \Sigma_{r_C} \cdot \mathbf{P}^T \quad (24)$$

With the individual standard deviations for the rate estimates computed from the variances on its diagonal, the standard deviation of the biomass estimate becomes

$$\sigma_{X_j} = \left( \Sigma_{X_j}(j, j) \right)^{1/2} \quad (25)$$

In practice, the standard deviation of the net conversion rates can be reduced by means of independent repetitions of the measurements under the same experimental conditions. The standard deviation of the average of  $r$  independent measurements can be estimated by dividing the standard deviation of a single measurement by the square root of the total number of measurements  $r$ :

$$\sigma_{X_j, r} = \sigma_{X_j} / r^{1/2} \quad (26)$$

**Table 5** Overview of the tested mass balances.

System number	System description	Number of mass balances	Number of unknowns	Rank	Rel. std. dev. of AMX conc.
1	Catabolic reactions	7 NH <sub>4</sub> , NO <sub>2</sub> , NO <sub>3</sub> , Ac, H, O <sub>2</sub> , TIC	6 $\Gamma_{\text{HET},\text{O}_2}$ , $\Gamma_{\text{HET},\text{NO}_2}$ , $\Gamma_{\text{HET},\text{NO}_3}$ , $\Gamma_{\text{AOB}}$ , $\Gamma_{\text{NOB}}$ , $\Gamma_{\text{AMX}}$	4	-
2	Catabolic and anabolic reactions, no kinetics, no bacterial conc.	7 NH <sub>4</sub> , NO <sub>2</sub> , NO <sub>3</sub> , Ac, H, O <sub>2</sub> , TIC	12 $\alpha_{\text{HET},\text{O}_2,\text{growth}}$ , $\alpha_{\text{HET},\text{O}_2,\text{end.resp}}$ , $\alpha_{\text{HET},\text{NO}_2,\text{growth}}$ , $\alpha_{\text{HET},\text{NO}_2,\text{end.resp}}$ , $\alpha_{\text{HET},\text{NO}_3,\text{growth}}$ , $\alpha_{\text{HET},\text{NO}_3,\text{end.resp}}$ , $\alpha_{\text{AOB},\text{growth}}$ , $\alpha_{\text{AOB},\text{end.resp}}$ , $\alpha_{\text{NOB},\text{growth}}$ , $\alpha_{\text{NOB},\text{end.resp}}$ , $\alpha_{\text{AMX},\text{growth}}$ , $\alpha_{\text{AMX},\text{end.resp}}$	6	-
3	Catabolic and anabolic reactions, no kinetics, 1 type of HET	12 NH <sub>4</sub> , NO <sub>2</sub> , NO <sub>3</sub> , Ac, H, O <sub>2</sub> , TIC, X <sub>I</sub> , X <sub>HET</sub> , X <sub>AOB</sub> , X <sub>NOB</sub> , X <sub>AMX</sub>	12 $\alpha_{\text{HET},\text{O}_2,\text{growth}}$ , $\alpha_{\text{HET},\text{O}_2,\text{end.resp}}$ , $\alpha_{\text{HET},\text{NO}_2,\text{growth}}$ , $\alpha_{\text{HET},\text{NO}_2,\text{end.resp}}$ , $\alpha_{\text{HET},\text{NO}_3,\text{growth}}$ , $\alpha_{\text{HET},\text{NO}_3,\text{end.resp}}$ , $\alpha_{\text{AOB},\text{growth}}$ , $\alpha_{\text{AOB},\text{end.resp}}$ , $\alpha_{\text{NOB},\text{growth}}$ , $\alpha_{\text{NOB},\text{end.resp}}$ , $\alpha_{\text{AMX},\text{growth}}$ , $\alpha_{\text{AMX},\text{end.resp}}$	9	-
4	Catabolic and anabolic reactions, no kinetics, 3 types of HET	14 NH <sub>4</sub> , NO <sub>2</sub> , NO <sub>3</sub> , Ac, H, O <sub>2</sub> , TIC, X <sub>I</sub> , X <sub>HET,O2</sub> , X <sub>HET,NO2</sub> , X <sub>HET,NO3</sub> , X <sub>AOB</sub> , X <sub>NOB</sub> , X <sub>AMX</sub>	12 $\alpha_{\text{HET},\text{O}_2,\text{growth}}$ , $\alpha_{\text{HET},\text{O}_2,\text{end.resp}}$ , $\alpha_{\text{HET},\text{NO}_2,\text{growth}}$ , $\alpha_{\text{HET},\text{NO}_2,\text{end.resp}}$ , $\alpha_{\text{HET},\text{NO}_3,\text{growth}}$ , $\alpha_{\text{HET},\text{NO}_3,\text{end.resp}}$ , $\alpha_{\text{AOB},\text{growth}}$ , $\alpha_{\text{AOB},\text{end.resp}}$ , $\alpha_{\text{NOB},\text{growth}}$ , $\alpha_{\text{NOB},\text{end.resp}}$ , $\alpha_{\text{AMX},\text{growth}}$ , $\alpha_{\text{AMX},\text{end.resp}}$	11	-
5	Catabolic and anabolic reactions, with kinetics, 3 types of HET	7 NH <sub>4</sub> , NO <sub>2</sub> , NO <sub>3</sub> , Ac, H, O <sub>2</sub> , TIC	6 X <sub>HET,O2</sub> , X <sub>HET,NO2</sub> , X <sub>HET,NO3</sub> , X <sub>AOB</sub> , X <sub>NOB</sub> , X <sub>AMX</sub>	6	5,280%
6	Catabolic and anabolic reactions, with kinetics and sludge loss, 3 types of HET	8 NH <sub>4</sub> , NO <sub>2</sub> , NO <sub>3</sub> , Ac, H, O <sub>2</sub> , TIC, X <sub>tot</sub>	6 X <sub>HET,O2</sub> , X <sub>HET,NO2</sub> , X <sub>HET,NO3</sub> , X <sub>AOB</sub> , X <sub>NOB</sub> , X <sub>AMX</sub>	6	1,210%

## RESULTS

The setup of the mass balances and the main results are summarised in Table 5. The results will be explained in more detail in the following paragraphs.

### Mass balances based on catabolic reactions only

Catabolic reactions alone do not allow determining the activities of the different bacterial groups. The linear system consists of seven equations but the rank of the matrix is only four (Table 5, system 1), which means that three out of the seven equations can be expressed as linear combinations of four independent equations. The lack of observability is thus structural in

the sense that it is impossible to conceive of any experiment, even idealized, that permits simultaneous estimation of all reaction rates. In contrast to ASM reactions (see "Mass balances based on the activated sludge model"), the stoichiometric coefficients are known constants that follow directly from the definition of the considered chemical reactions. As such, this result is universal in the sense that it does not depend on any adjustable model parameter.

Even if the linear equation system for the catabolic reactions were solvable, the resulting bacterial reaction rates would most probably not be accurate due to some coarse simplifications. The basic assumption that biomass growth and decay are in equilibrium is practically never the case in a wastewater treatment plant, there is always some biomass loss with the effluent or some biomass withdrawal. Furthermore, the catabolic reaction for AMX does not consider an important contribution of AMX to nitrate production: in order to generate the required energy for carbon fixation, AMX oxidise nitrite to nitrate, accounting for 11% of the total N conversion by AMX (Strous et al. 1998).

### **Mass balances based on the activated sludge model**

When considering microbial metabolism according to ASM the number of unknowns increases to twelve: for each of the six bacterial groups, two bacterial rates - growth and endogenous respiration - are included. In the equation system there are now more unknowns (twelve) than mass balances (seven) which means no unique solution exists under any scenario (Table 5, system 2). Concentrations for NOB, AOB, AMX, HET and for inert biomass can be included to provide additional measurements and associated balancing equations. Despite the inclusion of such measurements which are hard to obtain in practice, it remains impossible to determine the microbial activities (Table 5, system 3). This is also the case when the HET are divided in three subgroups, which use oxygen, nitrite or nitrate as electron acceptors (Table 5, system 4). The same classification was obtained for 10'000 random sets for the parameter values. This suggests that the lack of observability is most probably structural and not due to a particular combination of estimated parameters.

Even if it were possible to compute values for the considered respiration rates, it is worth considering that empirical stoichiometric coefficients have to be included in the mass balances (Table 1). These are considered to be known exactly although such parameters are estimated in practice. This means that the balancing equations as described here are subject to additional unaccounted uncertainty in practice.

### **Mass balances based on the activated sludge model including kinetics**

When the kinetics are known, one can combine the growth and endogenous respiration for each type of bacteria into a single net growth rate. This reduces the number of unknowns from



twelve to six and allows determining the biomass concentrations and thereby the bacterial activities (Table 5, system 5). In this case, and for the first time in this study, the balancing matrix  $A$  is full-rank. This means that the concentrations of AOB, NOB, AMX and the hypothetical concentrations of the three groups of HET can be estimated (structural observability). The activities for growth and endogenous respiration can later be calculated with the assumed kinetic expressions.

Although the biomass concentrations can be determined, the uncertainty of the resulting values is immense when using a single set of rate measurements (Table 6). Assuming that all necessary stoichiometric and kinetic parameters (Table 1 and Table 3) are known exactly, the relative standard deviations of the bacterial activities equal the relative standard deviations of the calculated biomass concentrations and only depend on the measurement accuracy of the net conversion rates. Even if a low standard deviation of 5% is assumed for the conversion rates, the resulting standard deviations are extremely high: the relative standard deviation for AMX is 5,280% (Table 6). This value can be reduced, if a mass balance for the biomass is included (Table 5, equation system 6). In our example, the relative standard deviation becomes 1,210%. However, this standard deviation is still unrealistically high for practical purposes.

**Table 6** Calculated concentrations and standard deviations of the six main types of bacteria in a nitrification/anammox reactor with high HET activity with mass balances based on the activated sludge model including kinetics (left) and including both kinetics and a biomass balance (right).

	including kinetics			including kinetics and biomass balance		
	mg COD·L <sup>-1</sup> concentration	mg COD·L <sup>-1</sup> st.dev.	% st.dev.	mg COD·L <sup>-1</sup> concentration	mg COD·L <sup>-1</sup> st.dev.	% st.dev.
$X_{H,O_2}$	3,470	326,000	9,420	3,510	74,500	2,120
$X_{H,NO_3}$	1,290	192,000	14,900	1,310	47,100	3,590
$X_{H,NO_2}$	483	553,000	115,000	413	130,000	31,600
$X_{AOB}$	2,040	74,000	3,620	2,030	17,200	846
$X_{NOB}$	-181	626,000	345,000	-103	159,000	154,000
$X_{AMX}$	1,080	57,200	5,280	1,090	13,300	1,210

In practice, the standard deviations of the net conversion rates can be reduced with multiple measurements. As an example, the required number of measurements and the corresponding standard deviation of the net conversion rate to reach a certain standard deviation for the calculated biomass concentration of AMX are listed in Table 7. To achieve a relative standard deviation of 50% for the AMX concentration, about 600 measurements of the net conversion rates would be necessary under the same experimental conditions. By far, this number is still too

high for measurements based on conventional grab sampling. Therefore, we conclude that neither AMX activity nor any other of the considered bacterial activities is practically observable with mass balances and conventional grab sampling.

**Table 7** Required number of measurements and the corresponding standard deviation of the net conversion rate to reach a certain standard deviation for the calculated biomass concentration of anammox bacteria with mass balances based on the activated sludge model including both kinetics and a biomass balance.

<b>Desired % st.dev. of <math>X_{AMX}</math></b>	<b>Required % st.dev. of the net conversion rates</b>	<b>Required # of measurements if % st.dev. of one measurement is 5 %</b>
50	0.205	595
40	0.164	929
30	0.123	1'651
20	0.082	3'713
10	0.041	14'851

## DISCUSSION

### **Constraints are necessary for the structural observability of the linear equation system**

By including constraints, i.e., kinetic expressions, we achieved complete structural observability of all unknown parameters (Table 5, systems 5 and 6). This approach is similar to the flux balance analysis, which is a common method to analyse the metabolic networks of single microorganisms (Edward et al., 2002). To overcome the lack of detailed information about the metabolism of a bacterial cell, the metabolic network is represented by a stoichiometric matrix describing the relation of conversion rates and metabolic reactions at steady state. The resulting equation system has essentially the same form as our equation systems (Noorman et al., 1991) and it is usually not observable because the number of unknown reactions is larger than the number of compounds (Orth et al., 2010). Constraints are introduced, e.g., measured fluxes or boundaries for certain rates, to allow quantitative predictions. Concentrations, e.g., of metabolites, cannot be predicted, because accurate kinetic parameters are usually not available (Orth et al., 2010). Here is the difference to our approach: our systems do not consist of single cells but of bacterial populations, for which macroscopic kinetic data are available. By including the kinetic data (systems 5 and 6 in Table 5), all unknown variables, i.e. bacterial concentrations, are observable.

Including kinetics makes the linear equation system structurally observable but also affects the accuracy of the final result. Systematic errors can be included in the mass balance. As the data

compilation in Table 3 shows, literature values for kinetic parameters vary widely and the chosen kinetic expressions might not include critical influences such as inhibition of AMX or AOB. However, unexpected inhibition effects by unknown compounds are a frequent problem in wastewater treatment plants (Lackner et al., 2014).

It would be desirable to achieve observability of all reaction rates by increasing the number of independent mass balance equations and not using kinetics. In theory, at least two additional mass balances could be included in our systems: one for  $\text{H}_2\text{O}$  and one for  $\text{N}_2$ . Unfortunately, no conversion rates for the two compounds can be measured, because their background concentrations are far too high. Furthermore, the two additional equations are not independent from the others (data not shown), so that the rank of the previous mass balances does not increase. Another option would be to include side-products such as nitrous oxide ( $\text{N}_2\text{O}$ ) or nitric oxide ( $\text{NO}$ ). Both compounds can be measured in the off-gas (Schreiber et al., 2012) or with sensors directly in the water (Jenni et al., 2012). The isotopic signatures of  $\text{N}_2\text{O}$  even allow the differentiation of the production pathway (Wunderlin et al., 2012b). However, both compounds are side-products, which only occur under certain circumstances. Additional reaction rates would have to be included to balance those compounds, so that structural observability of the bacterial activities would still not be achieved without introducing kinetics. Based on these considerations, including constraints (e.g. as kinetic expressions) seems to be the only way to achieve structural observability of the bacterial activities with the linear equation systems in our study.

### **Additional mass balances could be used to achieve practical observability**

Our study showed that not only increasing the number of measurements but also increasing the number of equations can improve the precision of the biomass concentrations. Adding one more equation (biomass balance) to equation 5 led to a substantial reduction of the variability of the estimated biomass concentrations in equation 6. This is due to the fact that some conversion rates are redundant and could also be calculated by combining other mass balances. In other words, some conversion rates are balanceable (van der Heijden et al., 1994). In practical systems, such redundancy can be used to detect and remove systematic balancing errors (gross error detection) and to reduce random measurement errors in measured data. This method is also known as data reconciliation (Noorman et al., 1996).

Data reconciliation is a common procedure for industrial processes. They have been proposed for wastewater treatment as well (Meijer et al. 2002), but are not commonly applied. This is partly due the fact that municipal wastewater treatment plants usually do not comply with certain requirements of data reconciliation: most of the processes are not at steady state, the variances of process variables are not known and some measurements often have gross errors (Spindler, 2014). Recently, methods have been adapted for wastewater treatment and now allow

the identification of periods with gross measurement errors, e.g. based on the CUSUM statistic for linear mass balancing errors (Spinder and Vanrolleghem, 2012) or based on bilinear mass balancing equations (Villez et al, 2013). Furthermore, the ability to detect measurement errors via mass balancing can be ensured by optimising the location of sampling (Villez et al., 2015). Long periods at quasi steady state conditions and without gross errors can provide a sufficiently high number of measurements to allow the calculation of precise biomass concentrations (Table 7). The result would be an average biomass concentration during an extended period of time.

Our study showed that not only increasing the number of measurements but also increasing the number of equations can improve the precision of the biomass concentrations. Adding one more equation (biomass balance) led to a substantial reduction of the variability of the final result.

### **Observing dynamics and separating bacterial processes can provide additional information**

The approach used in this study is based on two basic requirements for reactor operation: first, the soluble and particulate compounds are in steady state, and second, all processes occur concomitantly in one single reactor. However, reactors with higher dynamics, such as sequencing batch reactors, and separating the aerobic and the anoxic process steps in two different reactors, could be more suitable to determine the bacterial activities. Short-term changes from single-stage operation to a cyclic multi-stage operation could also be used as an online experimental design method to obtain observability at regular time intervals.

Dynamic measurements allow for more information about the processes, but a prerequisite for practical applications is the use of sensors. If online measurements are available, not only the actual concentrations but also mathematical derivatives such as the oxygen consumption or the change of the oxygen consumption can be used to determine unknown parameters (Dochain et al., 1995). Oxygen and ammonia sensors have been applied successfully for online observation of AMX activity in large scale wastewater treatment plants (Joss et al., 2009). Nitrite sensors would further simplify the observation of AMX activity, but reliable nitrite sensors, especially for high nitrite concentrations, still have to be developed (Joss et al., 2011; Mašić and Villez, 2014).

By operating the nitrification/anammox process in two reactors (van Dongen et al., 2001) or during two phases in the same reactor (Joss et al., 2011), aerobic processes such as the activities of AOB, NOB and aerobic HET could be separated from anoxic activities such as AMX and heterotrophic denitrification. While such an approach would greatly simplify the quantification of AMX activity, operational problems such as N<sub>2</sub>O production (Kampschreur et al., 2008a), high NOB activity (Fux et al., 2004) or inhibition of AMX can occur due to nitrite overloading (Joss et al., 2009). For such reasons, by far most full scale nitrification/anammox reactors are operated

as single-stage systems (Lackner et al., 2014), although two-stage systems would be more suitable for observing the AMX activity. However, in single-stage systems short phases with alternating aeration could be introduced to determine the AMX activity.

## CONCLUSIONS

- In theory mass balances can be used to determine the AMX activity in a nitrification/anammox reactor, but the requirements are challenging. Based on our study the following three conditions have to be fulfilled:
  - Accurate values for the stoichiometric and the kinetic parameters are available for all considered reactions.
  - The process can be assumed to operate in steady state.
  - A large number of reliable measurements are available for flow rates, COD, nitrite, nitrate, ammonium, alkalinity, TIC, pH and oxygen.
- To achieve a satisfying precision for the estimated AMX activity, an immense number of independent measurements are required. In our example, the conversion rates would need to have standard deviation as low as 0.2% to achieve a precision of 50% for the AMX concentration. This high precision for the conversion rates is practically unachievable with grab samples and laboratory measurements. In the future, high-frequency measurements with sensors and data reconciliation methods could allow for such a high precision of conversion rates.

## ACKNOWLEDGEMENTS

This work was financed by the Swiss National Science Foundation under grant 200020\_144498 (Decentralized urine treatment with the nitrification/anammox process, DUNOX, Part 2).



**SUPPORTING INFORMATION**

**FOR CHAPTER 2**

**Observability of anammox activity in single-stage  
nitritation/anammox reactors using mass balances**

Sarina Schielke-Jenni, Kris Villez, Eberhard Morgenroth, Kai M. Udert

*Submitted*

### S1 Mass balances with catabolic equations only

The equation system for mass balances with catabolic equations only is given in equation S1.

$$\begin{pmatrix} 0 & 0 & 0 & -1 & 0 & -1 \\ 0 & -8/3 & 0 & 1 & -1 & -1 \\ 0 & 0 & -8/5 & 0 & 1 & 0 \\ -1 & -1 & -1 & 0 & 0 & 0 \\ -1 & -11/3 & -13/5 & 2 & 0 & 0 \\ -2 & 0 & 0 & -3/2 & -1/2 & 0 \\ 2 & 2 & 2 & 0 & 0 & 0 \end{pmatrix} \cdot \begin{pmatrix} r_{R,HET,O2} \\ r_{R,HET,NO2} \\ r_{R,HET,NO3} \\ r_{R,AOB} \\ r_{R,NOB} \\ r_{R,AMX} \end{pmatrix} = \begin{pmatrix} r_{NH_4^+} \\ r_{NO_2^-} \\ r_{NO_3^-} \\ r_{C_2H_3O_2^-} \\ r_{H^+} \\ r_{O_2} \\ r_{TIC} \end{pmatrix} \quad (S1)$$

### S2 Mass balances based on the activated sludge model

The equation system 2, where only mass balances for dissolved compounds were considered, is given in equation S2.

$$\begin{pmatrix} -0.587 & -0.820 & 0 & 0 & 0 & 0 & -15.3 & -0.820 & -23.8 & -0.820 & 0 & 0 \\ -1.59 & 0 & -1.85 & 0 & -1.85 & 0 & 0 & 0 & 0 & 0 & 0 & 0 \\ -0.0875 & 0.0803 & -0.0875 & 0 & -0.0875 & 0.0803 & -4.85 & 0.0803 & -0.0875 & 0.0803 & -6.72 & 0.0505 \\ 0 & 0 & -0.298 & -0.287 & 0 & 0 & 0 & 0 & 21.7 & 0 & 1.63 & 0 \\ 0 & 0 & 0 & 0 & -0.497 & -0.478 & 4.76 & 0 & -21.7 & 0 & -8.80 & -0.478 \\ -0.0186 & -0.00574 & -0.0440 & -0.0262 & -0.058 & -0.0400 & 0.687 & -0.00574 & 0.00625 & -0.00574 & -0.0318 & -0.0378 \\ 0.220 & 0.308 & 0.319 & 0.308 & 0.319 & 0.3082 & -0.375 & 0.308 & -0.375 & 0.308 & -0.330 & 0.262 \end{pmatrix} \cdot \begin{pmatrix} \alpha_{R,HET,growth,O2} \\ \alpha_{R,HET,end.rep,O2} \\ \alpha_{R,HET,growth,NO2} \\ \alpha_{R,HET,end.resp,NO2} \\ \alpha_{R,HET,growth,NO3} \\ \alpha_{R,HET,end.resp,NO3} \\ \alpha_{R,AOB,growth} \\ \alpha_{R,AOB,end.resp} \\ \alpha_{R,NOB,growth} \\ \alpha_{R,NOB,end.resp} \\ \alpha_{R,AMX,growthj} \\ \alpha_{R,AMX,end.resp} \end{pmatrix} = \begin{pmatrix} r_{O_2} \\ r_{C_2H_3O_2^-} \\ r_{NH_4^+} \\ r_{NO_3^-} \\ r_{NO_2^-} \\ r_{H^+} \\ r_{TIC} \end{pmatrix} \quad (S2)$$

The equation system 3, with one type of HET and including the concentrations for the bacterial groups and inert biomass, is given in equation S3.



$$\begin{pmatrix}
 -0.587 & -0.820 & 0 & 0 & 0 & 0 & -15.3 & -0.820 & -23.8 & -0.820 & 0 & 0 \\
 -1.59 & 0 & -1.85 & 0 & -1.85 & 0 & 0 & 0 & 0 & 0 & 0 & 0 \\
 -0.0875 & 0.0803 & -0.0875 & 0 & -0.0875 & 0.0803 & -4.85 & 0.0803 & -0.0875 & 0.0803 & -6.72 & 0.0505 \\
 0 & 0 & -0.298 & -0.287 & 0 & 0 & 0 & 0 & 21.7 & 0 & 1.63 & 0 \\
 0 & 0 & 0 & 0 & -0.497 & -0.478 & 4.76 & 0 & -21.7 & 0 & -8.80 & -0.478 \\
 -0.0186 & -0.00574 & -0.0440 & -0.0262 & -0.058 & -0.0400 & 0.687 & -0.00574 & 0.00625 & -0.00574 & -0.0318 & -0.0378 \\
 0.220 & 0.308 & 0.319 & 0.308 & 0.319 & 0.3082 & -0.375 & 0.308 & -0.375 & 0.308 & -0.330 & 0.262 \\
 0 & 0.180 & 0 & 0.180 & 0 & 0.180 & 0 & 0.180 & 0 & 0.180 & 0 & 0.180 \\
 1 & -1 & 1 & -1 & 1 & -1 & 0 & 0 & 0 & 0 & 0 & 0 \\
 0 & 0 & 0 & 0 & 0 & 0 & 1 & -1 & 0 & 0 & 0 & 0 \\
 0 & 0 & 0 & 0 & 0 & 0 & 0 & 0 & 1 & -1 & 0 & 0 \\
 0 & 0 & 0 & 0 & 0 & 0 & 0 & 0 & 0 & 0 & 1 & -1
 \end{pmatrix} \cdot
 \begin{pmatrix}
 \alpha_{R,HET,growth,O2} \\
 \alpha_{R,HET,end.rep,O2} \\
 \alpha_{R,HET,growth,NO2} \\
 \alpha_{R,HET,end.resp,NO2} \\
 \alpha_{R,HET,growth,NO3} \\
 \alpha_{R,HET,end.resp,NO3} \\
 \alpha_{R,AOB,growth} \\
 \alpha_{R,AOB,end.resp} \\
 \alpha_{R,NOB,growth} \\
 \alpha_{R,NOB,end.resp} \\
 \alpha_{R,AMX,growth} \\
 \alpha_{R,AMX,end.resp}
 \end{pmatrix} =
 \begin{pmatrix}
 r_{O_2} \\
 r_{C_2H_3O_2^-} \\
 r_{NH_4^+} \\
 r_{NO_3^-} \\
 r_{NO_2^-} \\
 r_{H^+} \\
 r_{TIC} \\
 r_{X_I} \\
 r_{X_{HET}} \\
 r_{X_{AOB}} \\
 r_{X_{NOB}} \\
 r_{X_{AMX}}
 \end{pmatrix} \quad (S3)$$

The equation system 4, with three types of HET and including the concentrations for the bacterial groups and inert biomass, is given in equation S4.

$$\begin{pmatrix}
 -0.587 & -0.820 & 0 & 0 & 0 & 0 & -15.3 & -0.820 & -23.8 & -0.820 & 0 & 0 \\
 -1.59 & 0 & -1.85 & 0 & -1.85 & 0 & 0 & 0 & 0 & 0 & 0 & 0 \\
 -0.0875 & 0.0803 & -0.0875 & 0 & -0.0875 & 0.0803 & -4.85 & 0.0803 & -0.0875 & 0.0803 & -6.72 & 0.0505 \\
 0 & 0 & -0.298 & -0.287 & 0 & 0 & 0 & 0 & 21.7 & 0 & 1.63 & 0 \\
 0 & 0 & 0 & 0 & -0.497 & -0.478 & 4.76 & 0 & -21.7 & 0 & -8.80 & -0.478 \\
 -0.0186 & -0.00574 & -0.0440 & -0.0262 & -0.058 & -0.0400 & 0.687 & -0.00574 & 0.00625 & -0.00574 & -0.0318 & -0.0378 \\
 0.220 & 0.308 & 0.319 & 0.308 & 0.319 & 0.3082 & -0.375 & 0.308 & -0.375 & 0.308 & -0.330 & 0.262 \\
 0 & 0.180 & 0 & 0.180 & 0 & 0.180 & 0 & 0.180 & 0 & 0.180 & 0 & 0.180 \\
 1 & -1 & 0 & 0 & 0 & 0 & 0 & 0 & 0 & 0 & 0 & 0 \\
 0 & 0 & 1 & -1 & 0 & 0 & 0 & 0 & 0 & 0 & 0 & 0 \\
 0 & 0 & 0 & 0 & 1 & -1 & 0 & 0 & 0 & 0 & 0 & 0 \\
 0 & 0 & 0 & 0 & 0 & 0 & 1 & -1 & 0 & 0 & 0 & 0 \\
 0 & 0 & 0 & 0 & 0 & 0 & 0 & 0 & 1 & -1 & 0 & 0 \\
 0 & 0 & 0 & 0 & 0 & 0 & 0 & 0 & 0 & 0 & 1 & -1
 \end{pmatrix} \cdot
 \begin{pmatrix}
 \alpha_{R,HET,growth,O2} \\
 \alpha_{R,HET,end.rep,O2} \\
 \alpha_{R,HET,growth,NO2} \\
 \alpha_{R,HET,end.resp,NO2} \\
 \alpha_{R,HET,growth,NO3} \\
 \alpha_{R,HET,end.resp,NO3} \\
 \alpha_{R,AOB,growth} \\
 \alpha_{R,AOB,end.resp} \\
 \alpha_{R,NOB,growth} \\
 \alpha_{R,NOB,end.resp} \\
 \alpha_{R,AMX,growth} \\
 \alpha_{R,AMX,end.resp}
 \end{pmatrix} =
 \begin{pmatrix}
 r_{O_2} \\
 r_{C_2H_3O_2^-} \\
 r_{NH_4^+} \\
 r_{NO_3^-} \\
 r_{NO_2^-} \\
 r_{H^+} \\
 r_{TIC} \\
 r_{X_I} \\
 r_{X_{HET}} \\
 r_{X_{AOB}} \\
 r_{X_{NOB}} \\
 r_{X_{AMX}}
 \end{pmatrix}$$

$$\begin{pmatrix}
\alpha_{R,HET,growth,O2} \\
\alpha_{R,HET,end.rep,O2} \\
\alpha_{R,HET,growth,NO2} \\
\alpha_{R,HET,end.resp,NO2} \\
\alpha_{R,HET,growth,NO3} \\
\alpha_{R,HET,end.resp,NO3} \\
\alpha_{R,AOB,growth} \\
\alpha_{R,AOB,end.resp} \\
\alpha_{R,NOB,growth} \\
\alpha_{R,NOB,end.resp} \\
\alpha_{R,AMX,growth} \\
\alpha_{R,AMX,end.resp}
\end{pmatrix}
=
\begin{pmatrix}
r_{O_2} \\
r_{C_2H_3O_2^-} \\
r_{NH_4^+} \\
r_{NO_3^-} \\
r_{NO_2^-} \\
r_{H^+} \\
r_{TIC} \\
r_{X_I} \\
r_{X_{HET,O_2}} \\
r_{X_{HET,NO_3}} \\
r_{X_{HET,NO_2}} \\
r_{X_{AOB}} \\
r_{X_{NOB}} \\
r_{X_{AMX}}
\end{pmatrix}
\quad (S4)$$

### S3 Mass balances based on the activated sludge model including kinetics

The equation system 5, for mass balances based on the activated sludge model and including kinetics, is given in equation S5.

$$\begin{pmatrix}
-0.0351 & 0 & 0 & -0.189 & -0.00404 & 0 \\
-0.0490 & -0.0572 & -0.0487 & 0 & 0 & 0 \\
-0.00103 & -0.00103 & -0.000877 & -0.0592 & 0.0000664 & -0.0764 \\
0 & -0.0152 & 0 & 0 & 0.00295 & 0.0185 \\
0 & 0 & -0.0216 & 0.0583 & -0.00295 & -0.101 \\
-0.000691 & -0.00190 & -0.00224 & 0.00839 & -0.00000474 & -0.000412 \\
0.0132 & 0.0163 & 0.0139 & -0.000389 & 0.000249 & -0.00340
\end{pmatrix}$$

$$\begin{pmatrix}
X_{HET,O_2} \\
X_{HET,NO_3} \\
X_{HET,NO_2} \\
X_{AOB} \\
X_{NOB} \\
X_{AMX}
\end{pmatrix}
=
\begin{pmatrix}
r_{O_2} \\
r_{C_2H_3O_2^-} \\
r_{NH_4^+} \\
r_{NO_3^-} \\
r_{NO_2^-} \\
r_{H^+} \\
r_{TIC}
\end{pmatrix}
\quad (S5)$$

### S4 Mass balances based on the activated sludge model including kinetics and a biomass balance

The equation system 6, for mass balances based on the activated sludge model and including both kinetics and a biomass balance, is given in equation S6.

$$\begin{pmatrix} -0.0351 & 0 & 0 & -0.189 & -0.00404 & 0 \\ -0.0490 & -0.0572 & -0.0487 & 0 & 0 & 0 \\ -0.00103 & -0.00103 & -0.000877 & -0.0592 & 0.0000664 & -0.0764 \\ 0 & -0.0152 & 0 & 0 & 0.00295 & 0.0185 \\ 0 & 0 & -0.0216 & 0.0583 & -0.00295 & -0.101 \\ -0.000691 & -0.00190 & -0.00224 & 0.00839 & -0.00000474 & -0.000412 \\ 0.0132 & 0.0163 & 0.0139 & -0.000389 & 0.000249 & -0.00340 \\ 0.0138 & 0.0138 & 0.0118 & 0.0104 & -0.000664 & 0.0103 \end{pmatrix} \cdot \begin{pmatrix} X_{HET,O2} \\ X_{HET,NO3} \\ X_{HET,NO2} \\ X_{AOB} \\ X_{NOB} \\ X_{AMX} \end{pmatrix} = \begin{pmatrix} r_{O_2} \\ r_{C_2H_3O_2^-} \\ r_{NH_4^+} \\ r_{NO_3^-} \\ r_{NO_2^-} \\ r_{H^+} \\ r_{TIC} \\ r_{X_{tot}} \end{pmatrix} \quad (S6)$$

### S5 Initial conditions and influent concentrations

The initial conditions and the influent concentrations of the modelled compounds are given in Table S1.

**Table S1** Initial conditions and influent concentrations of the modelled compounds.

	Unit	Initial condition	Influent concentration
$S_H$	$10^3 \text{ mol}\cdot\text{m}^{-3}$	$5.97\cdot 10^{-7}$	$2.42\cdot 10^{-9}$
$S_{HCO3}$	$\text{mol}\cdot\text{m}^{-3}$	0.63	31.7
$S_{H2CO3}$	$\text{mol}\cdot\text{m}^{-3}$	0.62	0.12
$S_{HNO2}$	$\text{g N}\cdot\text{m}^{-3}$	0	0
$S_{HPO4}$	$\text{g P}\cdot\text{m}^{-3}$	7.6	43.2
$S_{H2PO4}$	$\text{g P}\cdot\text{m}^{-3}$	36.4	0.7
$S_{N2,AMX}$	$\text{g N}\cdot\text{m}^{-3}$	0	0
$S_{N2,HET}$	$\text{g N}\cdot\text{m}^{-3}$	0	0
$S_{NH3}$	$\text{g N}\cdot\text{m}^{-3}$	0.11	132
$S_{NH4}$	$\text{g N}\cdot\text{m}^{-3}$	8.29	566

$S_{NO2}$	$g\ N\cdot m^{-3}$	0.1	0
$S_{NO3}$	$g\ N\cdot m^{-3}$	6.5	0
$S_{O2}$	$g\ O_2\cdot m^{-3}$	0	0
$S_S$	$g\ COD\cdot m^{-3}$	0	0
$S_{Sneg}$	$g\ COD\cdot m^{-3}$	0	890
$S_{S,NO2}$	$g\ COD\cdot m^{-3}$	0	0
$S_{S,NO3}$	$g\ COD\cdot m^{-3}$	0	0
$S_{S,O2}$	$g\ COD\cdot m^{-3}$	0	0
$X_{AMX}$	$g\ COD\cdot m^{-3}$	100	0
$X_{AOB}$	$g\ COD\cdot m^{-3}$	100	0
$X_{H,NO2}$	$g\ COD\cdot m^{-3}$	100	0
$X_{H,NO3}$	$g\ COD\cdot m^{-3}$	100	0
$X_{H,O2}$	$g\ COD\cdot m^{-3}$	100	0
$X_I$	$g\ COD\cdot m^{-3}$	2000	0
$X_{NOB}$	$g\ COD\cdot m^{-3}$	100	0

### S6 Modelled compounds

The modelled compounds are listed in Table S2.

**Table S2** Dissolved and particulate compounds of the dynamic model.

		unit	$i_N$ [g N]	$i_{COD}$ [g COD]	$i_C$ [mol C]	$i_{charge}$ [mol]
$S_H$	dissolved hydrogen proton	$10^3\ mol\cdot m^{-3}$	0	0	0	1000
$S_{H2CO3}$	dissolved carbonic acid	$mol\cdot m^{-3}$	0	0	1	0
$S_{H2PO4}$	dissolved dihydrogen phosphate	$g\ P\cdot m^{-3}$	0	0	0	- 1/30.97
$S_{HCO3}$	dissolved bicarbonate	$mol\cdot m^{-3}$	0	0	1	-1
$S_{HNO2}$	dissolved nitrous acid	$g\ N\cdot m^{-3}$	1	-48/14	0	0
$S_{HPO4}$	dissolved hydrogen phosphate	$g\ P\cdot m^{-3}$	0	0	0	- 2/30.97
$S_{N2,AMX}$	dissolved dinitrogen produced by AMX	$g\ N\cdot m^{-3}$	1	-24/14	0	0
$S_{N2,HET}$	dissolved dinitrogen produced by HET	$g\ N\cdot m^{-3}$	1	-24/14	0	0
$S_{NH3}$	dissolved ammonia	$g\ N\cdot m^{-3}$	1	0	0	0
$S_{NH4}$	dissolved ammonium	$g\ N\cdot m^{-3}$	1	0	0	1/14
$S_{NO2}$	dissolved nitrite	$g\ N\cdot m^{-3}$	1	-48/14	0	-1/14
$S_{NO3}$	dissolved nitrate	$g\ N\cdot m^{-3}$	1	-64/14	0	-1/14

$S_{O_2}$	dissolved oxygen	$g\ O_2 \cdot m^{-3}$	0	-1	0	0
$S_S$	dissolved acetic acid	$g\ COD \cdot m^{-3}$	0	1	2/64	0
$S_{S,neg}$	dissolved acetate	$g\ COD \cdot m^{-3}$	0	1	2/64	-1/64
$S_{S,NO_2}$	dissolved acetic acid degraded by $X_{HET,NO_2}$	$g\ COD \cdot m^{-3}$	0	1	2/64	0
$S_{S,NO_3}$	dissolved acetic acid degraded by $X_{HET,NO_3}$	$g\ COD \cdot m^{-3}$	0	1	2/64	0
$S_{S,O_2}$	dissolved acetic acid degraded by $X_{HET,O_2}$	$g\ COD \cdot m^{-3}$	0	1	2/64	0
$X_{AOB}$	ammonia oxidising bacteria	$g\ COD \cdot m^{-3}$	14/160	1	5/160	0
$X_{AMX}$	anammox bacteria	$g\ COD \cdot m^{-3}$	0.15·14/36.4	1	1/36.4	0
$X_{H,NO_2}$	heterotrophic bacteria using nitrite	$g\ COD \cdot m^{-3}$	14/160	1	5/160	0
$X_{H,NO_3}$	heterotrophic bacteria using nitrate	$g\ COD \cdot m^{-3}$	14/160	1	5/160	0
$X_{H,O_2}$	heterotrophic bacteria using oxygen	$g\ COD \cdot m^{-3}$	14/160	1	5/160	0
$X_I$	inert particulate matter	$g\ COD \cdot m^{-3}$	0.035	1	5/160	0
$X_{NOB}$	nitrite oxidising bacteria	$g\ COD \cdot m^{-3}$	14/160	1	5/160	0

### S7 Simulation of pH equilibria and aeration

Parameters and process rates for the simulation of the pH equilibria and the aeration are listed in Table S3 and Table S4, respectively.

**Table S3** Parameters for the simulation of pH equilibria and aeration.

Symbol	Characterisation	Value / formula	Unit
cond	Conductivity	22	$mS \cdot cm^{-1}$
$f_1$	Activity coefficient for ions with charge 1	$10^{\left(-0.5 \cdot 1 \cdot \frac{\sqrt{ionicstrength}}{\sqrt{ionicstrength+1}} - 0.2 \cdot ionicstrength\right)}$	-
$f_2$	Activity coefficient for ions with charge 2	$10^{\left(-0.5 \cdot 4 \cdot \frac{\sqrt{ionicstrength}}{\sqrt{ionicstrength+1}} - 0.2 \cdot ionicstrength\right)}$	-
$H_{H_2CO_3}$	Henry coefficient of $H_2CO_3$	$\frac{1}{k_{H,T,H_2CO_3} \cdot 0.082057 \cdot (T + 273.15)}$	-

$H_{NH3}$	Henry coefficient of $NH_3$	$\frac{1}{k_{H,T,NH3} \cdot 0.082057 \cdot (T + 273.15)}$	-
<b>ionicstrength</b>	Ionic strength	$0.01001047 \cdot cond + 0.0005188$	$mol \cdot L^{-1}$
$k_{H,T,H2CO3}$	Temperature dependency of $H_{H2CO3}$	$0.0345294 \cdot \exp\left(2428.57 \cdot \left(\frac{1}{T+273.15} - \frac{1}{1298.15}\right)\right)$	$K^{-1}$
$k_{H,T,NH3}$	Temperature dependency of $H_{NH3}$	$55.8125 \cdot \exp\left(3708.33 \cdot \left(\frac{1}{T+273.15} - \frac{1}{1298.15}\right)\right)$	$K^{-1}$
$K_{LaH2CO3}$	$K_{La}$ value of $H_2CO_3$	$0.862 \cdot K_{LaO_2}$	$d^{-1}$
$K_{LaO_2}$	$K_{La}$ value of $O_2$	70	$d^{-1}$
$k_{aeq}$	Rate constant for equilibrium processes	$10^{10}$	$d^{-1}$
$p_{CO_2,air}$	Partial pressure of $CO_2$	0.000335	atm
$pK_{H2CO3}$	pK value of $H_2CO_3 \leftrightarrow HCO_3$	$-\log\left(10^{-6.37} \cdot \exp\left(7.6 \cdot \frac{1000}{8.314472} \cdot \left(\frac{1}{1298.15} - \frac{1}{T+273.15}\right)\right)\right)$	-
$pK_{H2PO4}$	pK value of $H_2PO_4 \leftrightarrow HPO_4$	$-\log\left(10^{-7.21} \cdot \exp\left(4.2 \cdot \frac{1000}{8.314472} \cdot \left(\frac{1}{1298.15} - \frac{1}{T+273.15}\right)\right)\right)$	-
$pK_{HNO_2}$	pK value of $HNO_2 \leftrightarrow NO_2$	$-\log\left(10^{-3.34} \cdot \exp\left(15.2 \cdot \frac{1000}{8.314472} \cdot \left(\frac{1}{1298.15} - \frac{1}{T+273.15}\right)\right)\right)$	-
$pK_{NH_4}$	pK value of $NH_4 \leftrightarrow NH_3$	$-\log\left(10^{-9.25} \cdot \exp\left(52.21 \cdot \frac{1000}{8.314472} \cdot \left(\frac{1}{1298.15} - \frac{1}{T+273.15}\right)\right)\right)$	-
$pK_{SS}$	pK value of $S \leftrightarrow S_{neg}$	$-\log\left(10^{-4.75} \cdot \exp\left(-0.2 \cdot \frac{1000}{8.314472} \cdot \left(\frac{1}{1298.15} - \frac{1}{T+273.15}\right)\right)\right)$	-
$pO_s$	Parameter for calculation of $S_{O_2,sat}$	$1.2 \cdot 10^{-6} \cdot T^4 + 0.00935467 \cdot T^2 - 0.412894 \cdot T + 14.6205$	-

<b>pw</b>	Parameter for calculation of $S_{O_2,sat}$	$4.79 \cdot 10^{-6} \cdot T^4 + 0.00021623 \cdot T^3 + 0.0148446 \cdot T^2 + 0.441893 \cdot T + 6.1145$	-
<b>Q<sub>air</sub></b>	Airflow rate	$0.195 \cdot \frac{1013}{971} \cdot \frac{273.14 + T}{273.14}$	$m^3 \cdot d^{-1}$
<b>Q<sub>in</sub></b>	Influent flow rate	0.003	$m^3 \cdot d^{-1}$
<b>Q<sub>eff</sub></b>	Effluent flow rate	0.003	$m^3 \cdot d^{-1}$
<b>SRT</b>	Sludge retention time	50 <i>resp.</i> 100	d
<b>S<sub>H2CO3,air</sub></b>	Concentration of H <sub>2</sub> CO <sub>3</sub> in the air	$p_{CO_2} \cdot 1000 \cdot \frac{1}{0.082057} \cdot \frac{1}{(T + 273.15)}$	$mol \cdot m^{-3}$
<b>S<sub>N2,tot</sub></b>	Total produced N <sub>2</sub>	$S_{N_2,AMX} + S_{N_2,HET}$	$gN \cdot m^{-3}$
<b>S<sub>O2,sat</sub></b>	Saturation concentration of dissolved oxygen	$pO_s \cdot \frac{975 - pw}{1013 - pw}$	$gO_2 \cdot m^{-3}$
<b>S<sub>S,tot</sub></b>	Total degraded S <sub>s</sub>	$S_{S,O_2} + S_{S,NO_3} + S_{S,NO_2}$	$gCOD \cdot m^{-3}$
<b>T</b>	Temperature	26	°C
<b>V</b>	Volume	0.01	$m^3$

**Table S4** Process rates for the simulation of pH equilibria and aeration.

	<b>Reaction</b>	<b>Reaction rate</b>
<b>aeration</b>	H <sub>2</sub> CO <sub>3</sub> strip	$(H_{H_2CO_3} \cdot S_{H_2CO_3} - S_{H_2CO_3,air}) \cdot \frac{Q_{air}}{V} \cdot \left(1 - \exp\left(\frac{K_L a_{H_2CO_3} \cdot V}{H_{H_2CO_3} \cdot Q_{air}}\right)\right)$
	O <sub>2</sub> input	$K_L a_{O_2} \cdot (S_{O_2,sat} - S_{O_2})$
<b>pH equilibria</b>	HCO <sub>3</sub> forward	$k_{aeq} \cdot S_{H_2CO_3}$
	HCO <sub>3</sub> backward	$k_{aeq} \cdot 10^{pK_{H_2CO_3}} \cdot f_1 \cdot S_H \cdot f_1 \cdot S_{HCO_3}$
	HPO <sub>4</sub> forward	$k_{aeq} \cdot f_1 \cdot S_{H_2PO_4}$
	HPO <sub>4</sub> backward	$k_{aeq} \cdot 10^{pK_{H_2PO_4}} \cdot f_1 \cdot S_H \cdot f_2 \cdot S_{HPO_4}$
	NH <sub>3</sub> forward	$k_{aeq} \cdot f_1 \cdot S_{NH_4}$
	NH <sub>3</sub> backward	$k_{aeq} \cdot 10^{pK_{NH_4}} \cdot f_1 \cdot S_H \cdot S_{NH_3}$
	NO <sub>2</sub> forward	$k_{aeq} \cdot S_{HNO_2}$
	NO <sub>2</sub> backward	$k_{aeq} \cdot 10^{pK_{HNO_2}} \cdot f_1 \cdot S_H \cdot f_1 \cdot S_{NO_2}$
S forward	$k_{aeq} \cdot S_S$	

## S8 Structural observability with one type of HET

To test whether the lack of observability is not only practical but also structural, we performed Monte Carlo simulations: 10,000 simulations were done with uniformly and randomly distributed parameter values in a range of  $\pm 50\%$  of the default values. This was done with the following Matlab code:

```

clc
clear all
close all

disp('Defining default or sampled parameter values')

a_def = 0.630 ; % YH,O2
b_def = 0.566 ; % YH,NO3
c_def = 0.566 ; % YH,NO2
d_def = 14/160 ; % iN,AOB,NOB,HET
e_def = 0.15*14/36.4 ; % iN,AMX
f_def = 0.035 ; % iN,XI
g_def = 0.180 ; % fxi
h_def = 0.210 ; % YAOB
i_def = 0.046 ; % YNOB
k_def = 0.150 ; % YAMX

approach = 'randomized' ;
switch approach
case 'default'
a = 0.630 ; % YH,O2
b = 0.566 ; % YH,NO3
c = 0.566 ; % YH,NO2
d = 14/160 ; % iN,AOB,NOB,HET
e = 0.15*14/36.4 ; % iN,AMX
f = 0.035 ; % iN,XI
g = 0.180 ; % fxi
h = 0.210 ; % YAOB
i = 0.046 ; % YNOB
k = 0.150 ; % YAMX
case 'randomized'
n_rand = 100 ; % number of repetitions

a = rand(1,n_rand)*a_def+1/2*a_def ;
b = rand(1,n_rand)*b_def+1/2*b_def ;
c = rand(1,n_rand)*c_def+1/2*c_def ;
d = 14/160 ; % iN,AOB,NOB,HET
e = 0.15*14/36.4 ; % iN,AMX
f = 0.035 ; % iN,XI
g = rand(1,n_rand)*g_def+1/2*g_def ;
h = rand(1,n_rand)*h_def+1/2*h_def ;
i = rand(1,n_rand)*i_def+1/2*i_def ;
k = rand(1,n_rand)*k_def+1/2*k_def ;

end

```



```

n_reagent = 12 ;
n_reactions = 12 ;
n_rep = length(a) ; % length of vector a = number of repetitions

for i_rep=1:n_rep
    disp(['Repetition ' num2str(i_rep) ' of ' num2str(n_rep)])
    % =====
    % Setup matrix:
    Matrix = nan(n_reagent,n_reactions) ;% initialize matrix

    % -----
    % reaction 1
    Matrix(:,1) = [    -1/(32*a(i_rep))+1/32 ;
                    -1/(64*a(i_rep)) ;
                    -d/14 ;
                    0 ;
                    0 ;
                    -1/(64*a(i_rep))+d/14 ;
                    2/(64*a(i_rep))-1/32 ;
                    0 ;
                    1/160 ;
                    0 ;
                    0 ;
                    0 ];

    % -----
    % reaction 2
    Matrix(:,2) = [    g(i_rep)/32-1/32 ;
                    0 ;
                    d/14-g(i_rep)*f/14 ;
                    0 ;
                    0 ;
                    (g(i_rep)*f-d)/14 ;
                    1/32-g(i_rep)/32 ;
                    g(i_rep)/160 ;
                    -1/160 ;
                    0 ;
                    0 ;
                    0 ];

    % -----
    % reaction 3
    Matrix(:,3) = [    0 ;
                    -1/(64*b(i_rep)) ;
                    -d/14 ;
                    1/40*(1-1/b(i_rep)) ;
                    0 ;
                    d/14-1/(64*b(i_rep))+1/40*(1-1/b(i_rep)) ;
                    1/(32*b(i_rep))-1/32 ;
                    0 ;
                    1/160 ;
                    0 ;
                    0 ;
                    0 ];

    % -----
    % reaction 4
    Matrix(:,4) = [    0 ;

```

```

0 ;
d/14-g(i_rep)*f/14 ;
(g(i_rep)-1)*1/40 ;
0 ;
(g(i_rep)*f-d)/14+(g(i_rep)-1)*1/40 ;
1/32-g(i_rep)/32 ;
g(i_rep)/160 ;
-1/160 ;
0 ;
0 ;
0 ];

% -----
% reaction 5

Matrix(:,5) = [ 0 ;
-1/(64*c(i_rep)) ;
-d/14 ;
0 ;
1/24*(1-1/c(i_rep)) ;
d/14-1/(64*c(i_rep))+1/24*(1-1/c(i_rep)) ;
1/(32*c(i_rep))-1/32 ;
0 ;
1/160 ;
0 ;
0 ;
0 ];

% -----
% reaction 6

Matrix(:,6) = [ 0 ;
0 ;
d/14-g(i_rep)*f/14 ;
0 ;
(g(i_rep)-1)*1/24 ;
(g(i_rep)*f-d)/14+(g(i_rep)-1)*1/24 ;
1/32-g(i_rep)/32 ;
g(i_rep)/160 ;
-1/160 ;
0 ;
0 ;
0 ];

% -----
% reaction 7

Matrix(:,7) = [ 1/32-3/(28*h(i_rep)) ;
0 ;
-1/(14*h(i_rep))-d/14 ;
0 ;
1/(14*h(i_rep)) ;
1/(7*h(i_rep))+d/14 ;
-1/32 ;
0 ;
0 ;
1/160 ;
0 ;
0 ];

% -----
% reaction 8

Matrix(:,8) = [ g(i_rep)/32-1/32 ;
0 ;

```

```

d/14-g(i_rep)*f/14      ;
0      ;
0      ;
(g(i_rep)*f-d)/14      ;
1/32-g(i_rep)/32      ;
g(i_rep)/160      ;
0      ;
-1/160      ;
0      ;
0      ];

% -----
% reaction 9

Matrix(:,9) = [      1/32-1/(28*i(i_rep))      ;
0      ;
-d/14      ;
1/(14*i(i_rep))      ;
-1/(14*i(i_rep))      ;
d/14      ;
-1/32      ;
0      ;
0      ;
0      ;
1/160      ;
0      ];

% -----
% reaction 10

Matrix(:,10) = [      g(i_rep)/32-1/32      ;
0      ;
d/14-g(i_rep)*f/14      ;
0      ;
0      ;
(g(i_rep)*f-d)/14      ;
1/32-g(i_rep)/32      ;
g(i_rep)/160      ;
0      ;
0      ;
-1/160      ;
0      ];

% -----
% reaction 11

Matrix(:,11) = [      0      ;
0      ;
-1/(14*k(i_rep))-e/14      ;
0.192/(14*k(i_rep))+1/40      ;
-1.32/(14*k(i_rep))      ;
e/14+1/40-0.064/(7*k(i_rep))      ;
-1/36.4      ;
0      ;
0      ;
0      ;
0      ;
1/36.4      ];

% -----
% reaction 12

Matrix(:,12) = [      0      ;
0      ;
e/14-g(i_rep)*f/14      ;

```

```

0 ;
(g(i_rep)-1)*1/24 ;
(g(i_rep)*f-e)/14+(g(i_rep)-1)*1/24 ;
1/36.4-g(i_rep)/32 ;
g(i_rep)/160 ;
0 ;
0 ;
0 ;
-1/36.4 ];

% =====
% Analyze matrix:
rank(Matrix)

[U,S,V]=svd(Matrix);

BooleanInclude = diag(S)<=1e-10 ;

disp(V(:,BooleanInclude))

end

```

## S9 Structural observability with three types of HET

To test whether the lack of observability is not only practical but also structural, we performed Monte Carlo simulations: 10,000 simulations were done with uniformly and randomly distributed parameter values in a range of  $\pm 50\%$  of the default values. This was done with the following Matlab code:

```

clc
clear all
close all

disp('Defining default or sampled parameter values')

a_def = 0.630 ; % YH,O2
b_def = 0.566 ; % YH,NO3
c_def = 0.566 ; % YH,NO2
d_def = 14/160 ; % iN,AOB,NOB,HET
e_def = 0.15*14/36.4 ; % iN,AMX
f_def = 0.035 ; % iN,XI
g_def = 0.180 ; % fxi
h_def = 0.210 ; % YAOB
i_def = 0.046 ; % YNOB
k_def = 0.150 ; % YAMX

approach = 'randomized' ;
switch approach
case 'default'
a = 0.630 ; % YH,O2
b = 0.566 ; % YH,NO3
c = 0.566 ; % YH,NO2
d = 14/160 ; % iN,AOB,NOB,HET
e = 0.15*14/36.4 ; % iN,AMX
f = 0.035 ; % iN,XI

```

```

g = 0.180 ; % fxi
h = 0.210 ; % YAOB
i = 0.046 ; % YNOB
k = 0.150 ; % YAMX
case 'randomized'
n_rand = 100 ; % number of repetitions

a = rand(1,n_rand)*a_def+1/2*a_def ;
b = rand(1,n_rand)*b_def+1/2*b_def ;
c = rand(1,n_rand)*c_def+1/2*c_def ;
d = 14/160 ; % iN,AOB,NOB,HET
e = 0.15*14/36.4 ; % iN,AMX
f = 0.035 ; % iN,XI
g = rand(1,n_rand)*g_def+1/2*g_def ;
h = rand(1,n_rand)*h_def+1/2*h_def ;
i = rand(1,n_rand)*i_def+1/2*i_def ;
k = rand(1,n_rand)*k_def+1/2*k_def ;

end

n_reagent = 14 ;
n_reactions = 12 ;
n_rep = length(a) ; % length of vector a = number of repetitions

for i_rep=1:n_rep
disp(['Repetition ' num2str(i_rep) ' of ' num2str(n_rep)])
% =====
% Setup matrix:
Matrix = nan(n_reagent,n_reactions) ;% initialize matrix

% -----
% reaction 1
Matrix(:,1) = [ -1/(32*a(i_rep))+1/32 ;
-1/(64*a(i_rep)) ;
-d/14 ;
0 ;
0 ;
-1/(64*a(i_rep))+d/14 ;
2/(64*a(i_rep))-1/32 ;
0 ;
1/160 ;
0 ;
0 ;
0 ;
0 ;
0 ] ;

% -----
% reaction 2
Matrix(:,2) = [ g(i_rep)/32-1/32 ;
0 ;
d/14-g(i_rep)*f/14 ;
0 ;
0 ;
(g(i_rep)*f-d)/14 ;
1/32-g(i_rep)/32 ;
g(i_rep)/160 ;
-1/160 ;
0 ;
0 ;
0 ] ;

```

```

                                0 ;
                                0 ];
% -----
% reaction 3

Matrix(:,3) = [      0 ;
                 -1/(64*b(i_rep)) ;
                 -d/14 ;
                 1/40*(1-1/b(i_rep)) ;
                 0 ;
                 d/14-1/(64*b(i_rep))+1/40*(1-1/b(i_rep)) ;
                 1/(32*b(i_rep))-1/32 ;
                 0 ;
                 0 ;
                 1/160 ;
                 0 ;
                 0 ;
                 0 ;
                 0 ];
% -----
% reaction 4

Matrix(:,4) = [      0 ;
                 0 ;
                 d/14-g(i_rep)*f/14 ;
                 (g(i_rep)-1)*1/40 ;
                 0 ;
                 (g(i_rep)*f-d)/14+(g(i_rep)-1)*1/40 ;
                 1/32-g(i_rep)/32 ;
                 g(i_rep)/160 ;
                 0 ;
                 -1/160 ;
                 0 ;
                 0 ;
                 0 ;
                 0 ];
% -----
% reaction 5

Matrix(:,5) = [      0 ;
                 -1/(64*c(i_rep)) ;
                 -d/14 ;
                 0 ;
                 1/24*(1-1/c(i_rep)) ;
                 d/14-1/(64*c(i_rep))+1/24*(1-1/c(i_rep)) ;
                 1/(32*c(i_rep))-1/32 ;
                 0 ;
                 0 ;
                 0 ;
                 1/160 ;
                 0 ;
                 0 ;
                 0 ];
% -----
% reaction 6

Matrix(:,6) = [      0 ;
                 0 ;
                 d/14-g(i_rep)*f/14 ;

```

```

0 ;
(g(i_rep)-1)*1/24 ;
(g(i_rep)*f-d)/14+(g(i_rep)-1)*1/24 ;
1/32-g(i_rep)/32 ;
g(i_rep)/160 ;
0 ;
0 ;
-1/160 ;
0 ;
0 ;
0 ];
% -----
% reaction 7

Matrix(:,7) = [ 1/32-3/(28*h(i_rep)) ;
0 ;
-1/(14*h(i_rep))-d/14 ;
0 ;
1/(14*h(i_rep)) ;
1/(7*h(i_rep))+d/14 ;
-1/32 ;
0 ;
0 ;
0 ;
0 ;
1/160 ;
0 ;
0 ];
% -----
% reaction 8

Matrix(:,8) = [ g(i_rep)/32-1/32 ;
0 ;
d/14-g(i_rep)*f/14 ;
0 ;
0 ;
(g(i_rep)*f-d)/14 ;
1/32-g(i_rep)/32 ;
g(i_rep)/160 ;
0 ;
0 ;
0 ;
-1/160 ;
0 ;
0 ];
% -----
% reaction 9

Matrix(:,9) = [ 1/32-1/(28*i(i_rep)) ;
0 ;
-d/14 ;
1/(14*i(i_rep)) ;
-1/(14*i(i_rep)) ;
d/14 ;
-1/32 ;
0 ;
0 ;
0 ;
0 ;
0 ;
1/160 ;
0 ];

```

```

% -----
% reaction 10

Matrix(:,10) = [   g(i_rep)/32-1/32      ;
                  0                      ;
                  d/14-g(i_rep)*f/14    ;
                  0                      ;
                  0                      ;
                  (g(i_rep)*f-d)/14      ;
                  1/32-g(i_rep)/32      ;
                  g(i_rep)/160           ;
                  0                      ;
                  0                      ;
                  0                      ;
                  0                      ;
                  -1/160                 ;
                  0                      ];

% -----

% reaction 11

Matrix(:,11) = [   0      ;
                  0      ;
                  -1/(14*k(i_rep))-e/14  ;
                  0.192/(14*k(i_rep))+1/40 ;
                  -1.32/(14*k(i_rep))    ;
                  e/14+1/40-0.064/(7*k(i_rep)) ;
                  -1/36.4                ;
                  0      ;
                  0      ;
                  0      ;
                  0      ;
                  0      ;
                  0      ;
                  0      ;
                  1/36.4 ];

% -----
% reaction 12

Matrix(:,12) = [   0      ;
                  0      ;
                  e/14-g(i_rep)*f/14    ;
                  0      ;
                  (g(i_rep)-1)*1/24     ;
                  (g(i_rep)*f-e)/14+(g(i_rep)-1)*1/24 ;
                  1/36.4-g(i_rep)/32    ;
                  g(i_rep)/160          ;
                  0      ;
                  0      ;
                  0      ;
                  0      ;
                  0      ;
                  0      ;
                  -1/36.4 ];

% =====
% Analyze matrix:
rank(Matrix)

[U,S,V]=svd(Matrix);

```



```
BooleanInclude = diag(S)<=1e-10 ;  
disp(V(:,BooleanInclude))  
end
```



## **CHAPTER 3**

### **Successful application of nitrification/anammox to wastewater with elevated organic carbon to ammonia ratios**

Sarina Jenni, Siegfried E. Vlaeminck, Eberhard Morgenroth, Kai M. Udert

*Water Research, 2014, 49, 316-326*

# Successful application of nitrification/anammox to wastewater with elevated organic carbon to ammonia ratios

Sarina Jenni<sup>1</sup>, Siegfried E. Vlaeminck<sup>2</sup>, Eberhard Morgenroth<sup>1,3</sup>, Kai M. Udert<sup>1</sup>

1: Eawag, Swiss Federal Institute for Aquatic Science and Technology, 8600 Dübendorf, Switzerland

2: Ghent University, Laboratory for Microbial Ecology and Technology (LabMET), 9000 Gent, Belgium

3: Institute of Environmental Engineering, ETH Zurich, 8093 Zurich, Switzerland

## ABSTRACT

The nitrification/anammox process has been mainly applied to high-strength nitrogenous wastewaters with very low biodegradable organic carbon content ( $< 0.5 \text{ g COD}\cdot\text{g N}^{-1}$ ). However, several wastewaters have biodegradable organic carbon to nitrogen (COD/N) ratios between 0.5 and  $1.7 \text{ g COD}\cdot\text{g N}^{-1}$  and thus, contain elevated amounts of organic carbon but not enough for heterotrophic denitrification. In this study, the influence of elevated COD/N ratios was studied on a nitrification/anammox process with suspended sludge. In a step-wise manner, the influent COD/N ratio was increased to  $1.4 \text{ g COD}\cdot\text{g N}^{-1}$  by supplementing digester supernatant with acetate. The increasing availability of COD led to an increase of the nitrogen removal efficiency from around 85% with pure digester supernatant to  $>95\%$  with added acetate while the nitrogen elimination rate stayed constant ( $275 \pm 40 \text{ mg N}\cdot\text{L}^{-1}\cdot\text{d}^{-1}$ ). Anammox activity and abundance of anammox bacteria (AMX) were strongly correlated, and with increasing influent COD/N ratio both decreased steadily. At the same time, heterotrophic denitrification with nitrite and the activity of ammonia oxidising bacteria (AOB) gradually increased. Simultaneously, the sludge retention time (SRT) decreased significantly with increasing COD loading to about 15 d and reached critical values for the slowly growing AMX. When the SRT was increased by reducing biomass loss with the effluent, AMX activity and abundance started to rise again, while the AOB activity remained unaltered. Fluorescent *in-situ* hybridisation (FISH) showed that the initial AMX community shifted within only 40 d from a mixed AMX community to “*Candidatus Brocadia fulgida*” as the dominant AMX type with an influent COD/N ratio of  $0.8 \text{ g COD}\cdot\text{g N}^{-1}$  and higher. “*Ca. Brocadia fulgida*” is known to oxidise acetate, and its ability to outcompete other types of AMX indicates that AMX participated in acetate oxidation. In a later phase, glucose was added to the influent instead of acetate. The new substrate composition did not significantly influence the nitrogen removal nor the AMX activity, and “*Ca. Brocadia fulgida*” remained the dominant type of AMX. Overall, this study showed that AMX can coexist with

heterotrophic bacteria at elevated influent COD/N ratios if a sufficiently high SRT is maintained.

## INTRODUCTION

The combination of nitrification and anammox is a cost saving alternative to conventional biological nitrogen removal via heterotrophic denitrification (Siegrist et al. 2008, Vlaeminck et al. 2012). Many studies have investigated various types of nitrification/anammox reactors with dedicated attention for the biomass growth mode as biofilm, flocs and/or granules (Vlaeminck et al. 2010), and the influence of process conditions such as the temperature (Vázquez-Padín et al. 2011), dissolved oxygen concentration (Strous et al. 1997a), salinity (Liu et al. 2009) and inhibitory substances (Dapena-Mora et al. 2007).

The term "biodegradable organic carbon" refers to the difference between the dissolved COD in the influent and the dissolved COD in the effluent, i.e. the organic carbon, which is actually degraded in a reactor. So far, nitrification/anammox has mainly been applied for wastewaters with high ammonia concentrations and low concentrations of biodegradable organic substances such as digester supernatant, in which the ratio of biodegradable organic carbon to ammonia nitrogen (COD/N) is lower than  $0.5 \text{ g COD}\cdot\text{g N}^{-1}$  (Joss et al. 2009, van der Star et al. 2007, Wett 2007). In contrast to this, complete heterotrophic denitrification via nitrite requires a COD/N ratio of more than  $1.71 \text{ g COD}\cdot\text{g N}^{-1}$ . However, several wastewaters have COD/N ratios between  $0.5$  and  $1.71 \text{ g COD}\cdot\text{g N}^{-1}$  and thus, contain elevated amounts of organic carbon but not enough for heterotrophic denitrification. If no organic substrate should be dosed, anammox bacteria (AMX) are needed for complete biological nitrogen removal. The application of the nitrification/anammox process has, for example, already been proposed as a cost efficient method for nitrogen removal from urine (Udert et al. 2008, Wilsenach and van Loosdrecht 2006). Stored urine has a theoretical COD/N ratio of approximately  $1 \text{ g COD}\cdot\text{g N}^{-1}$  (Udert et al. 2006) which can increase up to  $1.5 \text{ g COD}\cdot\text{g N}^{-1}$  (Bürgmann et al. 2011) due to ammonia volatilization during storage (i.e. a decrease of the ammonium concentration while the COD concentrations stays constant). AMX are also needed for a complete nitrogen removal in animal manure, especially piggery wastewater where the COD/N ratios can vary between  $4$  and  $6.5 \text{ g COD}\cdot\text{g N}^{-1}$ , but this is sometimes also too low to achieve complete denitrification (Bernet and Béline 2009). COD/N ratios of approximately  $1 \text{ g COD}\cdot\text{g N}^{-1}$  are also expected in the recently discussed integration of anammox into mainstream wastewater treatment (De Clippeleir et al. 2013, Winkler et al. 2012a).

The possible effects of COD on the nitrification/anammox process depend on the type of COD. Firstly, biodegradable organic carbon fosters the growth of heterotrophic bacteria (HET) which

compete with ammonia oxidising bacteria (AOB) for oxygen and with AMX for nitrite. Additionally, more heterotrophic growth will lead to a higher sludge production, which in turn often leads to a higher sludge loss, and thus to a decrease in the sludge retention time (SRT). Sludge loss is the total amount of sludge which leaves the system, i.e. the sludge in the effluent, the sludge in the samples and in case the SRT is regulated, also the sludge which is removed to maintain a certain SRT. A low SRT is particularly critical for the slowly growing AMX. Several studies reported decreasing AMX and AOB activities with high COD concentrations in the influent. Chamchoi et al. (2008) for instance, reported that AMX were outcompeted by HET when the COD/N ratio in the influent of a complete anoxic system was higher than 2.0 g COD·g N<sup>-1</sup> (SRT not mentioned). Zhu and Chen (2001) observed a 70% reduction of AOB activity when the influent COD/N ratio of a nitrification reactor was between 1.8 and 3.5 g COD·g N<sup>-1</sup> (SRT not mentioned). On the other hand, Desloover et al. (2011) successfully operated a partial nitrification reactor with an influent COD/N ratio of 3.70 g COD·g N<sup>-1</sup> (SRT 1.7 ± 0.5 d) and a subsequent anammox reactor with an influent COD/N ratio of 1.60 g COD·g N<sup>-1</sup> (SRT 46 d). None of these studies discussed whether competition for nitrite, oxygen or space (low SRT) caused the observed problems and which were the crucial factors for a successful operation with elevated COD/N influent ratios. Often, important information to judge this, as e.g. the SRT and the type of COD, is missing.

Secondly, specific organic compounds can also be directly toxic for AOB and AMX. Complete inhibition of AOB was for instance observed in the presence of 1000 mg·L<sup>-1</sup> propionate, 1000 mg·L<sup>-1</sup> butyrate, 2000 mg·L<sup>-1</sup> acetate (Gomez et al. 2000), 3.7 mg·L<sup>-1</sup> phenol or 1.3 mg·L<sup>-1</sup> cresol (Dyreborg and Arvin 1995). For AMX, Güven et al. (2005) observed a complete loss of activity in the presence of 23 mg·L<sup>-1</sup> methanol.

Thirdly, due to the ability of some anammox species to oxidise fatty acids while reducing nitrate (Güven et al. 2005, Kartal et al. 2007a), fatty acids could foster AMX activity and increase their competitiveness. Apparently, the fatty acids are not integrated into biomass but are instead oxidised to carbon dioxide, while the carbon for growth is fixed from CO<sub>2</sub> via acetyl-CoA. The oxidation of fatty acids might only occur for the conservation of energy, which could in turn lead to a higher biomass yield for AMX (Kartal et al. 2008), but this hypothesis has not yet been proven.

So far, one-stage nitrification/anammox systems have mainly been operated with influent COD/N ratios below 0.5 g COD·g N<sup>-1</sup>. In one of two studies which were performed with elevated COD/N influent ratios in biofilm systems, Chen et al. (2009) observed a significant reduction of the nitrogen removal efficiency (NRE) from 79% to below 52% when the influent COD/N ratio was increased from 0.5 to 0.75 g COD·g N<sup>-1</sup> (synthetic influent, type of COD and SRT not

mentioned). In contrast to this, Jia et al. (2012) achieved almost 95% total NRE with an influent COD/N ratio of 1.28 g COD·g N<sup>-1</sup> (synthetic solution with glucose, SRT not mentioned). In case of suspended sludge systems, Lackner and Horn (2013) reached 80-85% total nitrogen removal with an influent COD/N ratio of 1.00 ± 0.27 g COD·g N<sup>-1</sup> (wastewater with high COD concentration, but type of COD and SRT are not mentioned) in a sequencing batch reactor. In our own previous studies with a suspended sludge system and five-times diluted urine (1.4 -1.5 g COD·g N<sup>-1</sup>) we observed process instabilities (Udert et al. 2008) and a population shift to a new stable state characterised with a low nitrogen elimination rate and limited AMX activity (Bürgmann et al. 2011). In most of these studies the type of COD is not known and especially in case of urine, it is not possible to separate the influence of the elevated COD/N influent ratio from the influence of other wastewater compounds on the process.

Higher SRTs and having several zones with different redox conditions (oxic and anoxic zones) are advantages of biofilm systems for the slowly growing AMX. However, the handling and especially the start-up of suspended sludge systems is simpler, and most of the full-scale anammox applications in Switzerland are operated with suspended sludge (e.g. Joss et al. 2009). We therefore considered suspended sludge systems to be more relevant for practical applications and decided to use a suspended sludge system for our study. The goal of this study was to test the feasibility of the nitrification/anammox process for wastewaters with COD/N ratios of about 1.4 g COD·g N<sup>-1</sup>, which is relevant for stored urine. As acetate accounts for about 50% of the total COD in stored urine (Udert et al. 2013), we also wanted to test whether the oxidability of acetate provides a specific advantage for AMX. In order to minimise other influences from potentially toxic influent compounds, a sequencing batch reactor was operated with digester supernatant, which is a typical substrate for nitrification/anammox processes, and the influent COD/N ratio was increased stepwise up to 1.4 g COD·g N<sup>-1</sup> by adding increasing amounts of acetate. In the end, acetate was replaced with glucose, which supposedly cannot be degraded by AMX directly.

## **MATERIAL AND METHODS**

### **Reactor operation**

The lab-scale reactor was started with suspended biomass from a nitrification/anammox reactor treating sludge digester supernatant (WWTP Limmattal, Dietikon, Switzerland). This reactor is operated with hydrocyclones which enriches the granules (Wett et al. 2010). We collected a combined sample of the hydrocyclone under- and overflow that yielded an overall average volumetric particle size of 300 ± 6 µm. This mixture of granules and flocs is subsequently termed 'suspended biomass'. The initial concentration of volatile suspended solids (VSS) in the lab-scale reactor was ~ 4 g·L<sup>-1</sup>. In the first phase of the experiment, the sludge retention time

(SRT) was not controlled, i.e. sludge loss only occurred through washout in the effluent (the effluent withdrawal occurred at a constant depth) and sampling (for VSS concentration in the reactor and FISH samples). Subsequently, from day 129 onwards, the sludge from the effluent was returned to the reactor to increase the SRT. The SRT was calculated based on the VSS concentration in the reactor and the VSS loss per day. The reactor was operated with a liquid volume of 6.7 L and was equipped with sensors for online measurement of conductivity (Tetracon 325, WTW, Weilheim, Germany), dissolved oxygen (TriOxmatic 700, WTW, Weilheim, Germany), water level (Waterpilot FMX 167, Endress und Hauser, Reinach, Switzerland), pH, temperature, ammonia, nitrate and potassium (CAS40d, Endress und Hauser, Reinach, Switzerland). The reactor was fed with digester supernatant from the WWTP Werdhölzli in Zürich, Switzerland (composition see Table 1). The temperature was regulated at 30°C with a thermostat. pH was not controlled and fluctuated between 7.8 and 8.3 at the beginning of each cycle and 7.0 and 7.3 at the end.

**Table 1** Composition of the digester supernatant.

<b>Compound</b>	<b>Concentration (average <math>\pm</math> standard deviation)</b>	<b>Number of measurements</b>
<b>pH [-]</b>	8.3 $\pm$ 0.2	83
<b>Cond<sub>30°C</sub> [mS·cm<sup>-1</sup>]</b>	7.3 $\pm$ 0.3	83
<b>TIC [mg·L<sup>-1</sup>]</b>	710 $\pm$ 100	83
<b>NH<sub>4</sub><sup>+</sup> [mg N·L<sup>-1</sup>]</b>	740 $\pm$ 60	83
<b>NO<sub>2</sub><sup>-</sup> [mg N·L<sup>-1</sup>]</b>	< 0.50	22
<b>NO<sub>3</sub><sup>-</sup> [mg N·L<sup>-1</sup>]</b>	< 0.50	22
<b>COD [mg·L<sup>-1</sup>]</b>	140 $\pm$ 50	83
<b>COD<sub>inert</sub> [mg·L<sup>-1</sup>]</b>	180 $\pm$ 22	83
<b>PO<sub>4</sub><sup>3-</sup> [mg P·L<sup>-1</sup>]</b>	13 $\pm$ 3	22
<b>SO<sub>4</sub><sup>2-</sup> [mg·L<sup>-1</sup>]</b>	4.3 $\pm$ 0.1	2
<b>Cl<sup>-</sup> [mg·L<sup>-1</sup>]</b>	96 $\pm$ 2	2
<b>K<sup>+</sup> [mg·L<sup>-1</sup>]</b>	130 $\pm$ 9	12
<b>Na<sup>+</sup> [mg·L<sup>-1</sup>]</b>	230 $\pm$ 29	7
<b>Ca<sup>2+</sup> [mg·L<sup>-1</sup>]</b>	110 $\pm$ 40	5
<b>Mg<sup>2+</sup> [mg·L<sup>-1</sup>]</b>	20 $\pm$ 7	6

The reactor was operated in sequencing batch mode. After the feeding period (~ 3 min), a 20 min anoxic phase was followed by alternating aerobic (40 min) and anoxic phases (20 min) until the ammonia concentration decreased below 10 mg N·L<sup>-1</sup>. Afterwards, the sludge was



allowed to settle for 20 min prior to effluent withdrawal (~ 9 min). The effluent was withdrawn at a constant depth of 10 cm below the initial water level. Together with the sedimentation time of 20 min, this results in a minimum settling velocity of  $0.3 \text{ m}\cdot\text{h}^{-1}$ . The exchanged volume per cycle was 1.3 L, i.e. about 20% of the liquid volume present and the cycle time is varied between 8.5 and 18 h (Supporting Information S1). During aerobic phases, the reactor was aerated with  $81 \text{ mL}\cdot\text{min}^{-1}$  air, which resulted in average oxygen concentrations of  $0.07 \text{ mg}\cdot\text{L}^{-1}$ . On day 160, the aeration rate was accidentally increased from 81 to  $228 \text{ mL}\cdot\text{min}^{-1}$ . However, the average oxygen concentration did not change.

The influent COD/N ratio was increased in a stepwise manner every 2 weeks by adding the required volume of a sodium acetate solution (Figure 1). At first, sodium acetate was added to the influent tank (peak on day 14). However, with this method acetate was degraded in the influent tank, and the desired influent COD/N ratio could not be reached. In order to solve this problem, a separate pump (diaphragm metering pump, beta 4, ProMinent, Regensdorf, Switzerland) and tank were added for the sodium acetate solution. This pump was coupled to the influent pump (peristaltic pump, Vario Pumpsystem, Ismatec, Glattbrugg, Switzerland) which itself was coupled to a water level sensor. From day 159 onwards, the acetate was replaced by glucose maintaining a COD/N ratio of  $1.4 \text{ g COD}\cdot\text{g N}^{-1}$ .

### Sampling

Aliquots from the influent tank, the effluent tank, and the reactor were taken three times a week. Samples for the analysis of dissolved compounds were immediately filtered (MN GF-5, pore size  $0.45 \mu\text{m}$ , Macherey-Nagel, Düren, Germany) and stored in the fridge for 1-2 d prior to analysis. Total suspended solids (TSS) and VSS samples were processed immediately after sampling. Aliquots for the determination of the particle size distribution were taken on day 0, 115 and 194 and stored overnight prior to analysis. For the batch activity measurement, the necessary amount of sludge (based on the VSS concentration) was removed from the reactor immediately before the start of the experiment. Sludge samples for FISH analysis were taken once a week in triplicate.

### Batch activity measurements

For the batch activity measurements, biomass was taken from the reactor, washed once, and diluted with sodium phosphate buffer ( $0.01 \text{ mol}\cdot\text{L}^{-1}$ , pH 8.35) to a total volume of 0.6 L in order to obtain a VSS concentration of approximately  $1 \text{ g}\cdot\text{L}^{-1}$ . 1.2 mL of a trace element stock solution (Kuai and Verstraete 1998) was added. The temperature was kept at  $30^\circ\text{C}$ . For AMX activity tests, the reactor was closed and anaerobic conditions were established by sparging the solution with  $600 \text{ mL}\cdot\text{min}^{-1}$   $\text{N}_2$  gas containing 2%  $\text{CO}_2$  for 20 min prior to the experiment. The

pH was increased to 7.2 by adding NaOH solution and kept constant during the experiment ( $7.2 \pm 0.1$ ) by regulating the CO<sub>2</sub> flow (0-60 mL·min<sup>-1</sup>). 60 mg N·L<sup>-1</sup> of both NH<sub>4</sub><sup>+</sup> (NH<sub>4</sub>Cl) and NO<sub>2</sub><sup>-</sup> (NaNO<sub>2</sub>) were added, and liquid samples for the analysis of the nitrogen compounds were taken every 30 min for a total duration of 2 h. During the experiment, only the headspace was flushed with N<sub>2</sub> (540 mL·min<sup>-1</sup>) and 10-60 mL·min<sup>-1</sup> of 20% CO<sub>2</sub> in N<sub>2</sub> gas to keep the pH constant. After the 2 h, the anoxic phase continued until the NO<sub>2</sub><sup>-</sup> concentration reached values below 20 mg N·L<sup>-1</sup>. Then, the reactor was opened, the airflow was switched to synthetic air (80% N<sub>2</sub>, 20% O<sub>2</sub>), and the sludge was aerated until reaching at least 4 mg O<sub>2</sub>·L<sup>-1</sup> in order to determine the activity of AOB and nitrite oxidising bacteria (NOB). NH<sub>4</sub><sup>+</sup> (NH<sub>4</sub>Cl) was added to reach a minimum ammonia concentration of 80 mg N·L<sup>-1</sup>. Afterwards, aliquots were taken every 30 min for a total duration of 2 h for the analysis of the nitrogen compounds. Samples for the measurement of TSS and VSS were taken at the beginning (before AMX activity tests) and at the end (after AOB and NOB activity test) of each experiment. At the end of each batch experiment, the filtered sludge was returned to the reactor.

AMX (NH<sub>4</sub><sup>+</sup> consumption), AOB (NH<sub>4</sub><sup>+</sup> consumption), and NOB (NO<sub>3</sub><sup>-</sup> production) activities were calculated as the slopes from 5 data points using the least squares method. The measurement uncertainties of the resulting rate are given as the standard error of the calculated slopes. In order to determine the maximum possible activities in the sequencing batch reactor (SBR; mg N·L<sup>-1</sup>·d<sup>-1</sup>), the calculated values in mg N·gVSS<sup>-1</sup>·d<sup>-1</sup> were multiplied with the VSS concentration measured in the SBR on the same day.

In order to compare the AMX activity with the FISH data, we assumed that the conditions in the batch activity measurements allowed a maximum growth, that the assimilation of ammonium into biomass can be ignored due to the low yield of AMX, and thus that AMX quantities can be calculated with the measured rates as follows:

$$X_{AMX} = r_{NH4} \cdot \frac{Y_{AMX}}{\mu_{max,AMX}} \quad (1)$$

where  $X_{AMX}$  is the AMX concentration (mg COD·L<sup>-1</sup>),  $r_{NH4}$  is the measured maximum ammonia degradation rate (mg NH<sub>4</sub>-N·L<sup>-1</sup>·d<sup>-1</sup>),  $Y_{AMX}$  is the yield of AMX (mg COD·mg<sup>-1</sup> NH<sub>4</sub>-N), and  $\mu_{max,AMX}$  is the maximum growth rate of AMX (d<sup>-1</sup>). Yields and growth rates rather than substrate uptake rates ( $q_{max}$ ) were used for the calculations, because values for these two parameters are directly available in modelling studies. We used a maximum growth rate of 0.08 d<sup>-1</sup> and a yield of 0.159 g COD·g<sup>-1</sup> N according to Lackner et al. (2008). Some of the previous studies reported much faster growth rates for AMX with doubling times in the range of 2-4 d. However, it is not yet clear under which conditions AMX are able to grow that fast and doubling times in the range of 8-10 d have been reported far more often. The authors therefore think that

the use of a growth rate with a doubling time of 8.7 d is adequate in this case. For the conversion from  $\text{mg COD}\cdot\text{L}^{-1}$  to  $\text{mg VSS}\cdot\text{L}^{-1}$ , we assumed a biomass composition of  $\text{CH}_2\text{O}_{0.5}\text{N}_{0.15}$ , which results in a conversion factor of  $1.51 \text{ g COD}\cdot\text{g}^{-1} \text{ VSS}$ . As such,  $X_{\text{AMX}}$  ( $\text{mg VSS}\cdot\text{L}^{-1}$ ) =  $1.316 \cdot r_{\text{NH}_4}$ .

### Fluorescence *in situ* hybridization (FISH)

Biomass samples were fixed in a 4% paraformaldehyde solution, washed with phosphate-buffered saline, and stored in phosphate-buffered saline–ethanol (1:1) at  $-20^\circ\text{C}$  until further processing (Amann et al. 1990). Prior to hybridisation, the samples were diluted five times with PBS and homogenised by repeated drawings with a needle on a syringe (inner diameter 210  $\mu\text{m}$ ). Three 10  $\mu\text{L}$  aliquots of each sample were spotted on a Poly L-lysine coated slide. The oligonucleotide probes used are listed in the Supporting Information S2. For DAPI staining, 15  $\mu\text{L}$  of DAPI solution ( $0.33 \mu\text{g}\cdot\text{mL}^{-1}$  in ultra-pure water) was added to each spot, and the slides were incubated for 10 min at room temperature in the dark. Subsequently, the slides were washed with cold ( $4^\circ\text{C}$ ) ultra-pure water and dried at room temperature.

For microscopy, the slides were embedded with the embedding medium (Citifluor, Citifluor Ltd, Leicester, United Kingdom or Vectashield, Vector Laboratories Ltd, Peterborough, United Kingdom), covered with a cover slide, and analysed with an epifluorescence microscope (Axioskop 2 plus, Zeiss, Feldbach, Switzerland resp. DMI 6000B, Leica, Heerbrugg, Switzerland).

Four samples (day 4, 73, 157 and 194) were screened for the most common AMX types (probe sequences are listed in the Supporting Information S2). Clear signals in relevant quantities were only detected with Bfu613 and Amx820. Therefore, a combination of these two probes was used as an approximation for total AMX. The real amount of total AMX might be higher, as not all AMX types have yet been identified. However, based on the good agreement between the measured AMX quantities with FISH and the calculated AMX quantities from the batch activity measurements (Figure 3), the authors are confident that the main part of the present AMX were detected. Potential autofluorescence of “*Ca. Brocadia fulgida*” was tested and only registered in the FLUO channel. Because all AMX probes were used with Cy3 dye, the autofluorescence did not pose a problem in this study. The failure of AMX368, which is specific for all anammox bacteria including Bfu613, has also been observed by Liu et al. (2013).

For the quantification of “*Ca. Brocadia fulgida*” and ‘total AMX’, 15 pictures were taken at random locations and processed with the with ImageJ freeware (ImageJ 1.46r, Wayne Rasband, National Institutes of Health, USA). For the conversion of the measured quantities of AMX in % of total bacteria (DAPI) in  $\text{g VSS}\cdot\text{L}^{-1}$ , we assumed that the whole VSS mass in the reactor was active biomass. Thus we multiplied the measured percentages with the measured VSS concentrations in the reactor.

### Calculation of the sludge production

For the quantification of “*Ca. Brocadia fulgida*” and ‘total AMX’, 15 pictures were taken at random locations

The sludge production of AMX, AOB and HET was each calculated using the following formula, which can be derived from the biomass and the substrate mass balance (Supporting Information S3):

$$P_{Xi} = \frac{Q \cdot Y_i \cdot \Delta S_i}{1 + b_i \cdot SRT} \quad (2)$$

where  $P_{Xi}$  is the sludge production of bacteria  $i$  (mg VSS·d<sup>-1</sup>),  $Q$  is the flow rate (L·d<sup>-1</sup>),  $Y_i$  is the yield of bacteria  $i$  (mg COD·mg<sup>-1</sup> COD resp. mg COD·mg<sup>-1</sup> N),  $\Delta S_i$  is the degraded substrate by bacteria  $i$  (mg COD·L<sup>-1</sup> resp. mg N·L<sup>-1</sup>), and  $b_i$  is the endogenous respiration rate of bacteria  $i$  (d<sup>-1</sup>). Equation 2 is based on the assumption that the growth rate  $\mu$  is constant, which is not true in a SBR. However, the assumption is a good approximation if we consider average values over the whole cycle. Furthermore, as the exchange volume was rather low (about one-fifth of the reactor volume), concentration changes and thus also deviations from the average  $\mu$  over the cycle were also rather small.

The yields and the endogenous respiration rates used are listed in the Supporting Information S3. The total sludge production  $P_{X,tot}$  was then calculated as the sum of the sludge production by AMX, AOB, and HET.

### Analytical methods

NH<sub>4</sub><sup>+</sup> in the effluent and in the samples from the batch activity measurements was analysed on a flow injection analyser (Foss FIA star 5000, Rellingen, Germany). NH<sub>4</sub><sup>+</sup> in influent samples and COD were measured photometrically with vial tests (Hach Lange, Düsseldorf, Germany). NO<sub>2</sub><sup>-</sup> and NO<sub>3</sub><sup>-</sup> were analysed on an ion chromatograph (Compact IC 761, Metrohm, Herisau, Switzerland). TSS and VSS were determined according to standard methods (American Public Health Association 2005).

Particle size distribution analysis was performed on a mastersizer (Mastersizer 2000, Malvern Instruments Ltd, Malvern, United Kingdom). Samples were dispersed in water in the Hydro 2000s module until a laser obscuration of 10-15% was established prior to the measurement. The measurement range was 0.5 µm -2 mm. Each sample was analysed in triplicate.

## RESULTS

### Nitrogen removal

During the operation with digester supernatant and acetate addition, the NER remained stable at a level of  $270 \pm 30 \text{ mg N}\cdot\text{L}^{-1}\cdot\text{d}^{-1}$  (Figure 1). Following the switch from acetate to glucose on day 159, a significant change of the NER occurred when the NER reached values in the range of  $370 \pm 25 \text{ mg N}\cdot\text{L}^{-1}\cdot\text{d}^{-1}$ . This increase of the NER was most likely due to the (accidental) increase of the aeration rate on day 160. The increased nitrite effluent concentrations on day 161 and 164 (unbalance between AMX and AOB activity due to the increased availability of oxygen) support this hypothesis. As it was not the goal of this study to maximise the NER, the aeration rate was kept constant during the operation with acetate, and this most likely did not provide enough oxygen for the maximum nitrogen removal capacity of the reactor.

During the whole operation phase, the nitrogen removal efficiency (NRE) gradually increased from  $87.9 \pm 3.9\%$  with pure digester supernatant to  $94.9 \pm 0.6\%$  with acetate addition and finally to  $98.0 \pm 1.0\%$  with glucose addition (Figure 1). This coincided with a gradual decrease of the nitrate effluent concentration from above  $100 \text{ mg N}\cdot\text{L}^{-1}$  with pure digester supernatant to  $29.2 \pm 3.2 \text{ mg N}\cdot\text{L}^{-1}$  with acetate addition and finally to  $9.4 \pm 4.2 \text{ mg N}\cdot\text{L}^{-1}$  during the last operation phase with glucose addition.

### Activity measurements of nitrifiers and anammox bacteria

The maximum activities of AMX, AOB, and NOB are given in Figure 2. The AMX activity gradually decreased from an initial value of  $840 \text{ mg NH}_4^+\text{-N}\cdot\text{L}^{-1}\cdot\text{d}^{-1}$  with digester supernatant down to  $160 \text{ mg NH}_4^+\text{-N}\cdot\text{L}^{-1}\cdot\text{d}^{-1}$  after 6 weeks at an influent COD/N ratio of  $1.4 \text{ g COD}\cdot\text{g N}^{-1}$  with acetate. This decreasing AMX trend was countered by the increase of the SRT on day 129, which resulted in activities of 225 and  $220 \text{ mg NH}_4^+\text{-N}\cdot\text{L}^{-1}\cdot\text{d}^{-1}$  3 and 4 weeks after the SRT increase, respectively. After the change to glucose on day 159, the maximum AMX activity further increased to 275 and  $353 \text{ mg NH}_4^+\text{-N}\cdot\text{L}^{-1}\cdot\text{d}^{-1}$ .

The AOB activity increased from  $320 \text{ mg NH}_4^+\text{-N}\cdot\text{L}^{-1}\cdot\text{d}^{-1}$  with digester supernatant to  $1695 \text{ mg NH}_4^+\text{-N}\cdot\text{L}^{-1}\cdot\text{d}^{-1}$  after 2 weeks with an influent COD/N ratio of  $1.4 \text{ g COD}\cdot\text{g N}^{-1}$  with acetate. Afterwards, the AOB activity reached a stable level of around  $1830 \text{ mg NH}_4^+\text{-N}\cdot\text{L}^{-1}\cdot\text{d}^{-1}$  and was not influenced by the increase of the SRT on day 129 or the switch from acetate to glucose on day 159. The lower value on day 115 was probably an outlier.

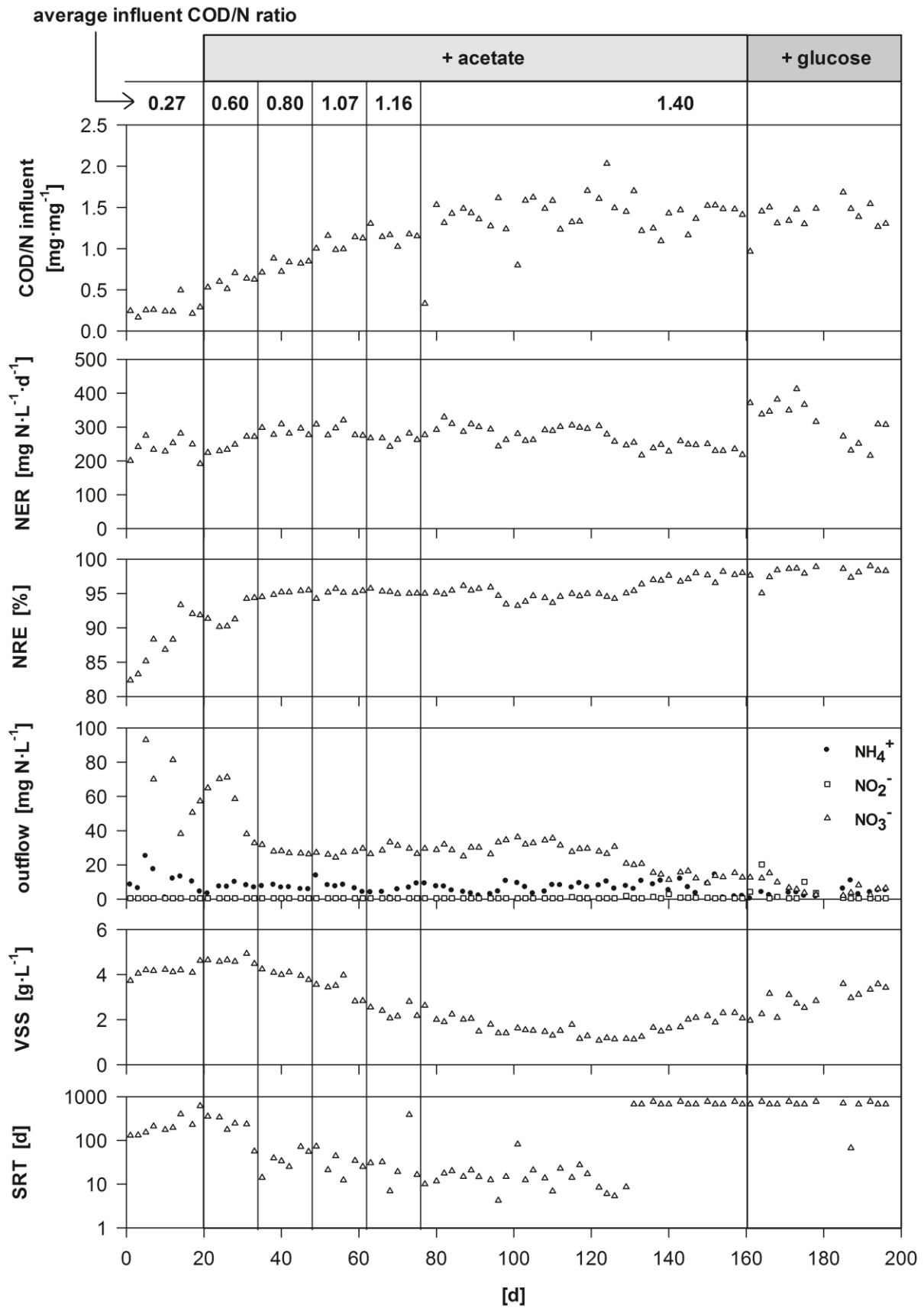


**Figure 1** SBR performance, including the nitrogen elimination rate (NER) and the nitrogen removal efficiency (NRE), during operation with pure digester supernatant and increasing influent COD/N ratios due to acetate and glucose addition.

The NOB activity developed very similarly to the AMX activity. After an initial increase from 410 mg NO<sub>3</sub>-N·L<sup>-1</sup>·d<sup>-1</sup> with digester supernatant to 860 mg NO<sub>3</sub>-N·L<sup>-1</sup>·d<sup>-1</sup> at an influent COD/N ratio of 0.6 g COD·g N<sup>-1</sup>, the maximum NOB activity continuously decreased to 350 mg NO<sub>3</sub>-N·L<sup>-1</sup>·d<sup>-1</sup> after 6 weeks at an influent COD/N ratio of 1.4 g COD·g N<sup>-1</sup>. However, after the increase of the SRT on day 129, NOB activity decreased to an even lower level of around 185 mg NO<sub>3</sub>-N·L<sup>-1</sup>·d<sup>-1</sup>. Similar to the AMX activity, NOB activity was not influenced by the switch from acetate to glucose on day 159

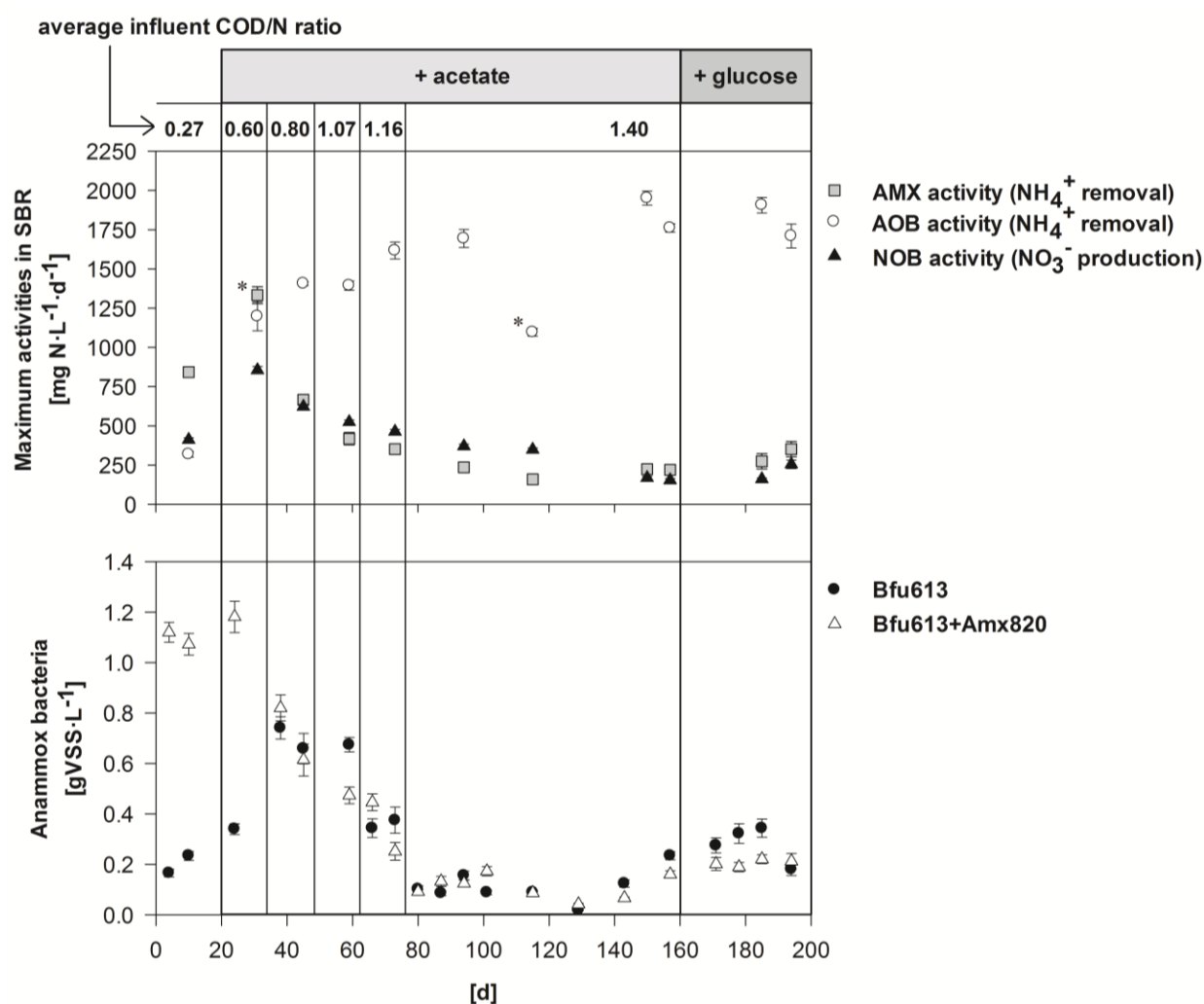


**Figure 2** Maximum AMX, AOB and NOB activities in the SBR measured in batch experiments, and quantification of AMX with FISH. Both were recalculated based on the VSS concentration at the moment of sampling. Outliers are marked with a star.

During the whole operation, the maximum NOB activity was relatively high and in the same range as the anammox activity. However, compared to the batch activity measurements where conditions for NOB were ideal with oxygen concentrations of at least 4 mg·L<sup>-1</sup>, very little oxy-

gen was available in the reactor. Regarding an average oxygen concentration around  $0.066 \text{ mg}\cdot\text{L}^{-1}$  and a half saturation constant of  $2.2 \text{ mg}\cdot\text{L}^{-1}$  (Lackner et al. 2008), the actual NOB activity in the reactor was on average only  $\sim 3\%$  of the maximum NOB activity. The actual NOB activity in the reactor was thus considered to be negligible for the total N turnover.

### **Anammox bacteria abundance**

The results from the FISH measurements are displayed in Figure 2. “*Ca. Brocadia fulgida*” increased from  $\sim 0.2 \text{ g VSS}\cdot\text{L}^{-1}$  during the operation with digester supernatant to  $\sim 0.7 \text{ g VSS}\cdot\text{L}^{-1}$  with an influent COD/N ratio of  $0.8 - 1.07 \text{ g COD}\cdot\text{g N}^{-1}$ . The increase of “*Ca. Brocadia fulgida*” together with the decrease of ‘total’ AMX (estimated with Bfu613+Amx820) indicates that “*Ca. Brocadia fulgida*” was able to out-compete other AMX types relatively quickly (40 d), and this is probably due to its ability to oxidise acetate. Afterwards, with an influent COD/N ratio of 1.16 and  $1.4 \text{ g COD}\cdot\text{g N}^{-1}$ , “*Ca. Brocadia fulgida*” continuously decreased to a minimum of  $0.04 \text{ g VSS}\cdot\text{L}^{-1}$  on day 129 but remained the dominant type of AMX, even after the switch from acetate to glucose on day 159.

In Figure 3, we plotted the measured AMX quantities with FISH against the calculated AMX quantities from the batch activity measurements. Because the measured maximum AMX activity on day 31 was much higher than the other activities (Figure 2) and also much too high for the corresponding quantity that was measured with FISH (most right point in Figure 3), this point is considered to be an outlier. The slope of a straight line that best fits the remaining ten points in Figure 3 according to the least square method was calculated to be  $1.05 \pm 0.09$ . In our study, the measured AMX quantities with FISH thus correlated surprisingly well (correlation coefficient 0.973) with the results from the batch activity measurements. However, it should be kept in mind that the uncertainty of FISH and activity based biomass estimations is high. Several assumptions contribute to the considerable uncertainty, e.g. the values of the growth rate and the yield of AMX was assumed based on literature values and the exact amount of active VSS is not known.

### **Organic substrate removal**

Based on the assumption that the yield of HET with acetate is much higher than the yield of AMX with acetate, we expected that an involvement of AMX in acetate oxidation could be demonstrated based on the sludge production in different scenarios. All three scenarios assume a complete autotrophic nitrogen removal and negligible NOB activity. Scenario 1 assumes a complete heterotrophic COD removal, while scenarios 2 and 3 assume a maximum possible COD oxidation by AMX (Supporting Information S4) and heterotrophic degradation of the remaining COD.



For heterotrophic COD removal, the yield was assumed to be the average value for COD removal with oxygen, nitrite and nitrate (Supporting Information S5). Due to the very low oxygen concentration, AMX activity and HET denitrification cannot be excluded during aerobic phases. It is therefore not possible to gain any information on the degradation pathways based on oxygen mass transfer data and cycle measurements. Furthermore, in single-stage nitrification/anammox processes with elevated COD/N influent ratios, it is generally not possible to assess the activities of the different bacterial groups based on mass balances.

To our knowledge, the effect of acetate oxidation on the yield of AMX has not yet been determined. Apparently, acetate is not integrated into biomass, but the oxidation probably occurs for the conservation of energy, which could lead to a higher biomass yield for AMX. For this study, we assumed that the true yield of AMX with acetate oxidation is between zero and the AMX yield with ammonia ( $0.159 \text{ g COD} \cdot \text{g N}^{-1}$ ; Strous et al. (1998)). These values are based on the assumption that, as ammonia is their main substrate, the AMX yield with ammonia is maximised and it is therefore unlikely, that the AMX yield with acetate is higher. As ammonia and acetate oxidation produce the same amount of energy per electrons released, we converted the normal AMX yield with ammonia to  $0.093 \text{ g COD} \cdot \text{g COD}^{-1}$  based on the electrons released during the two reactions (Supporting Information S3). We then calculated scenario 2 with no biomass growth and scenario 3 with the normal AMX yield of  $0.093 \text{ g COD} \cdot \text{g COD}^{-1}$  as the two extreme scenarios.

The measured and the calculated sludge productions for the three scenarios are displayed in Figure 4. However, the sludge production in all three scenarios was relatively similar, and there was no clear difference between complete heterotrophic acetate degradation (scenario 1) and an involvement by AMX (scenario 2 and 3). Furthermore, the measured sludge production was much higher than the calculated ones for the three scenarios, which could have been due to higher actual yields and/or lower actual endogenous respiration rates than the ones used for the calculation (Supporting Information S3). Therefore, this approach did not allow us to judge the involvement of AMX in acetate oxidation, but it did show that the sludge production exceeded stoichiometric expectations.

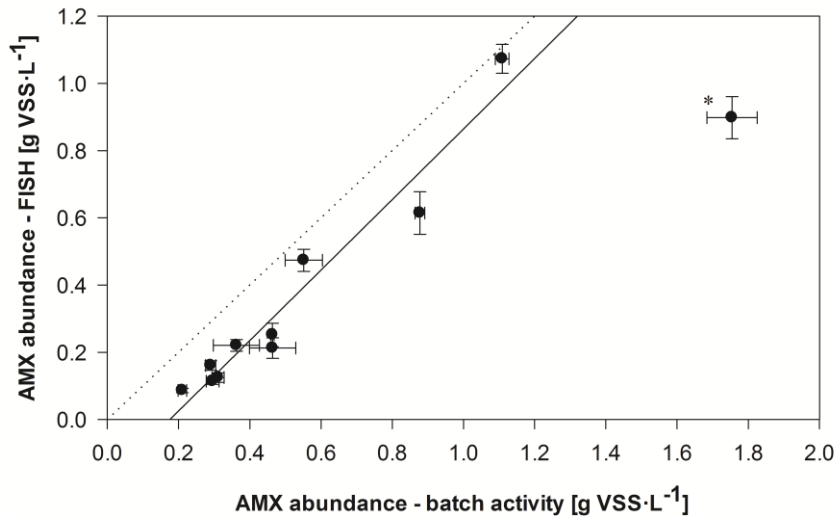


**Figure 3** Comparison of AMX abundance as calculated from the batch activity measurements and FISH with a linear regression (continuous line,  $y = 1.048 \cdot x - 0.184$ ,  $R^2 = 0.947$ ). For a perfect correlation, points would have to be on the dotted line. The data point marked with a star is considered to be an outlier. The error bars represent the standard deviations.

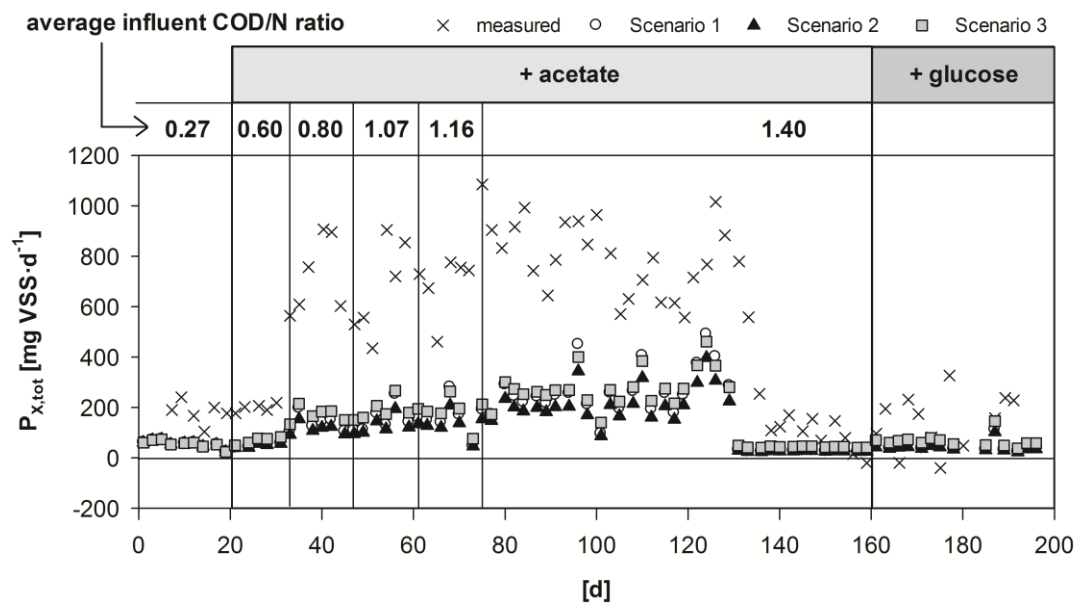


**Figure 4** Measured and calculated total sludge production for three different scenarios. Scenario 1 assumed that all COD was degraded by HET. Scenarios 2 and 3 assumed a maximum possible COD oxidation by AMX, with a zero and normal AMX yield, respectively.

### Sludge retention time

During the start-up phase with digester supernatant, the SRT increased from 130 d to ~ 350 d (Figure 1). Subsequently, when the influent COD/N ratio was increased, the SRT rapidly dropped to values below 50 d. At the same time, sludge washout in the effluent increased (Supporting Information S6). Based on visual observations, this was due to an increase of the sludge level at the end of the sedimentation phase and, thus cannot be attributed only to the turbidity of the supernatant.

Because the SRT was not controlled, and sludge loss only occurred through washout in the effluent and sampling, and because the sedimentation time and the sludge withdrawal regime was not changed, a decrease of the SRT was expected due to increasing heterotrophic growth with increasing availability of COD. However, a simultaneous decrease of the VSS concentration in the reactor (Figure 1) showed that the decrease of the SRT must have been, at least partly, caused by worse settleability of the sludge. The worse settleability could be due to a decrease of the particle size (Figure 5).

Between the beginning of the operation (day 1) and day 115, the average particle size decreased from  $300 \pm 6 \mu\text{m}$  to  $104 \pm 3 \mu\text{m}$ . Because smaller particles settle more slowly than bigger ones with the same density, the decreased floc size probably caused a general lower settleability. An influence of inorganic solids can be excluded because the VSS/TSS ratio remained constant during the whole operation period ( $0.843 \pm 0.033 \text{ g VSS} \cdot \text{g TSS}^{-1}$ ).

From day 129 onwards, the sludge from the effluent was returned to the reactor in order to increase the SRT. This resulted in an average SRT of  $702 \pm 48 \text{ d}$  for the remaining operation period.

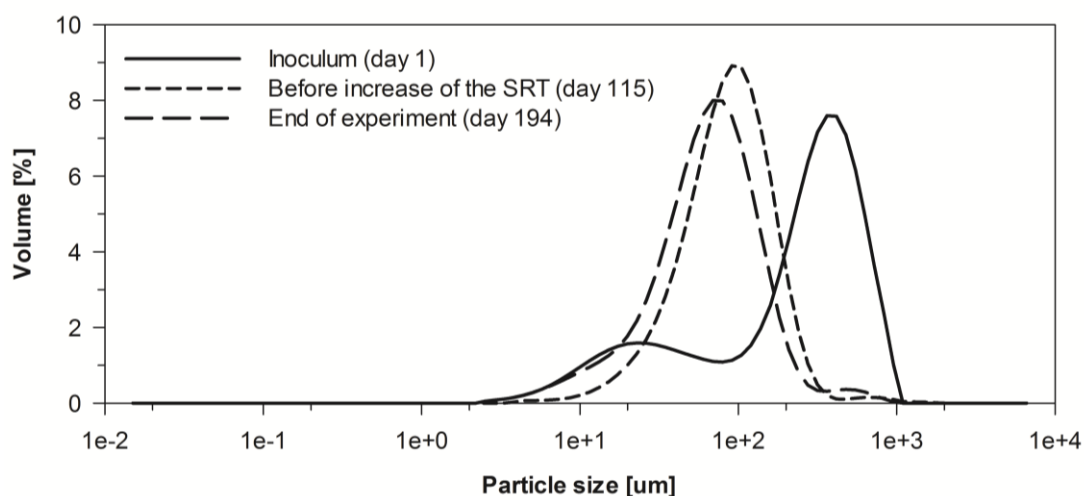


**Figure 5** Particle size distributions at different time points during the SBR operation.

## DISCUSSION

### Influence of the COD/N ratio on nitrogen removal

Despite the increasing influent COD/N ratio, the decreasing SRT, and the changing bacterial activities, the NER remained stable and was thus not influenced by the increase of the influent COD/N ratio from pure digester supernatant up to 1.4 g COD·g N<sup>-1</sup> with acetate. In contrast to this, the NRE clearly increased with increasing influent COD/N ratio. This was expected because the additional COD allows more denitrification of the nitrate produced by AMX.

Assuming no significant NOB activity and that all nitrogen is converted via nitrification/anammox, an influent COD/N ratio of 0.31 g COD·g N<sup>-1</sup> would already be sufficient to denitrify all nitrate produced by AMX (11% nitrate production, 2.86 g COD·g<sup>-1</sup> NO<sub>3</sub>-N, assuming complete COD degradation). Based on the influent COD/N ratio, complete denitrification should thus be possible from day 21 on (Figure 1). However, because this was a mixed aerobic/anoxic system, part of the COD would also have been degraded with oxygen. Furthermore, while the nitrate is produced continuously during the whole cycle, COD is only added once in the beginning, and it was rapidly degraded during the first 1-2 h of each cycle, part of it also with oxygen. These two factors can explain why denitrification was still incomplete at an influent COD/N ratio of 1.4 g COD·g N<sup>-1</sup>.

### Nitrite removal by AMX, HET and NOB

Batch experiments and FISH data indicated that the maximum AMX activity decreased in the SBR. According to Monod kinetics, this decrease of the maximally possible activity could have been balanced out by higher substrate concentrations, but ammonia and nitrite concentrations were similar in all cycles. Therefore, the actual activity of the AMX in the SBR must have decreased as well.

One possible explanation for decreasing AMX activity is increasing competition for nitrite by HET with increasing availability of COD. Because the NER remained constant up to the maximum influent COD/N ratio of 1.4 g COD·g N<sup>-1</sup> with acetate (day 1 - day 159; Figure 1) but the actual AMX activity in the SBR decreased, heterotrophic denitrification must have increased in order to still achieve the same nitrogen removal. This is supported by the fact that the actual AOB activity in the reactor, and thus the nitrite production, increased as well (because ammonia, nitrite and oxygen concentrations were similar in all cycles it can be assumed that the actual AOB activity developed proportionally to the maximum activity in Figure 2).

However, simultaneous to the decrease of the AMX activity and the increase of denitrification by HET, the SRT strongly decreased (Figure 1). Thus, the decrease of the AMX activity and abundance might also have been due to wash out, which could occur as soon as the SRT is lower

than the inverse of the actual growth rate of AMX. The fact that AMX activity started to increase again as soon as a high SRT was established by sludge recycling from day 129 onwards suggests, that the decrease of AMX activity was at least partly due to the decrease of the SRT. Furthermore, this increase clearly shows that AMX are able to stay in the system and compete with HET up to influent COD/N ratios of 1.4 g COD·g N<sup>-1</sup> if the SRT is high enough. However, the remaining experiment was too short to reach the initial high activity of AMX. Therefore, it remains unclear to what extent the AMX activity decreased due to competition by HET.

NOB activity developed very similarly to the AMX activity and also decreased with increasing COD/N ratio respectively decreasing SRT (Figure 2). This indicated that NOB also suffered from the increased competition by HET for nitrite and, because their actual growth rate was limited by nitrite, NOB were also affected by the decreasing SRT. However, in contrast to AMX activity, NOB activity did further decrease after the SRT was increased by sludge recycling from day 129 onwards. This could mean that AMX were mainly affected by the SRT decrease while the competition for nitrite by HET was more significant for NOB.

The initial presence of NOB can be explained with the fact that the inoculum was taken from a reactor which was operated with digester supernatant. Due to the lower availability of biodegradable COD, HET denitrification was low and therefore more nitrite was available for NOB. Therefore, NOB were able to grow in the original reactor and thus present in the inoculum. The fact that they sustained over longer periods in our reactor can be explained with the high initial SRT. Even with the lowest average SRT of 17 d and zero net growth (i.e. endogenous respiration equals growth), it would take 40 d for a 90% reduction of the NOB population.

### **Acetate oxidation by anammox bacteria**

Previous studies have shown that “*Ca. Brocadia fulgida*” is able to oxidise acetate and outcompetes other AMX types in the presence of acetate (Kartal et al. 2008, Winkler et al. 2012a, Winkler et al. 2012b). Our study confirmed that “*Ca. Brocadia fulgida*” was able to outcompete other AMX types in the presence of acetate (Figure 2). However, the dominance of “*Ca. Brocadia fulgida*” alone does not prove that AMX participated in acetate oxidation.

Because the sludge production in all three tested scenarios was very similar (Figure 4), it was not possible to prove or exclude an involvement of AMX in acetate oxidation based on the sludge production. The fact that “*Ca. Brocadia fulgida*” remained the dominant type of AMX after the switch from acetate to glucose does not support an involvement of AMX in acetate degradation. Güven et al. (2005) tested the influence of glucose on AMX and did not find any positive or adverse effect. Thus, it is not likely that AMX are able to oxidise glucose. If AMX and specifically “*Ca. Brocadia fulgida*” would have had an advantage with acetate, this should have resulted in a lower activity with glucose, probably also coupled with a switch of the domi-

nant type of AMX. The increasing trend of AMX activity can be explained with the increased SRT. Whether glucose would support another AMX type cannot be judged with our experiment, because the experiment was too short for another type of AMX to reach significant concentrations.

### **Causes for the decrease of the sludge retention time**

A high SRT is essential for the slowly growing AMX. A decrease of the SRT due to higher sludge production of HET with an increasing influent COD/N ratio could thus be critical for AMX. Indeed, the SRT rapidly decreased in our study and reached values in the range of the minimally required SRT for AMX. The lower SRT was caused by worse settleability of the sludge. However, the worse settleability of the sludge was not due to increased HET sludge production but was caused by a decrease of the floc size.

There are two possible reasons for the observed decrease of the floc size. First of all, the reactor from where the inoculum was taken was equipped with hydrocyclones and thus selecting for dense and coarse particles. The different operating conditions in the reactor used for this study, e.g. the low shear forces, might have induced a mechanical breakup of the bigger particles. Secondly, HET mainly grow in small and light flocs due to their fast growth. Therefore, the decrease of the SRT might still have been caused by HET, but rather due to the quality of the flocs than due to the amount of the produced biomass.

Based on our own observation, an elevated influent COD/N ratio does not necessarily cause a decrease of the SRT. During the operation of a one-stage nitrification/anammox process with five times diluted urine in the same sequencing batch reactor (Bürgmann et al. 2011), the average SRT was 170 d even though the biomass concentration was with an average of  $8.7 \text{ g TSS}\cdot\text{L}^{-1}$  much higher than in this study (average influent COD/N ratio of  $1.5 \pm 0.3 \text{ g COD}\cdot\text{g N}^{-1}$ ; constant minimum settling velocity). The sodium and the chloride concentrations of five times diluted urine are around 2.5 respectively 8.5 times higher than in digester supernatant and Fernández et al. (2008) showed that sodium chloride can increase the settleability (anammox process with activated sludge). A high salinity might thus be beneficial for the treatment of wastewaters with elevated influent COD/N ratios. However, in case of Schaubroeck et al. (2012), higher sodium chloride concentrations led to a higher proportion of small aggregates coupled to nitrite accumulation, and thus had a negative effect on the process.

In cases where the SRT reaches critical values for AMX, there are a number of measures to increase the SRT. Apart from the option chosen in this study (returning all sludge from the effluent back into the reactor), an increase of the SRT might also be achieved with a longer sedimentation time or by increasing the settleability of the sludge. The latter could be achieved by using another reactor setup, which allows the formation of larger or denser flocs or of granules.

While the mechanisms for aerobic (Adav et al. 2008) and anaerobic (Hulshoff Pol et al. 2004) granulation are well known, the exact physical or chemical triggers for granulation in one-stage nitrification/anammox systems are not clear yet Vlaeminck et al. (2010).

## CONCLUSIONS

Based on the results of our study we conclude the following:

- Nitrification/anammox with influent COD/N ratios of  $1.4 \text{ g COD} \cdot \text{g N}^{-1}$ , which is similar to the typical ratio for stored urine ( $1.5 \text{ g COD} \cdot \text{g N}^{-1}$ ), is feasible provided a sufficiently high SRT is maintained.
- The observed decrease of the SRT was the most critical factor for the slowly growing AMX. As the VSS concentration in the reactor decreased and the minimum settling velocity remained constant, the SRT decrease was not caused by a higher sludge production. Instead, the sludge settleability decreased due to a decrease of the average floc size. Potential reasons for this were increased HET growth in small flocs and the breakup of bigger particles, presumably due to different operational conditions compared to the inoculum reactor.
- The availability of acetate quickly and strongly influenced the anammox community. “*Ca. Brocadia fulgida*” became the dominant AMX type, which is most probably due to its ability to oxidise acetate. It was, however, not possible to prove nor exclude an involvement of AMX in acetate oxidation based on the sludge production.
- The switch from acetate to glucose addition did not negatively influence the activity of “*Ca. Brocadia fulgida*”. This suggests that “*Ca. Brocadia fulgida*” can also successfully compete with HET in the presence of other types of COD as long as the organic compounds are not toxic.

## ACKNOWLEDGEMENTS

This work was financed by the Swiss National Science Foundation. Siegfried E. Vlaeminck was supported with a postdoctoral fellowship from the Research Foundation Flanders (FWO Vlaanderen). We thank Brian Sinnet for the particle size distribution measurements, Alexandra Hug and Hanspeter Zöllig for their help with the sampling, and Karin Rottermann and Claudia Bänniger for their support in the laboratory.





## **SUPPORTING INFORMATION**

### **FOR CHAPTER 3**

#### **Successful application of nitrification/anammox to wastewater with elevated organic carbon to ammonia ratios**

Sarina Jenni, Siegfried E. Vlaeminck, Eberhard Morgenroth, Kai M. Udert

*Water Research, 2014, 49, 316-326*

## S1 Cycle time

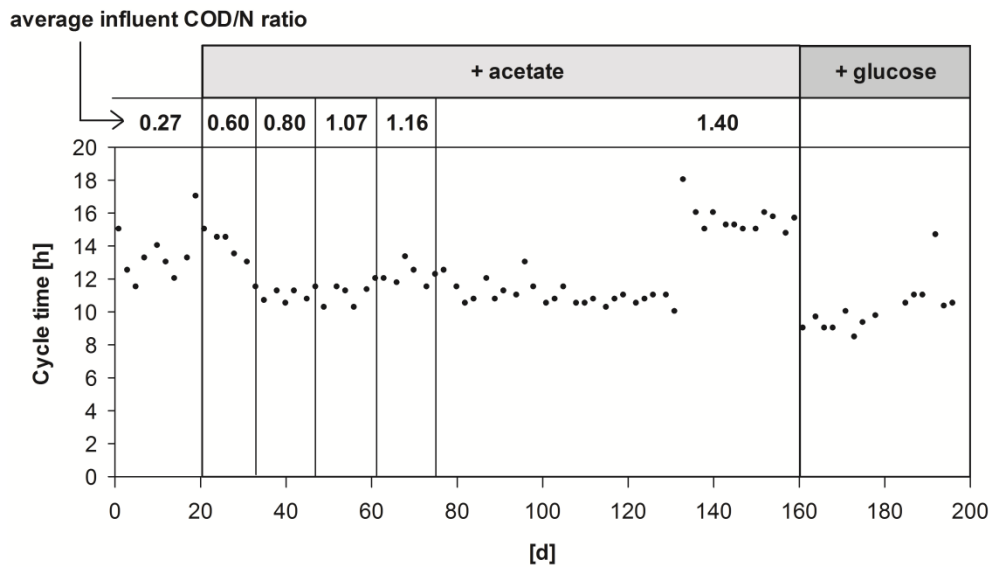


**Figure S1** Cycle time during the whole experiment.

## S2 Oligonucleotide probes

**Table S1** Oligonucleotide probes used for the screening of AMX, sequences according to Loy et al. (2003).

Probe	Target organism(s)
Amx368	Ca. Brocadia, Ca. Kuenenia and Ca. Scalindua
Amx820	Ca. Brocadia anammoxidans and Ca. Kuenenia stuttgartiens
Amx1015	Ca. Brocadia anammoxidans
Amx1240	Ca. Brocadia anammoxidans
Amx1900	Ca. Brocadia anammoxidans and Ca. Kuenenia stuttgartiens
Apr820	Ca. Anammoxoglobus propionicus
Ban162	Ca. Brocadia anammoxidans
Bfu613	Ca. Brocadia fulgida
BS820	Ca. Scalindua wangeri and Ca. Scalindua sorokinii
Kst157	Ca. Kuenenia stuttgartiensis
Kst1275	Ca. Kuenenia stuttgartiensis
Sca1309	Ca. Scalindua
Scabr1114	Ca. Scalindua brodae

### S3 Sludge production

The rate of substrate concentration change due to utilization by bacteria can be calculated as:

$$r_{su} = -\frac{\mu_{max}}{Y} \cdot \frac{S}{K_S + S} \cdot X$$

where  $r_{su}$  is the rate of substrate concentration change ( $\text{mg S}\cdot\text{L}^{-1}\cdot\text{d}^{-1}$ ),  $\mu_{max}$  is the maximum growth rate of the bacteria ( $\text{d}^{-1}$ ),  $Y$  is the yield of the bacteria ( $\text{mg COD}\cdot\text{mg S}^{-1}$ ),  $X$  is the bacteria concentration ( $\text{mg COD}\cdot\text{L}^{-1}$ ),  $S$  is the substrate concentration ( $\text{mg}\cdot\text{L}^{-1}$ ) and  $K_S$  is the half saturation constant for substrate  $S$  ( $\text{mg}\cdot\text{L}^{-1}$ ).

The growth rate of the bacteria can be formulated as:

$$r_g = \mu_{max} \cdot \frac{S}{K_S + S} \cdot X - b \cdot X$$

where  $r_g$  is the growth rate of the bacteria ( $\text{mg COD}\cdot\text{L}^{-1}\cdot\text{d}^{-1}$ ) and  $b$  is the endogenous respiration rate of the bacteria ( $\text{d}^{-1}$ ).

The mass balance for substrate utilisation is:

$$\frac{dS}{dt} \cdot V = Q \cdot \Delta S + \frac{\mu_{max}}{Y} \cdot \frac{S}{K_S + S} \cdot X \cdot V$$

where  $V$  is the reactor volume (L),  $Q$  is flowrate ( $\text{L}\cdot\text{d}^{-1}$ ) and  $\Delta S$  is the degraded amount of substrate  $S$  ( $\text{mg}\cdot\text{L}^{-1}$ ). Assuming steady state, this equation can be solved for the biomass concentration  $X$  as:

$$X = \frac{1}{HRT} \cdot \frac{\Delta S \cdot Y}{\mu_{max} \cdot \frac{S}{K_S + S}}$$

where  $HRT$  is the hydraulic retention time.

Assuming that the influent does not contain any biomass, the biomass mass balance is:

$$\frac{dX}{dt} \cdot V = (Q_e \cdot X_e - Q_s \cdot X_s) + \left( \mu_{max} \cdot \frac{S}{K_S + S} - b \right) \cdot X \cdot V$$

where  $Q_e$  is the effluent flowrate ( $\text{L}\cdot\text{d}^{-1}$ ),  $X_e$  is the concentration of biomass in the effluent ( $\text{mg VSS}\cdot\text{L}^{-1}$ ),  $Q_s$  is the sampling volume ( $\text{L}\cdot\text{d}^{-1}$ ) and  $X_s$  is the concentration of biomass in the sampling volume ( $\text{mg VSS}\cdot\text{L}^{-1}$ ). Assuming steady state, this equation can be transferred to

$$\mu_{max} \cdot \frac{S}{K_S + S} = \frac{1}{SRT} + b$$

where SRT is the sludge retention time (d).

If we substitute this equation into the above equation for the biomass concentration  $X$ , we get:

$$X = \frac{SRT}{HRT} \cdot \frac{\Delta S \cdot Y}{1 + b \cdot SRT}$$

In steady state, the total biomass production of a reactor can be expressed as:

$$P_{X,tot} = \frac{X_{tot} \cdot V}{SRT}$$

where  $P_{X,tot}$  is the total sludge production ( $\text{mg COD} \cdot \text{d}^{-1}$ ) and  $X_{tot}$  is the total sludge concentration in the reactor ( $\text{mg COD} \cdot \text{L}^{-1}$ ). Assuming that the total sludge in a reactor is a homogenous mixture of different types of bacteria, this equation can also be used to calculate the sludge production of any type of bacteria present in the reactor:

$$P_{X,i} = \frac{X_i \cdot V}{SRT}$$

where the concentration of bacteria  $X_i$  can be substituted with the above equation for  $X_i$ :

$$P_{X,i} = \frac{Q \cdot Y_i \cdot \Delta S_i}{1 + b_i \cdot SRT}$$

For the conversion of  $\text{mg COD} \cdot \text{d}^{-1}$  to  $\text{mg VSS} \cdot \text{d}^{-1}$ , we assumed a biomass composition of  $\text{C}_5\text{H}_7\text{O}_2\text{N}$  for HET and AOB respectively  $\text{CH}_2\text{O}_{0.5}\text{N}_{0.15}$  for AX, which results in conversion factors of  $1.42 \text{ g COD} \cdot \text{g VSS}^{-1}$  and  $1.51 \text{ g COD} \cdot \text{g VSS}^{-1}$ , respectively.

The yields and the endogenous respiration rates that were used for the calculation of the sludge productions are composed in the following table. The yield of AMX during acetate oxidation was calculated from the normal AMX yield during ammonium oxidation based on the produced electrons during ammonium and acetate oxidation, respectively. The half reactions according to Metcalf and Eddy (2003) are:



During ammonium oxidation,  $3/14$  mole  $e^-$  are released per g N. The normal AMX yield of  $0.159 \text{ g COD} \cdot \text{g N}^{-1}$  can thus be converted to  $0.742 \text{ g COD} \cdot \text{mole } e^{-1}$ . Together with an electron release of  $1/8$  mole  $e^-$  per g COD (1 mole acetate equals 64 g COD) during acetate oxidation, this results in a maximum yield of  $0.093 \text{ g COD} \cdot \text{g COD}^{-1}$  for AMX during acetate oxidation.

**Table S2** Yields end endogenous respiration rates for the calculation of the sludge production of HET, AOB and AMX.

	Y	Unit	Reference	b	Unit	Reference
HET with acetate	0.591	g COD·g COD <sup>-1</sup>	SI S5	0.62	d <sup>-1</sup>	Lackner et al. (2008)
HET with glucose	0.726	g COD·g COD <sup>-1</sup>	SI S5	0.62	d <sup>-1</sup>	Lackner et al. (2008)
AOB	0.15	g COD·g N <sup>-1</sup>	Lackner et al. (2008)	0.13	d <sup>-1</sup>	Lackner et al. (2008)
AMX	0.159	g COD·g N <sup>-1</sup>	Lackner et al. (2008)	0.003	d <sup>-1</sup>	Lackner et al. (2008)
AMX	0.093	g COD·g COD <sup>-1</sup>	calculated			

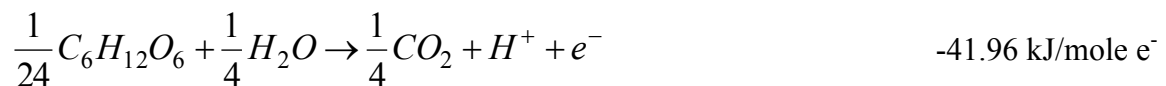
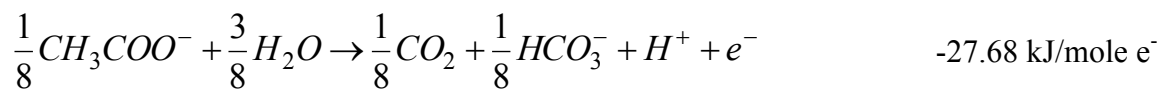
#### S4 Maximum possible COD oxidation by AMX

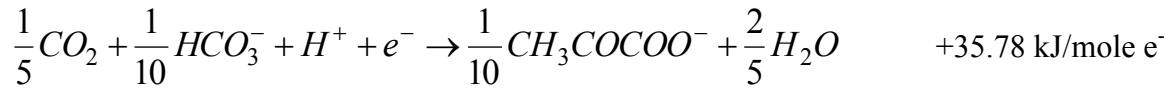
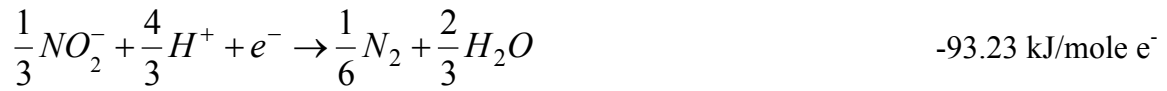
According to the stoichiometry of the AMX reaction (Strous et al. 1998), AMX produce 0.26 mole nitrate per mole ammonium degraded. Assuming a complete autotrophic nitrogen removal and neglecting NOB activity, the maximum possible nitrate production can be calculated.

Since the exact stoichiometry of acetate oxidation by AMX is not known, we decided to calculate the required amount of nitrate reduced per amount of acetate oxidised based on the COD difference between nitrate and ammonium, which is 4.57 g COD·g N<sup>-1</sup>. Together with the maximum possible nitrate production, this allows to estimate the maximum possible acetate oxidation by AMX.

#### S5 Yield of heterotrophic bacteria

The yield of heterotrophic bacteria with acetate and with glucose was calculated according to the procedure in Metcalf and Eddy (2003). The calculation based on the following oxidation and reduction reactions:





The energy released from the oxidation reduction reactions  $\Delta G_R$  can be calculated by combining the oxidation reaction with the respective reduction reactions and are composed in the following table for heterotrophic growth with acetate or glucose as substrate as well as oxygen, nitrite and nitrate as electron acceptors.

**Table S3** Energy released from the oxidation (acetate and glucose) reduction (oxygen, nitrite and nitrate) reactions  $\Delta G_R$  in kJ/mole  $e^-$ .

	oxygen	nitrite	nitrate
acetate	105.82	120.91	99.35
glucose	120.10	135.19	113.63

The free energy to convert one electron equivalent of the carbon source to cell material  $\Delta G_S$  (kJ/mole  $e^-$ ) can be calculated with the following equation:

$$\Delta G_S = \frac{\Delta G_P}{K^m} + \Delta G_C$$

where  $\Delta G_P$  is the free energy to convert one electron equivalent ( $e^-$  eq) of the carbon source to the pyruvate intermediate (kJ/ $e^-$  eq),  $K$  is the fraction of energy transfer captured (-),  $m$  is +1 if  $\Delta G_P$  is positive and -1 if energy is produced (-) and  $\Delta G_C$  is the free energy to convert one electron equivalent of pyruvate intermediate to one electron equivalent of cells (kJ/ $e^-$  eq).

The value of  $\Delta G_C$  is +31.41 kJ/ $e^-$  eq (McCarty 1975),  $K$  is 0.6 and  $\Delta G_P$  can be calculated from combining the oxidation of acetate resp. glucose to carbon dioxide with the reduction of carbon dioxide to pyruvate as 8.10 kJ/mole  $e^-$  and -6.18 kJ/mole  $e^-$ , respectively.

The fraction of  $e^-$  mole of substrate used for cell synthesis per  $e^-$  mole of substrate used  $f_s$  (-) resp. the yield can then be calculated by combining the following two equations:

$$K \cdot \Delta G_R \cdot \frac{f_e}{f_s} = -\Delta G_S$$

$$f_e + f_s = 1$$

where  $f_e$  is  $e^-$  mole of substrate oxidised per  $e^-$  mole of substrate used (-) and solving them for  $f_s$ :

$$f_s = \frac{1}{1 + \frac{-\Delta G_S}{K \cdot \Delta G_R}}$$

The so calculated yields of HET growth for the substrates acetate and glucose and the different electron acceptors oxygen, nitrite and nitrate are composed in the following table.

**Table S4** Yields of HET growth for the substrates acetate and glucose and the three different electron acceptors oxygen, nitrite and nitrate as well as the average yield for all three electron acceptors in  $\text{g COD} \cdot \text{g COD}^{-1}$ .

	oxygen	nitrite	nitrate	average
acetate	0.585	0.618	0.570	0.591
glucose	0.723	0.745	0.711	0.726

For the calculations in this chapter we assumed that HET consumed all three electron acceptors with the same ratio and thus average yields of  $0.591 \text{ g COD} \cdot \text{g COD}^{-1}$  for acetate and  $0.726 \text{ g COD} \cdot \text{g COD}^{-1}$  for glucose.

## S6 VSS loss with the effluent

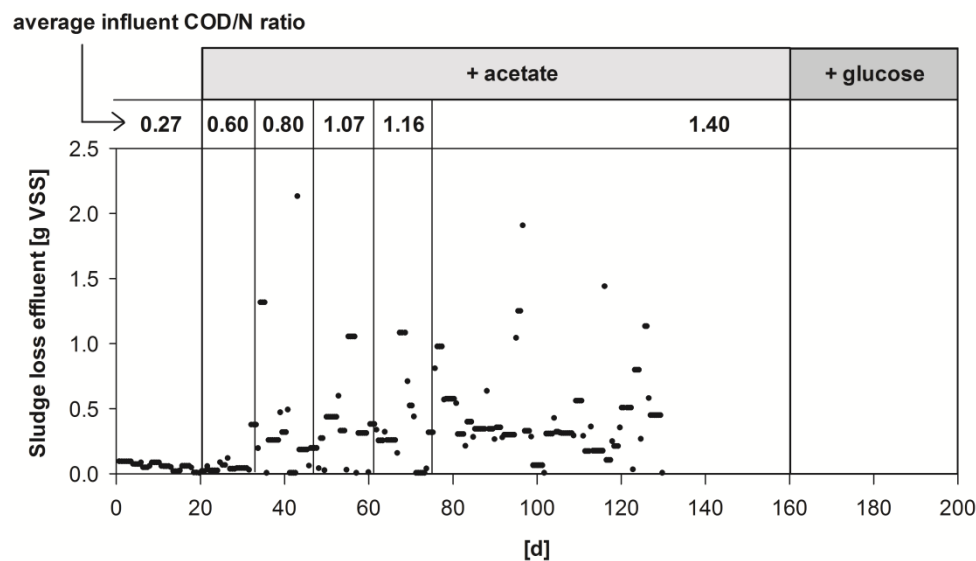


**Figure S2** VSS loss per effluent. From day 129 on, the sludge in the effluent was returned to the reactor in order to increase the SRT.





## **CHAPTER 4**

### **Temperature dependence and interferences of NO and N<sub>2</sub>O microelectrodes used in wastewater treatment**

Sarina Jenni, Joachim Mohn, Lukas Emmenegger, Kai M. Udert

*Environmental Science & Technology*, 2012, 46(4), 2257-2266

# Temperature dependence and interferences of NO and N<sub>2</sub>O microelectrodes used in wastewater treatment

Sarina Jenni<sup>1</sup>, Joachim Mohn<sup>2</sup>, Lukas Emmenegger<sup>2</sup>, Kai M. Udert<sup>1</sup>

*1: Eawag, Swiss Federal Institute for Aquatic Science and Technology, 8600 Dübendorf, Switzerland*

*2: Empa, Swiss Federal Laboratories for Materials Science and Technology, 8600 Dübendorf, Switzerland*

## ABSTRACT

Electrodes for nitric and nitrous oxide have been on the market for some time, but have not yet been tested for an application in wastewater treatment processes. Both sensors were therefore assessed with respect to their (non)linear response, temperature dependence and potential cross sensitivity to dissolved compounds, which are present and highly dynamic in nitrogen conversion processes (nitric oxide, nitrous oxide, nitrogen dioxide, ammonia, hydrazine, hydroxylamine, nitrous acid, oxygen and carbon dioxide). Off-gas measurements were employed to differentiate between cross sensitivity to interfering components and chemical nitric oxide or nitrous oxide production. Significant cross sensitivities were detected for both sensors: by the nitrous oxide sensor to nitric oxide and by the nitric oxide sensor to ammonia, hydrazine, hydroxylamine and nitrous acid. These interferences could, however, be removed by correction functions. Temperature fluctuations in the range of  $\pm 1^\circ\text{C}$  lead to artefacts of  $\pm 3.5\%$  for the nitric oxide and  $\pm 3.9\%$  for the nitrous oxide sensor and can be corrected with exponential equations. The results from this study help to significantly shorten and optimise the determination of the correction functions and are therefore relevant for all users of nitric and nitrous oxide electrodes.

## INTRODUCTION

Emissions of nitric oxide (NO) and nitrous oxide (N<sub>2</sub>O) have been frequently observed during nitrogen removal in wastewater treatment plants (Gustavsson and La Cour Jansen 2011, Kampschreur et al. 2009b, Weissenbacher et al. 2010). Both gases are critical atmospheric pollutants: N<sub>2</sub>O is a potent contributor to global warming (Solomon et al. 2007) and the most important ozone-depleting substance in the stratosphere (Ravishankara et al. 2009). NO is rapidly oxidised in the troposphere. Its product, nitrogen dioxide (NO<sub>2</sub>) is a precursor of ozone and is, together with sulphur dioxide (SO<sub>2</sub>), responsible for acid rain. In addition to its negative effects

on the atmosphere, NO is toxic for bacteria (Zumft 1993) and can lead to severe process instabilities in wastewater treatment (Fux et al. 2006).

NO and N<sub>2</sub>O can be produced by ammonium-oxidising bacteria, nitrite-oxidising bacteria and denitrifying bacteria. While NO is an intermediate in the anammox process, N<sub>2</sub>O does not seem to play a role in the anammox metabolism (Kampschreur et al. 2009a). Among other factors, high ammonium (NH<sub>4</sub><sup>+</sup>) and nitrite (NO<sub>2</sub><sup>-</sup>) concentrations can cause imbalances in the microbial processes and lead to the accumulation of NO and N<sub>2</sub>O (Wunderlin et al. 2012a). Whereas novel nutrient removal strategies from high-strength nitrogen wastewaters potentially improve the effluent quality and the efficiency of wastewater treatment, there is thus a risk that the environmental problem is displaced from water bodies to the atmosphere (Kampschreur et al. 2009a).

To control emissions from wastewater treatment more effectively, much research has been done recently into the causes of NO and N<sub>2</sub>O production. Both substances are usually analysed in the off-gas: NO is usually measured with chemoluminescence detectors (Udert et al. 2005, Yu et al. 2010) or Fourier transform infrared spectroscopy (Joss et al. 2009), while N<sub>2</sub>O is generally quantified by gas filter correlation (Udert et al. 2005, Yu et al. 2010), gas chromatography with an electron capture detector (Kampschreur et al. 2008b) or Fourier transform infrared spectroscopy (Joss et al. 2009). Off-gas measurements require reactor setups with a continuous gas flow to strip the target species. This can be problematic, particularly during anoxic/anaerobic periods: the purge gas not only strips NO and N<sub>2</sub>O, but also other gaseous compounds. The stripping of carbon dioxide (CO<sub>2</sub>) in particular can change the chemical conditions considerably. Time delays are another problem of indirect measurements in the gas phase, as they can hamper the effective detection of short but crucial peaks (Kampschreur et al. 2008b, Schreiber et al. 2009).

In view of these limitations of off-gas measurements, NO and N<sub>2</sub>O analysis in the liquid phase with Clark-type microsensors can be an attractive alternative. The most important advantages of liquid phase measurements are that they allow differentiating between production and emission of the two gases (Ahn et al. 2010) as well as measuring concentration gradients in stratified (e.g. biofilm) reactors. Electrodes for NO and N<sub>2</sub>O measurement have been on the market for some time, and both sensors have already been applied to measurements in wastewater treatment plants (Fux et al. 2006, Kampschreur et al. 2008b, Schreiber et al. 2009), in sediments (Meyer et al. 2008, Schreiber et al. 2008), as well as in medical research (Hetrick and Schoenfisch 2009). In NO sensors, the NO is generally oxidised at the anode because possible severe interferences from oxygen reduction make the reductive approach undesirable (Bedioui and Villeneuve 2003) while N<sub>2</sub>O is usually reduced at the cathode in the N<sub>2</sub>O sensor (Andersen et al. 2001).

In principle, any substance which can pass through a silicone membrane and whose reduction potential is higher or lower than the microsensor potential can interfere with the NO or N<sub>2</sub>O measurement. Both sensors have already been tested for interference with a few compounds (Andersen et al. 2001, Schreiber et al. 2008). However, these tests were not designed for sensor applications to nitrogen conversion processes in high-strength wastewater. Thus, many compounds of the nitrogen cycle were not considered or only at very low concentrations. Furthermore, to our knowledge, the temperature dependence of the two sensors has not yet been systematically described in the literature. However, this is a fundamental precondition for many applications, because the temperature can change by several degrees during nitrogen removal processes due to diurnal changes in the ambient temperature or the heat produced by the biological process itself (Joss et al. 2009).

The aim of this study was thus to test common NO and N<sub>2</sub>O microsensors with respect to their application during nitrogen removal from high-strength nitrogen wastewater. This involved a general characterisation of the sensors (linearity, temperature dependence) and the quantification of their cross-sensitivity to compounds with high variability during nitrogen removal processes: NO, N<sub>2</sub>O, NO<sub>2</sub>, ammonia (NH<sub>3</sub>), nitrous acid (HNO<sub>2</sub>), hydroxylamine (NH<sub>2</sub>OH), hydrazine (N<sub>2</sub>H<sub>4</sub>), oxygen (O<sub>2</sub>) and carbon dioxide (CO<sub>2</sub>).

## **EXPERIMENTAL SECTION**

### **Microsensors**

The N<sub>2</sub>O microsensor (Unisense A/S, Aarhus, Denmark) used was a Clark-type sensor with an internal reference and a guard cathode. It was connected to a high-sensitivity picoammeter (PA 2000, Unisense A/S, Aarhus, Denmark) and a voltage of -0.80 V was applied between the cathode and the internal reference electrode (material not known). The measurement medium and the picoammeter were ground connected with a wire. Driven by the external partial pressure, N<sub>2</sub>O from the solution penetrated through the silicone membrane at the sensor tip and was reduced at the metal cathode surface. The flow of electrons from the N<sub>2</sub>O reducing cathode to the anode, measured in [pA], reflects the N<sub>2</sub>O partial pressure in front of the sensor tip. Capacitors (Unisense A/S, Aarhus, Denmark) were used to minimise the noise caused by other electronic equipment. Prior to all measurements, the sensors had to be pre-activated by applying a voltage of -1.30 V for 5 minutes and pre-polarised at -0.80 V for at least 12 h to obtain a stable output signal. During this period, the internal guard cathode scavenged any oxygen that may have accumulated in the electrolyte. The sensor was also equipped with an oxygen front guard which contains an alkaline solution in which O<sub>2</sub> is reduced (Unisense 2010a).

The basic principle of the NO microsensor (Unisense A/S, Aarhus, Denmark) used in this study is described by Schreiber et al.<sup>16</sup> In our experiments, the NO sensor was polarised at +1.25 V (PA 2000 or Microsensor Multimeter, both from Unisense A/S, Aarhus, Denmark) in order to oxidise NO at the anode. In order to remove NO and other oxidisable compounds from the electrode electrolyte, the anode had to be polarised at +1.25 V against the internal reference electrode (material not known) for at least 12 h or until the signal was stable before the measurement started (Unisense 2010b).

The response time of the setup used in this study was determined as the time required to reach 90% of the new equilibrium signal (40, 80 and 160 ppm NO or N<sub>2</sub>O, starting from zero). The limit of quantitation and the limit of detection were determined by measuring eight different concentrations for each sensor and analysing the resulting data series at a confidence level of 95% according to Funk et al. (1985).

Most NO sensors tested in this study had a tip diameter of 100 µm. The system specific response time was  $140 \pm 30$  s (one sensor tested, response time independent of the concentration). The limits of quantitation and detection (one sensor tested) were  $3.64 \cdot 10^{-4}$  mgN·L<sup>-1</sup> and  $2.43 \cdot 10^{-4}$  mgN·L<sup>-1</sup>, respectively. The sensors used to measure the temperature dependence in digester supernatant had a wider diameter: 500 µm. Their system specific response time was  $84 \pm 28$  s (three sensors tested, response time independent of the concentration).

In the case of the N<sub>2</sub>O sensor, most sensors tested in this study had a tip diameter of 100 µm and a system specific response time of  $30 \pm 5$  s (one sensor tested, response time increases slightly with the N<sub>2</sub>O concentration). The limit of quantitation and detection (one sensor tested) were  $1.00 \cdot 10^{-2}$  mgN·L<sup>-1</sup> and  $8.02 \cdot 10^{-3}$  mgN·L<sup>-1</sup>, respectively. A newer type of the sensor, specifically built for wastewater applications, was used to determine the temperature dependence in digester supernatant and the interference from NO. These sensors had a tip diameter of 500 µm and a system specific response time of  $28 \pm 22$  s (three sensors tested, response time independent of the concentration). The limit of quantitation and detection (three sensors tested) were  $1.38 \cdot 10^{-3} \pm 7.73 \cdot 10^{-4}$  mgN·L<sup>-1</sup> and  $9.22 \cdot 10^{-4} \pm 5.18 \cdot 10^{-4}$  mgN·L<sup>-1</sup>, respectively.

### **Experimental setup for electrode measurements**

The measurements were carried out in a 1.7 L glass reactor. This was stirred magnetically and the temperature was regulated with a thermostat. The reactor was equipped with sensors for oxygen (O<sub>2</sub>) (Oxi 340, WTW, Weilheim, Germany or LDO HQ20, Hach Lange, Düsseldorf, Germany), pH (pH 340, WTW, Weilheim, Germany) and temperature (LDO HQ20, Hach Lange, Düsseldorf, Germany or pH 196, WTW, Weilheim, Germany). Mass flow controllers (Vögtlin Instruments, Aesch BL, Switzerland) were applied to adjust the gas flow through the reactor.

## Solutions

Nearly all experiments were conducted in 0.1 M sodium phosphate buffer solutions (pH 7). The temperature dependence, however, was determined in this buffer solution and in digester supernatant taken from the wastewater treatment plant Werdhölzli in Zurich, Switzerland (the composition and the pretreatment can be found in the Supporting Information S1).

The substance to be tested was either added as salt or the solution was sparged with the respective gas. The following salts were used:  $\text{NaH}_2\text{PO}_4 \cdot \text{H}_2\text{O}$  ( $\geq 99\%$ , Sigma Aldrich, Buchs, Switzerland),  $\text{Na}_2\text{HPO}_4 \cdot \text{H}_2\text{O}$  ( $\geq 98\%$ , Sigma Aldrich, Buchs, Switzerland),  $\text{NH}_2\text{OH} \cdot \text{HCl}$  ( $\geq 99\%$ , Sigma Aldrich, Buchs, Switzerland),  $\text{NaNO}_2$  ( $\geq 99\%$ , Merck, Zug, Switzerland),  $\text{NH}_4\text{Cl}$  ( $\geq 99.8\%$ , Merck, Zug, Switzerland),  $\text{N}_2\text{H}_4 \cdot \text{H}_2\text{SO}_4$  ( $> 99\%$ , Sigma Aldrich, Buchs, Switzerland). All gases had a purity of  $\pm 2\%$  and were supplied by Messer Schweiz AG (Lenzburg, Switzerland): high purity nitrogen gas, 10 ppm  $\text{NO}_2$  in  $\text{N}_2$ , 90 ppm  $\text{N}_2\text{O}$  in  $\text{N}_2$ , 5001 ppm  $\text{N}_2\text{O}$  in  $\text{N}_2$ , 91 ppm  $\text{NO}$  in  $\text{N}_2$ , 901 ppm  $\text{NO}$  in  $\text{N}_2$ , 2500 ppm  $\text{NO}$  in  $\text{N}_2$ , 10%  $\text{NO}$  in  $\text{N}_2$ , 10%  $\text{CO}_2$  in  $\text{N}_2$ , synthetic air (20.5%  $\text{O}_2$  in  $\text{N}_2$ ). Apart from the experiment for oxygen interference, all experiments were performed in anoxic solutions (purging with  $1 \text{ L} \cdot \text{min}^{-1} \text{ N}_2$ ), so that any chemical reactions between dissolved compounds and oxygen can be excluded.

## Concentration units

Concentrations in [ppm] refer to the concentration in the gas which was used to sparge the solution, and concentrations in [ $\text{mgN} \cdot \text{L}^{-1}$ ] to the concentration in the liquid phase. Assuming equilibrium, the concentration in the gas  $C_G$  can be calculated from the concentration in the liquid phase  $C_L$  with the dimensionless Henry coefficient  $H$  as follows:

$$C_G = C_L \cdot H \quad (1)$$

$C_G$  Concentration in the gas phase [ $\text{mg} \cdot \text{L}^{-1}$ ]

$C_L$  Concentration in the liquid phase [ $\text{mg} \cdot \text{L}^{-1}$ ]

The conversion from [ $\text{mg} \cdot \text{L}^{-1}$ ] to [ppm] can be performed as follows:

$$C_G[\text{ppm}] = C_G[\text{mg} \cdot \text{L}^{-1}] \cdot \frac{1}{M} \cdot \frac{R \cdot T}{p} \cdot 10^6 \quad (2)$$

$M$  Molecular weight [ $\text{g} \cdot \text{mol}^{-1}$ ]

$R$  Universal gas constant  $8.3145 \text{ [J} \cdot \text{mol}^{-1} \cdot \text{K}^{-1}]$

$T$  Temperature [K]

$p$  Pressure [Pa]

The average atmospheric pressure in Dübendorf is 96.650 kPa. Together with the pressure of the water column (the sensors were mounted 10 cm below the water surface), this results in a pressure of 97.630 kPa which was used for the conversion of the concentrations measured in this study. For converting the literature values where no pressure was given, we used standard pressure (101.325 kPa).

As the Henry coefficient depends on the temperature, the same  $C_G$  corresponds to different  $C_L$  at different temperatures. The inverse of the Henry coefficient, the absorption coefficient  $k_H$ , can be calculated as follows as a function of the temperature (the values for  $k_{H,i}(T_0)$  and  $B$  can be found in the Supporting Information S2):

$$k_{H,i}(T) = k_{H,i}(T_0) \cdot \exp\left(B \cdot \left(\frac{1}{T} - \frac{1}{T_0}\right)\right) \quad (3)$$

$k_{H,i}(T_0)$  Absorption coefficient of compound  $i$  at  $T_0 = 298.15$  K [ $\text{mol} \cdot \text{L}^{-1} \cdot \text{bar}^{-1}$ ]

$B$  Temperature dependence constant [K]

$T$  Temperature [K]

The dimensionless Henry coefficient can be calculated from the absorption coefficient as follows:

$$H_i = \frac{1}{k_{H,i} \cdot R \cdot T \cdot 10^2} \quad (4)$$

$R$  Universal gas constant 8.314 [ $\text{J} \cdot \text{mol}^{-1} \cdot \text{K}^{-1}$ ]

$T$  Temperature [K]

### Coefficient of variation

The accuracy of all calibration and correction curves was assessed with the coefficient of variation of the method  $v_{X0}$  (in [%]). We decided to use  $v_{X0}$  instead of the more common coefficient of determination  $R^2$  because  $v_{X0}$  is a measure of the precision of the measurement method and directly reflects the expected standard deviation of a sample with a concentration that lies in the middle of the calibration range. By contrast,  $R^2$  is a measure of how much the calculated standard curve deviates from the measured standards. The calibration curves and their sensitivities can be found in the Supporting Information S3.

$$v_{X0} = \frac{s_{X0}}{\bar{x}} \cdot 100 = \frac{s_y / E}{\bar{x}} \cdot 100 \quad (5)$$

$s_{X0}$  Standard deviation of the method

$\bar{x}$	Mean of concentrations
$s_y$	Residual standard deviation
$E$	Sensitivity of the calibration curve = $\left. \frac{dy}{dx} \right _{\bar{x}}$
$x$	Concentration or temperature
$y$	Measured signal

### Linearity of sensor response

The linearity of the sensor response (signal change per concentration change) was determined in sodium phosphate buffer (pH 7) sparged with different concentrations of NO or N<sub>2</sub>O in N<sub>2</sub> gas (one N<sub>2</sub>O and one NO sensor tested). For both gases, eight different concentrations were measured starting from ~10% in equidistant steps up to 100% of the maximal expected concentration. The measurements were conducted at  $25.2 \pm 0.1^\circ\text{C}$ .

The standard deviation of the residuals (measured minus calculated signals) of a linear (ISO 8466-1) and a non-linear (ISO 8466-2) calibration function were used to calculate the difference of the variances  $DS^2$ .  $DS^2$  and the variance of the non-linear calibration function  $s_{y2}$  were then submitted to an F-test to determine whether there was a significant difference between both calibrations: if so, the non-linear calibration curve leads to a significantly better adjustment and must be used instead of the linear calibration function.

$$DS^2 = (N - 2) \cdot s_{y1}^2 - (N - 3) \cdot s_{y2}^2 \quad (6)$$

$N$	Number of data points
$s_{y1}$	Residual standard deviation obtained by linear regression calculation
$s_{y2}$	Residual standard deviation obtained by non-linear regression calculation

### Temperature dependence

The signal of the sensors consists of a zero current (i.e. the current in an NO and N<sub>2</sub>O free environment) and a signal that depends on the amount of NO and N<sub>2</sub>O (target signal) present. The temperature dependence of the zero currents  $Z$  of both sensors was determined in sodium phosphate buffer (pH 7) for a temperature range of 10 - 30°C (one N<sub>2</sub>O and two NO sensors tested). The measurements started at 10°C and the temperature was slowly increased to 30°C within 3 h. The solutions were sparged with dinitrogen gas and did not contain any N<sub>2</sub>O or NO.



The temperature dependence of the signal caused by the actual target compounds NO or N<sub>2</sub>O (target signal  $U$ ) was tested by measuring the signals of the sensors at different temperatures (10/15/20/25/30°C) in a sodium phosphate buffer (pH 7; one N<sub>2</sub>O and NO sensor tested) and in digester supernatant (three N<sub>2</sub>O and three NO sensors tested). The solutions were sparged with different mixtures of NO or N<sub>2</sub>O and N<sub>2</sub>. Target concentrations were 0, 500, 2500 and 4500 ppm N<sub>2</sub>O with digester supernatant and 0, 100, 500 and 900 ppm N<sub>2</sub>O (phosphate buffer) or NO (digester supernatant and phosphate buffer).

The parameters of the expected equations were estimated with the computer software R (version 2.12.0, R foundation for Statistical Computing; Venables et al. (2009)) using the “optim” function with the “Nelder-Mead” method (Nelder and Mead 1965).

For unknown reasons, the zero current of the N<sub>2</sub>O sensor was slightly negative during these experiments. To describe the data with an exponential curve, a constant offset of 1 pA was added before the fit.

### **Interfering substances**

Possible interferences with the gases NO<sub>2</sub>, N<sub>2</sub>O, NO, CO<sub>2</sub> and O<sub>2</sub> were tested by first measuring the zero currents of the NO and N<sub>2</sub>O electrodes (buffer solution (pH 7) sparged with 1000 mL·min<sup>-1</sup> N<sub>2</sub>) and then repeating the measurements in buffer solution (pH 7) that was saturated with the maximum concentrations as given in Table 1 (sparged with 1000 mL·min<sup>-1</sup>). The measurements were conducted at 25.0 ± 0.2°C. Because NO interfered with the N<sub>2</sub>O measurement, eight equidistant concentrations were measured (four sensors tested) so that the linearity of the interference could be assessed (according to the method described in "Linearity of sensor response").

The N<sub>2</sub>O and NO concentrations in the off-gas were analysed by FTIR spectroscopy (Gasmeter CX-4000, Temet Instruments, Helsinki, Finland, equipped with a heated (40°C) flow-through gas cell with 9.8 m path-length, 1 min<sup>-1</sup> measurement frequency; Mohn et al. (2008)). Details of the FTIR measurement and the experimental setup can be found in the Supporting Information S4.

**Table 1** Maximum reference concentrations and tested concentrations of potentially interfering substances.

	<b>Maximum reference concentration</b>	<b>Type of process</b>	<b>Reference</b>	<b>Maximum tested concentration</b>
<b>NO<sub>2</sub></b>	5.80·10 <sup>-4</sup> mgN·L <sup>-1</sup>	Two-reactor nitrification-anammox system with reject water	Kampschreur et al. (2008a)	3.03·10 <sup>-3</sup> mgN·L <sup>-1</sup> (10 ppm)
	1.70·10 <sup>-3</sup> mgN·L <sup>-1</sup>	Test effect of NO <sub>2</sub> with bacteria on agar plates	Mancinelli and McKay (1983)	
<b>N<sub>2</sub>O</b>	1.68 mgN·L <sup>-1</sup>	Combined C/N/P removal from synthetic municipal wastewater	Meyer et al. (2005)	3.34 mgN·L <sup>-1</sup> (5000 ppm)
	2.67 mgN·L <sup>-1</sup>	Two-reactor nitrification-anammox system with reject water	Kampschreur et al. (2008a)	
<b>NO</b>	9.20·10 <sup>-3</sup> mgN·L <sup>-1</sup>	Nitrification/anammox with five-times diluted urine	Own unpublished data	6.07·10 <sup>-2</sup> mgN·L <sup>-1</sup> (2500 ppm)
	3.00·10 <sup>-2</sup> mgN·L <sup>-1</sup>	Batch experiments with heterotrophic bacteria in a citrate nutrient medium	Anderson et al. (1993)	
<b>CO<sub>2</sub></b>	100 mgC·L <sup>-1</sup>	Nitrification/anammox with five-times diluted urine	Own unpublished data	38.5 mgC·L <sup>-1</sup> (100,000 ppm)
	60 mgC·L <sup>-1</sup>	Anammox bacteria in gel carriers and a synthetic ammonium-nitrite-solution	Kimura et al. (2011)	
<b>O<sub>2</sub></b>	Air saturation	Nitrification reactors with high-strength nitrogen wastewater		8.04 mgO <sub>2</sub> ·L <sup>-1</sup> (205,000 ppm)
<b>NH<sub>2</sub>OH</b>	2 mgN·L <sup>-1</sup>	Batch culture of anammox bacteria with synthetic enrichment medium	Suneethi and Joseph (2011)	14.5 mgN·L <sup>-1</sup>
	35 mgN·L <sup>-1</sup>	Batch experiments with anammox bacteria and a synthetic ammonium-nitrite solution	Hu et al. (2011)	
<b>N<sub>2</sub>H<sub>4</sub></b>	28 mgN·L <sup>-1</sup>	Batch experiments with anammox bacteria and a synthetic ammonium-nitrite solution	Hu et al. (2011)	84 mgN·L <sup>-1</sup>
	56 mgN·L <sup>-1</sup>	Batch culture with anammox bacteria and a synthetic ammonium-nitrite medium	Jetten et al. (1998), Schalk et al. (1998)	
<b>HNO<sub>2</sub></b>	0.1 mgN·L <sup>-1</sup>	Nitrification/anammox with five-times diluted urine	Own unpublished data	1.69 mgN·L <sup>-1</sup>
	2 mgN·L <sup>-1</sup>	Nitrification with source-separated urine	Udert et al. (2003)	
<b>NH<sub>3</sub></b>	35 mgN·L <sup>-1</sup>	Nitrification/anammox with five-times diluted urine	Own unpublished data	462 mgN·L <sup>-1</sup>
	130 mgN·L <sup>-1</sup>	Nitrification with source-separated urine	Udert et al. (2003)	

The interference caused by  $\text{NH}_2\text{OH}$ ,  $\text{N}_2\text{H}_4$ ,  $\text{HNO}_2$  or  $\text{NH}_3$  on the NO electrode (one sensor tested) was determined by measuring at least seven equidistant concentrations up to the maximum concentration (details are given in the Supporting Information S5). The pH buffer solutions had different pH values depending on the tested compound and its acid-base constant. The acid-base equilibria were calculated with dissociation constants from Lide (2009) and activity coefficients according to the Davies approximation (Stumm and Morgan 1996). The measurements were conducted at  $25.2 \pm 0.1^\circ\text{C}$  ( $\text{NH}_2\text{OH}$ ,  $\text{HNO}_2$ ) and  $23.9 \pm 0.3^\circ\text{C}$  ( $\text{N}_2\text{H}_4$ ,  $\text{NH}_3$ ) respectively. The linearity of the interferences was assessed with the same method as described above (see "Linearity of sensor response").

## RESULTS AND DISCUSSION

### Linearity of sensor response

The concentration range for the calibration curves were chosen according to the  $\text{N}_2\text{O}$  and NO concentrations reported in the literature and the available gases. Concentrations of up to  $1.68 \text{ mgN}\cdot\text{L}^{-1}$  with synthetic wastewater (Meyer et al. 2005) and up to  $2.67 \text{ mgN}\cdot\text{L}^{-1}$  in a reject water treatment (Kampschreur et al. 2008a) were reported for  $\text{N}_2\text{O}$ . For NO, previously measured maximum concentrations range from  $9.20\cdot 10^{-3} \text{ mgN}\cdot\text{L}^{-1}$  with five-times diluted urine (own unpublished data) to  $3.00\cdot 10^{-2} \text{ mgN}\cdot\text{L}^{-1}$  (synthetic wastewater; Anderson et al. (1993)). Values of  $3.34 \text{ mgN}\cdot\text{L}^{-1}$  (5000 ppm)  $\text{N}_2\text{O}$  and  $6.07\cdot 10^{-2} \text{ mgN}\cdot\text{L}^{-1}$  (2500 ppm) NO were used as the maximum concentrations in this study.

The  $\text{N}_2\text{O}$  sensor responded linearly up to the maximum tested concentration of  $3.34 \text{ mgN}\cdot\text{L}^{-1}$  with a coefficient of variation  $v_{x0}$  of 0.3%. The NO sensor signal followed an asymptotic curve which could be described by a quadratic function ( $v_{x0}$  of 1.4%) and can be explained by saturation (Supporting Information S6). The measurement uncertainties of both sensors are very low compared to other measurement methods, e.g. vial tests for nitrogen compounds (Hach Lange, Düsseldorf, Germany) which have average standard deviations of between 2.5% and 4.0% (according to the specifications on the package).

### Temperature dependence

The signal of the sensors consists of a zero current (i.e. the current in a NO and  $\text{N}_2\text{O}$  free environment) and a signal that depends on the amount of NO or  $\text{N}_2\text{O}$  (target signal  $U$ ) present. Both parts of the signals are temperature dependent and the overall signal  $S$  of the sensors can therefore be described as a sum of the zero current  $Z(T)$  and the target signal  $U$  depending on the temperature  $T$  and the concentration  $C$ :

$$S(T, C) = Z(T) + U(T, C) \quad (7)$$

The zero current arises from unspecific oxidation/reduction of other compounds which may be present in the electrolyte at low concentrations and was therefore expected to show the exponential temperature dependence typical of chemical reactions (Arrhenius equation):

$$Z(T) = a_1 \cdot e^{b_1 \cdot T} \quad (8)$$

$a_i, b_i$  Fitting parameters [-]

Measurements of the zero currents of both sensors at different temperatures in a phosphate buffer solution confirm the exponential temperature dependence (Figure 1). Equation 8 can describe the temperature dependence of the zero currents of two different NO sensors with coefficients of variation of 0.9% and 1.1% respectively and the respective temperature dependence of an N<sub>2</sub>O sensor with a coefficient of variation of 4.1%. The zero currents of the NO sensors increased by 7.3% and 8.4% respectively per 1°C while the zero current of the N<sub>2</sub>O sensor increased only by 1.4% per 1°C.

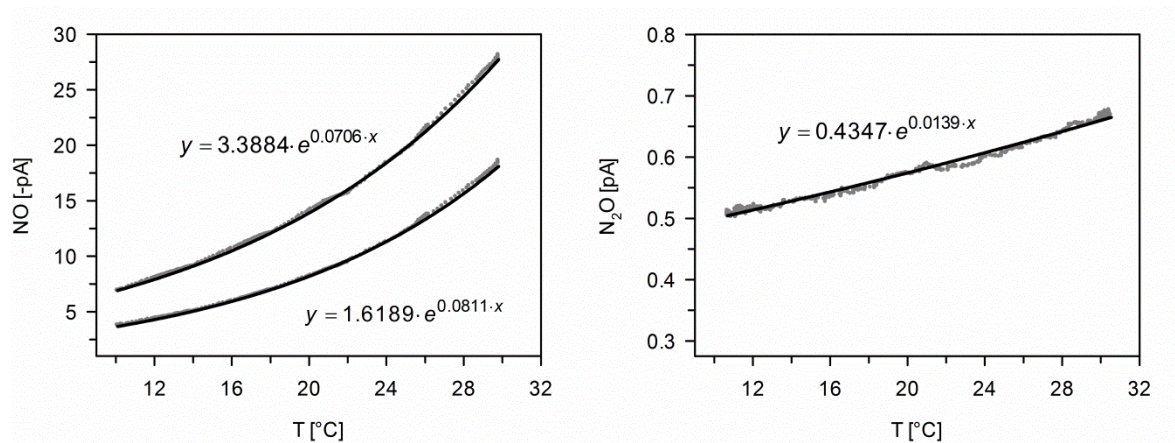


**Figure 1** Measured zero currents (dots) and exponential approximation of two NO sensors (left) and one N<sub>2</sub>O sensor (right) between 10°C and 30°C in a buffer solution.

The temperature dependence of the target signal is caused by that of several chemical and physical processes such as solubility, diffusion in water and in the silicone membrane and reduction or oxidation at the electrode (Gundersen et al. 1998). The target signal is therefore also expected to show the exponential temperature dependence typical of chemical reactions (Arrhenius equation). On the basis of determining the linearity of the sensor signals (see "Linearity of sensor response") it is assumed that the dependence on the concentration  $C$  is quadratic for the NO sensor and linear for the N<sub>2</sub>O sensor:

$$U_{NO}(C) = a_2 \cdot C^2 + a_3 \cdot C + a_4 \quad (9a)$$

$$U_{N_2O}(C) = a_2 \cdot C \quad (9b)$$

Combined with an exponential temperature dependence and the zero current, we obtain:

$$S_{NO}(T, C) = a_1 \cdot e^{b_1 \cdot T} + (a_2 \cdot C^2 + a_3 \cdot C + a_4) \cdot e^{b_2 \cdot T} \quad (10a)$$

$$S_{N_2O}(T, C) = a_1 \cdot e^{b_1 \cdot T} + a_2 \cdot C \cdot e^{b_2 \cdot T} \quad (10b)$$

or

$$C_{NO}(T, S) = \frac{-a_3 + \sqrt{a_3^2 - 4 \cdot a_2 \cdot \left( a_4 - \left( \frac{S - a_1 \cdot e^{b_1 T}}{e^{b_2 T}} \right) \right)}}{2 \cdot a_2} \quad (11a)$$

$$C_{N_2O}(T, S) = \frac{S - a_1 \cdot e^{b_1 T}}{a_2 \cdot e^{b_2 T}} \quad (11b)$$

Measurements of the signals of both sensors at different temperatures and concentrations in a buffer solution confirmed the exponential temperature dependence (Figure 2). Equations 10a and 10b can predict the signals of the two sensors at different concentrations and temperatures with a coefficient of correlation of 3.06% (NO) and 1.04% (N<sub>2</sub>O) respectively. The signal of the NO sensor at 30°C is about 240% higher than at 10°C while the signal of the N<sub>2</sub>O sensor increases by about 190% (Supporting Information S7).

Neglecting the temperature effect can result in large measurement errors. For example, if the sensors were calibrated for 20°C and the measurements were conducted at 25°C, the NO would be overestimated by 19% and the N<sub>2</sub>O by 21%. Another example is the error caused by temperature fluctuations. If the sensors were calibrated at 25°C and temperature fluctuations were in the range of ± 1°C, the temperature artefacts would be ± 3.5% for the NO and ± 3.9% for the N<sub>2</sub>O. As these examples show, the temperature effect can significantly increase the measurement uncertainties of 1.4% (NO sensor) and 0.3% (N<sub>2</sub>O sensor). The calibration of the sensors should consequently include the temperature dependence according to Equations 10a and 10b if high measurement accuracy is required.

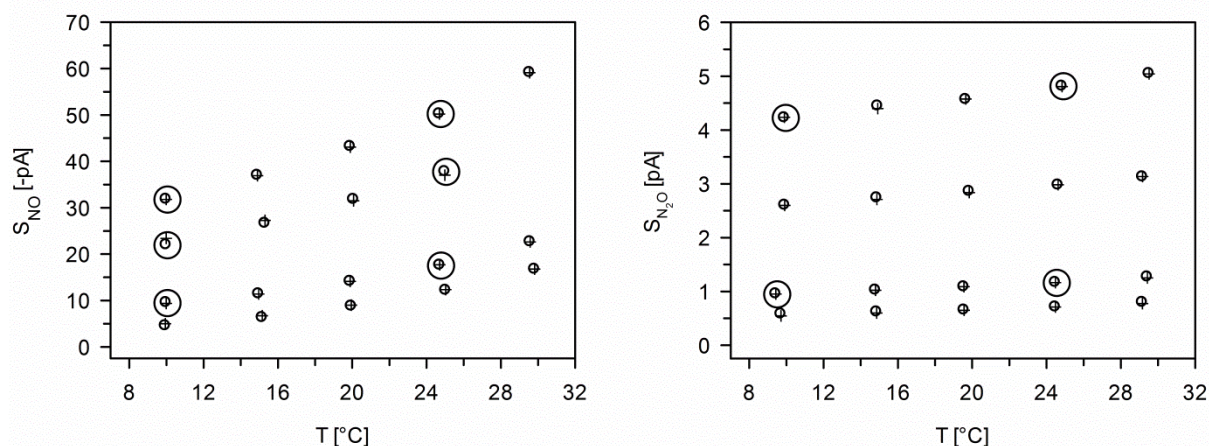


**Figure 2** Measured (small circles) and fitted (crosses) signals for 0, 100, 500 and 900 ppm NO (left) and N<sub>2</sub>O (right) in a buffer solution. The fitted calibration curves are  $S_{NO}(T, C) = 1.22 \cdot e^{0.0770 \cdot T} + (-12200 \cdot C^2 + 1010 \cdot C + 1.68) \cdot e^{0.0342 \cdot T}$  and  $S_{N_2O}(T, C) = 0.459 \cdot e^{0.0179 \cdot T} + 2.57 \cdot C \cdot e^{0.0386 \cdot T}$ . The large circles mark the measurements used for calibration.

As Equations 10a and 10b contain 4 and 6 parameters respectively and depend on two variables – the concentration and temperature – a calibration with redundant measurement points would require too much time for short experiments. In order to minimise the time and effort needed, we estimated the parameters of Equations 10a and 10b with the minimal number of data points required (= number of parameters), and by applying only two different temperatures. The chosen points are marked with circles in Figure 2. With this approach, the signals of both sensors could be fitted very well: the calculated coefficient of variation was 3.13% (NO sensor) and 1.11% (N<sub>2</sub>O sensor) respectively. If all measurement points (NO sensor 19 points and N<sub>2</sub>O sensor 20 points) were used, the fit was hardly better: a coefficient of variation of 3.06% for NO and 1.04% for N<sub>2</sub>O. By measuring only the minimum number of required points for the parameter estimation, therefore, the parameters of Equations 10a and 10b can be determined with much less effort and hardly any loss of accuracy. The chosen points must include two different temperatures and two (N<sub>2</sub>O, linear dependency on concentration) or three (NO, quadratic dependency on concentration) different concentrations at the same temperature. Furthermore, the chosen temperatures and concentrations should cover the whole expected temperature and concentration range during the measurement.

To test whether the temperature dependence found in the synthetic buffer solutions is also valid for wastewater, we conducted experiments with real digester supernatant (Figures can be found in the Supporting Information S8).

We tested the N<sub>2</sub>O sensors for a larger temperature range than with synthetic buffer solutions because we wanted to cover the maximum concentration range as given in Table 1. The meas-

ured data shows that Equation 10b is valid over the whole expected concentration range in digester supernatant. The coefficient of correlation was  $2.26 \pm 0.72\%$  (three sensors), which is only slightly higher than in the phosphate buffer solution (1.04%, one sensor). In these measurements, the three  $N_2O$  sensors behaved very similarly with respect to temperature: the signal increase between  $10^\circ\text{C}$  and  $30^\circ\text{C}$  varied only  $\pm 1.2\%$  ( $197 \pm 2\%$  higher) between the three sensors. Nevertheless, the fitted coefficients of Equation 10b varied considerably, which shows that the parameters of Equation 10b must thus be fitted for each sensor individually in order to reach high measurement accuracy.

In case of  $NO$ , two of the three sensors had unstable signals and could not be included in the data interpretation. The signal of the third  $NO$  sensor also fluctuated strongly ( $\pm 1.9\%$ , compared to  $\pm 0.1\%$  for the  $N_2O$  sensor), but it was sufficiently stable to determine a calibration curve. The strong fluctuations were probably the reason why the fit was not as good as in the experiments with the phosphate buffer: the coefficient of correlation was (15.9% in the digester supernatant instead of 3.06% in the phosphate buffer). Nevertheless, Figure 3 shows that Equation 10a could fit the measurement data considerably well.

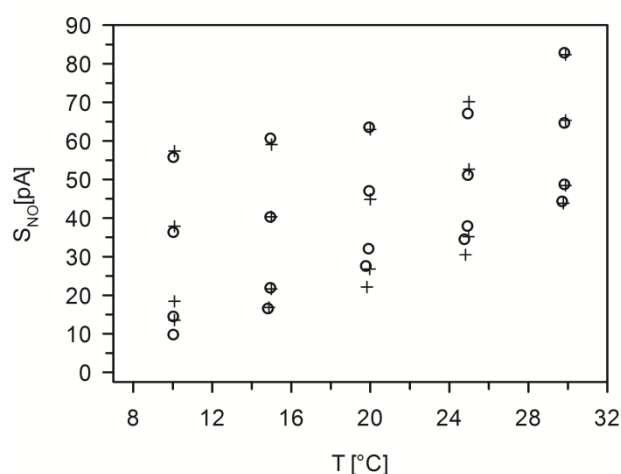


**Figure 3** Measured (circles) and fitted (crosses) signals for 0, 500, 2500 and 4500 ppm  $NO$  in digester supernatant. The fitted calibration curve is  $S_{NO}(T,C) = 1.68 \cdot e^{0.0998 \cdot T} + (177 \cdot C^2 + 1360 \cdot C + 8.03) \cdot e^{0.0109 \cdot T}$ .

It is known that the sensor signals are not stable, i.e. a drift occurs, so that the zero current will increase while the target signal for the same amount of measured compound will decrease over time. This could lead to problems when the sensors are used for longer experiments (e.g. for several days) or require recalibration of the sensors at regular intervals during the experiment.

This may necessitate shortening the time and effort needed for the calibration. However, that was not the focus of this study and was therefore not assessed in more detail.

### Interfering substances

The tested substances were chosen on the basis of their presence and strong dynamics in nitrogen conversion processes, their ability to penetrate the sensor tip membrane (small uncharged molecules) and their potential reducibility/oxidability. The first two criteria led to the selection of NO, N<sub>2</sub>O, NO<sub>2</sub>, NH<sub>3</sub>, HNO<sub>2</sub>, NH<sub>2</sub>OH, N<sub>2</sub>H<sub>4</sub>, O<sub>2</sub> and CO<sub>2</sub>. Because the materials of the electrodes and electrolyte as well as the latter's pH value are confidential, and the concentrations of the oxidants and reductants in the electrolyte cannot be measured, the exact reduction potentials  $E_H$  of the reactions and the sensors could not be calculated according to Equation 12. We therefore estimated them assuming a pH value of 7, activities of 1 for all the substances and a temperature of 25°C (Supporting Information S9). The potentials of the two sensors were assumed to be slightly higher than those necessary to oxidise NO to NO<sub>2</sub><sup>-</sup> or NO<sub>3</sub><sup>-</sup> (end product unknown) or slightly lower than the potential necessary to reduce N<sub>2</sub>O to N.

$$E_H = E_H^\circ + \frac{2.3 \cdot R \cdot T}{F} \cdot \log \frac{\{ox\}}{\{red\}} \quad (12)$$

$E_H^\circ$  Standard redox potential [V]

$R$  Universal gas constant 8.3145 [J·mol<sup>-1</sup>·K<sup>-1</sup>]

$T$  Temperature [K]

$F$  Faraday constant 96,485.3365 [C·mol<sup>-1</sup>]

{ox} Activity of oxidised compound [mol]

{red} Activity of reduced compound [mol]

On the basis of the estimated potentials of the reactions and sensors, all the chosen substances could theoretically be oxidised in the NO sensor apart from NO<sub>2</sub>, N<sub>2</sub>O and O<sub>2</sub> (whose calculated oxidation potentials were lower than that of the NO sensor) and CO<sub>2</sub> (which cannot be further oxidised). Apart from NH<sub>3</sub> (which cannot be further reduced), all the chosen substances can be reduced in the N<sub>2</sub>O sensor.

For the tests of possible interference by the chosen substances, the maximum concentrations were set on the basis of the highest values found in the literature (Table 1). We specifically scanned the literature for measured concentrations in biological treatment processes of high-strength nitrogen wastewater and, if necessary, completed them with data from other experiments. The chosen maximum concentrations for some tests differed from those found in the literature due to practical limitations (e.g. availability of gases).



In the test for the interference due to other nitrogen compounds, a signal on the electrodes could either be caused by interference, by actual chemically produced NO or N<sub>2</sub>O or a combination of both. The chemical production of NO and N<sub>2</sub>O thus needed to be assessed in order to differentiate between real interference and signals from chemically-produced NO or N<sub>2</sub>O. As the experiments were conducted in anaerobic solutions, the seven tested N compounds (NO, N<sub>2</sub>O, NO<sub>2</sub>, HNO<sub>2</sub>, NH<sub>2</sub>OH, N<sub>2</sub>H<sub>4</sub> and NH<sub>3</sub>) could only dissociate or react with themselves, H<sub>2</sub>O and/or N<sub>2</sub> to form NO or N<sub>2</sub>O. On this basis, we set up reactions with regard to the conservation of mass and calculated the Gibbs free energy of reaction  $\Delta G_R^0$  with standard molar Gibbs free energy of formation values  $\Delta_f G^0$  from Lide (2009). The following equations show the reactions which have a negative  $\Delta G_R^0$  and are therefore thermodynamically possible, although this is not a sufficient criterion for the reaction to really occur. The chemical production of N<sub>2</sub>O is theoretically possible in the presence of NO, NH<sub>2</sub>OH or HNO<sub>2</sub>, and chemical NO production is theoretically possible in the presence of N<sub>2</sub>O, N<sub>2</sub>H<sub>4</sub>, NH<sub>2</sub>OH or HNO<sub>2</sub>.



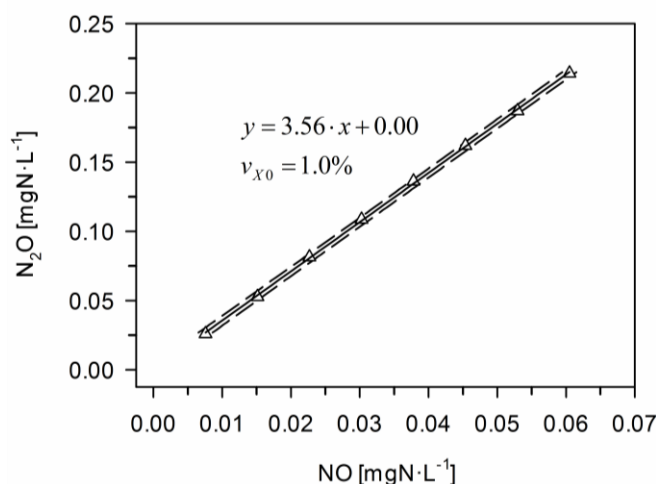
The possible pathways for chemical N<sub>2</sub>O production were tested by putting the sensor in buffer solutions containing NO, N<sub>2</sub>O, HNO<sub>2</sub>, NH<sub>2</sub>OH or N<sub>2</sub>H<sub>4</sub> (Table 2). N<sub>2</sub>O production from NO (Equation 13) can be excluded because NO is kinetically inert and generally requires a catalyst to undergo this disproportionation reaction (Franz and Lippard 1998). The measured signal on the N<sub>2</sub>O sensor must thus be due to interference from NO (Figure 4).

**Table 2** Measurements to evaluate interferences.

	NO sensor	N <sub>2</sub> O sensor	NO gas phase	N <sub>2</sub> O gas phase
NO	-	Signal	-	-
N <sub>2</sub> O	No signal	-	-	-
N <sub>2</sub> H <sub>4</sub>	Signal	No signal	-	-
HNO <sub>2</sub>	Signal	Signal	Signal	No signal
NH <sub>2</sub> OH	Signal	Signal	No signal	Signal

In case of HNO<sub>2</sub> and NH<sub>2</sub>OH, where signals on the N<sub>2</sub>O sensor indicated the possibility of chemical N<sub>2</sub>O production, off-gas measurements were conducted to differentiate between interference and the signal from chemically-produced N<sub>2</sub>O. The off-gas measurements confirmed the chemical N<sub>2</sub>O production from NH<sub>2</sub>OH (Equation 14), but there was no N<sub>2</sub>O production from HNO<sub>2</sub> (Equation 15). Equation 14 has been postulated previously (Feelisch and Stamler 1996) and Schmidt et al. (2004) also observed chemical N<sub>2</sub>O production from NH<sub>2</sub>OH.

In the case of NH<sub>2</sub>OH, where the N<sub>2</sub>O was chemically produced, the measured signal of the N<sub>2</sub>O sensor was equal to the measured N<sub>2</sub>O concentration in the gas phase (Supporting Information S10). Any interference from NH<sub>2</sub>OH on the N<sub>2</sub>O measurement can therefore be excluded. Because NO interferes with the N<sub>2</sub>O measurement (Figure 4), the chemically produced NO from HNO<sub>2</sub> (see below) produced a signal on the N<sub>2</sub>O sensor. A comparison of the measured N<sub>2</sub>O signals with the measured NO concentration in the gas phase showed that the signal on the N<sub>2</sub>O sensor was entirely due to the chemically produced NO (Supporting Information S10). Interference from HNO<sub>2</sub> on the N<sub>2</sub>O sensor can thus also be excluded.

**Figure 4** Interference from NO on the N<sub>2</sub>O sensor: calibration curve (straight line) and 95% prediction interval (dashed lines).

The possible pathways for chemical NO production were also tested by putting the sensor in buffer solutions containing NO, N<sub>2</sub>O, HNO<sub>2</sub>, NH<sub>2</sub>OH or N<sub>2</sub>H<sub>4</sub> (Table 2). Any NO production from N<sub>2</sub>O (Equation 16) can be excluded because there was no signal on the NO sensor. Chemical production of NO from N<sub>2</sub>H<sub>4</sub> (Equation 17) can also be excluded because this NO would interfere with the N<sub>2</sub>O measurement (Table 3), but there was no signal on the N<sub>2</sub>O sensor. The measured signal on the NO sensor must therefore be due to interference from N<sub>2</sub>H<sub>4</sub> (Table 3).

In the case of HNO<sub>2</sub> and NH<sub>2</sub>OH, where the signals on the NO sensor indicated the possibility of chemical NO production, off-gas measurements were conducted to differentiate between interference and a signal from chemically produced NO. The off-gas measurements confirmed chemical NO production from HNO<sub>2</sub> (Equation 19), but there was no production of NO from NH<sub>2</sub>OH (Equation 18). Equation 19 had been postulated previously (Beake and Moodie 1995) and Udert et al. (2005) also observed chemical NO production from HNO<sub>2</sub>.

In the case of NH<sub>2</sub>OH, the measured signal on the NO sensor must be due to interference because there was no chemical production of NO. In the case of HNO<sub>2</sub>, a comparison of the measured NO signal with the measured NO concentration in the gas phase showed that the signal on the NO sensor must be a sum of the chemically produced NO and additional interference from HNO<sub>2</sub> (Supporting Information S10). For the further characterisation of the interference from HNO<sub>2</sub> on the NO measurement, the signal from the chemically produced NO therefore had to be subtracted from the measured signal. We were able to measure the actual NO concentrations as an interference on the N<sub>2</sub>O sensor. We had quantified the interference of NO on the N<sub>2</sub>O sensor just before the experiment.

**Table 3** Influence of tested substances on NO and N<sub>2</sub>O measurements (the ‘N<sub>2</sub>O signal’ and ‘NO signal’ columns contain the type of curve that describes the interference).

Substance	Maximum tested concentration	N <sub>2</sub> O signal	NO signal	Coefficient of variation	Interference
NO <sub>2</sub>	3.03·10 <sup>-3</sup> mgN·L <sup>-1</sup>	None	None		
N <sub>2</sub> O	3.34 mgN·L <sup>-1</sup>	-	None		
NO	6.07·10 <sup>-2</sup> mgN·L <sup>-1</sup>	Linear	-	1.0%	1 mgN·L <sup>-1</sup> → 3.56 mgN·L <sup>-1</sup>
CO <sub>2</sub>	38.5 mgC·L <sup>-1</sup>	None	None		
O <sub>2</sub>	8.04 mgO <sub>2</sub> ·L <sup>-1</sup>	None	None		
NH <sub>2</sub> OH	15 mgN·L <sup>-1</sup>	None	Quadratic	1.0%	1 mgN·L <sup>-1</sup> → 1.07·10 <sup>-4</sup> mgN·L <sup>-1</sup>
N <sub>2</sub> H <sub>4</sub>	84 mgN·L <sup>-1</sup>	None	Linear	1.9%	1 mgN·L <sup>-1</sup> → 1.27·10 <sup>-5</sup> mgN·L <sup>-1</sup>
HNO <sub>2</sub>	1.69 mgN·L <sup>-1</sup>	None	Linear	1.0%	1 mgN·L <sup>-1</sup> → 6.22·10 <sup>-3</sup> mgN·L <sup>-1</sup>
NH <sub>3</sub>	462 mgN·L <sup>-1</sup>	None	Quadratic	1.7%	1 mgN·L <sup>-1</sup> → 8.22·10 <sup>-5</sup> mgN·L <sup>-1</sup>

The influence of all the tested compounds on N<sub>2</sub>O and NO measurement is summarised in Table 3. The NO measurement is influenced by four of the tested substances. The interference from HNO<sub>2</sub> and N<sub>2</sub>H<sub>4</sub> is linear, while NH<sub>2</sub>OH and NH<sub>3</sub> have a quadratic interference on the NO measurement (Figures can be found in the Supporting Information S11). The N<sub>2</sub>O measurement is only influenced by NO. The influence was further characterised by measuring eight different concentrations and is linear with a coefficient of variation of 1.0% (Figure 4). As no other compound interferes with the N<sub>2</sub>O measurement, the N<sub>2</sub>O sensor can be used to measure NO in the absence of N<sub>2</sub>O.

For the NO sensor, the results in Table 3 correspond to the prediction made on the basis of the estimated redox potentials, i.e. that only NH<sub>2</sub>OH, N<sub>2</sub>H<sub>4</sub>, HNO<sub>2</sub> and NH<sub>3</sub> interfere with the NO measurement. In contrast to this, all tested compounds apart from NH<sub>3</sub> could theoretically interfere with the N<sub>2</sub>O measurement on the basis of the estimated redox potentials, but only NO actually interfered in the tested concentration range.

Because all the sensors are built in the same way and with the same material, it can be expected that all sensors show similar interferences. This was proved by measuring the influence of NO on three different N<sub>2</sub>O sensors (Figures can be found in the Supporting Information 12). All three sensors reacted linear (coefficient of variation of  $4.0 \pm 0.6\%$ ) and the interference caused by  $1 \text{ mgNO-N}\cdot\text{L}^{-1}$  varied only  $\pm 20.7\%$  between the three sensors ( $3.5 \pm 0.7 \text{ mgN}_2\text{O-N}\cdot\text{L}^{-1}$ ). Nevertheless, individual correction functions must be determined for each sensor to reach high measurement accuracy.

The significance of the determined interferences by the two sensors was assessed on the basis of the maximum reference concentrations given in Table 1 (Table 4). The presence of NH<sub>3</sub>, HNO<sub>2</sub>, NH<sub>2</sub>OH, N<sub>2</sub>H<sub>4</sub> or NO can lead to overestimations of the measured NO and N<sub>2</sub>O concentrations of up to 21.9% if the interference is not considered and corrected. High concentrations of NH<sub>3</sub> and HNO<sub>2</sub> are especially critical. We would therefore always recommend to first determine the expected concentrations of NH<sub>3</sub>, HNO<sub>2</sub>, NH<sub>2</sub>OH, N<sub>2</sub>H<sub>4</sub> and NO during the experiment, i.e. measure them in a preliminary experiment, and to calculate the expected interference from these five compounds with the data in Table 3 before starting the actual NO and N<sub>2</sub>O measurements.

**Table 4** Assessment of the interference on NO and N<sub>2</sub>O measurement from NO, NH<sub>2</sub>OH, N<sub>2</sub>H<sub>4</sub>, HNO<sub>2</sub> and NH<sub>3</sub>, calculated for the maximum reference concentrations given in Table 1.

Compound	Maximum reference concentration	Interference	% of maximum reference concentration
<b>N<sub>2</sub>O sensor</b>	2.67 mgN·L <sup>-1</sup>		
NO	3.00·10 <sup>-2</sup> mgN·L <sup>-1</sup>	1.07·10 <sup>-1</sup> mgN·L <sup>-1</sup>	4.1
<b>NO sensor</b>	3.00·10 <sup>-2</sup> mgN·L <sup>-1</sup>		
NH <sub>2</sub> OH	20.0 mgN·L <sup>-1</sup>	2.14·10 <sup>-3</sup> mgN·L <sup>-1</sup>	7.1
N <sub>2</sub> H <sub>4</sub>	40.0 mgN·L <sup>-1</sup>	5.08·10 <sup>-4</sup> mgN·L <sup>-1</sup>	1.7
HNO <sub>2</sub>	1.00 mgN·L <sup>-1</sup>	6.22·10 <sup>-3</sup> mgN·L <sup>-1</sup>	20.7
NH <sub>3</sub>	80.0 mgN·L <sup>-1</sup>	6.58·10 <sup>-3</sup> mgN·L <sup>-1</sup>	21.9

Depending on the required measurement accuracy, the signals of the two electrodes must then be corrected with a previously established correction function. Depending on the type of interference (linear or quadratic), this requires the measurement of the electrode signal at least at two or three different concentrations of the dissolved compound concerned, preferably at the same temperature as that at which the measurements are conducted. In case of HNO<sub>2</sub>, the chemically produced NO must be subtracted from the measured signal to determine the interference. Here we can make a positive use of the NO interference on the N<sub>2</sub>O sensor. As NO interferes with the N<sub>2</sub>O measurement while HNO<sub>2</sub> does not (Table 3 and Figure 4), the chemically produced NO can be calculated from the N<sub>2</sub>O signal (after previously determining the NO interference on the N<sub>2</sub>O signal).

#### ACKNOWLEDGEMENTS

This work was financed by the Swiss National Science Foundation and with Eawag discretionary funds. We thank Unisense for providing us with five free N<sub>2</sub>O and several free NO electrodes as well as an additional multimeter. We thank Frank Schreiber for his critical comments and helpful suggestions.



## **SUPPORTING INFORMATION**

### **FOR CHAPTER 4**

#### **Temperature dependence and interferences of NO and N<sub>2</sub>O microelectrodes used in wastewater treatment**

Sarina Jenni, Joachim Mohn, Lukas Emmenegger, Kai M. Udert

*Environmental Science & Technology*, 2012, 46(4), 2257-2266

### S1 Measurements in digester supernatant

Prior to the measurements, most of the inorganic carbon was stripped (purging with 1 L·min<sup>-1</sup> N<sub>2</sub>) and the pH value was adjusted to 6.5 by adding HCl. This was done to prevent pH changes by CO<sub>2</sub> volatilisation during the experiment. The digester supernatant was characterised as follows: < 5 mg TIC·L<sup>-1</sup>, 330 mgCOD·L<sup>-1</sup>, 34 mg PO<sub>4</sub>-P·L<sup>-1</sup>, 10 mg SO<sub>4</sub>·L<sup>-1</sup>, 2740 mg Cl·L<sup>-1</sup>, 300 mg Na·L<sup>-1</sup>, 130 mg K·L<sup>-1</sup>, 18 mg Mg·L<sup>-1</sup>, 72 mg Ca·L<sup>-1</sup>, < 2 mg NO<sub>2</sub>-N·L<sup>-1</sup>, < 2 mg NO<sub>3</sub>-N·L<sup>-1</sup>. The NH<sub>4</sub> concentration decreased slightly from 790 mg N·L<sup>-1</sup> to 760 mg N·L<sup>-1</sup> during the experiments (20 h) probably due to NH<sub>3</sub> volatilisation.

### S2 Temperature dependence of absorption coefficients

The temperature dependence of the absorption coefficients was calculated with:

$$k_{H,i}(T) = k_{H,i}(T_0) \cdot \exp\left(B \cdot \left(\frac{1}{T} - \frac{1}{T_0}\right)\right)$$

**Table S1** Mean values for  $k_{H,i}(T_0)$  and  $B$  according to NIST.

	$k_{H,i}(T_0)$ [mol·L <sup>-1</sup> ·bar <sup>-1</sup> ]	$B$ [K]
<b>NO</b>	0.0018	1533
<b>N<sub>2</sub>O</b>	0.0247	2675
<b>NO<sub>2</sub></b>	0.0225	2150
<b>CO<sub>2</sub></b>	0.0345	2429
<b>O<sub>2</sub></b>	0.0013	1650

### S3 Coefficient of variation

The sensitivities of the calibration curves were calculated with:

$$E = \frac{dy}{dx} \Big|_{\bar{x}}$$

$\bar{x}$  Mean of concentrations

Linear calibration curves:  $y = a + b \cdot x$

$$E = b$$

Quadratic calibration curves:  $y = a + b \cdot x + c \cdot x^2$

$$E = b + 2 \cdot c \cdot \bar{x}$$

Zero currents:  $Z(T) = a_1 \cdot e^{b_1 \cdot T}$



$$E = \frac{dZ}{dT} \Big|_{\bar{T}} = a_1 \cdot b_1 \cdot e^{b_1 \cdot \bar{T}}$$

N<sub>2</sub>O sensor signal:

$$S_{N_2O}(T, C) = a_1 \cdot e^{b_1 \cdot T} + a_2 \cdot C \cdot e^{b_2 \cdot T}$$

$$E = \frac{dS_{N_2O}}{dC} \Big|_{\bar{C}} = a_2 \cdot e^{b_2 \cdot \bar{T}}$$

NO sensor signal:

$$S_{NO}(T, C) = a_1 \cdot e^{b_1 \cdot T} + (a_2 \cdot C^2 + a_3 \cdot C + a_4) \cdot e^{b_2 \cdot T}$$

$$E = \frac{dS_{NO}}{dC} \Big|_{\bar{C}} = 2 \cdot a_2 \cdot \bar{C} \cdot e^{b_2 \cdot \bar{T}} + a_3 \cdot e^{b_2 \cdot \bar{T}}$$

#### S4 FTIR measurements

Quantification limits for N<sub>2</sub>O and NO analysis by FTIR are 0.25 and 5 ppm, respectively, and the expanded standard uncertainty for both components is around 10% (95% confidence level). The off-gas was recirculated after the spectrometer and supplemented with 50 ml·min<sup>-1</sup> N<sub>2</sub> to avoid oxygen intrusion. Analysed N<sub>2</sub>O and NO concentrations were corrected for this dilution with nitrogen gas.

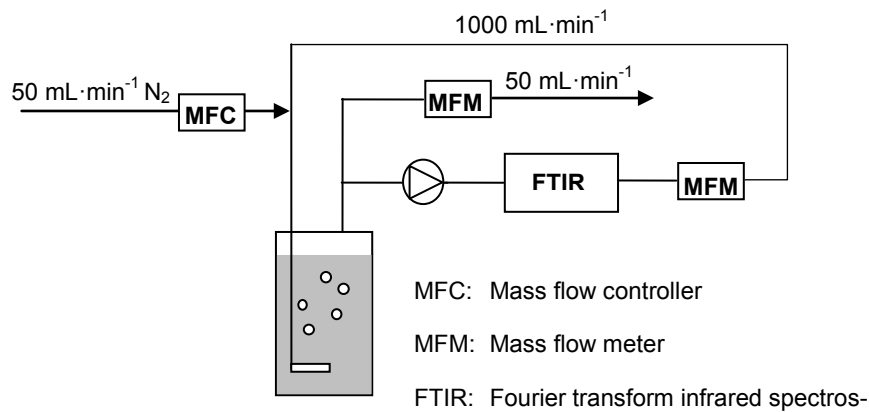


**Figure S1** Experimental setup for the off-gas measurements.

## S5 Characterisation of the interference caused by $\text{NH}_2\text{OH}$ , $\text{N}_2\text{H}_4$ , $\text{HNO}_2$ or $\text{NH}_3$ on the NO electrode

**Table S2** Solutions used to determine the interference from  $\text{NH}_2\text{OH}$ ,  $\text{HNO}_2$ ,  $\text{NH}_3$  and  $\text{N}_2\text{H}_4$ . The concentrations refer to the specified protonation state and not to the total amount of the compound, e.g. only  $\text{NH}_3$  and not the sum of  $\text{NH}_3$  and  $\text{NH}_4$ .

	Buffer solution	Added solution	Low	Interval	High
$\text{NH}_2\text{OH}$	pH 9	$\text{NH}_2\text{OH}\cdot\text{HCl}$	$0.5 \text{ mgN}\cdot\text{L}^{-1}$	$2 \text{ mgN}\cdot\text{L}^{-1}$	$14.5 \text{ mgN}\cdot\text{L}^{-1}$
$\text{HNO}_2$	pH 6	$\text{NaNO}_2$	$0.2 \text{ mgN}\cdot\text{L}^{-1}$	$0.21 \text{ mgN}\cdot\text{L}^{-1}$	$1.69 \text{ mgN}\cdot\text{L}^{-1}$
$\text{NH}_3$	pH 8	$\text{NH}_4\text{Cl}$	$42 \text{ mgN}\cdot\text{L}^{-1}$	$42 \text{ mgN}\cdot\text{L}^{-1}$	$462 \text{ mgN}\cdot\text{L}^{-1}$
$\text{N}_2\text{H}_4$	pH 10	$\text{N}_2\text{H}_4 \text{ H}_2\text{SO}_4$	$1.4 \text{ mgN}\cdot\text{L}^{-1}$	$14 \text{ mgN}\cdot\text{L}^{-1}$	$84 \text{ mgN}\cdot\text{L}^{-1}$

## S6 Linearity of sensor response

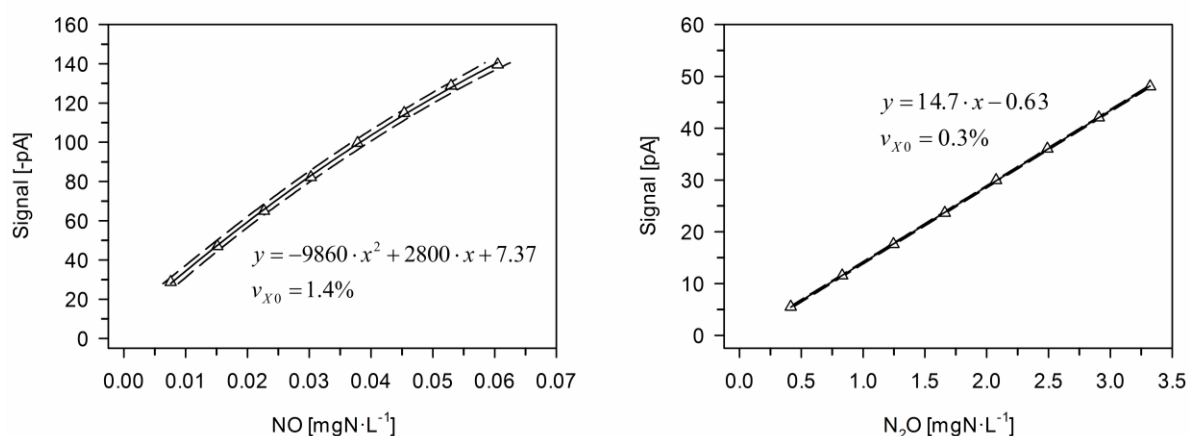


**Figure S2** Quadratic (NO, left side) and linear ( $\text{N}_2\text{O}$ , right side) sensor response of the two electrodes: calibration curve (straight line) and 95% prediction interval (dashed lines).

### S7 Temperature dependence in phosphate buffer solution

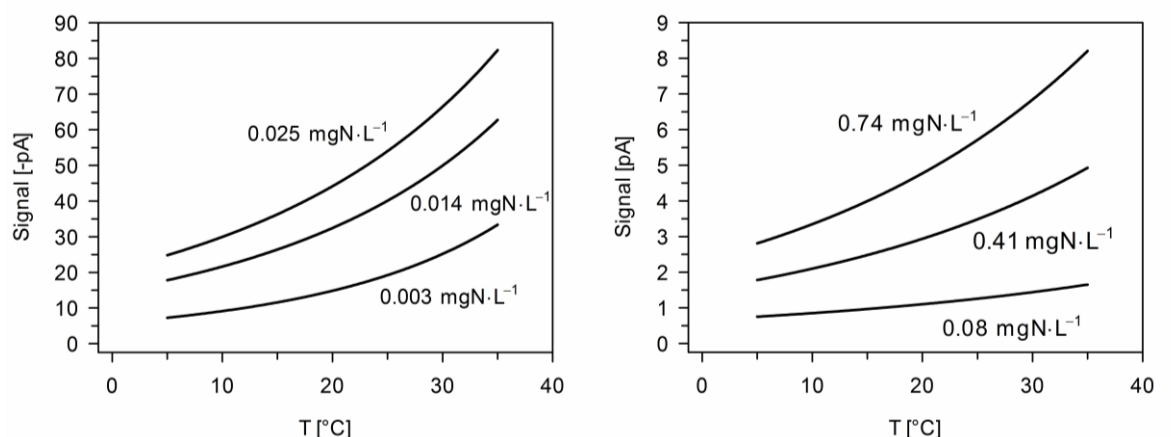


**Figure S3** Temperature dependence of the signals of NO electrodes (left) and N<sub>2</sub>O electrodes (right) at various concentrations in phosphate buffer solution.

### S8 Temperature dependence in digester supernatant

The temperature dependence of the N<sub>2</sub>O sensor signal in digester supernatant was measured with three different N<sub>2</sub>O sensors (Figure S4, Figure S5 and Figure S6). The temperature dependence of the NO sensor signal in digester supernatant was also measured with three different NO sensors, but only one of them worked properly (Figure S7).

In the figures below, the data on the left side corresponds to constant concentrations in the gas which was used to sparge the solution while the data on the right side corresponds to constant liquid phase concentrations. Due to the temperature dependence of the Henry coefficients, NO or N<sub>2</sub>O liquid phase concentrations decrease with temperature if the concentration in the gas used to sparge the solution stays constant. Therefore, the signals on the left side increase less strong with temperature than the ones on the right side.

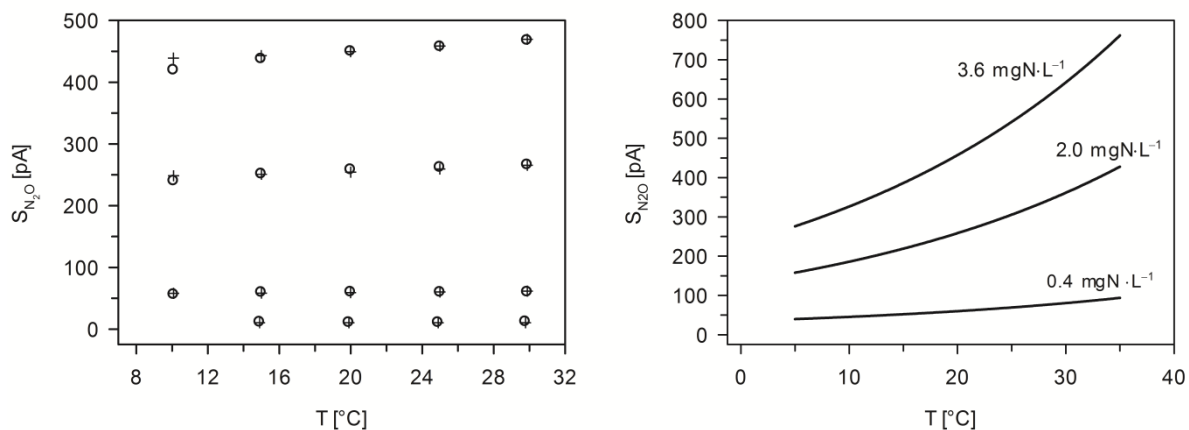


**Figure S4** Measured (circles) and fitted (crosses) signals for 0, 500, 2500 and 4500 ppm N<sub>2</sub>O (left) and fitted temperature dependence of the signal of an N<sub>2</sub>O electrode at various concentrations (right) in digester supernatant. The fitted calibration curve is  $S_{N_2O}(T,C) = 10.4 \cdot e^{0.00 \cdot T} + 62.1 \cdot e^{0.0346 \cdot T}$ .

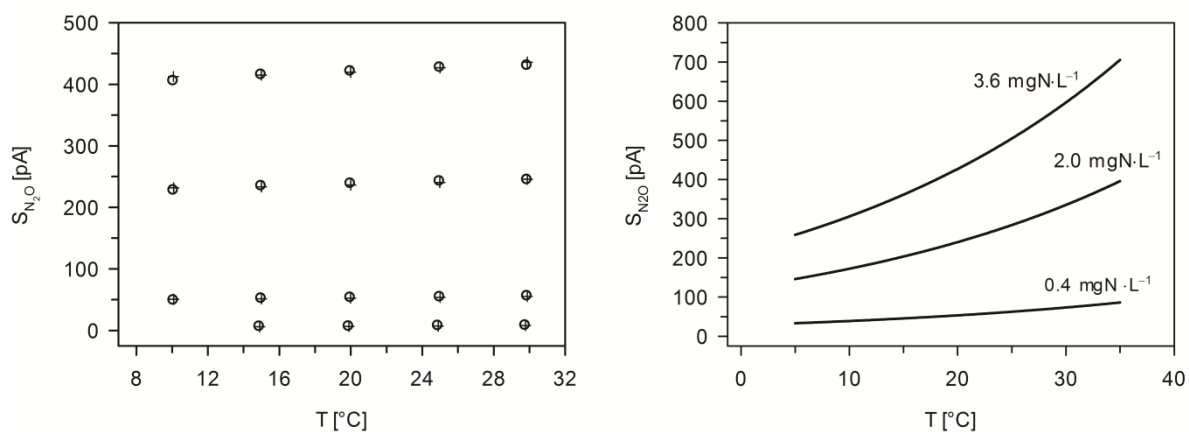


**Figure S5** Measured (circles) and fitted (crosses) signals for 0, 500, 2500 and 4500 ppm N<sub>2</sub>O (left) and fitted temperature dependence of the signal of an N<sub>2</sub>O electrode at various concentrations (right) in digester supernatant. The fitted calibration curve is  $S_{N_2O}(T,C) = 4.54 \cdot e^{0.0182 \cdot T} + 59.5 \cdot e^{0.0337 \cdot T}$ .

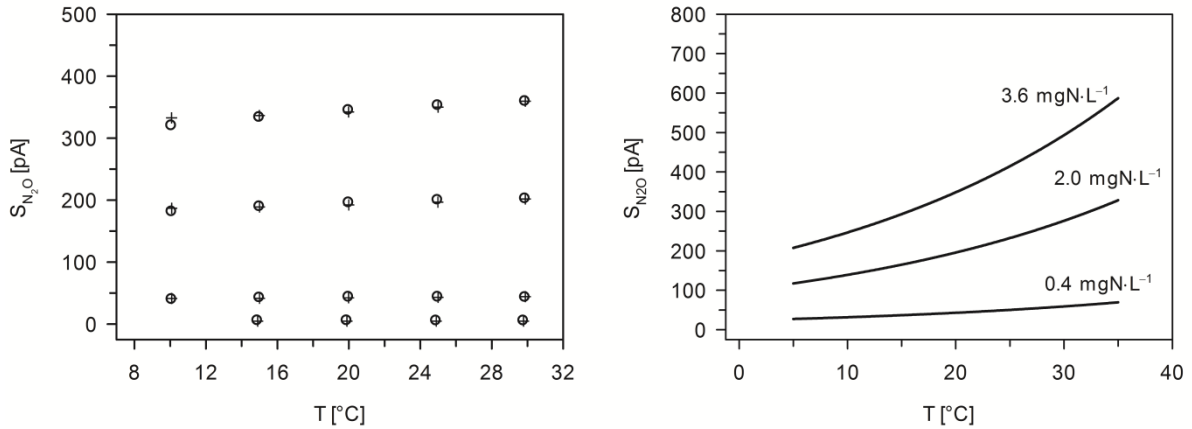


**Figure S6** Measured (circles) and fitted (crosses) signals for 0, 500, 2500 and 4500 ppm  $N_2O$  (left) and fitted temperature dependence of the signal of an  $N_2O$  electrode at various concentrations (right) in digester supernatant. The fitted calibration curve is  $S_{N_2O}(T,C) = 4.69 \cdot e^{0.0000561 \cdot T} + 47.3 \cdot e^{0.0352 \cdot T}$ .

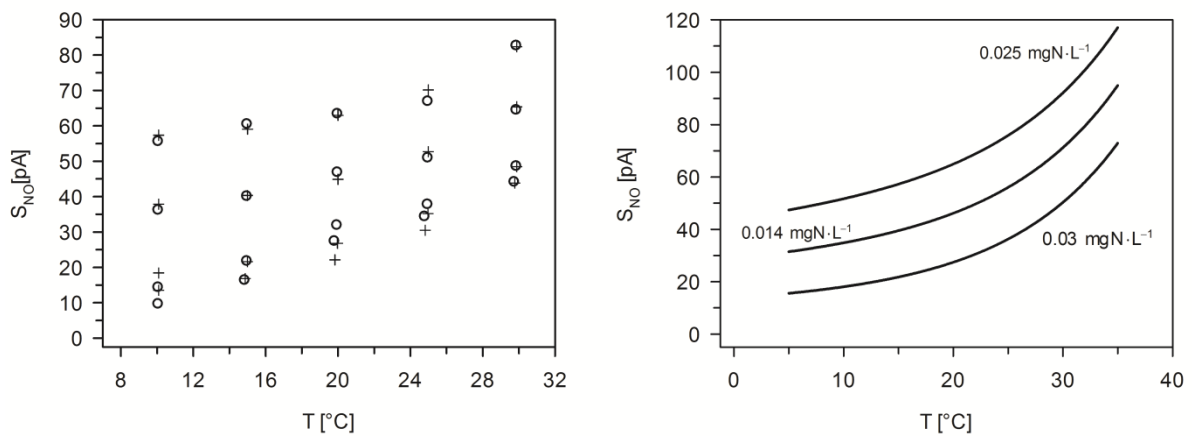


**Figure S7** Measured (circles) and fitted (crosses) signals for 0, 500, 2500 and 4500 ppm  $NO$  (left) and fitted temperature dependence of the signal of an  $NO$  electrode at various concentrations (right) in digester supernatant. The fitted calibration curve is  $S_{NO}(T,C) = 1.68 \cdot e^{0.0998 \cdot T} + (177 \cdot C^2 + 1360 \cdot C + 8.03) \cdot e^{0.0109 \cdot T}$ .

## S9 Estimation of reduction potentials

The reduction potentials  $E_H$  of the reactions were estimated with:

$$E_H = E_H^\circ + \frac{2.3 \cdot R \cdot T}{F} \cdot \log \frac{\{ox\}}{\{red\}}$$

assuming a pH value of 7, activities of 1 for all substances and a temperature of 25°C. The standard potentials were taken from Bard et al (1986).

**Table S3** Redox potentials for reactions with NO, N<sub>2</sub>O and potentially interfering compounds.

Sensor / compound	Reaction	Redox potential [V]
NO sensor	$NO(g) + H_2O \rightarrow NO_2^- + 2H^+ + 2e^-$	- 0.376
	$\frac{1}{3}NO(g) + \frac{2}{3}H_2O \rightarrow \frac{1}{3}NO_3^- + \frac{4}{3}H^+ + e^-$	- 0.407
HNO <sub>2</sub>	$\frac{1}{2}NO_2^- + \frac{1}{2}H_2O \rightarrow \frac{1}{2}NO_3^- + H^+ + e^-$	- 0.422
NH <sub>3</sub>	$\frac{1}{2}NH_4^+ + \frac{1}{2}H_2O \rightarrow \frac{1}{2}NH_3OH^+ + H^+ + e^-$	- 0.937
	$NH_4^+ \rightarrow \frac{3}{2}N_2H_5^+ + \frac{3}{2}H^+ + e^-$	- 0.661
	$\frac{1}{8}NH_4^+ + \frac{3}{8}H_2O \rightarrow \frac{1}{8}NO_3^- + \frac{5}{4}H^+ + e^-$	- 0.359
	$\frac{1}{6}NH_4^+ + \frac{1}{3}H_2O \rightarrow \frac{1}{6}NO_2^- + \frac{4}{3}H^+ + e^-$	- 0.346
	$\frac{1}{5}NH_4^+ + \frac{1}{5}H_2O \rightarrow \frac{1}{5}NO(g) + \frac{6}{5}H^+ + e^-$	- 0.340
	$NH_4^+ + \frac{1}{8}H_2O \rightarrow \frac{1}{8}N_2O(g) + \frac{5}{4}H^+ + e^-$	- 0.131
	$\frac{1}{3}NH_4^+ \rightarrow \frac{1}{6}N_2(g) + \frac{4}{3}H^+ + e^-$	+ 0.281
N <sub>2</sub> H <sub>4</sub>	$\frac{1}{2}N_2H_5^+ + H_2O \rightarrow NH_3OH^+ + \frac{1}{2}H^+ + e^-$	- 1.204
	$\frac{1}{4}N_2H_5^+ \rightarrow \frac{1}{4}N_2(g) + \frac{5}{4}H^+ + e^-$	+ 0.746
NH <sub>2</sub> OH	$\frac{1}{6}NH_3OH^+ + \frac{1}{3}H_2O \rightarrow \frac{1}{6}NO_3^- + \frac{4}{3}H^+ + e^-$	- 0.176
	$\frac{1}{4}NH_3OH^+ + \frac{1}{4}H_2O \rightarrow \frac{1}{4}NO_2^- + \frac{3}{2}H^+ + e^-$	- 0.054
	$\frac{1}{3}NH_3OH^+ \rightarrow \frac{1}{3}NO(g) + \frac{4}{3}H^+ + e^-$	+ 0.051
	$\frac{1}{2}NH_3OH^+ \rightarrow \frac{1}{4}N_2O(g) + \frac{1}{4}H_2O + \frac{3}{2}H^+ + e^-$	+ 0.670

	$NH_3OH^+ \rightarrow \frac{1}{2}N_2(g) + H_2O + 2H^+ + e^-$	+ 2.696
<b>NO<sub>2</sub></b>	$NO_2(g) + H_2O \rightarrow NO_3^- + 2H^+ + e^-$	- 0.596
<b>N<sub>2</sub>O</b>	$\frac{1}{2}N_2O(g) + \frac{1}{2}H_2O \rightarrow NO + H^+ + e^-$	- 1.177
	$\frac{1}{6}N_2O(g) + \frac{1}{2}H_2O \rightarrow \frac{1}{3}NO_2(g) + H^+ + e^-$	- 0.816
	$\frac{1}{4}N_2O(g) + \frac{3}{4}H_2O \rightarrow \frac{1}{2}NO_2^- + \frac{3}{2}H^+ + e^-$	- 0.777
	$\frac{1}{8}N_2O(g) + \frac{5}{8}H_2O \rightarrow \frac{1}{4}NO_3^- + \frac{5}{4}H^+ + e^-$	- 0.600
<b>O<sub>2</sub></b>	$\frac{1}{2}O_2 + \frac{1}{2}H_2O \rightarrow \frac{1}{2}O_3 + H^+ + e^-$	- 1.662
<b>N<sub>2</sub>O sensor</b>	$\frac{1}{2}N_2O(g) + H^+ + e^- \rightarrow \frac{1}{2}N_2(g) + H_2O$	<b>+ 1.357</b>
<b>N<sub>2</sub>H<sub>4</sub></b>	$\frac{3}{2}N_2H_5^+ + \frac{3}{2}H^+ + e^- \rightarrow NH_4^+$	+ 0.661
<b>NH<sub>2</sub>OH</b>	$\frac{1}{2}NH_3OH^+ + H^+ + e^- \rightarrow \frac{1}{2}NH_4^+ + \frac{1}{2}H_2O$	+ 0.937
	$NH_3OH^+ + \frac{1}{2}H^+ + e^- \rightarrow \frac{1}{2}N_2H_5^+ + H_2O$	+ 1.204
<b>HNO<sub>2</sub></b>	$\frac{1}{4}NO_2^- + \frac{3}{2}H^+ + e^- \rightarrow \frac{1}{4}NH_3OH^+ + \frac{1}{4}H_2O$	+ 0.054
	$NO_2^- + 2H^+ + e^- \rightarrow NO(g) + H_2O$	+ 0.376
	$\frac{1}{2}NO_2^- + \frac{3}{2}H^+ + e^- \rightarrow \frac{1}{4}N_2O(g) + \frac{3}{4}H_2O$	+ 0.777
	$\frac{1}{6}NO_2^- + \frac{4}{3}H^+ + e^- \rightarrow \frac{1}{6}NH_4^+ + \frac{1}{3}H_2O$	+ 0.799
	$\frac{1}{3}NO_2^- + \frac{4}{3}H^+ + e^- \rightarrow \frac{1}{6}N_2(g) + \frac{2}{3}H_2O$	+ 0.969
<b>NO<sub>2</sub></b>	$\frac{1}{7}NO_2(g) + \frac{8}{7}H^+ + e^- \rightarrow \frac{1}{7}NH_4^+ + \frac{1}{7}H_2O$	+ 0.425
	$\frac{1}{2}NO_2(g) + H^+ + e^- \rightarrow \frac{1}{2}NO(g) + \frac{1}{2}H_2O$	+ 0.632
	$NO_2(g) + H^+ + e^- \rightarrow HNO_2$	+ 0.678
	$\frac{1}{4}NO_2(g) + H^+ + e^- \rightarrow \frac{1}{8}N_2(g) + \frac{1}{2}H_2O$	+ 0.950
<b>NO</b>	$\frac{1}{5}NO(g) + \frac{6}{5}H^+ + e^- \rightarrow \frac{1}{5}NH_4^+ + \frac{1}{5}H_2O$	+ 0.340
	$NO(g) + H^+ + e^- \rightarrow \frac{1}{2}N_2O(g) + H_2O$	+ 1.177
	$\frac{1}{4}NO(g) + H^+ + e^- \rightarrow \frac{1}{4}N_2(g) + \frac{1}{2}H_2O$	+ 1.265

$O_2$	$\frac{1}{2}O_2(g) + H^+ + e^- \rightarrow \frac{1}{2}H_2O_2$	+ 0.282
	$\frac{1}{4}O_2(g) + H^+ + e^- \rightarrow \frac{1}{2}H_2O$	+ 0.816
$CO_2$	$\frac{1}{8}CO_2(g) + H^+ + e^- \rightarrow \frac{1}{8}CH_4 + \frac{1}{4}H_2O$	- 0.244
	$\frac{1}{4}CO_2(g) + H^+ + e^- \rightarrow \frac{1}{4}C + \frac{1}{2}H_2O$	- 0.207

### S10 Comparison of sensor signal with off-gas measurements

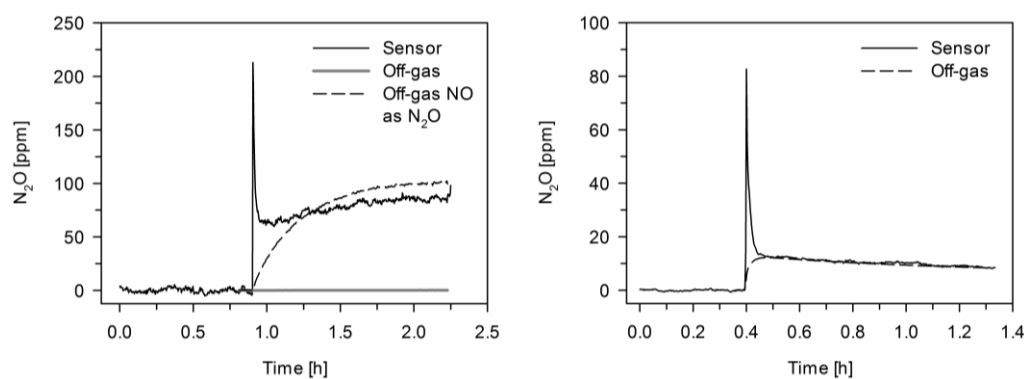


**Figure S8** Comparison of the  $N_2O$  sensor signals with  $N_2O$  measurements in the gas phase and the  $N_2O$  signal caused by  $NO$  interference. This  $N_2O$  signal was calculated from the measured  $NO$  concentration in the off-gas using the calibration curve in Figure 3. On the left, solution with  $1.1 \text{ mgN}\cdot\text{L}^{-1} \text{ HNO}_2$ , on the right, solution with  $15.0 \text{ mgN}\cdot\text{L}^{-1} \text{ NH}_2\text{OH}$ .



## S11 Interferences on NO sensor

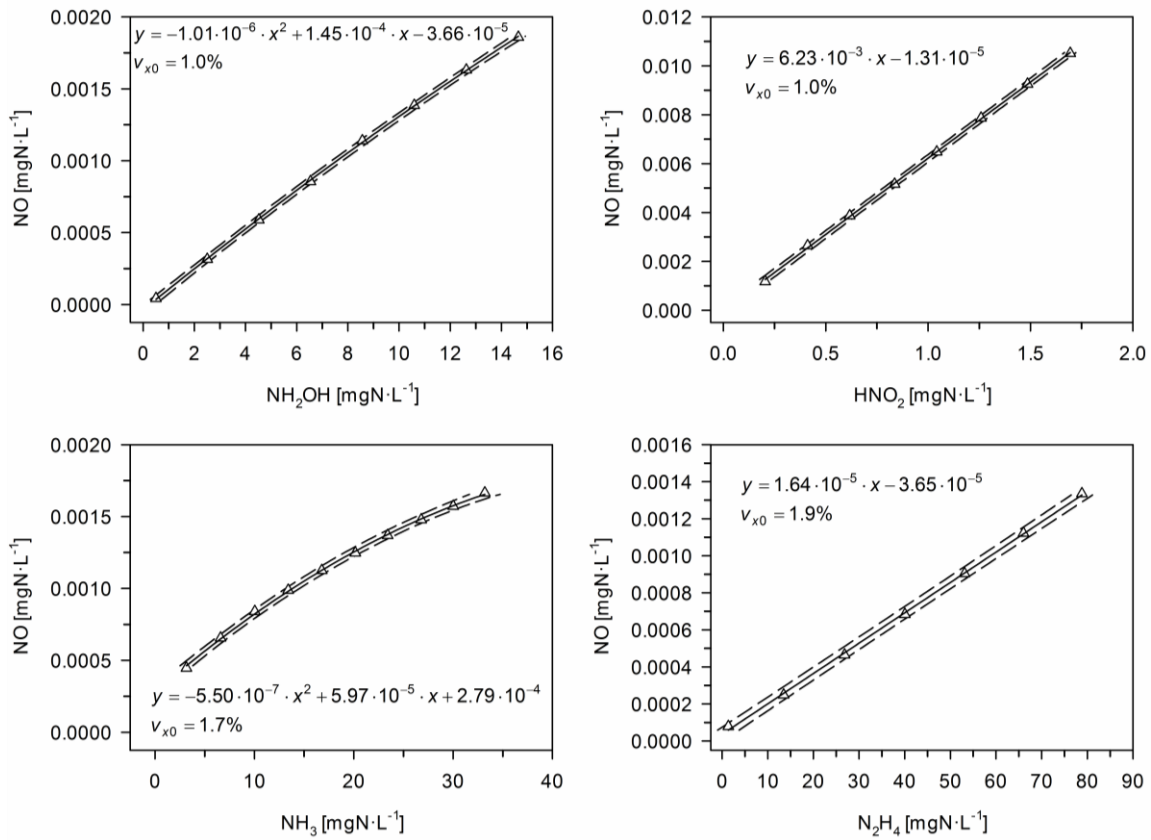


**Figure S9** Influence of NH<sub>2</sub>OH, HNO<sub>2</sub>, NH<sub>3</sub> and N<sub>2</sub>H<sub>4</sub> on NO measurement: fitted interference curve (straight line), 95% prediction interval (dashed lines) and coefficient of variation.

**S12 Variability of individual sensor responses**

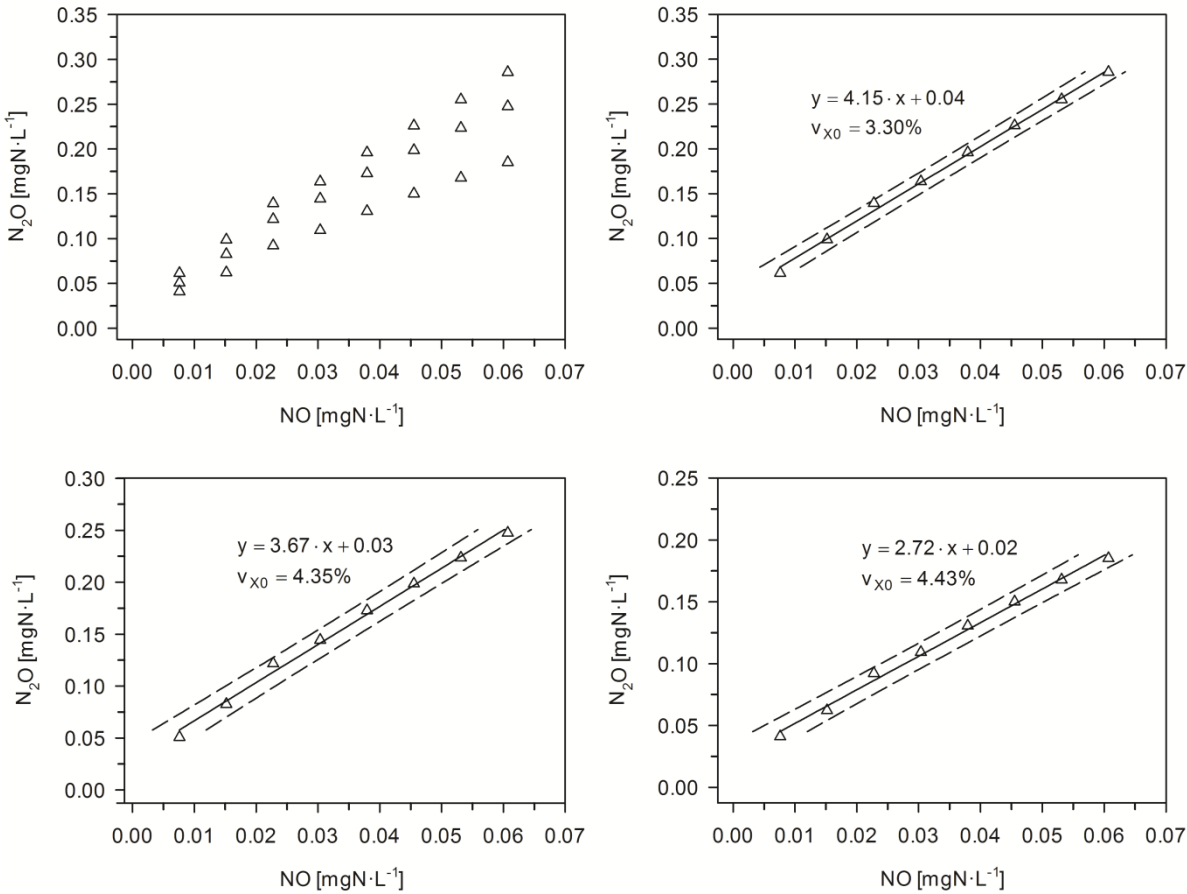


**Figure S10** Influence of NO on three  $N_2O$  sensors: measured signals of all three sensors (triangles) combined in one graph and for each sensor separately with the fitted interference curve (straight line), the 95% prediction interval (dashed lines) and the coefficient of variation.

## **CHAPTER 5**

# **Evaluation of critical factors for the operation of a nitritation/anammox process with urine**

Sarina Schielke-Jenni

# **Evaluation of critical factors for the operation of a nitrification/anammox process with urine**

## **ABSTRACT**

Nitrogen removal from source-separated urine is potentially cheaper and less energy intensive than from wastewater, because urine has substantially higher nitrogen concentrations. However, urine does not contain enough biodegradable organic compounds for conventional nitrogen removal via nitrification and denitrification. If no organic substrate is added, a process combination of aerobic ammonium oxidation (nitrification) and anaerobic ammonium oxidation (anammox) can be used for nitrogen removal from urine. In this study, three different process configurations for nitrification/anammox treatment of undiluted urine were tested: (1) a single-stage nitrification/anammox reactor, (2) a reactor for pre-oxidation of organic substances followed by a single-stage nitrification/anammox reactor, and (3) a two reactor setup with an oxic step for nitrification and oxidation of organic substances and an anoxic step for anammox. All three process configurations were initially operated with digester supernatant, and in all three process configurations, the switch from digester supernatant to urine led to a fast decrease and finally to a complete breakdown of AMX activity within less than 45 d. A detailed evaluation of all potential influence factors, including urine compounds, intermediates of nitrogen conversion and operating parameters, revealed three factors, which could be the most critical for AMX: (1) a high sludge loss caused by floc destabilisation due to the high ratio of monovalent to divalent cations in urine, (2) a direct inhibition of AMX by non-biodegradable organic substances, and (3) a direct inhibition of AMX by pharmaceuticals. The identification of these three critical factors can guide the further research on nitrification/anammox treatment of source-separated urine. Inhibition of AMX by non-biodegradable organic substances or pharmaceuticals can be reduced by diluting urine. Operating biofilm systems could help to reduce the sludge loss due to floc stabilization.

## **INTRODUCTION**

Urine contains over 80% of the total nitrogen in wastewater but accounts for less than 1% of the total volume. Due to higher concentrations, nitrogen removal from source-separated urine is potentially much cheaper and less energy intensive than from wastewater (Maurer et al. 2003, Wilsenach and van Loosdrecht 2006). In many parts of the world, nitrogen removal rather than nitrogen recovery will be the process of choice, because producing nitrogen fertilizer with the well-established Haber-Bosch process can be economically more interesting than recovering nitrogen from urine.

The most conventional process for biological nitrogen removal from wastewater is a combination of autotrophic nitrification with heterotrophic denitrification. However, this process requires a biodegradable organic substrate to ammonia nitrogen (COD/N) ratio of at least 1.7 g COD·g N<sup>-1</sup>. The COD/N ratio of stored urine is though approximately 1 g COD·g N<sup>-1</sup> (Udert et al. 2006) and can increase up to 1.5 g COD·g N<sup>-1</sup> due to ammonia volatilisation during storage (Bürgmann et al. 2011). Therefore, if no organic substrate is added, conventional nitrification/denitrification is not feasible with urine.

In contrast to nitrification/denitrification, the combination of aerobic ammonium oxidation (nitritation) and anaerobic ammonium oxidation (anammox) does not require any biodegradable organic substrate. In addition, nitritation/anammox is economically favourable as it saves up to 58% oxygen compared to conventional nitrification/denitrification. Nitritation/anammox is thus a cost saving alternative for all wastewaters which do not contain enough organic matter for sufficient heterotrophic activity such as urine (Siegrist et al. 2008, Vlaeminck et al. 2012).

However, the composition of urine is very different from common influents of nitritation/anammox processes as, e.g., digester supernatant. For one thing, urine has a much higher COD/N ratio than digester supernatant. Organic substances can be directly toxic for the bacteria (Gomez et al. 2000, Yang et al. 2013) or foster the growth of heterotrophic bacteria (HET), which compete with ammonia oxidising bacteria (AOB) for oxygen and with anammox bacteria (AMX) for nitrite (Chamchoi et al. 2008, Zhu and Chen 2001). Urine also has an about 4 times higher total salinity than digester supernatant. Both the total salinity (Dapena-Mora et al. 2010, Moussa et al. 2006) and high concentrations of single ions (Dapena-Mora et al. 2007, Mosquera-Corral et al. 2005) could inhibit the bacteria. Urine, e.g., contains much higher concentrations of sodium and potassium than digester supernatant. Furthermore, it is likely that the anaerobic conditions in collection and storage tanks allow growth of sulphate-reducing bacteria. Due to the much higher sulphate concentration compared to digester supernatant, this most likely results in much higher sulphide concentrations. Sulphide is another potential inhibitor for the bacteria (Dapena-Mora et al. 2007, Sears et al. 2004). Finally, many pharmaceuticals are excreted via urine (Lienert et al. 2007) and could also have a toxic effect on the bacteria (Fernández et al. 2009, van de Graaf et al. 1995).

So far, only Udert et al. (2003) tried to operate a nitritation/anammox process with undiluted urine. In this case, the system was operated as a two-stage process. Nitritation was successfully operated for 35 d. The second stage, anammox, was though only tested in a batch experiment. The results were promising, however, due to the dilution with the anammox sludge, the concentration of the urine compounds were much lower than in undiluted urine and the experiment only lasted for 90 min. The operation of a nitritation/anammox process with diluted urine was tested in two previous studies (Udert et al. 2008, Bürgmann et al. 2011). Both experiments

showed that nitrogen removal from diluted urine via nitritation/anammox is feasible, but prone to process instabilities.

The goal of this study was to test the operation of a nitritation/anammox process with undiluted urine. Because AMX activity is required for a nearly complete nitrogen removal from urine and thus the crucial factor for a successful operation, three process configurations were chosen, with all of them offering different physiological conditions for AMX: (1) a single-stage nitritation/anammox process, (2) a reactor for pre-oxidation of organic substances followed by a single-stage nitritation/anammox process, which allows the removal of oxidisable compounds prior to the contact with AMX, and (3) a two-stage process, which offers the same advantage as configuration number 2 but additionally complete anoxic conditions for AMX in the second reactor. During all three experiments, the activities of AMX, AOB and nitrite oxidising bacteria (NOB) were followed with batch activity measurements. Additional batch experiments were performed to characterise the influence of selected urine compounds on AMX.

## **MATERIAL AND METHODS**

### **Single-stage nitritation/anammox with untreated urine**

The operation of a nitritation/anammox process with digester supernatant plus glucose (COD/N ratio of 1.4 g N·g COD<sup>-1</sup>) has been described in Jenni et al. (2014). The influent of this lab-scale reactor with a liquid volume of 6.7 L was then switched to undiluted urine. The average influent composition is listed in Table 1. In order to reach the same ammonium concentration as with digester supernatant, the exchange volume per cycle was reduced from 1.3 L to 0.35 L per cycle. The temperature was regulated to 30°C. The cycle scheme was not changed and consisted of a feeding period (~ 3 min), a subsequent 20 min anoxic phase followed by alternating aerobic (40 min) and anoxic phases (20 min) until the ammonium concentration decreased below the set-point (initially 10 mgN·L<sup>-1</sup>, afterwards increased as the ammonium concentration did not further decrease) and a final settling phase of 20 min followed by effluent withdrawal (~ 9 min). Due to problems with the ammonium electrode, the control set-point was switched from ammonium to pH on day 17 after the switch to urine.

During the previous experiment with digester supernatant, the aeration rate was 228 mL·min<sup>-1</sup>. On day 3 after the switch to urine, the aeration rate was switched to 81 mL·min<sup>-1</sup>. Since the measured oxygen concentrations were still very high, i.e. > 0.2 mg·L<sup>-1</sup> in the second half of each cycle, the aeration rate was further reduced to 63 mL·min<sup>-1</sup> and 51 mL·min<sup>-1</sup> on day 22 and day 24 after the switch to urine, respectively.

The effluent was withdrawn at a constant depth of 10 cm below the initial water level. Together with the sedimentation time of 20 min, this resulted in a minimum settling velocity of 0.3 m·h<sup>-1</sup>. In order to maintain a high sludge retention time (SRT), the sludge from the effluent was re-

turned to the reactor during the previous experiment with digester supernatant. Due to very low sludge loss with the effluent, the sludge was not returned to the reactor anymore after day 35 with urine.

**Table 1** Average concentrations  $\pm$  standard deviations in the untreated (20 samples) and the pre-oxidised (12 samples) urine.

	[mgN·L <sup>-1</sup> ] NH <sub>4</sub> <sup>+</sup>	[mg·L <sup>-1</sup> ] COD	[mg·L <sup>-1</sup> ] TIC	[pH] pH	[mS·cm <sup>-1</sup> ] Cond 25°C
<b>untreated urine</b>	2230 $\pm$ 165	3420 $\pm$ 395	1130 $\pm$ 145	9.16 $\pm$ 0.17	26.6 $\pm$ 1.2
<b>pre-oxidised urine</b>	2150 $\pm$ 105	885 $\pm$ 125	1500 $\pm$ 65	9.07 $\pm$ 0.23	23.5 $\pm$ 7.4

### Single-stage nitrification/anammox with pre-oxidised urine

Pre-oxidation of organic substances in urine was achieved in an open Erlenmeyer flask with a total volume of 5 L. Settled sludge (300 mL out of 1 L, volatile suspended solids (VSS) concentration not known) from the nitrification stage of the wastewater treatment plant at Eawag and urine were filled into the flask (total volume of 4 L) and stirred on a magnetic mixer at high speed to ensure high surface aeration. The system was operated as a sequencing batch reactor: as soon as the concentration of the chemical oxygen demand (COD) reached values below 1000 mg COD·L<sup>-1</sup> (corresponding to > 85% biodegradable COD removal), the sludge was settled and 2 L of the supernatant were exchanged with fresh urine. A cycle typically lasted for 7 d. Sulphide was measured during one batch and found to be completely oxidised after 1 d. Based on the average cycle length of 7 d, it was therefore assumed that sulphide was always completely oxidised during the pre-oxidation.

The pre-oxidised urine was used as influent for a single-stage nitrification/anammox reactor. The experiment was performed in the same reactor as used for the operation of the single-stage nitrification/anammox reactor with untreated urine. The temperature was regulated to 30°C. The cycle scheme was identical as in the experiment with untreated urine. Prior to the operation with pre-oxidised urine, the reactor was restarted with fresh sludge from a nitrification/anammox reactor running with digester supernatant at the WWTP Werdhölzli in Zurich. The reactor was first operated with digester supernatant from the WWTP Werdhölzli in Zurich and afterwards, the influent was switched to pre-oxidised urine. The average influent concentrations are listed in Table 1. The exchange volume per cycle was reduced from 1.3 L to 0.45 L in order to reach the same initial ammonium concentration. The initial aeration rate was 81 mL·min<sup>-1</sup>. Afterwards, due to high oxygen concentrations, the aeration rate was reduced to 69 mL·min<sup>-1</sup> at day 3, 57

$\text{mL}\cdot\text{min}^{-1}$  at day 6 and  $40\text{ mL}\cdot\text{min}^{-1}$  at day 7 after the switch to urine. The set-point for the cycle length was initially  $5\text{ mg NH}_4\text{-N}\cdot\text{L}^{-1}$  and afterwards increased up to  $340\text{ mg NH}_4\text{-N}\cdot\text{L}^{-1}$  (Figure 1D) if the ammonium concentration did not decrease further. This resulted in cycle lengths between 15 h in the beginning and up to 120 h at the end of the experiment.

### **Two-stage nitrification/anammox**

The reactor for the nitrification stage had a liquid volume of 7 L. The reactor was inoculated with suspended sludge from the nitrification stage of the wastewater treatment plant at Eawag. The reactor was stirred and aerated with  $1\text{ L}\cdot\text{min}^{-1}$  air. The temperature was regulated to  $30^\circ\text{C}$ . The reactor was operated as a continuous flow stirred tank reactor (CSTR). The influent pump was controlled via the pH, i.e. was switched on at a lower pH level (6.7 – 7.0) and turned off again after reaching a higher pH level (6.9 – 7.5). The so controlled influent flow rate varied between  $0.27$  and  $4.68\text{ L}\cdot\text{d}^{-1}$ . The SRT was not regulated, i.e. sludge loss only occurred via the effluent (overflow at 7 L) and sampling. The average SRT was  $18.0 \pm 11.8\text{ d}$  and the average VSS concentration was  $1.2 \pm 0.5\text{ g}\cdot\text{L}^{-1}$ . From day 45 on, additional base (sodium hydroxide) was dosed to the influent.

The anammox stage was operated in a second reactor with a liquid volume of 6.7 L. The reactor was inoculated with suspended biomass from a nitrification/anammox reactor treating sludge digester supernatant (WWTP Limmattal, Dietikon, Switzerland). The reactor was stirred but not aerated and the temperature was regulated to  $30^\circ\text{C}$ . The pH was controlled between 7.6 and 7.8 by adding hydrochloric acid. The effluent from the nitrification stage was filtered with coffee filters (Kafino n°2, Migros, Switzerland) before it was used as influent for the anammox stage. Initially, the length of the cycles was time-controlled (12 h) and the exchange volume per cycle was 0.5 or 0.75 L per cycle (depending on the performance of the nitrification stage). From day 10 on, when the process performance started to decrease, the length of the cycle was controlled via the ammonium concentration in order to prevent ammonia inhibition. When the ammonium concentration did not decrease any further, additional nitrite (sodium nitrite) was added to the reactor until the ammonium concentration decreased at least below  $50\text{ mg N}\cdot\text{L}^{-1}$ . The effluent was withdrawn at a constant depth of 10 cm below the initial water level. Together with the sedimentation time of 10 min, this resulted in a minimum settling velocity of  $0.6\text{ m}\cdot\text{h}^{-1}$ . The SRT was not controlled, i.e. sludge loss only occurred via the effluent and sampling.

### **Anammox batch activity measurements**

For the batch activity measurements during the operation of the single-stage processes, the necessary amount of sludge to reach the desired VSS concentration as described below was sampled from the reactor immediately before the start of the batch experiments. The batch experiments to test the influence of nitrite and salts on anammox activity were conducted with sus-



pended biomass from a nitrification/anammox reactor treating sludge digester supernatant (WWTP Limmattal, Dietikon, Switzerland). The sludge was collected one (influence of nitrite) respectively two (influence of salts) days prior to the experiments and stored at room temperature.

The collected biomass was washed once, and diluted with sodium phosphate buffer ( $0.01 \text{ mol}\cdot\text{L}^{-1}$ , pH 8.35) to a total volume of 0.6 L in order to obtain a VSS concentration of approximately  $1 \text{ g}\cdot\text{L}^{-1}$ . In case of the batch experiments to test the influence of nitrite, the sludge was diluted to a final volume of 1 L and a VSS concentration of approximately  $5 \text{ g}\cdot\text{L}^{-1}$ . In case of the batch experiments on salt influence, a salt solution (Supporting information S1) was used instead of the sodium phosphate buffer and the sludge was diluted to a total volume of 1 L and a VSS concentration of approximately  $2.5 \text{ g}\cdot\text{L}^{-1}$ .

A trace element stock solution (Kuai and Verstraete 1998) was added to all experiments. The temperature was always kept at  $30^\circ\text{C}$ . Anaerobic conditions were established by sparging the solution with  $600 \text{ mL}\cdot\text{min}^{-1}$  (experiments with total volume of 0.6 L) respectively  $1000 \text{ mL}\cdot\text{min}^{-1}$  (experiments with total volume of 1 L)  $\text{N}_2$  gas containing 2%  $\text{CO}_2$  for 20 min prior to the experiment. During the experiment, only the headspace was flushed (with the same gas mixture) to minimise stripping. The pH was always adjusted to 7.2 by adding NaOH respectively HCl solution and kept constant during the experiment ( $7.2 \pm 0.1$ ) by regulating the  $\text{CO}_2$  flow ( $0\text{--}250 \text{ mL}\cdot\text{min}^{-1}$  of 20%  $\text{CO}_2$  in  $\text{N}_2$  gas) and adding more HCl solution, if necessary.

For the standard experiments, concentrations of  $60 \text{ mg N}\cdot\text{L}^{-1}$  of both  $\text{NH}_4^+$  and  $\text{NO}_2^-$  were established by adding  $\text{NH}_4\text{Cl}$  and  $\text{NaNO}_2$ , respectively, and liquid samples for the analysis of the nitrogen compounds were taken every 30 min for a total duration of 2 h. In case of the experiments on nitrite influence,  $\text{NH}_4^+$  concentrations of approximately  $85 \text{ mg N}\cdot\text{L}^{-1}$  and  $\text{NO}_2^-$  concentrations of 50, 80, 120, 160 respectively  $200 \text{ mg N}\cdot\text{L}^{-1}$  were established by dosing  $\text{NH}_4\text{Cl}$  and  $\text{NaNO}_2$ . In case of 50 and  $80 \text{ mg N}\cdot\text{L}^{-1}$   $\text{NO}_2^-$  liquid samples for the analysis of the nitrogen compounds were taken every 5 min for a total duration of 20 min. In case of 120, 160 and  $200 \text{ mg N}\cdot\text{L}^{-1}$   $\text{NO}_2^-$  liquid samples for the analysis of the nitrogen compounds were taken every 15 min for a total duration of 1 h. In case of the experiments on salt influence,  $\text{NH}_4^+$  and  $\text{NO}_2^-$  concentrations of approximately  $85 \text{ mg N}\cdot\text{L}^{-1}$  each were established by dosing  $\text{NH}_4\text{Cl}$  and  $\text{NaNO}_2$ , respectively. In case of the standard experiment with phosphate buffer,  $\text{NaNO}_3$  was added to reach a concentration of  $110 \text{ mg N}\cdot\text{L}^{-1}$   $\text{NO}_3^-$  to match the nitrate concentration in the salt solution (Supporting information S1). Liquid samples for the analysis of the nitrogen compounds were taken every 15 min for a total duration of 1 h.

AMX ( $\text{NH}_4^+$  consumption), AOB ( $\text{NH}_4^+$  consumption), and NOB ( $\text{NO}_3^-$  production) activities were calculated as the slopes from 5 data points using the least squares method. The measurement uncertainties of the resulting rates are given as the standard error of the calculated slopes

(linear estimation function in excel). In case of the batch activity measurements during the operation of the single-stage processes, the calculated values in  $\text{mg N}\cdot\text{gVSS}^{-1}\cdot\text{d}^{-1}$  were multiplied with the VSS concentration measured in the SBR on the same day in order to determine the maximum possible activities in the SBR ( $\text{mg N}\cdot\text{L}^{-1}\cdot\text{d}^{-1}$ ).

### **Alkalinity simulation**

According to the study of Bürgmann et al. (2011), pH values around 6.3 to 6.5 in the end of the cycles allow a successful operation of a nitrification/anammox process with five times diluted urine. Lower pH values were not tested and based on the fact that AMX activity was reported to decrease to around 10% of the maximum possible value at pH values 6.0 (Strous et al. 1997b), we decided to choose 6.3 as the lowest possible value which still allows a successful operation of a nitrification/anammox process with urine. Therefore, only the alkalinity that buffers above pH 6.3 should be consumed during the process.

For the alkalinity simulation, we used the concentrations according to Table 1 and Table 2. We assumed that 40% of the biodegradable organic substrate was present as acetate (relevant for alkalinity calculation) and the remaining 60% as uncharged organic substances (not relevant for alkalinity calculation). The simulation was performed with the software Phreeqc (version phreeqi-2.13.2-1727, USGS (2014), <http://wwwbrr.cr.usgs.gov>). In a first step, the chloride concentration was adjusted in order to equilibrate the charge balance at the initial pH value. Subsequently, an alkalinity measurement respectively a dosage of HCl was simulated by adjusting the chloride concentration to meet the charge balance at the final pH value of 6.3. CO<sub>2</sub> stripping was included in the simulation by defining a gas phase with a fix CO<sub>2</sub> partial pressure of 0.000316 atm (partial pressure of CO<sub>2</sub> in the atmosphere). Phreeqc adjusts the chloride concentration in a first step and then equilibrates the CO<sub>2</sub> in a second step, which causes an increase of the pH value. Therefore, the chloride concentration at the end pH value 6.3 could only be calculated iteratively. Due to numerical reasons, the final pH value in the simulations was 6.318.

### **Analytical methods**

Samples for the analysis of dissolved compounds were immediately filtered (MN GF-5, pore size 0.45  $\mu\text{m}$ , Macherey-Nagel, Düren, Germany) and stored in the fridge for 1 to 2 days prior to analysis. Total suspended solids (TSS) and VSS samples were processed immediately after sampling. NH<sub>4</sub><sup>+</sup> in the effluent and in the samples from the batch activity measurements was analysed on a flow injection analyser (Foss FIA star 5000, Rellingen, Germany). NH<sub>4</sub><sup>+</sup> in the influent and COD were measured photometrically with vial tests (Hach Lange, Düsseldorf, Germany). NO<sub>2</sub><sup>-</sup> and NO<sub>3</sub><sup>-</sup> were analysed on an ion chromatograph (Compact IC 761, Metrohm, Herisau, Switzerland). TSS and VSS were determined according to standard methods (Ameri-

can Public Health Association 2005), using ashless black ribbon filter papers (MN 64 w, average retention of 7 – 12  $\mu\text{m}$ , Macherey-Nagel, Düren, Germany).

## RESULTS

### Single-stage nitrification/anammox with untreated undiluted urine

Almost immediately after the switch from digester supernatant to urine, the nitrogen elimination rate (NER) started to decline and continuously decreased from values above  $200 \text{ mgN}\cdot\text{L}^{-1}\cdot\text{d}^{-1}$  to values around  $70 \text{ mgN}\cdot\text{L}^{-1}\cdot\text{d}^{-1}$  after 45 d with urine (Figure 1A). At the same time, the  $\text{NO}_2^-$  and  $\text{NH}_4^+$  effluent concentrations increased from values below  $10 \text{ mg N}\cdot\text{L}^{-1}$  to values around  $70 \text{ mg N}\cdot\text{L}^{-1}$ , indicating decreasing AMX activity (Figure 1C).

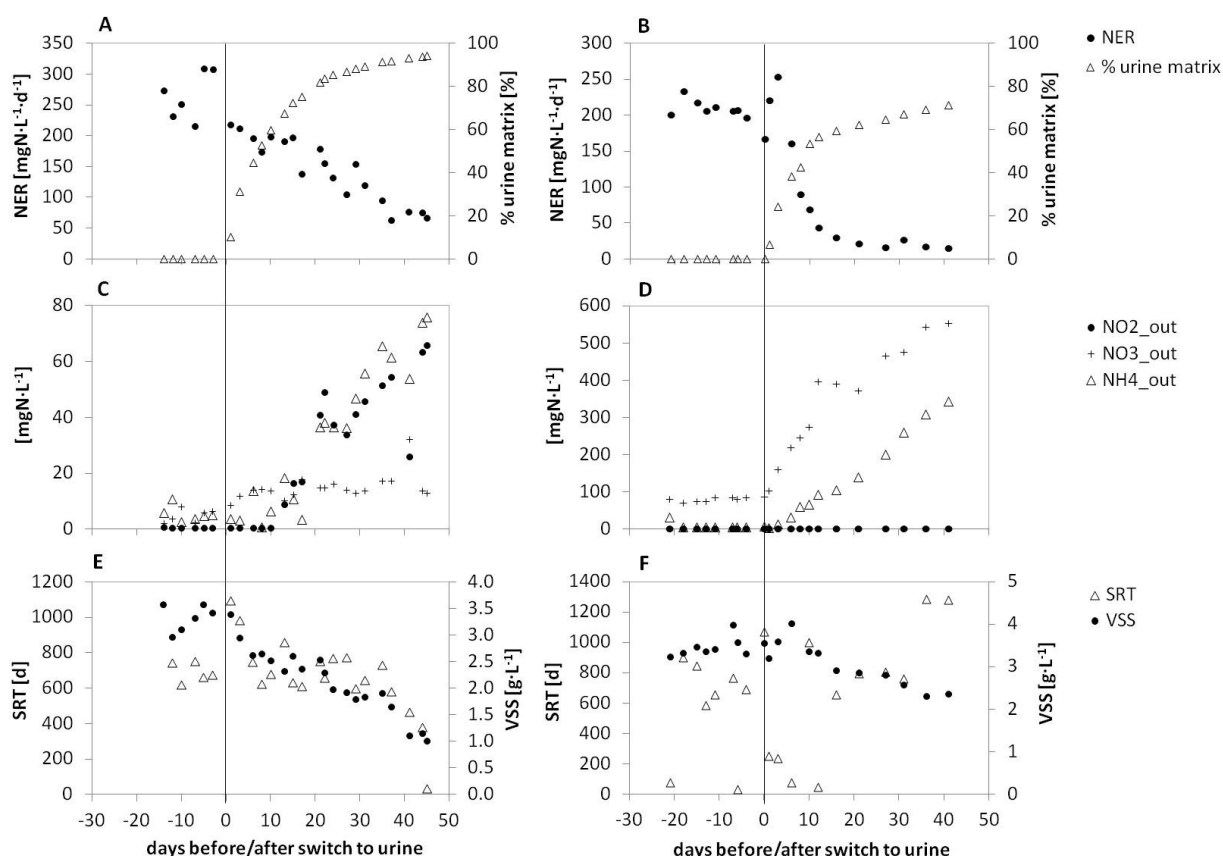


**Figure 1** Single stage nitrification/anammox with (A, C, E) and without (B, D, F) pre-oxidation of urine: Nitrogen elimination rates and extent of reactor exchange with urine matrix (A, B), the nitrogen effluent concentrations (C,D) and SRT and VSS concentrations in the reactor (E,F) before and after the switch from digester supernatant to urine.

Batch activity measurements before and after the switch to urine confirmed that AMX activity significantly decreased and was not detectable any more after 42 d with urine (Figure 2A).

While AOB activity was not affected by the switch to urine, NOB activity showed a similar pattern as the AMX activity and also completely ceased after 42 d with urine.

The SRT remained at a very high level during the entire operation period ( $670 \pm 200$  d; Figure 1E) which was in part possible by recycling the suspended solids captured in the effluent. The high fluctuations can be explained with the fact that the SRT was not regulated and sludge loss only occurred irregularly via the effluent and sampling. After day 35 with urine, the sludge from the effluent was not returned to the reactor anymore, which resulted in a decrease of the average SRT to  $440 \pm 260$  d. Interestingly, the VSS concentration strongly decreased from values around  $3.3 \text{ g}\cdot\text{L}^{-1}$  with digester supernatant to values only slightly higher than  $1.0 \text{ g}\cdot\text{L}^{-1}$  after 40 d with urine.

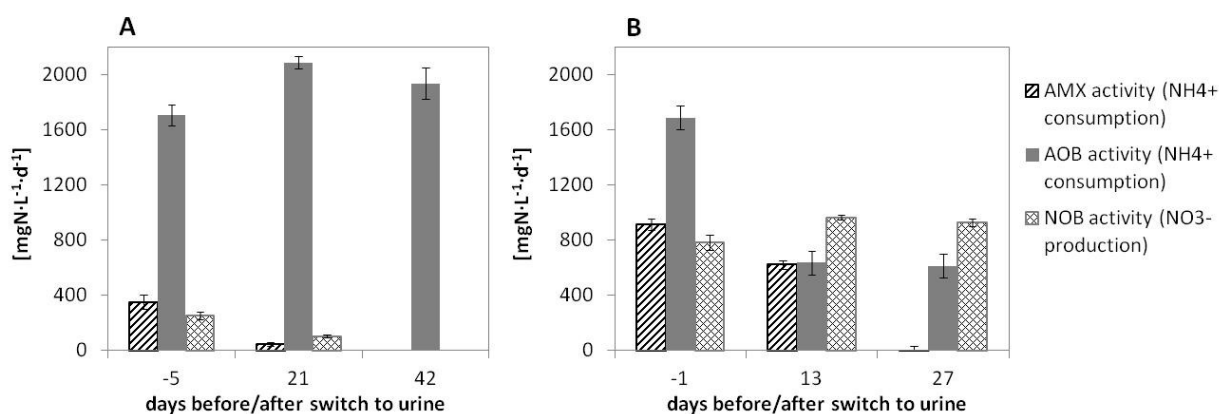


**Figure 2** Batch activity measurements before and after the switch from digester supernatant to urine during single stage nitritation/anammox with (A) and without (B) pre-oxidation of urine.

### Single-stage nitritation/anammox with pre-oxidised undiluted urine

A pre-oxidation of undiluted urine allowed removing  $> 85\%$  of the biodegradable organic substrate without losing significant amounts of nitrogen. The pre-oxidised undiluted urine was then used as influent for a single-stage nitritation/anammox process. As in case of the untreated undiluted urine (see "Single-stage nitritation/anammox with untreated urine"), the NER started to decrease almost immediately after the switch from digester supernatant to urine (Figure 1B). The decrease was even faster and the NER reached values as low as  $15 \text{ mg N}\cdot\text{L}^{-1}\cdot\text{d}^{-1}$  after 40 d with pre-oxidized undiluted urine. In contrast to the operation with untreated undiluted urine (Figure 1C), the ammonium and the nitrate effluent concentrations increased much stronger while the nitrite effluent concentration remained at a very low level (Figure 1D). The much higher initial nitrate effluent concentration can be explained with the fact, that the digester supernatant used as influent prior to the switch to untreated undiluted urine contained additional

glucose (COD/N ratio  $1.4 \text{ g COD} \cdot \text{g N}^{-1}$ ), which allowed higher denitrification of the nitrate produced by AMX.

The average SRT remained at a high level ( $640 \pm 400 \text{ d}$ ) during the entire experiment but varied a lot since it was not regulated (sludge loss only occurred via the effluent and sampling; Figure 1F). As in case of the single-stage process with untreated urine, the VSS concentration in the reactor decreased during the experiment. The decrease was less strong, but the VSS concentration still decreased from values around  $3.6 \text{ g} \cdot \text{L}^{-1}$  with digester supernatant to values around  $2.4 \text{ g} \cdot \text{L}^{-1}$  after 40 d with urine.

The strong increase of the ammonium and the nitrate effluent concentrations indicate decreasing AMX and AOB activity and increasing NOB activity (Figure 1D). Batch activity measurements before and after the switch to urine confirmed that both AMX and AOB activity significantly decreased (Figure 2B). AOB activity stabilised at a level around  $620 \text{ mg N} \cdot \text{L}^{-1} \cdot \text{d}^{-1}$  while AMX activity was close to zero after 27 d with urine. In contrast to our expectations based on the strong increase of the nitrate effluent concentration, NOB activity did not increase but remained at the same level before and after the switch to urine.

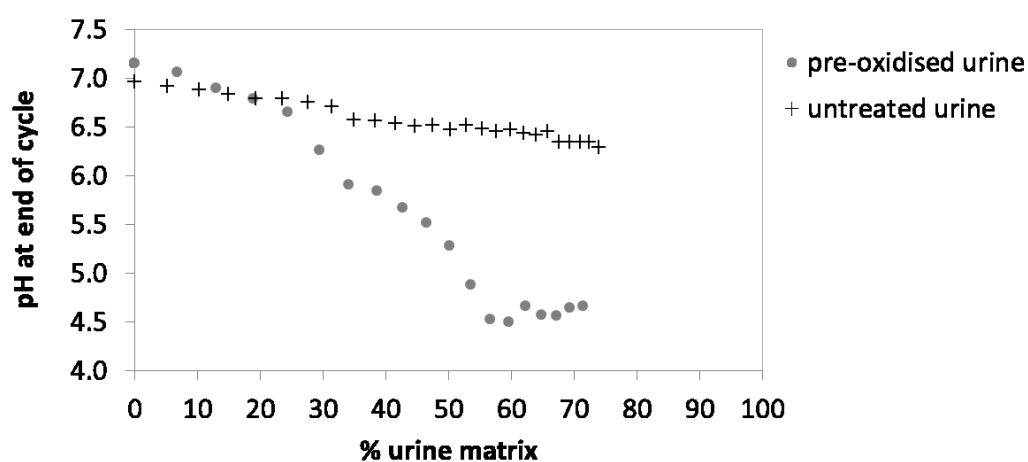


**Figure 3** pH values in the end of each cycle of single-stage nitrification/anammox reactors operated with untreated and pre-oxidised urine, respectively, against the reactor volume that was already exchanged with urine.

Interestingly, the pre-oxidised undiluted urine led to an unexpected and very strong decrease of the pH value in the nitrification/anammox reactor (Figure 3). The pH value at the end of each cycle decreased from values around 7.1 with digester supernatant to values as low as 4.5 after 14 days with urine. In contrast to this, the pH value only decreased to a level around 6.3 with untreated urine. Most likely, the much lower pH value explains the different effluent concentrations and the different bacterial activities compared to the experiment with untreated urine. Ap-

parently, NOB were less affected by the low pH value than AOB and AMX and then profited from the lower oxygen consumption by AOB and the lower nitrite consumption by AMX. Most likely, the higher NOB activity and thus higher nitrate effluent concentrations compared to the single-stage reactor with untreated urine was also due to the higher oxygen concentrations (Figure 9).

### **Two-stage nitrification/anammox with undiluted urine**

Nitrification of urine was tested in a semi-continuous flow stirred tank reactor with activated sludge (Figure 4). The performance was unstable during most part of the experiment. Considering the points when the influent tank was filled with a fresh batch of urine (arrows in Figure 4A), the sudden decreases of the ammonium removal rate and the nitrite production rate on day 10 and 55 were most likely caused by inhibiting compounds in the influent. Both times the rates started to increase again as soon as the influent was changed on day 24 and 64. One possible explanation for this could be that cleaning agent was accidentally flushed into the urine storage tank during the cleaning of the toilets. The fact, that a similar decrease of the ammonium removal rate was also observed in another nitrification reactor which was operated with the same urine (data not shown), supports this hypothesis.

Between the two process breakdowns, the performance was more stable with an average ammonium oxidation rate of  $270 \pm 30 \text{ mg N}\cdot\text{L}^{-1}\cdot\text{d}^{-1}$ . The good agreement of the ammonium oxidation rate with the nitrite production rate and the low nitrate production rate shows that only minor nitrite oxidation occurred. Furthermore, this also indicates that only minor amounts of nitrogen were lost as gaseous nitrogen compounds.

After an increase in the beginning, the nitrite to ammonium ratio reached a stable level around  $0.91 \pm 0.06 \text{ mg NO}_2^- \cdot \text{N} \cdot \text{mg NH}_4^+ \cdot \text{N}^{-1}$  after 10 d (Figure 4B). This is much lower than the minimal ratio of  $1.32 \text{ mg NO}_2^- \cdot \text{N} \cdot \text{mg NH}_4^+ \cdot \text{N}^{-1}$  which is required for the anammox process. Because further ammonium oxidation requires more alkalinity, additional base was added to the influent from day 45 on. Subsequently, the nitrite to ammonium ratio reached a suitable level around  $1.35 \pm 0.06 \text{ mg NO}_2^- \cdot \text{N} \cdot \text{mg NH}_4^+ \cdot \text{N}^{-1}$ .

The anammox stage was operated as a SBR and fed with the effluent of the nitrification stage. In the beginning, the nitrification stage was slower than the anammox stage, which led to a significant decrease of the NER and the ammonium removal rate (corresponding to AMX activity) between day 4 and 7 in the anammox stage (Figure 5). Subsequently, both the NER and the ammonium removal rate only slightly decreased till a turning point on day 24, when both rates suddenly decreased very fast and finally reached values close to zero on day 44.

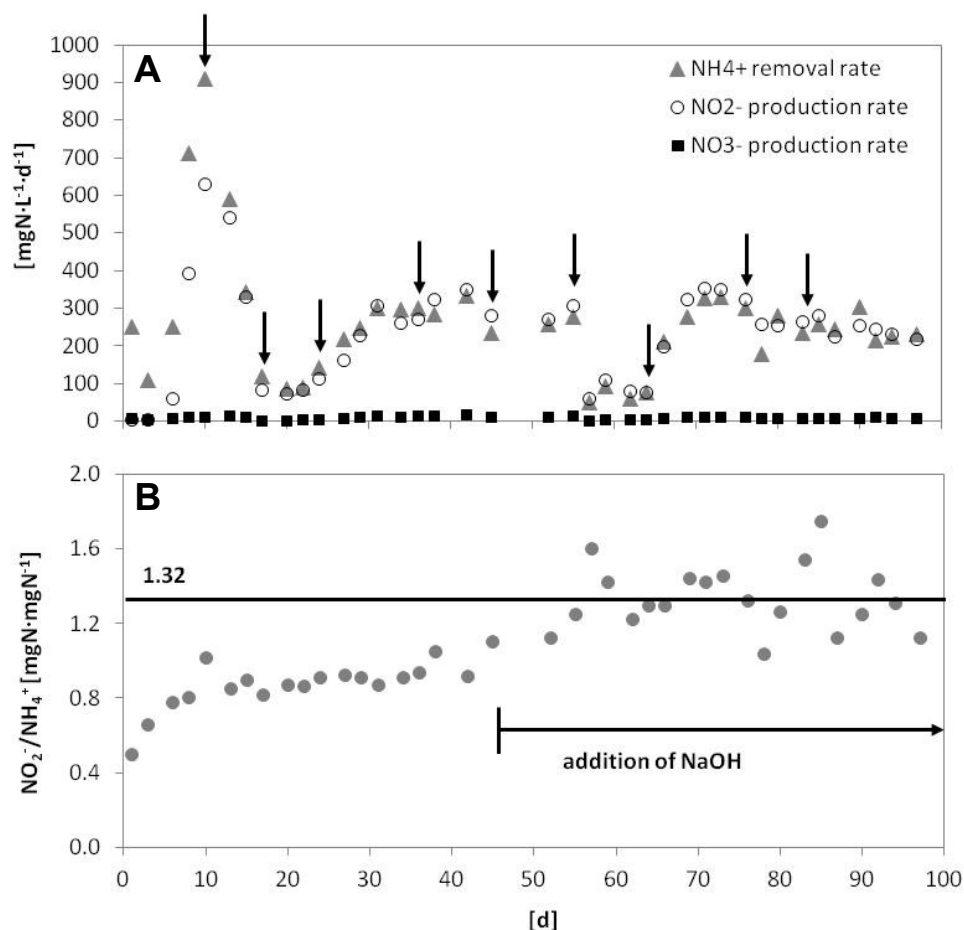


**Figure 4** (A) Process rates of the nitrogen compounds (arrows mark points when the influent tank was filled with a new batch of urine) and (B) the nitrite to ammonium ratio in the effluent of the nitrification reactor.

The decreasing AMX activity was coupled to a simultaneous, but due to the high HRT slower decrease, of the nitrate effluent concentration from values above  $150 \text{ mg N}\cdot\text{L}^{-1}$  down to  $80 \text{ mg N}\cdot\text{L}^{-1}$  (Figure 5B). This can be explained with the fact that AMX activity is the only source of nitrate in an anoxic reactor. In order to avoid ammonia toxicity, the ammonium concentration at the end of each cycle was kept below  $50 \text{ mg N}\cdot\text{L}^{-1}$ . When the ammonium concentration did not further decrease, additional nitrite was dosed to the reactor (arrows in Figure 5D). Nitrite was the limiting compound and therefore, the effluent nitrite concentrations remained at a very low level during the whole experiment. Towards the end of the experiment, the required nitrite to ammonium ratio to keep the ammonium concentration in the effluent below  $50 \text{ mg N}\cdot\text{L}^{-1}$  increased significantly up to  $4 \text{ g NO}_2^- \text{N per g NH}_4^+ \text{-N}$ .

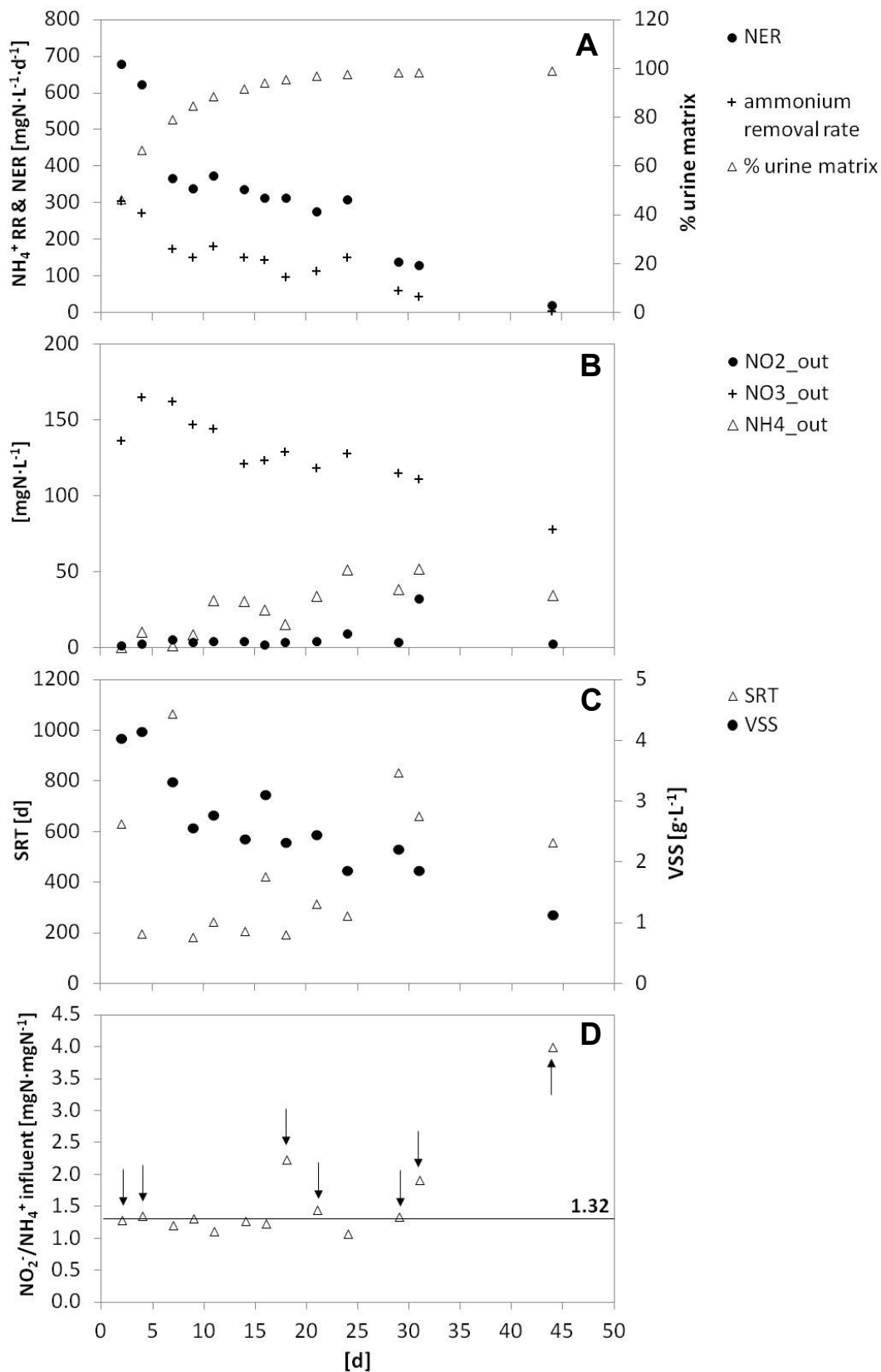


**Figure 5** (A) Ammonium removal rate, nitrogen elimination rate, urine matrix i.e. percentage of the reactor volume already exchanged with urine, (B) the nitrogen effluent concentrations, (C) SRT and VSS in the reactor and (D) the nitrite to ammonium ratio in the influent of the anammox reactor (arrows mark the cycles where additional nitrite was dosed into the reactor).



With an average value of  $450 \pm 280$  d the SRT remained at a high level during the entire experiment, but fluctuated strongly as it was not controlled (sludge loss only occurred via the effluent and sampling; Figure 5D). As observed in the single-stage system with untreated urine, the VSS concentration decreased strongly from initial values around  $4 \text{ g}\cdot\text{L}^{-1}$  to values around  $1 \text{ g}\cdot\text{L}^{-1}$  at the end of the experiment.

### Effect of salts on AMX activity

The effect of salt on AMX activity was tested in batch activity measurements with phosphate buffer solution (blank) and a synthetic salt solution which contained the same salts at the same concentrations as measured in urine (Supporting information S1). With the salt solution, AMX activity decreased to less than 5% of the activity measured in the standard experiment with phosphate buffer solution (Figure 6) and was thus almost completely inhibited.

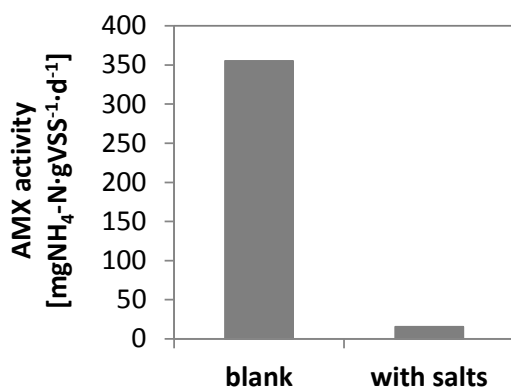


**Figure 6** AMX batch activity measurements to characterise the influence of salts, with a phosphate buffer solution (blank) and a synthetic salt solution that contained the same salts at the same concentrations as measured in urine (Supporting information S1).

### Effect of nitrite on AMX activity

The effect of nitrite on AMX activity was characterised in batch activity measurements with different initial nitrite concentrations (other conditions identical; Figure 7). ). Compared to the standard experiment with an initial nitrite concentration of  $52 \text{ mg N}\cdot\text{L}^{-1}$ , AMX activity only slightly decreased to 83% between  $80$  and  $123 \text{ mg N}\cdot\text{L}^{-1}$  nitrite. There was no significant difference with initial nitrite concentrations between  $123$  and  $202 \text{ mg N}\cdot\text{L}^{-1}$ .

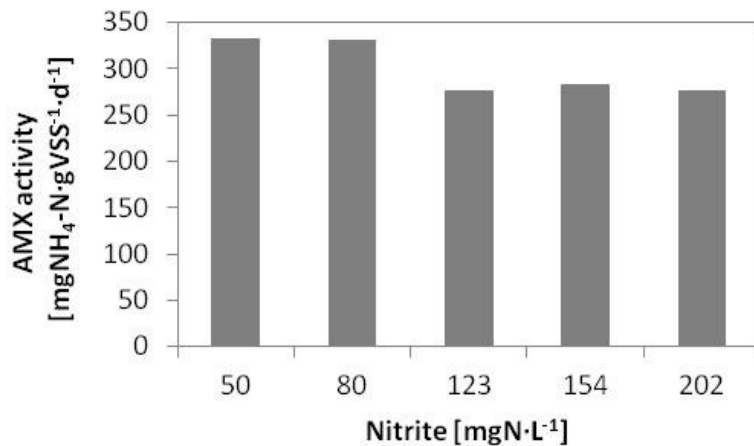


**Figure 7** AMX batch activity measurements with different initial nitrite concentrations to characterise the influence of nitrite.

## DISCUSSION

### Direct inhibition of AMX activity

In all three process configurations, AMX activity decreased very fast and almost completely ceased 45 d after the switch to urine at the latest. Apart from a direct inhibition by urine compounds, AMX could also have been inhibited or limited by operating parameters (e.g. dissolved oxygen) or by nitrogen intermediates (e.g. nitrite) which were built during the process. Table 3 contains an overview of all possible inhibition factors as well as their conditions in the three different process configurations, which are subsequently discussed in more detail.

There are only two factors for which a significant inhibition is likely or cannot be excluded in all three reactor configurations: non-biodegradable organic substrate and pharmaceuticals. Both factors are sum parameters and their individual composition in urine is not known. Especially in case of pharmaceuticals, the concentration and presence of single products is expected to be highly variable as e.g. the use of antibiotics is much less restricted in some low-income countries compared to Europe. A further characterisation of the influence of these two factors on AMX activity is thus difficult. In any case, the best solution to reduce an inhibition of AMX by these two factors would be a dilution of the urine prior to the treatment with nitrification/anammox.

**Table 3** Overview of potentially inhibiting factors for AMX activity in the three tested process configurations (grey: inhibition likely, shaded: inhibition not completely excluded, white: significant inhibition excluded).

		single-stage untreated urine	single-stage pre-oxidised urine	two-stage
Operating parameters	pH	6.3 – 7.9	4.5 – 8.5	7.6 – 7.8 (regulated)
	Dissolved oxygen	~ 0.2 mg·L <sup>-1</sup>	< 0.5 mg·L <sup>-1</sup>	anoxic
	Temperature	30°C	30°C	30°C
	SRT	670 ± 220 d	690 ± 440 d	450 ± 280 d
Nitrogen intermediates	NO <sub>2</sub> <sup>-</sup>	< 66 mg N·L <sup>-1</sup>	< 0.5 mg N·L <sup>-1</sup>	< 130 mg N·L <sup>-1</sup>
	NO	only coupled to high nitrite concentrations	n.d.	< 800 ppm
	N <sub>2</sub> O	only coupled to high nitrite concentrations	n.d.	< 17'300 ppm
Urine compounds	COD as substrate for HET	1.37 ± 0.15 g COD·g N <sup>-1</sup>	0.30 ± 0.07 g COD·g N <sup>-1</sup>	0.12 ± 0.10 g COD·g N <sup>-1</sup>
	Toxic biodegradable COD	100%	~25%	~5%
	Toxic non-biodegradable COD	100%	100%	100%
	NH <sub>3</sub>	< 5 mg N·L <sup>-1</sup>	< 20 mg N·L <sup>-1</sup>	< 3.5 mg N·L <sup>-1</sup>
	Sulphide	100%	n.d.	n.d.
	Salinity	slow increase	slow increase	slow increase
	Salt ions	below inhibition threshold values	below inhibition threshold values	below inhibition threshold values
	Pharmaceuticals	100%	partly reduced	partly reduced

### Operating parameters

#### pH value

AMX activity was reported to be the highest at pH values between 7.0 and 8.5, and to decrease to around 40% and 10% at pH values between 6.5 and 6.0, respectively (Strous et al. 1997b). However, during the operation with five-times diluted urine in a SBR (Bürgmann et al. 2011), a strong increase of AMX abundance over time was observed when the lower pH setpoint was in

the range of 6.3 to 6.5 (Figure 8). Therefore, I conclude that pH values in the range of 6.3 – 8.5 do not significantly inhibit AMX.

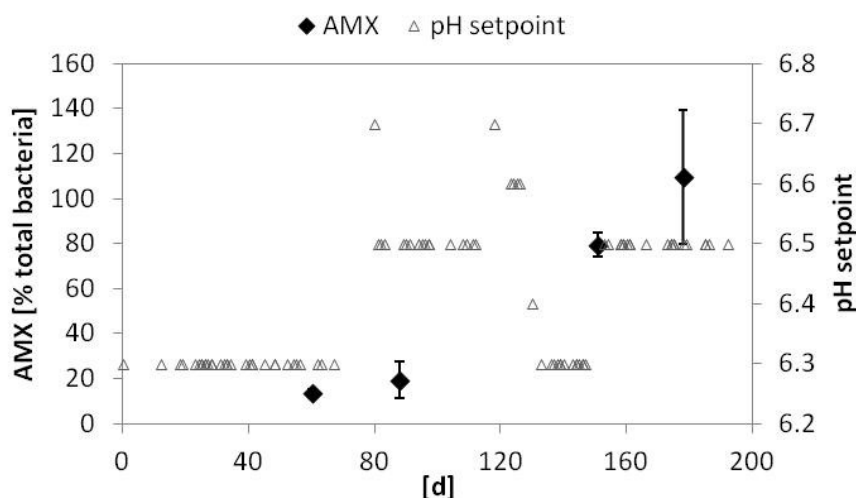


**Figure 8** pH at the end of the cycles (pH setpoint) and anammox bacteria abundance during the operation of a nitrification/anammox reactor with five-times diluted urine (adapted from Bürgmann et al. 2011).

### Dissolved oxygen

AMX prefer completely anoxic conditions and can be inhibited at very low dissolved oxygen concentrations. Strous et al. (1997a) e.g. reported that AMX were completely but reversibly inhibited at 0.5% air saturation, which equals  $0.036 \text{ mg O}_2 \cdot \text{L}^{-1}$  at  $30^\circ\text{C}$ . The maximum tolerable oxygen concentration though strongly depends on the sludge structure as AMX can cope with much higher bulk oxygen concentrations if they are located in the centre of larger aggregates (Winkler et al. 2012a).

In case of the single-stage nitrification/anammox reactor with untreated undiluted urine, the inoculum was from a nitrification/anammox reactor that has been successfully operated with dissolved oxygen concentrations around  $0.2 \text{ mg} \cdot \text{L}^{-1}$ . In our reactor, the dissolved oxygen concentration was also regulated around  $0.2 \text{ mg} \cdot \text{L}^{-1}$ , i.e. the aeration stopped when the concentration reached  $0.2 \text{ mg} \cdot \text{L}^{-1}$  and started again when the concentration dropped below  $0.2 \text{ mg} \cdot \text{L}^{-1}$ . Due to the high response time, the oxygen concentration highly fluctuated and reached values up to  $0.6 \text{ mg} \cdot \text{L}^{-1}$  (Figure 9A). From day 15 on, high signals were partially caused by interfering substances (increase of the baseline; See nitric oxide and nitrous oxide) and the dissolved oxygen concentration itself mainly stayed below  $0.2 \text{ mg} \cdot \text{L}^{-1}$ . In the first 15 days, an inhibition of AMX activity by the short but high peaks above  $0.2 \text{ mg O}_2 \cdot \text{L}^{-1}$  can though not be excluded. As oxygen inhibition is reversible, AMX might though have been able to recover during the anoxic periods.

In case of the single-stage nitrification/anammox reactor with pre-oxidised undiluted urine, the inoculum was from a nitrification/anammox reactor that has been successfully operated with regular oxygen concentrations between 0.2 and 0.5 mg·L<sup>-1</sup> and short peaks up to 0.8 mg O<sub>2</sub>·L<sup>-1</sup>. Therefore, it is assumed that AMX were not inhibited by the dissolved oxygen concentrations during single-stage nitrification/anammox with pre-oxidised undiluted urine, although the oxygen concentrations during aerobic phases reached values above 0.4 mg·L<sup>-1</sup> for most of the cycle duration (Figure 9B).

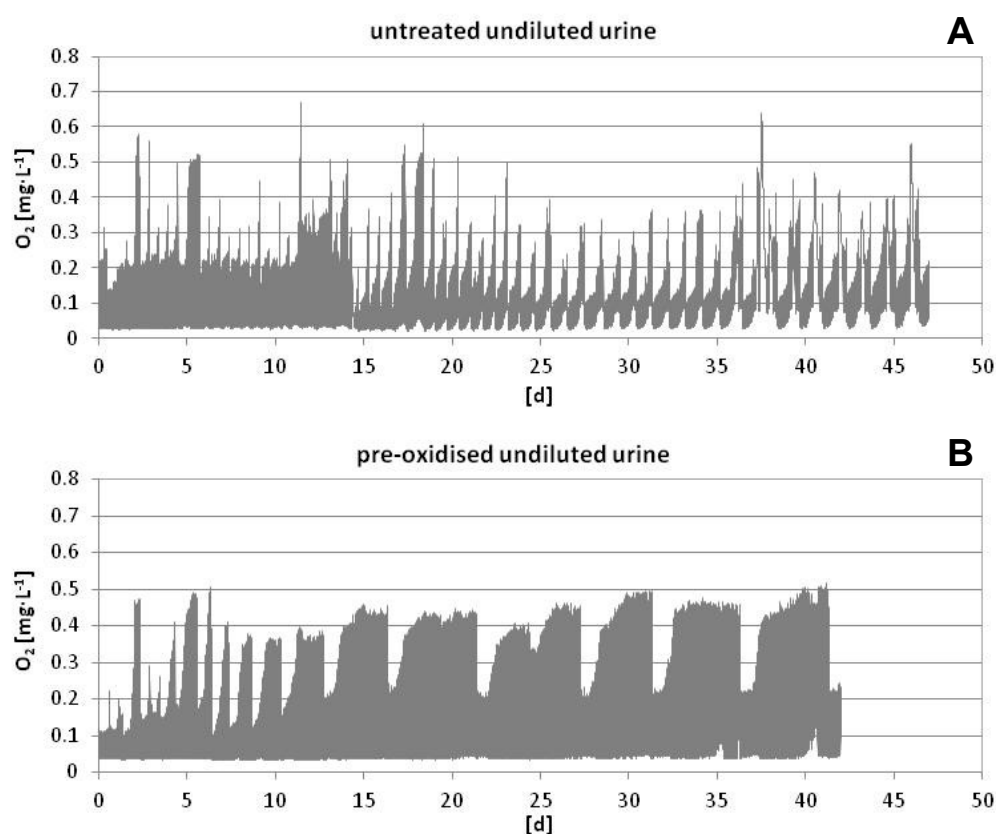


**Figure 9** Dissolved oxygen concentrations during the operation of single-stage nitrification/anammox reactors with (A) untreated undiluted urine and (B) pre-oxidised undiluted urine.

### Temperature

According to Strous et al. (1997b), the highest AMX activity occurs at 40°C. However, AMX activity at 30°C is only slightly lower and allows saving energy for the heating. 30°C is thus considered as optimal temperature for AMX.

### Sludge retention time

Based on a maximum growth rate of 0.073 d<sup>-1</sup> for AMX at 30°C (Schneider et al. 2013), a minimum required SRT of 30 d in the single-stage processes (1/3 anoxic time) and 10 d in the

two-stage process (completely anoxic), respectively, is assumed. The measured SRT was much higher in all three cases and should thus have been sufficient to maintain a high AMX activity in all three cases.

### *Nitrogen intermediates*

#### Nitrite

According to Lotti et al. (2012), nitrite rather than nitrous acid is the actual inhibiting compound for AMX. Numerous studies confirmed that nitrite is critical for the stability of an anammox reactor. The reported threshold concentrations though vary between 5 and 280 mg N·L<sup>-1</sup> (Jin et al. 2012). Most likely, the differences among the various studies are due to differences in the sludge characteristics (e.g. floc size) and the operational conditions (e.g. other inhibiting factors).

In case of the single-stage nitrification/anammox process with pre-oxidised urine, the nitrite concentration was always below 0.5 mg N·L<sup>-1</sup> and can thus definitely be excluded as an inhibition factor for AMX. In case of the single-stage process with untreated urine and the two-stage process, where the nitrite concentration reached values up to 66 mg N·L<sup>-1</sup> and 130 mg N·L<sup>-1</sup>, respectively, it was not possible to exclude an inhibition based on the available literature. Therefore, the influence of nitrite on AMX was characterised in batch activity measurements with the same sludge that was used in the two experiments and under optimal operation conditions for AMX (Figure 7). Based on these measurements, I conclude that AMX activity was not significantly inhibited in all three process configurations.

#### Nitric oxide and nitrous oxide

NO and N<sub>2</sub>O were not directly measured during the three different experiments with undiluted urine. Both gases though interfere with the signal of the sensor that was used for the measurement of the dissolved oxygen concentration in the three experiments (TriOxmatic 700, WTW, Weilheim, Germany; Supporting information S2). Both, in the single-stage (Figure 9A) and in the two-stage process (Supporting information S3) with untreated undiluted urine, an increase of the oxygen baseline signal (during anoxic phases) was observed towards the end of the experiment. Interestingly, this increase was though not observed in case of the single-stage process with pre-oxidised undiluted urine (Figure 9B), where the oxygen baseline remained constant during the whole experiment apart from two-peaks in the middle of the last two cycles.

One difference between the single-stage process with pre-oxidised urine and the other two processes, where an increase of the oxygen baseline signal was observed, was that the nitrite concentration was always < 0.5 mg N·L<sup>-1</sup> and thus much lower than in the other two experiments. Previous studies, e.g. Kampschreur et al. (2009a), showed that nitrite accumulation

clearly results in increased NO and N<sub>2</sub>O concentrations. This hypothesis is further supported by the fact that there is a clear correlation between high nitrite concentrations and the observed increase of the oxygen baseline signal in the single-stage processes with five-times diluted (Bürgmann et al. 2011; Figure 10A) and untreated undiluted urine (Figure 10B).

In a single-stage process, nitrite only accumulates if AMX are already inhibited or AOB activity rapidly increased e.g. due to an increased aeration rate. In the single-stage process with diluted urine (Bürgmann et al. 2011), the increase of the nitrite effluent concentration and the oxygen baseline signal was indeed coupled to an increase of the aeration rate. It can thus not be excluded that NO and N<sub>2</sub>O significantly contributed to the observed decrease of the AMX activity. However, in case of the single-stage process with untreated undiluted urine, the conditions for AOB did not change and thus, it is not possible that NO and N<sub>2</sub>O caused the initial inhibition of AMX. NO and N<sub>2</sub>O might though have further decreased the AMX activity once enough nitrite had accumulated due to an already reduced AMX activity.

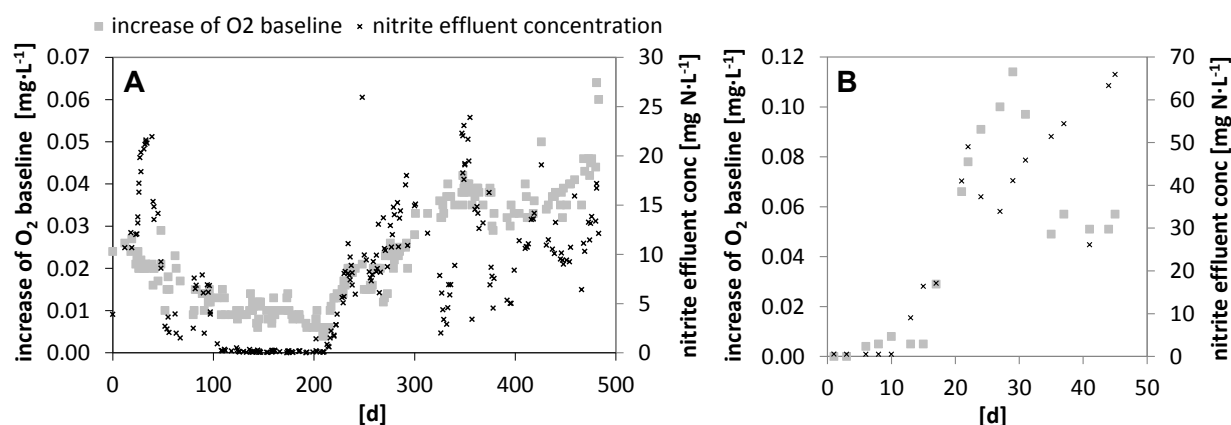


**Figure 10** Increase of the oxygen sensor baseline (NO and N<sub>2</sub>O interference) and the nitrite effluent concentration during the operation of single-stage nitrification/anammox processes with (A) five-times diluted (Bürgmann et al. 2011) and (B) untreated undiluted urine.

In case of the two-stage process, high nitrite concentrations naturally occur in the beginning of the cycle because the AMX stage is fed both with ammonium and nitrite. During the experiment, the oxygen baseline signal continuously increased from 0.042 to 0.068 mg·L<sup>-1</sup> (Supporting information S3). This increase of 0.026 mg O<sub>2</sub>·L<sup>-1</sup> could be caused by 800 ppm NO, 17'300 ppm N<sub>2</sub>O or a mixture of both gases in lower concentrations (Supporting information S2).

NO is known to be toxic for bacteria (Zumft 1993). Apparently, concentrations as low as 1-2 ppm NO can already affect bacterial growth and survival rates, but the effect of NO varies strongly among different types of bacteria. In case of AMX, Kartal et al. (2010) reported that 3500 ppm NO even enhanced AMX activity. NO is an intermediate of the AMX pathway

(Strous et al. 2006) and apparently, AMX are also able to use NO directly for the oxidation of additional ammonium. AMX were exposed to less than 800 ppm NO in the two-stage process and therefore, a significant inhibition of AMX by NO can be excluded.

Inactivation of vitamin B<sub>12</sub> is the main toxic action of N<sub>2</sub>O (Weimann 2003). To the best of my knowledge, the effect of N<sub>2</sub>O on AMX has not yet been tested and it is not clear, whether AMX require vitamin B<sub>12</sub> or not. The highest N<sub>2</sub>O concentration in an anammox process was measured by Kampschreur et al. (2008a). They measured up to 4500 ppm N<sub>2</sub>O in the off-gas of a successfully operated full-scale anammox process treating digester supernatant. Most likely, AMX are therefore not inhibited by N<sub>2</sub>O concentrations up to 4500 ppm. It can though not be excluded, that AMX were inhibited in the two-stage process, where up to 17'300 ppm N<sub>2</sub>O were measured.

### *Urine compounds*

#### Organic substances

In general, organic substances can influence AMX in two different ways: (1) as substrate for heterotrophic bacteria (HET) which compete with AMX for nitrite and space (by decreasing the SRT) or (2) as potentially toxic compounds. The extent of the influence on AMX will depend on the influent COD/N ratio in the first case and on the influent COD concentration in the second case. While the COD must be biodegradable in order to allow HET growth, both biodegradable and non-biodegradable COD can be toxic for AMX.

#### (a) COD as substrate for HET

The availability of biodegradable COD fosters the growth of HET. HET can oxidise COD with oxygen or the nitrate produced by AMX, but also compete with AMX for nitrite. Furthermore, HET growth could increase the sludge concentration in a reactor and with this, decrease the SRT and thus compete with AMX for space. The influence of biodegradable COD on a nitrification/anammox process has been tested by Jenni et al. (2014). Increasing amounts of acetate, and subsequently also glucose, were added to digester supernatant up to an influent COD/N ratio of 1.4 g COD·g N<sup>-1</sup>. This experiment showed that AMX are able to coexist with HET up to influent COD/N ratios of 1.4 g COD·g N<sup>-1</sup> provided a high SRT is sustained.

#### (b) Direct toxicity of biodegradable COD

In case of the single-stage process with untreated undiluted urine, the exchange volume per cycle with undiluted urine was adjusted so that the same amount of ammonium and COD was added per cycle than with five times diluted urine (Bürgmann et al. 2011). Because the degradable compounds do not accumulate in the reactor, the concentrations of the biodegradable COD in the reactor were identical both with undiluted and with five times diluted urine. In case of the single-stage process with pre-oxidised undiluted urine and the two-stage process, most part of



the biodegradable COD (75% and 95%, respectively) was degraded prior to the contact with AMX and thus, AMX were exposed to even lower concentrations of biodegradable COD than with five times diluted urine. Based on the successful operation phase with five times diluted urine (Bürgmann et al. 2011) I therefore conclude that AMX were not significantly inhibited by biodegradable COD in all three experiments with undiluted urine.

#### (c) Direct toxicity of non-biodegradable COD

During the operation of a nitrification/anammox reactor with five-times diluted urine (Bürgmann et al. 2011), the influent and the effluent were screened for organic compounds (Supporting information S4). In total, 68% of the total dissolved COD in the influent was identified. However, none of the identified compounds was detected in the effluent and thus, the non-biodegradable COD remains completely unknown. It was thus not possible to test the influence of the non-biodegradable organic urine compounds on AMX and a significant inhibition cannot be excluded in all three process configurations.

#### Ammonia

According to Caravajal-Arroyo et al. (2013) free ammonia ( $\text{NH}_3$ ) rather than ammonium ( $\text{NH}_4^+$ ) is believed to be the actual inhibitor of AMX. Fernández et al. (2012) characterised the influence of ammonia on AMX activity in different experiments. The short-term effect was tested both with floccular sludge and with biofilm carriers and resulted in very similar 50% inhibition ( $\text{IC}_{50}$ ) values around  $38 \text{ mg NH}_3\text{-N}\cdot\text{L}^{-1}$ . The long-term effect was though only tested with biofilm carriers, where up to  $20 \text{ mg NH}_3\text{-N}\cdot\text{L}^{-1}$  did not have an effect, but efficiency was totally lost at concentrations between 35 and  $40 \text{ mg NH}_3\text{-N}\cdot\text{L}^{-1}$ . It can not be excluded, that the threshold values for the long-term effect are lower with floccular sludge.

In case of the single-stage nitrification/anammox process with pre-oxidised urine, the ammonia concentration reached values up to  $20 \text{ mg N}\cdot\text{L}^{-1}$ . Inhibition of AMX by ammonia can thus not be excluded in this case. Significant inhibition of AMX by ammonia can though be excluded both in case of the single-stage reactor with untreated urine and in case of the two-stage process, as the ammonia concentration was always below  $5 \text{ mg N}\cdot\text{L}^{-1}$ .

#### Sulphide

Previous studies showed that AMX are inhibited by sulphide. Dapena-Mora et al. (2007) e.g. observed a 50% reduced AMX activity in the presence of  $9.6 \text{ mg S}\cdot\text{L}^{-1}$  sulphide. Based on a one-point measurement, the sulphide concentration in stored urine is rather low ( $1\text{-}2 \text{ mg S}\cdot\text{L}^{-1}$ ) and will be even lower in the reactor as only 5% of the volume is exchanged per cycle. Combined with the fact that sulphide is oxidised very fast in the presence of oxygen, a significant inhibition of AMX by sulphide is not likely in all three process configurations.

## Salinity

Urine has an electric conductivity in the range of 27 - 32  $\text{mS}\cdot\text{cm}^{-1}$  which corresponds to a total salinity in the range of 13.6 - 16.2  $\text{g NaCl}\cdot\text{L}^{-1}$ . Dapena-Mora et al. (2010) tested the effect of NaCl on AMX activity and reported an  $\text{IC}_{50}$  value (concentration which causes a 50% inhibition) of 13.5  $\text{g NaCl}\cdot\text{L}^{-1}$ . In a batch activity measurement with a synthetic solution that contained the same salts at the same concentrations as in urine (Figure 6), AMX activity even decreased to 5%.

However, Liu et al. (2009) was able to maintain AMX activity at NaCl concentrations up to 30  $\text{g}\cdot\text{L}^{-1}$  by slowly increasing the salt concentration in steps of 2.5  $\text{g}\cdot\text{L}^{-1}$  every 5 or 10 d. Apparently, AMX are able to adapt to high salt concentrations. According to Welsh (2000), osmoadaptation of bacteria involves one or more of a restricted range of low molecular mass organic solutes termed compatible solutes. The synthesis of these compatible solutes requires some time which explains why sudden increases of the salt concentration can be problematic.

In Figure 11, the increase of the salinity in the three different process configurations with undiluted urine is compared with the increase of the salinity in Liu et al. (2009). The salinity was increased in two big steps in the experiment by Liu et al. (2009). In case of the three experiments with urine, the salinity increased more continuously and reached similar values after 5, 10, 15 and 20 d. Therefore, I conclude that AMX had enough time to adapt to the salt concentrations and were not significantly inhibited by the salinity increase in all three experiments with undiluted urine.

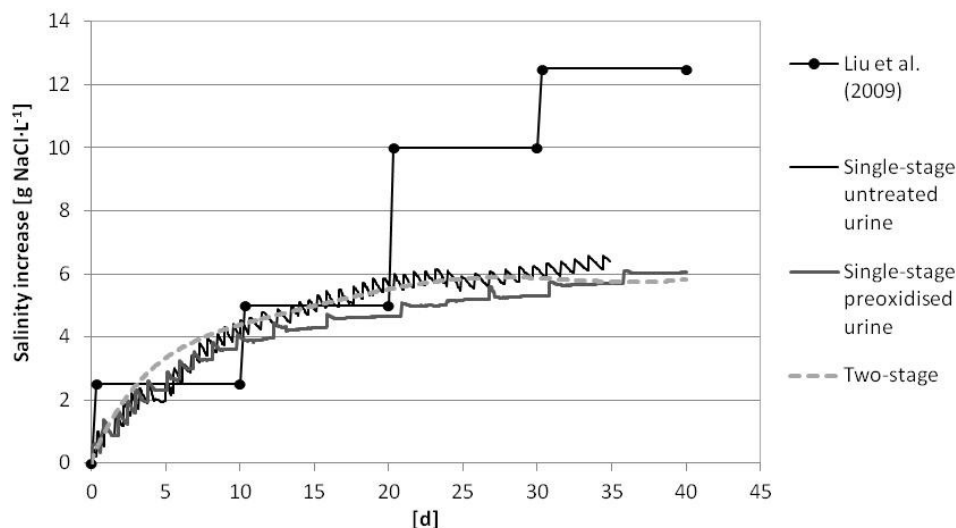


**Figure 11** Increase of salinity with the three different process configurations and a reference from literature (Liu et al. (2009); anammox fix-bed reactor fed with synthetic wastewater). In case of the two stage process, a trendline (Supporting information S5) was used because the conductivity signal was disturbed during the whole experiment.

### Salt ions

Apart from the total salinity, AMX might also be inhibited by one or more of the ions present in urine. This hypothesis is supported by the fact that the observed activity decrease in the batch experiment with a synthetic salt solution that contained the same ions at the same concentrations as in urine (- 95%; Figure 6) was much stronger than the one observed by Dapena-Mora et al. (2010) at similar salt concentrations with sodium chloride (-50%).

According to Table 2, the concentrations of chloride, phosphate, sulphate, sodium and potassium are much higher in urine than in digester supernatant, which allows a successful operation of nitrification/anammox processes. In case of sodium and chloride, which are discussed above as ‘model compounds’ for salinity, it is known that AMX can adapt to concentrations much higher than the ones in urine if the concentration is increased step-wise. The effect of phosphate, sulphate and potassium on AMX activity has been tested by Dapena-Mora et al. (2007) in short-time batch experiments. Concentrations up to 3900 mg K<sup>+</sup>·L<sup>-1</sup>, 4800 mg SO<sub>4</sub><sup>2-</sup>·L<sup>-1</sup> and 465 mg PO<sub>4</sub>-P·L<sup>-1</sup> had no effect on AMX activity. It can thus be excluded that the single ions present in urine significantly inhibited AMX activity in the three experiments with undiluted urine.

**Table 2** Ion concentrations in urine (average from three measurements) and in digester supernatant (Jenni et al. 2014).

	mg·L <sup>-1</sup>	mg·L <sup>-1</sup>	mg·L <sup>-1</sup>	mg·L <sup>-1</sup>	mg·L <sup>-1</sup>	mg·L <sup>-1</sup>	mg·L <sup>-1</sup>	mg·L <sup>-1</sup>
	Cl <sup>-</sup>	PO <sub>4</sub> -P	SO <sub>4</sub> <sup>2-</sup>	Na <sup>+</sup>	K <sup>+</sup>	Mg <sup>2+</sup>	Ca <sup>2+</sup>	NH <sub>4</sub> <sup>+</sup> -N
<b>Digester supernatant</b>	96	13	4.3	230	130	20	110	740
<b>Urine</b>	3780	285	917	1830	1840	<4	20	2110

### Pharmaceuticals

Lienert et al. (2007) analysed the excretion pathways of 212 pharmaceuticals active ingredients, equalling 1409 products. On average, 64% (± 27%) of each active ingredient was excreted via urine. The individual composition in the urine used for the three experiment is not known and probably anyway highly variable.

The effect of pharmaceuticals on AMX has only been tested for a few substances yet. Fernández et al. (2009) and van de Graaf et al. (1995) both tested the effect of some broad-spectrum antibiotics (chloramphenicol, tetracycline hydrochloride and ampicillin) on AMX activity. AMX activity decreased to around 20% at concentration levels between 20 and 400 mg·L<sup>-1</sup>. In case of AOB, Ghosh et al. (2003) reported an 80% inhibition in the presence of a

mixture of five antibiotics (clarithromycin, enrofloxacin, sulfamethoxazole, tetracycline and trimethoprim) at concentrations of  $0.3 \text{ g}\cdot\text{L}^{-1}$  each. The concentrations in wastewater are generally lower (e.g. Giger et al. 2003), but urine is more concentrated and other pharmaceuticals or a combination of different pharmaceuticals could already inhibit AMX at lower concentrations.

Joss et al. (2006) studied the degradation of pharmaceuticals in municipal wastewater treatment plants. Based on the degradation of a heterogeneous group of 35 compounds, state of the art biological treatment schemes for municipal wastewater are not efficient in degrading pharmaceuticals: only 4 out of 35 compounds are degraded by more than 90% while 17 compounds are removed by less than 50%. Most likely, the degradation in the pre-oxidation step and in the nitrification step of the two-stage process was at most similar and thus, pharmaceuticals at most partly reduced in the subsequent anammox step.

### **Decrease of the biomass concentration**

In all three process configurations, a strong decrease of the VSS concentration in the reactor was observed (Figure 1E, Figure 1F and Figure 5C). Interestingly, the decrease cannot be explained with the VSS loss through sampling and via effluent. In Figure 12, the measured VSS concentration and the calculated VSS concentration (biomass in the reactor minus VSS loss through sampling and via effluent) are compared. In all three process configurations, the measured VSS concentration decreases much stronger than the calculated VSS concentration even though the calculated VSS concentration is based on the assumption that no biomass growth occurs in the reactor. Unmonitored sludge accumulation in the reactors can be excluded due to the fact that the reactors were well mixed, and all sensors and the reactor walls were cleaned regularly (at least once a week).

The strong decrease of the VSS concentration in the three experiments could be explained with unmonitored sludge loss via the effluent in case the pore size of the filter papers used for the VSS measurement was larger than the smallest biomass flocs in the reactor. The ashless filter papers used for VSS measurement had an average retention of  $7 - 12 \text{ }\mu\text{m}$ , which is rather large compared to the size of a single bacteria cell. Single cells of "*Candidatus Brocadia fulgida*" e.g. measure less than  $1 \text{ }\mu\text{m}$  (Kartal et al. 2007b) so that even a microcolony could still easily pass through the filter papers. The fact that the VSS concentration in the reactor did not decrease during the initial operation phase with digester supernatant in both single-stage processes (Figure 1E and 1F) indicates that the increased biomass loss with the effluent and thus the reduced settleability of the sludge was related to the switch to urine. One explanation for the observed substantial decrease of the biomass content in all three process configurations could be that the much higher ratio of monovalent to divalent cations in urine caused a floc destabilisation.

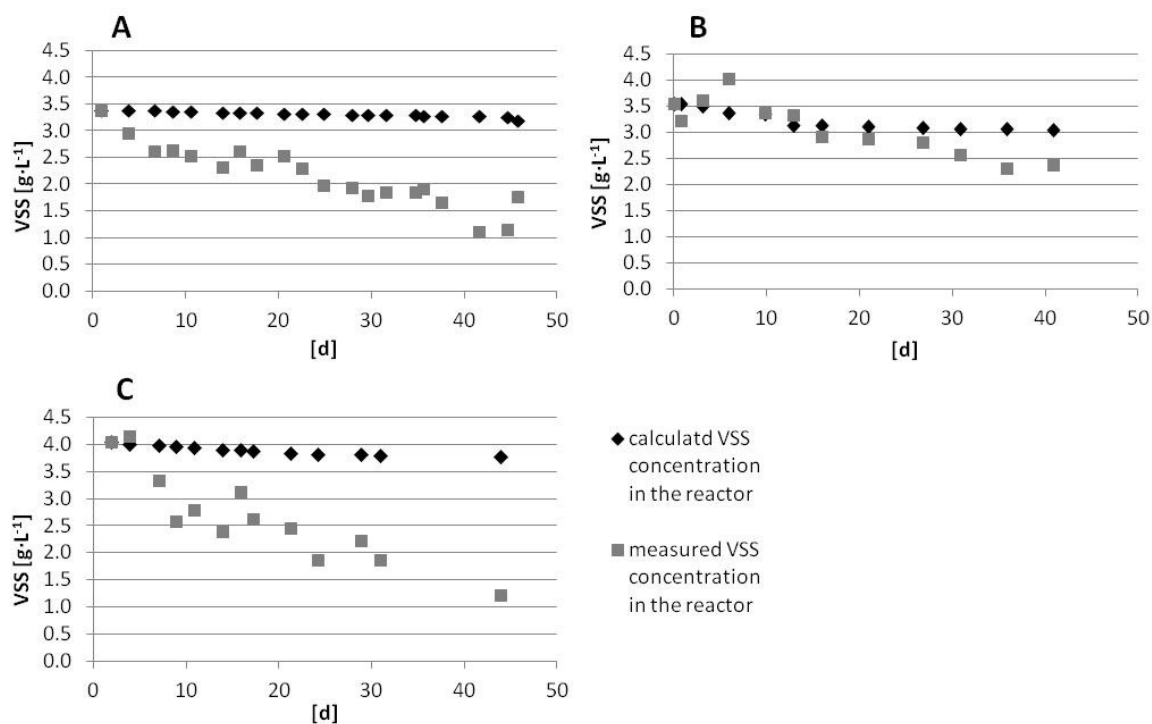


**Figure 12** Measured VSS concentration and calculated VSS concentration based on the VSS loss through sampling and via effluent (assuming zero biomass production) in the reactor during (A) single-stage nitritation/anammox with untreated urine, (B) single-stage nitritation/anammox with pre-oxidised urine and (C) two-stage nitritation/anammox.

The ratio of monovalent to divalent cations is much higher in stored urine ( $420 \text{ mol} \cdot \text{mol}^{-1}$ ) than in digester supernatant ( $19 \text{ mol} \cdot \text{mol}^{-1}$ ; Table 2). Sobek and Higgins (2002) reported that the addition of either calcium or magnesium resulted in improvements of the floc properties, while the addition of sodium resulted in a deterioration of floc properties. According to the divalent cation bridging (DCB) theory, divalent cations can bridge negatively charged functional groups within the exocellular polymeric substances and this bridging helps to aggregate and stabilize the matrix of biopolymer and bacteria and therefore promotes bioflocculation. The implications of the DCB theory suggests that activated sludge systems should attempt to lower the ratio of monovalent (sodium, potassium and ammonium) to divalent (calcium and magnesium) cations to improve floc properties and treatment performance. This was also observed by de Graaff et al. (2011) who reported that the calcium concentration in black water was too low to obtain sufficient granulation of anammox biomass. A decrease of the monovalent to bivalent cations from 19 to 12 by adding extra calcium to the black water though led to a considerable improvement of granulation and retention of the biomass. In case of the operation of a nitritation/anammox process with diluted urine (Bürgmann et al. 2011), where de-ionised water was

used for the dilution and thus resulted in the same ratio of monovalent to divalent cations, sufficient biomass retention in the reactor was though not an issue.

Another explanation for the observed substantial decrease of the biomass content could be that the elevated salt concentrations increase the water density and cause a washout of small and poor settling flocs as suggested by Bassin et al. (2012). However, they did not prove this hypothesis and the observed decrease of the biomass concentration from 2.4 to 2.0 g VSS·L<sup>-1</sup> when the salt concentration in their nitrifying sequencing batch reactor was increased from 0 to 5 g NaCl·L<sup>-1</sup> could also have been due to floc destabilisation. Furthermore, the density of urine is with 1.015 kg·L<sup>-1</sup> only remotely higher than the density of nanopure water (0.997 kg·L<sup>-1</sup>; Ciba-Geigy 1997).

Unmonitored sludge loss with the effluent is of extreme significance for the whole process because it leads to a systematic overestimation of the SRT, which is one of the most crucial factors for the slowly growing AMX. Assuming zero biomass growth in the reactor, the SRT can be calculated based on the measured VSS decrease in the reactor (Supporting information S6). The so calculated SRT are significantly lower than the measured ones, i.e. 53 ± 13 d instead of 660 ± 220 d in case of the single-stage process with untreated urine, 90 ± 14 d instead of 690 ± 440 d in case of the single-stage process with pre-oxidised urine and 40 ± 12 d instead of 450 ± 280 d in case of the two-stage process (anammox step). Because biomass growth in the reactor was not zero, the actual SRT must have been even lower. Compared with the fact that AMX were most likely not growing at their maximum growth rate, the low SRT could have caused a wash out of AMX and thus, could also have been the main limiting factor of AMX activity in all three process configurations. Further research is required to characterise the effect of the high ratio of monovalent to divalent cations in urine on the nitrification/anammox process and to test if the addition of divalent cations allows higher biomass retention.

### **Alkalinity aspects**

Nitrification/anammox requires 1.104 mol alkalinity·mol<sup>-1</sup> NH<sub>4</sub> (Supporting information S7) but urine only provides 0.853 mol alkalinity·mol<sup>-1</sup> NH<sub>4</sub> (simulated alkalinity). The low alkalinity of urine was no problem in the single-stage process with untreated urine, but caused a strong decrease of the pH value in case of the single-stage process with pre-oxidised urine. The different behaviour was not expected because mainly the same reactions occur, just in different places. There must though be some significant differences in order to be able to explain the different development of the pH values in the two cases (Figure 3).

Due to the much higher pH values in urine (9.16 ± 0.17) compared to the pH values in the nitrification/anammox reactor (max. 7.9), around 4% of the total ammonium (NH<sub>3</sub> and NH<sub>4</sub>) is stripped during pre-oxidation while ammonia stripping from the reactor is negligible. For each

mol NH<sub>3</sub> that is striped, one mol alkalinity is consumed. NH<sub>3</sub> striping during pre-oxidation therefore reduces the available alkalinity. However, with untreated urine, where this NH<sub>3</sub> is not striped, the same amount of ammonium has to be degraded in the reactor, which requires 1.104 mol alkalinity·mol<sup>-1</sup> NH<sub>4</sub>. Thus, in total, the striping of NH<sub>3</sub> even increases the available amount of alkalinity and can thus not be responsible for the strong decrease of the pH value in case of the single-stage process with pre-oxidised urine.

Heterotrophic growth and endogenous respiration are the main occurring processes during pre-oxidation of urine. Both with pre-oxidised and untreated urine, all biodegradable COD had been removed at the end of the cycles in the nitrification/anammox reactor. Though while with untreated urine all biodegradable COD had been degraded in the nitrification/anammox reactor, most part of the biodegradable COD had been degraded in the pre-oxidation step in case of the pre-oxidised urine. The main difference between the two cases could then be that while only oxygen is available in the pre-oxidation step, HET can also use nitrite or nitrate in the nitrification/anammox step. Indeed, as listed in Table 4, both heterotrophic growth and endogenous respiration with oxygen produces much less alkalinity compared to heterotrophic reactions with nitrite or nitrate. Aerobic heterotrophic growth on glucose even consumes alkalinity. The much stronger pH decrease in the nitrification/anammox reactor with pre-oxidised urine than with untreated urine was though most likely caused by a lower alkalinity production by HET in case of the pre-oxidised urine.

**Table 4** Alkalinity consumption/production in reactions that involve HET (Supporting information S7)

<b>Glucose</b>	Growth with oxygen	- 0.252	mol alkalinity·mol <sup>-1</sup> COD glucose
	Growth with nitrate	+ 0.468	mol alkalinity·mol <sup>-1</sup> COD glucose
	Growth with nitrite	+ 0.931	mol alkalinity·mol <sup>-1</sup> COD glucose
<b>Acetate</b>	Growth with oxygen	+ 0.748	mol alkalinity·mol <sup>-1</sup> COD acetate
	Growth with nitrate	+ 1.468	mol alkalinity·mol <sup>-1</sup> COD acetate
	Growth with nitrite	+ 1.931	mol alkalinity·mol <sup>-1</sup> COD acetate
<b>Biomass</b>	End. respiration with oxygen	+ 0.928	mol alkalinity·mol <sup>-1</sup> COD biomass
	End. respiration with nitrate	+ 4.208	mol alkalinity·mol <sup>-1</sup> COD biomass
	End. respiration with nitrite	+ 6.395	mol alkalinity·mol <sup>-1</sup> COD biomass

The same problem also occurred in the two-stage process. Without addition of base, the nitrite to ammonium ratio in the effluent of the nitrification step was with  $0.91 \pm 0.06$  mg NO<sub>2</sub><sup>-</sup>-N·mg

$\text{NH}_4^+ \text{-N}^{-1}$  (Figure 4B) much lower than the minimal ratio of 1.32 mg  $\text{NO}_2^- \text{-N} \cdot \text{mg NH}_4^+ \text{-N}^{-1}$  which is required for the anammox process. Even though nitrite was also available in this case, HET most likely still mainly used oxygen, which is their preferred electron acceptor, and thus, produced less alkalinity compared to the single-stage process with untreated urine.

In contrast to the single-stage process with pre-oxidised urine, the required additional base was added to the nitrification step of the two-stage process from day 45 on (Figure 4B). Apart from the fact that the additional base caused such high pH values in the anammox step that additional acid had to be dosed, AMX activity decreased just as fast as in the single-stage process. Therefore, in contrast to our initial expectation, a separation of the biodegradable organic substrate and other oxidisable compounds from AMX is not beneficial for the process. On the contrary, in this context, the high concentration of biodegradable organic substrate in urine is actually even positive for the process because heterotrophic activity produces the missing alkalinity for a nearly complete nitrogen removal and thus allows the operation of a nitrification/anammox process without dosing of additional base.

## CONCLUSIONS

Based on the results of this study, I conclude the following:

- With a detailed evaluation of the possible influence factors, including urine compounds, intermediates of nitrogen conversion and operating parameters, the number of potentially critical factors could be reduced to three: (1) a high sludge loss caused by floc destabilisation due to the high ratio of monovalent to divalent cations in urine, (2) a direct inhibition of AMX by non-biodegradable organic substances, and (3) a direct inhibition of AMX by pharmaceuticals.
- At this point, further research is required to evaluate whether all three factors or only one or two of them are critical. While a strong influence from the non-biodegradable organic compounds or the pharmaceutical could be reduced with dilution of the urine, additional divalent cations would be necessary to decrease the high ratio of monovalent to divalent cations in urine. If the ratio of monovalent to divalent cations could not be reduced, biomass retention could be improved with a biofilm system.
- In contrast to my initial expectation, a separation of the biodegradable organic substrate from AMX is not beneficial for the process. Regarding the low alkalinity of urine, the high concentration of biodegradable organic substrate in urine is even positive for the process, because heterotrophic denitrification of nitrite and nitrate produces the missing alkalinity, which is necessary to completely remove nitrogen. This implies that a single-stage nitrification/anammox reactor is the best choice for nitrogen removal from urine.



# **SUPPORTING INFORMATION**

## **FOR CHAPTER 5**

### **Evaluation of critical factors for the operation of a nitritation/anammox process with urine**

Sarina Schielke-Jenni

## S1 Salt solution

In Table S1, the components and the used concentrations for a salt solution that contains the same salts at the same concentrations as in urine are listed.

**Table S1** Components of a salt solution that contains the same salts at approximately the same concentrations as urine. The sodium and the chloride concentration had to be slightly adjusted because it was not possible to meet the exact concentrations of urine with the available salts.

	Mg	Ca	K	Na	SO <sub>4</sub>	PO <sub>4</sub>	Cl	CO <sub>3</sub>	NO <sub>3</sub>	Alkalinity	mM
CaCl <sub>2</sub> · 2H <sub>2</sub> O		1					2				0.2246
K <sub>2</sub> HPO <sub>4</sub> · 3H <sub>2</sub> O			2			1				1	3.871
KCl			1				1				30.11
MgCl <sub>2</sub> · 6H <sub>2</sub> O	1						2				0.04114
NaCl				1			1				67.78
NaH <sub>2</sub> PO <sub>4</sub> · 2H <sub>2</sub> O				1		1					1.941
NaHCO <sub>3</sub>				1				1		1	7.909
NaNO <sub>3</sub>				1					1		7.782
Na <sub>2</sub> SO <sub>4</sub>				2	1						9.057
<b>Salt solution</b>	0.04114	0.2246	37.85	103.5	9.057	5.811	98.42	7.909	7.782	11.78	<b>mM</b>
<b>Urine</b>	0.04114	0.2246	37.85	97.87	9.057	5.811	104.1	7.909	7.782	11.78	<b>mM</b>

## S2 NO and N<sub>2</sub>O interference on oxygen sensor signal

In all three process configurations, the same sensor was used for the measurement of the dissolved oxygen concentration (TriOxmatic 700, WTW, Weilheim, Germany). The interference of NO and N<sub>2</sub>O on the signal of this sensor was measured in a close reactor that was filled with a neutral phosphate buffer solution and aerated with a gas mixture containing dinitrogen and different amounts of NO and N<sub>2</sub>O (Figure S1).

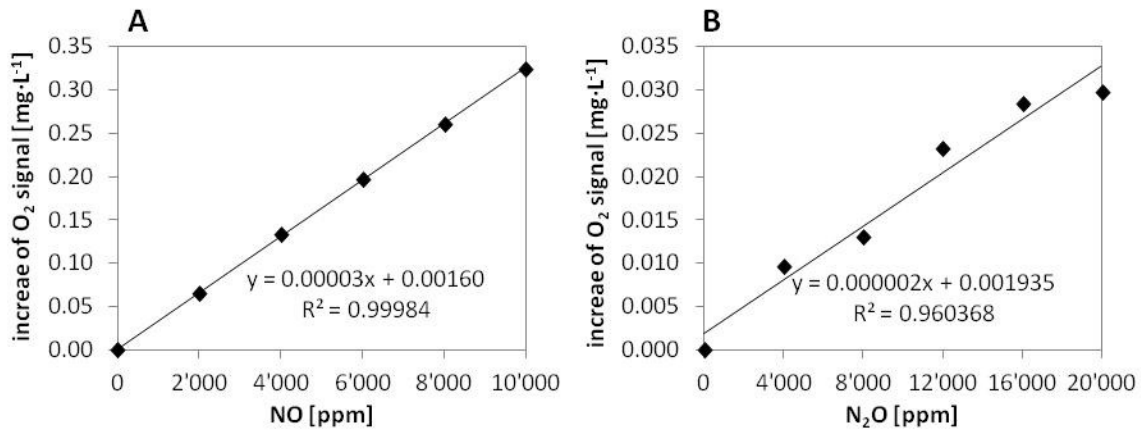


**Figure S1** Interference of (A) NO and (B) N<sub>2</sub>O on the signal of the oxygen sensor that was used for the measurement of the dissolved oxygen concentration in all three process configurations. The concentrations in ppm are referring to the concentrations in the gas that was used to aerate the neutral phosphate buffer solutions.

### S3 Dissolved oxygen concentration in the two-stage process

The signal of the oxygen sensor during the operation of the anammox step of the two-stage process with urine is displayed in Figure S2.

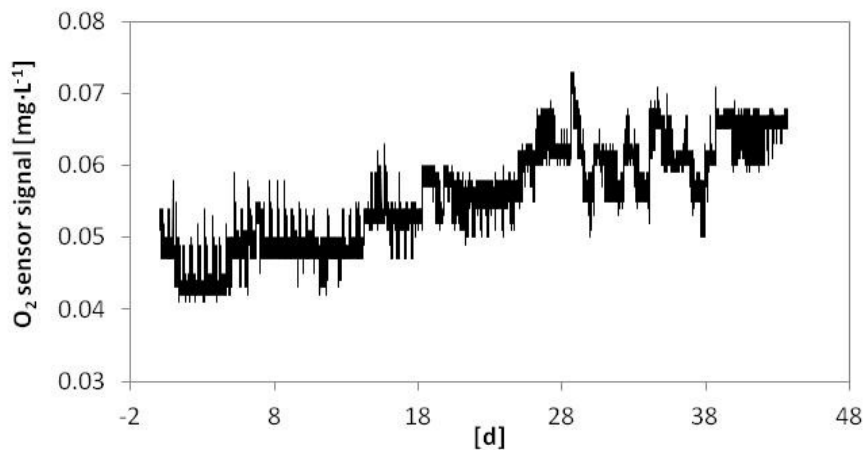


**Figure S2** Signal of the oxygen sensor during the operation of the anammox step of the two-stage nitritation/anammox process with urine.

### S4 Organic compounds in urine

On day 157 of the operation of a single-stage nitritation/anammox process with five-times diluted urine (Bürgmann et al. 2011), the influent and the effluent of the reactor were screened for organic compounds. In total, 68% of the dissolved COD in the influent was identified (Table S2). In the effluent, all measured concentrations were below the detection limit (0.5 mg·L<sup>-1</sup>).

The dissolved COD concentrations in the influent and in the effluent (accounting for the non-biodegradable COD) were 1050 and 98 mg·L<sup>-1</sup>, respectively.

**Table S2** Measured organic compounds in the influent on day 157 of the operation of a single-stage nitrification/anammox process with five-times diluted urine (Bürgmann et al. 2011).

	[mg·L <sup>-1</sup> ]	[mg COD·L <sup>-1</sup> ]	[% of total dissolved COD]
Acetic acid	417	446	42.5
Propionic acid	24.5	37	3.5
Iso butyric acid	2.8	5.0	0.5
Butyric acid	30.4	55.4	5.3
Iso-valeric acid	2.8	5.6	0.5
Valeric acid	0.8	1.6	0.2
Benzoic acid	65.0	128	12.2
Phenylacetic acid	10.0	21.2	2.0
Salicylic acid	0.9	1.5	0.1
Phenol	1.7	4.0	0.4
Cresol	1.7	4.3	0.4
Palmitinic acid	0.7	2.0	0.2
Linolic acid	1.4	4.0	0.4
Total		715	<b>68.1</b>

### S5 Increase of salinity in the anammox step of the two-stage process

The measured salinity increase in the anammox step during the operation of a two-stage process with urine and the calculate trendline are displayed in Figure S3.

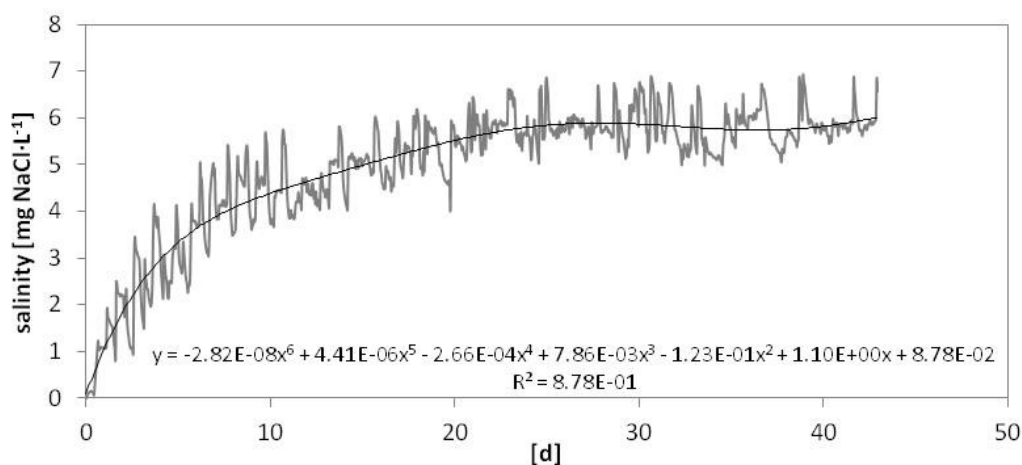


**Figure S3** Measured salinity increase in the anammox step during the operation of a two-stage process with urine (grey) and the with Excel calculate trendline (black).

### S6 SRT calculation based on measured VSS decrease in the reactor

Assuming zero biomass growth, the VSS decrease in the reactor equals the sludge loss with sampling and via effluent. For the calculation of the SRT based on the VSS decrease in the reactor (Figure S4), a linear decrease of the VSS concentration in the reactor was assumed (Figure S5).

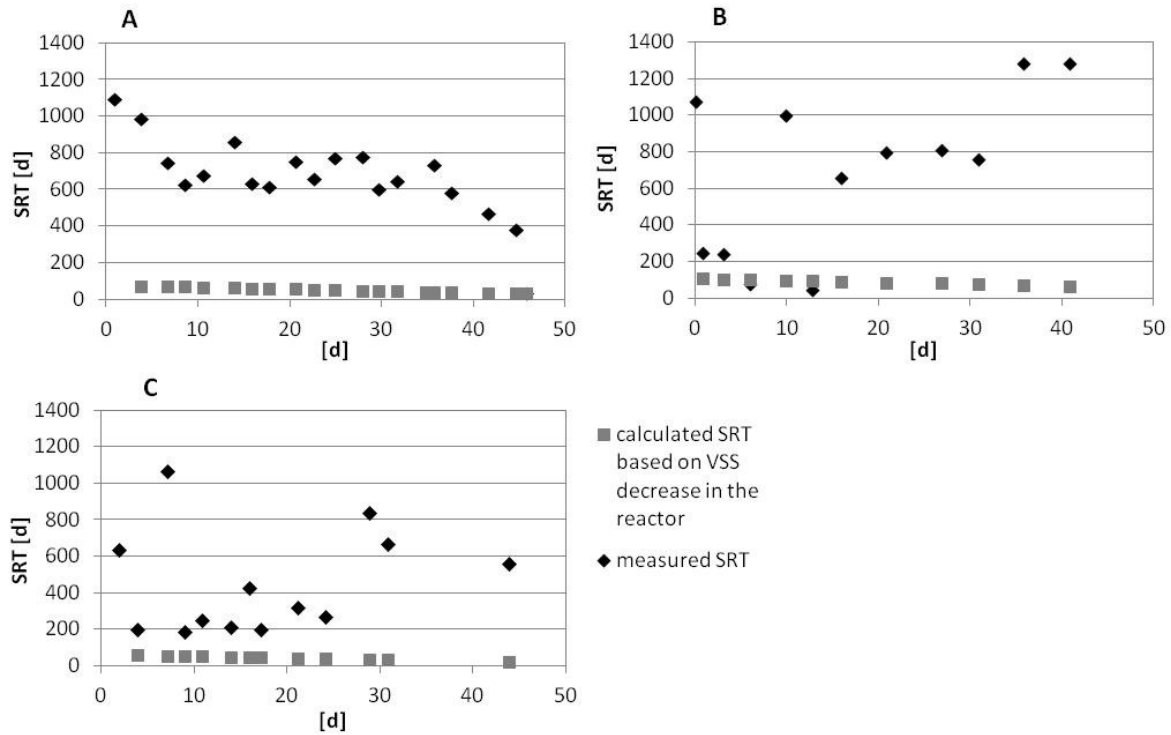


**Figure S4** Measured and calculated SRT during (A) single-stage nitritation/anammox with untreated urine, (B) single-stage nitritation/anammox with pre-oxidised urine and (C) two-stage nitritation/anammox.

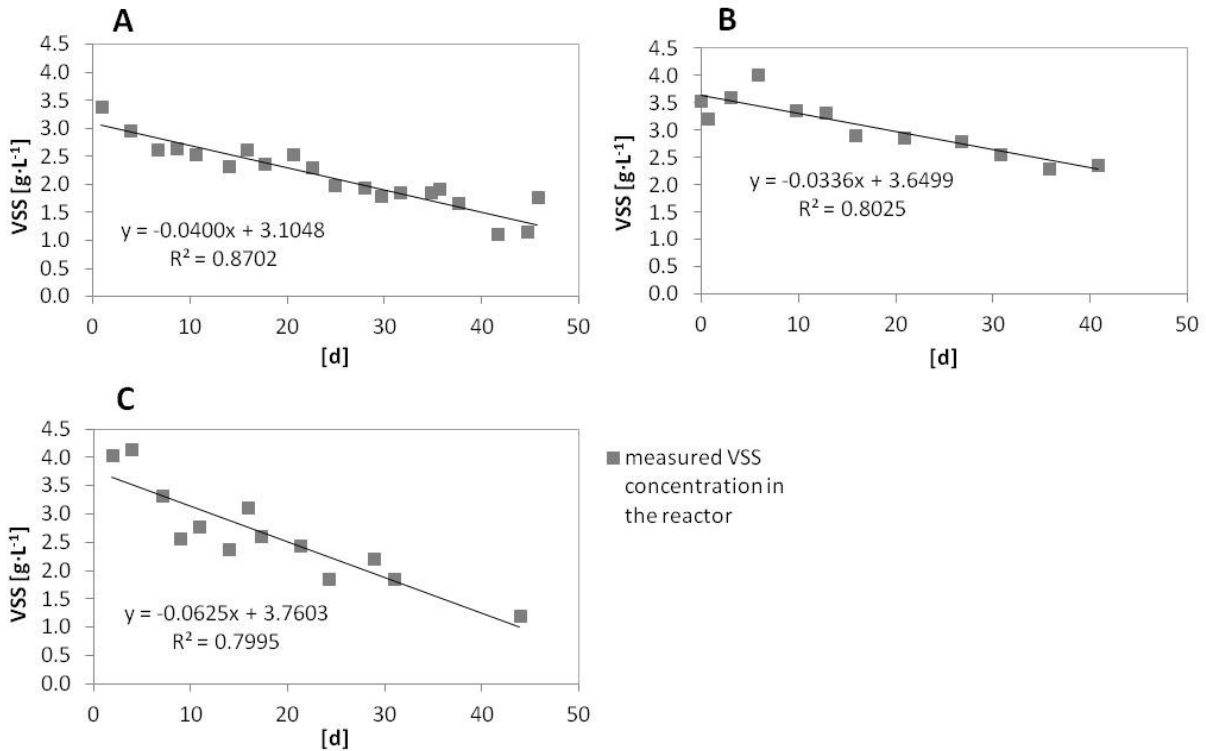


**Figure S5** Measured VSS concentration and assumed linear decrease for the SRT calculation during (A) single-stage nitrification/anammox with untreated urine, (B) single-stage nitrification/anammox with pre-oxidised urine and (C) two-stage nitrification/anammox.

### S7 Alkalinity consumption/production in bacterial reactions

The parameters used for the calculation of the stoichiometric matrices are listed in Table S3. The stoichiometric matrices for nitrification and anammox (Table S4), for heterotrophic growth with acetate (Table S6) and glucose (Table S8) as well as for heterotrophic endogenous respiration (Table S10) were calculated by balancing nitrogen, COD, carbon and charge according to the composition matrices (Table S5, Table S7, Table S9 and Table S11).

The alkalinity consumption by the nitrification/anammox process was calculated with the ammonium consumption by AOB

$$d\text{NH}_4\text{AOB} = \frac{628.1 \cdot \frac{346.1}{339.9}}{480.0 + 628.1 \cdot \frac{346.1}{339.9}} \cdot d\text{NH}_4 = 0.571 \cdot d\text{NH}_4$$

and the ammonium consumption by AMX

$$d\text{NH}_4\text{AMX} = 1 - d\text{NH}_4\text{AOB} = 0.429 \cdot d\text{NH}_4$$

as follows:

$$d\text{Alk, Nit} / \text{Amx} = -\frac{686.5}{346.1} \cdot d\text{NH}_4\text{AOB} + \frac{31.83}{480.0} \cdot d\text{NH}_4\text{AMX} = -1.104 \frac{\text{mol}_{\text{ALK}}}{\text{mol}_{\text{NH}_4}}$$

The alkalinity consumption by heterotrophic growth with acetate was calculated as follows:

$$d\text{Alk, HET}_{\text{growth}}, \text{O}_2, \text{acetate} = \frac{-18.55}{-24.80} = 0.748 \frac{\text{mol}_{\text{ALK}}}{\text{mol}_{\text{COD}}}$$

$$d\text{Alk, HET}_{\text{growth}}, \text{NO}_3, \text{acetate} = \frac{-40.53}{-27.61} = 1.468 \frac{\text{mol}_{\text{ALK}}}{\text{mol}_{\text{COD}}}$$

$$d\text{Alk, HET}_{\text{growth}}, \text{NO}_2, \text{acetate} = \frac{-53.31}{-27.61} = 1.931 \frac{\text{mol}_{\text{ALK}}}{\text{mol}_{\text{COD}}}$$

The alkalinity consumption by heterotrophic growth with glucose was calculated as follows:

$$d\text{Alk, HET}_{\text{growth}}, \text{O}_2, \text{glucose} = \frac{6.250}{-24.80} = -0.252 \frac{\text{mol}_{\text{ALK}}}{\text{mol}_{\text{COD}}}$$

$$d\text{Alk, HET}_{\text{growth}}, \text{NO}_3, \text{glucose} = \frac{-12.92}{-27.61} = 0.468 \frac{\text{mol}_{\text{ALK}}}{\text{mol}_{\text{COD}}}$$

$$d\text{Alk, HET}_{\text{growth}}, \text{NO}_2, \text{glucose} = \frac{-25.70}{-27.61} = 0.931 \frac{\text{mol}_{\text{ALK}}}{\text{mol}_{\text{COD}}}$$

The alkalinity consumption by heterotrophic endogenous respiration was calculated as follows:

$$d\text{Alk, HET}_{\text{end.respiration}}, \text{O}_2 = \frac{-5.800}{-6.250} = 0.928 \frac{\text{mol}_{\text{ALK}}}{\text{mol}_{\text{COD}}}$$

$$d\text{Alk, HET}_{\text{end.respiration}}, \text{NO}_3 = \frac{-26.30}{-6.250} = 4.208 \frac{\text{mol}_{\text{ALK}}}{\text{mol}_{\text{COD}}}$$

$$d\text{Alk, HET}_{\text{end.respiration}}, \text{NO}_2 = \frac{-39.97}{-6.250} = 6.395 \frac{\text{mol}_{\text{ALK}}}{\text{mol}_{\text{COD}}}$$

**Table S3** Parameters for the calculation of the stoichiometric matrices.

Symbol	Description	Value	Unit
$Y_{\text{HET},\text{O}_2}$	Yield for growth of $X_{\text{HET}}$ with oxygen	0.630	$\text{g COD}\cdot\text{g COD}^{-1}$
$Y_{\text{HET},\text{NO}_2}$	Yield for growth of $X_{\text{HET}}$ with nitrite	0.566	$\text{g COD}\cdot\text{g COD}^{-1}$
$Y_{\text{HET},\text{NO}_3}$	Yield for growth of $X_{\text{HET}}$ with nitrate	0.566	$\text{g COD}\cdot\text{g COD}^{-1}$
$Y_{\text{AOB}}$	Yield for growth of $X_{\text{AOB}}$	0.210	$\text{g COD}\cdot\text{g N}^{-1}$
$Y_{\text{AMX}}$	Yield for growth of $X_{\text{AMX}}$	0.150	$\text{g COD}\cdot\text{g N}^{-1}$
$i_{\text{N},\text{X}_1}$	Nitrogen content of inorganic biomass $X_1$	0.035	$\text{g N}\cdot\text{g COD}^{-1}$
$i_{\text{N},\text{X}}$	Nitrogen content of $X_{\text{HET}}$ and $X_{\text{AOB}}$	0.088	$\text{g N}\cdot\text{g COD}^{-1}$
$i_{\text{N},\text{XAMX}}$	Nitrogen content of $X_{\text{AMX}}$	0.058	$\text{g N}\cdot\text{g COD}^{-1}$
$f_{\text{X}_1}$	Fraction of biomass converted into $X_1$ during endogenous respiration	0.18	-

**Table S4** Stoichiometric matrix for nitrification and anammox in two different units.

	$\text{SO}_2$	$\text{SNH}_4$	$\text{SNO}_3$	$\text{SNO}_2$	$\text{SN}_2$	$\text{SH}$	$\text{SH}_2\text{CO}_3$	$\text{XAOB}$	$\text{XAMX}$
	$[\text{gO}_2\cdot\text{m}^{-3}]$	$[\text{gN}\cdot\text{m}^{-3}]$	$[\text{gN}\cdot\text{m}^{-3}]$	$[\text{gN}\cdot\text{m}^{-3}]$	$[\text{gN}\cdot\text{m}^{-3}]$	$[\text{mol}\cdot\text{m}^{-3}]$	$[\text{mol}\cdot\text{m}^{-3}]$	$[\text{gCOD}\cdot\text{m}^{-3}]$	$[\text{gCOD}\cdot\text{m}^{-3}]$
Growth	-23.8447	-0.0875	21.7391	-21.7391		0.00625	-0.03125	1	
Growth		-6.72436	1.63000	-8.80000	13.8367	-0.03183	-0.02747		1

	$\text{SO}_2$	$\text{SNH}_4$	$\text{SNO}_3$	$\text{SNO}_2$	$\text{SN}_2$	$\text{SH}$	$\text{SH}_2\text{CO}_3$	$\text{XAOB}$	$\text{XAMX}$
	$[\mu\text{M}]$	$[\mu\text{M}]$	$[\mu\text{M}]$	$[\mu\text{M}]$	$[\mu\text{M}]$	$[\mu\text{M}]$	$[\mu\text{M}]$	$[\mu\text{M}]$	$[\mu\text{M}]$
Growth	-479.3	-346.1		339.9		686.5	-31.25	6.250	
Growth	-480.0	116.3	-628.1	987.6	-31.83	-27.47	-480.0		27.47

**Table S5** Composition matrix for the calculation of the stoichiometric matrix for nitrification and anammox.

	$\text{SO}_2$	$\text{SNH}_4$	$\text{SNO}_3$	$\text{SNO}_2$	$\text{SN}_2$	$\text{SH}$	$\text{SH}_2\text{CO}_3$	$\text{XAOB}$	$\text{XAMX}$
	$[\text{gO}_2]$	$[\text{gN}]$	$[\text{gN}]$	$[\text{gN}]$	$[\text{gN}]$	$[\text{mol}]$	$[\text{mol}]$	$[\text{gCOD}]$	$[\text{gCOD}]$
$[\text{gN}]$	0	0	1	1	1	1	0	0	0.035
$[\text{gCOD}]$	-1	1	0	-4.57	-3.43	-1.71	0	0	1
$[\text{mol C}]$	0	0.0313	0	0	0	0	0	1	0.031
$[\text{mol charge}]$	0	-0.016	0.07	-0.07	-0.07	0	1	0	0



**Table S6** Stoichiometric matrix for heterotrophic growth with acetate in two different units.

	<b>SO<sub>2</sub></b> [gO <sub>2</sub> ·m <sup>-3</sup> ]	<b>SS</b> [gCOD·m <sup>-3</sup> ]	<b>SNH<sub>4</sub></b> [gN·m <sup>-3</sup> ]	<b>SNO<sub>3</sub></b> [gN·m <sup>-3</sup> ]	<b>SNO<sub>2</sub></b> [gN·m <sup>-3</sup> ]	<b>SN<sub>2</sub></b> [gN·m <sup>-3</sup> ]	<b>SH</b> [mol·m <sup>-3</sup> ]	<b>SH<sub>2</sub>CO<sub>3</sub></b> [mol·m <sup>-3</sup> ]	<b>XHET</b> [gCOD·m <sup>-3</sup> ]
Growth with oxygen	-0.58730	-1.58730	-0.0875				-0.01855	0.01835	1
Growth with nitrate		-1.76678	-0.0875	-0.26837		0.26837	-0.04053	0.02396	1
Growth with nitrite		-1.76678	-0.0875		-0.44729	0.44729	-0.05331	0.02396	1
	<b>SO<sub>2</sub></b> [μM]	<b>SS</b> [μM]	<b>SNH<sub>4</sub></b> [μM]	<b>SNO<sub>3</sub></b> [μM]	<b>SNO<sub>2</sub></b> [μM]	<b>SN<sub>2</sub></b> [μM]	<b>SH</b> [μM]	<b>SH<sub>2</sub>CO<sub>3</sub></b> [μM]	<b>XHET</b> [μM]
Growth with oxygen	-18.36	-24.80	-6.246				-18.55	18.35	6.250
Growth with nitrate		-27.61	-6.246	-19.16		19.16	-40.53	23.96	6.250
Growth with nitrite		-27.61	-6.246		-31.93	31.93	-53.31	23.96	6.250

**Table S7** Composition matrix for the calculation of the stoichiometric matrix for heterotrophic growth with acetate.

	<b>SO<sub>2</sub></b> [gO <sub>2</sub> ]	<b>SS</b> [gCOD]	<b>SNH<sub>4</sub></b> [gN]	<b>SNO<sub>3</sub></b> [gN]	<b>SNO<sub>2</sub></b> [gN]	<b>SN<sub>2</sub></b> [gN]	<b>SH</b> [mol]	<b>SH<sub>2</sub>CO<sub>3</sub></b> [mol]	<b>XHET</b> [gCOD]
[gN]	0	0	1	1	1	1	0	0	0.088
[gCOD]	-1	1	0	-4.57	-3.43	-1.71	0	0	1
[mol C]	0	0.0313	0	0	0	0	0	1	0.031
[mol charge]	0	-0.016	0.07	-0.07	-0.07	0	1	0	0

**Table S8** Stoichiometric matrix for heterotrophic growth with glucose in two different units.

	<b>SO<sub>2</sub></b> [gO <sub>2</sub> ·m <sup>-3</sup> ]	<b>SS</b> [gCOD·m <sup>-3</sup> ]	<b>SNH<sub>4</sub></b> [gN·m <sup>-3</sup> ]	<b>SNO<sub>3</sub></b> [gN·m <sup>-3</sup> ]	<b>SNO<sub>2</sub></b> [gN·m <sup>-3</sup> ]	<b>SN<sub>2</sub></b> [gN·m <sup>-3</sup> ]	<b>SH</b> [mol·m <sup>-3</sup> ]	<b>SH<sub>2</sub>CO<sub>3</sub></b> [mol·m <sup>-3</sup> ]	<b>XHET</b> [gCOD·m <sup>-3</sup> ]
Growth with oxygen	-0.58730	-1.58730	-0.0875				0.00625	0.01835	1
Growth with nitrate		-1.76678	-0.0875	-0.26837		0.26837	-0.01292	0.02396	1
Growth with nitrite		-1.76678	-0.0875		-0.44729	0.44729	-0.02570	0.02396	1

	<b>SO<sub>2</sub></b> [μM]	<b>SS</b> [μM]	<b>SNH<sub>4</sub></b> [μM]	<b>SNO<sub>3</sub></b> [μM]	<b>SNO<sub>2</sub></b> [μM]	<b>SN<sub>2</sub></b> [μM]	<b>SH</b> [μM]	<b>SH<sub>2</sub>CO<sub>3</sub></b> [μM]	<b>XHET</b> [μM]
Growth with oxygen	-18.36	-24.80	-6.246				6.250	18.35	6.250
Growth with nitrate		-27.61	-6.246	-19.16		19.16	-12.92	23.96	6.250
Growth with nitrite		-27.61	-6.246		-31.93	31.93	-25.70	23.96	6.250

**Table S9** Composition matrix for the calculation of the stoichiometric matrix for heterotrophic growth and endogenous respiration with glucose.

	<b>SO<sub>2</sub></b> [gO <sub>2</sub> ]	<b>SS</b> [gCOD]	<b>SNH<sub>4</sub></b> [gN]	<b>SNO<sub>3</sub></b> [gN]	<b>SNO<sub>2</sub></b> [gN]	<b>SN<sub>2</sub></b> [gN]	<b>SH</b> [mol]	<b>SH<sub>2</sub>CO<sub>3</sub></b> [mol]	<b>XHET</b> [gCOD]
[gN]	0	0	1	1	1	1	0	0	0.088
[gCOD]	-1	1	0	-4.57	-3.43	-1.71	0	0	1
[mol C]	0	0.0313	0	0	0	0	0	1	0.031
[mol charge]	0	0	0.07	-0.07	-0.07	0	1	0	0

**Table S10** Stoichiometric matrix for heterotrophic endogenous respiration in two different units.

	<b>SO<sub>2</sub></b>	<b>SNH<sub>4</sub></b>	<b>SNO<sub>3</sub></b>	<b>SNO<sub>2</sub></b>	<b>SN<sub>2</sub></b>	<b>SH</b>	<b>SH<sub>2</sub>CO<sub>3</sub></b>	<b>XI</b>	<b>XHET</b>
	[gO <sub>2</sub> ·m <sup>-3</sup> ]	[gN·m <sup>-3</sup> ]	[gN·m <sup>-3</sup> ]	[gN·m <sup>-3</sup> ]	[gN·m <sup>-3</sup> ]	[mol·m <sup>-3</sup> ]	[mol·m <sup>-3</sup> ]	[gCOD·m <sup>-3</sup> ]	[gCOD·m <sup>-3</sup> ]
End. respiration with oxygen	-0.82	0.0812				-0.00580	0.02563	0.18	-1
End. respiration with nitrate		0.0812	-0.2870		0.2870	-0.02630	0.02563	0.18	-1
End. respiration with nitrite		0.0812		-0.47833	0.47833	-0.03997	0.02563	0.18	-1

	<b>SO<sub>2</sub></b>	<b>SNH<sub>4</sub></b>	<b>SNO<sub>3</sub></b>	<b>SNO<sub>2</sub></b>	<b>SN<sub>2</sub></b>	<b>SH</b>	<b>SH<sub>2</sub>CO<sub>3</sub></b>	<b>XI</b>	<b>XHET</b>
	[μM]	[μM]	[μM]	[μM]	[μM]	[μM]	[μM]	[μM]	[μM]
End. respiration with oxygen	-25.64	5.796				-5.800	25.63	1.125	-6.250
End. respiration with nitrate		5.796	-20.49		20.49	-26.30	25.63	1.125	-6.250
End. respiration with nitrite		5.796		-34.14	34.14	-39.97	25.63	1.125	-6.250

**Table S11** Composition matrix for the calculation of the stoichiometric matrix for heterotrophic endogenous respiration.

	<b>SO<sub>2</sub></b>	<b>SNH<sub>4</sub></b>	<b>SNO<sub>3</sub></b>	<b>SNO<sub>2</sub></b>	<b>SN<sub>2</sub></b>	<b>SH</b>	<b>SH<sub>2</sub>CO<sub>3</sub></b>	<b>XI</b>	<b>XHET</b>
	[gO <sub>2</sub> ]	[gN]	[gN]	[gN]	[gN]	[mol]	[mol]	[gCOD]	[gCOD]
[gN]	0	1	1	1	1	0	0	0.035	0.088
[gCOD]	-1	0	-4.57	-3.43	-1.71	0	0	1	1
[mol C]	0	0	0	0	0	0	1	0.031	0.031
[mol charge]	0	0.07	-0.07	-0.07	0	1	0	0	0



## **General Conclusions and Outlook**

## General Conclusions and Outlook

So far, nitrification/anammox has mainly been applied for high-strength nitrogen wastewaters with very low biodegradable organic substrate contents. The results from this thesis though clearly show that nitrification/anammox is also suitable for nitrogen removal from wastewaters with elevated amounts of biodegradable organic substrate. Provided the SRT is high enough, AMX are able to coexist with HET at least up to influent COD/N ratios of  $1.4 \text{ g COD} \cdot \text{g N}^{-1}$ . Oxidisable acetate did not seem to constitute an advantage for AMX compared to glucose, which suggests that AMX can also compete with HET in the presence of different types of organic substances as long as the organic compounds are not toxic. These results also confirm that the recently discussed integration of anammox into mainstream wastewater treatment should be further pursued.

Nevertheless, the presence of HET and their competition with AMX bears a potential for process instabilities. It was therefore expected that a separation of the biodegradable organic substrate from AMX would be beneficial for the operation of nitrification/anammox process with urine. However, a comparison of three different process configurations, i.e. (1) a single-stage nitrification/anammox reactor, (2) a reactor for pre-oxidation of organic substances followed by a single-stage nitrification/anammox reactor, and (3) a two reactor setup with an oxic step for nitrification and oxidation of organic substances and an anoxic step for anammox did not confirm this. The decrease of AMX activity was comparable in all three process configurations.

Moreover, additional base was required to allow complete nitrogen removal in the second and third set-up, where the biodegradable organic substrate was oxidised under aerobic conditions. Apparently, heterotrophic degradation of the biodegradable organic matter with nitrite and nitrate produces the missing alkalinity for a complete nitrogen removal from urine in a single-stage nitrification/anammox process. Regarding the low ratio of alkalinity to ammonium in urine, the high concentration of biodegradable organic substrate in urine is though even positive for the process. This also implies that a single-stage configuration is the best option for a nitrification/anammox process with urine.

Apart from the elevated amount of biodegradable organic substrate, many other urine components, such as salts and non-biodegradable organic substances, could hinder nitrogen removal via nitrification/anammox. A detailed evaluation of all possible influence factors revealed three potentially critical factors: (1) a strong decrease of the biomass content caused by a floc destabilisation due to the high ratio of monovalent to divalent cations in urine, (2) a direct inhibition of AMX by non-biodegradable organic substances and (3) a direct inhibition of AMX by pharmaceuticals.

Further research is required to evaluate whether all three factors or only one or two of them are critical. A strong influence of non-biodegradable organic compounds and/or pharmaceuticals could be reduced with dilution of the urine. One option for this could be to already collect the urine together with part of the flushing water. The high ratio of monovalent to divalent cations could be decreased with additional divalent cations. Another option could be to directly treat fresh urine, because urea hydrolysis and the related precipitation of struvite and hydroxyapatite significantly reduces the amount of dissolved divalent cations in urine during storage. If the ratio of monovalent to divalent cations cannot be reduced, biomass retention could also be improved with a biofilm system.

The operation of a single-stage nitritation/anammox process with diluted urine confirmed that a dilution of the urine is beneficial for the process. Though even with diluted urine, the complex interactions between the different bacterial groups and the influence from numerous urine compounds make single-stage nitritation/anammox processes prone to system instabilities and the occurrence of potentially irreversible regime shifts. Therefore, a good process control is required for a stable operation. Especially due to the elevated amounts of biodegradable organic substrate in urine, detection of decreasing AMX activity is difficult. HET are able to take over part of the nitrogen removal from urine so that decreasing AMX activity does not necessarily lead to an accumulation of nitrite.

In this context, it would be especially useful to have a simple and fast tool that allows detecting changes of bacterial activities in time, and thus taking appropriate measures to omit impending regime shifts. Mass balances based on regularly measured parameters such as ammonium and nitrite would be a convenient alternative to the existing analytical and experimental methods which all require sophisticated equipment and expertise. However, if heterotrophic activity with oxygen, nitrite and nitrate is included in the mass balances, the calculated bacterial activities are coupled to very high uncertainties. Mass balances are therefore not suitable for a fast and reliable assessment of the current bacterial activities.

Nutrient removal strategies from high-strength nitrogen wastewaters bear the risk to displace the environmental problem from water bodies to the atmosphere because both high ammonium and nitrite concentrations can lead to increased NO and N<sub>2</sub>O production. In this study, significant NO and N<sub>2</sub>O emissions only occurred as a consequence of increased nitrite concentrations due to decreasing AMX activity. The hypothesis that NO and N<sub>2</sub>O emissions are negligible during stable operation of a nitritation/anammox process with urine though still requires further proof.

Microsensors for the measurement of NO and N<sub>2</sub>O in the liquid phase have a number of significant advantages compared to the more established measurement in the gas phase. Measurements in the liquid phase e.g. allow measuring concentration gradients in biofilm reactors and

they do not require a purge gas to strip NO and N<sub>2</sub>O during anoxic phases. Depending on the conditions during the measurement, the temperature dependency, the interference from NO on the N<sub>2</sub>O measurement and the interference from ammonia, nitrous acid, hydroxylamine and hydrazine on the NO measurement must be corrected with previously established correction functions in order to reach high measurement accuracy. These results establish a sound basis for all further applications of the two sensors and make NO and N<sub>2</sub>O measurement more reliable.

To conclude, this thesis contributes many new insights and directs the way of further research for the development of a reliable and simple process configuration for nitrogen removal from urine. The operation of a single-stage nitritation/anammox reactor with urine is challenging, but, in my opinion, the best option for biological nitrogen removal from urine. Further research should focus on an evaluation of the three remaining potentially critical factors, first, a floc destabilisation due to high ratio of monovalent to divalent cations in urine, second, a direct inhibition of AMX by non-biodegradable organic substances and third, a direct inhibition of AMX by pharmaceuticals. Subsequently, with the additional knowledge from this evaluation, a suitable operation strategy for reliable nitrogen removal from urine via the nitritation/anammox process can be developed.



## **REFERENCES**

## REFERENCES

- Adav S.S., Lee D.-J., Show K.-Y. and Tay J.-H. (2008) Aerobic granular sludge: Recent advances. *Biotechnology Advances* **26**, 411-423.
- Ahn J.H., Kim S., Park H., Katehis D., Pagilla K. and Chandran K. (2010) Spatial and temporal variability in atmospheric nitrous oxide generation and emission from full-scale biological nitrogen removal and non-BNR processes. *Water Environment Research* **82**, 2362–2372.
- Allison S.D. and Martiny J.B.H. (2008) Resistance, resilience, and redundancy in microbial communities. *Proceedings of the National Academy of Sciences U. S. A.* **105**, 11512–11519.
- Alpkvist E., Picioreanu C., van Loosdrecht M.C.M. and Heyden A. (2006) Three-dimensional biofilm model with individual cells and continuum EPS matrix. *Biotechnology and Bioengineering* **94**, 961-979.
- Amann R.I., Krumholz L. and Stahl D.A. (1990) Fluorescent-oligonucleotide probing of whole cells for determinative, phylogenetic, and environmental studies in microbiology. *Journal of Bacteriology* **172**, 762-770.
- American Public Health Association (2005) *Standard methods for the examination of water & wastewater*, 21st ed. American Public Health Association, American Water Works Association, and Water Environment Federation, Washington, DC.
- Andersen K., Kjær T. and Revsbech N.P. (2001) An oxygen insensitive microsensor for nitrous oxide. *Sensors and Actuators B* **81**, 42–48.
- Anderson I.C., Poth M., Homstead J. and Burdige D. (1993) A comparison of NO and N<sub>2</sub>O production by the autotrophic nitrifier *Nitrosomonas europaea* and the heterotrophic nitrifier *Alcaligenes faecalis*. *Applied and Environmental Microbiology* **59**, 3525–3533.
- Baas-Becking L.G.M. (1934) *Geobiologie of inleiding tot de milieukunde*. W.P. van Stockum and N.V. Zoon, The Hague, Netherlands.
- Bard A.J., Parson R. and Jordan J., Eds. *Standard Potentials in Aqueous Solutions*; Marcel Dekker: New York, 1985.
- Bassin J.P., Kleerebezem R., Muyzer G., Rosado A.S., van Loosdrecht M.C.M. and Dezotti M. (2012) Effect of different salt adaption strategies on the microbial diversity, activity, and settling of nitrifying sludge in sequencing batch reactor. *Applied and Microbiology Biotechnology* **93**, 1281-1294.
- Beake B.D. and Moodie R.B. (1995) Role of the reaction of nitric oxide with oxygen in the decomposition of nitrous acid in aqueous acid solution. *Journal of the Chemical Society, Perkin Transactions* **2**, 1045–1048.
- Bedioui F. and Villeneuve N. (2003) Electrochemical nitric oxide sensors for biological samples - Principle, selected examples and applications. *Electroanalysis* **15**, 5–18.
- Bernet N. and Béline F. (2009) Challenges and innovations on biological treatment of livestock effluents. *Bioresource Technology* **100**, 5431-5436.
- Blackburne R., Yuan Z. and Keller J. (2008) Partial nitrification to nitrite using low dissolved oxygen concentrations as the main selection factor. *Biodegradation* **19**, 303-312.

- Botton S., van Heusden M., Parsons J. R., Smidt H. and van Straalen N. (2006) Resilience of microbial systems towards disturbances. *Critical Reviews in Microbiology* **32**, 101–112.
- Briones A. and Raskin L. (2003) Diversity and dynamics of microbial communities in engineered environments and their implications for process stability. *Current Opinion in Biotechnology* **4**, 270–276.
- Bürgmann H., Meier S., Bunge M., Widmer F. and Zeyer J. (2005) Effects of model root exudates on structure and activity of a soil diazotroph community. *Environmental Microbiology* **7**, 1711–1724.
- Bürgmann H., Jenni S., Vazquez F. and Udert K.M. (2011) Regime shift and microbial dynamics in a sequencing batch reactor for nitrification and anammox treatment of urine. *Applied and Environmental Microbiology* **77**, 5897–5907.
- Buesing N., Filippini M., Bürgmann H. and Gessner M. O. (2009) Microbial communities in contrasting freshwater marsh microhabitats. *FEMS Microbiology Ecology* **69**, 84–97.
- Carvajal-Arroyo J.M., Sun W., Sierre-Alvarez R. and Field J.A. (2013) Inhibition of anaerobic ammonium oxidizing (anammox) enrichment cultures by substrates, metabolites and common wastewater constituents. *Chemosphere* **91**, 22–27.
- Chamchoi N., Nitisoravut S. and Schmidt, J.E. (2008) Inactivation of ANAMMOX communities under concurrent operation of anaerobic ammonium oxidation (ANAMMOX) and denitrification. *Bioresource Technology* **99**, 3331–3336.
- Chen H., Liu S., Yang F., Xue Y. and Wang T. (2009) The development of simultaneous partial nitrification, ANAMMOX and denitrification (SNAD) process in a single reactor for nitrogen removal. *Bioresource Technology* **100**, 4531–4534.
- Ciba-Geigy (1977) *Wissenschaftliche Tabellen Geigy*, Teilband Körperflüssigkeiten, 8. Auflage, Basel.
- Climate Change 2007: The Physical Science Basis. Contribution of Working Group I to the Fourth Assessment Report of the Intergovernmental Panel on Climate Change*; Solomon S., Qin D., Manning M., Marquis M., Averyt K., Tignor M.M.B., Henry LeRoy Miller J. and Chen Z., Eds.; Cambridge University Press: Cambridge, U.K., 2007.
- Collie J.S., Richardson K. and Steele J.H. (2004) Regime shifts: can ecological theory illuminate the mechanisms? *Progress in Oceanography* **60**, 281–302.
- Curtis T.P., Head I.M. and Graham D.W. (2003) Theoretical Ecology for engineering biology. *Environmental Science and Technology* **37**, 64A–70A.
- Dapena-Mora A., Van Hulle S.W.H., Campos J.L., Mendez R., Vanrolleghem P.A. and Jetten M.S.M. (2004) Enrichment of Anammox biomass from municipal activated sludge: experimental and modelling results. *Journal of Chemical Technology and Biotechnology* **79**, 1421–1428.
- Dapena-Mora A., Fernandez I., Campos J.L., Mosquera-Corral A., Mendez R. and Jetten M.S.M. (2007) Evaluation of activity and inhibition effects on anammox process by batch tests based on the nitrogen gas production. *Enzyme and Microbial Technology* **40**, 859–865.

- Dapena-Mora A., Vázquez-Padín J.R., Campos J.L., Mosquera-Corral A., Jetten M.S.M. and Méndez R. (2010) Monitoring the stability of an anammox reactor under high salinity conditions. *Biochemical Engineering Journal* **51**, 167-171.
- Daverey A., Su S.-H., Huang Y.-T. and Lin J.-G. (2012) Nitrogen removal from opto-electronic wastewater using the simultaneous partial nitrification, anaerobic ammonium oxidation and denitrification (SNAD) process in sequencing batch reactor. *Bioresource Technology* **113**, 225-231.
- De Clippeleir H., Vlaeminck S., Wilde F., Daeninck K., Mosquera M., Boeckx P., Verstraete W. and Boon N. (2013) One-stage partial nitritation/anammox at 15°C on pretreated sewage: feasibility demonstration at lab-scale. *Applied Microbiology and Biotechnology* **97**, 10199-10210.
- de Graaff M.S., Temmink H., Zeeman G., van Loosdrecht M.C.M. and Buisman C.J.N. (2011) Autotrophic nitrogen removal from black water : Calcium addition as a requirement for settleability. *Water Research* **45**, 63-74.
- Desloover J., De Clippeleir H., Boeckx P., Du Laing G., Colsen J., Verstraete W. and Vlaeminck S.E. (2011) Floc-based sequential partial nitritation and anammox at full scale with contrasting N<sub>2</sub>O emissions. *Water Research* **45**, 2811-2821.
- Dochain D., Vanrolleghem P.A. and Van Daele M. (1995) Structural identifiability of biokinetic models of activated sludge respiration. *Water Research* **29**, 2571-2578.
- Dyrborg S. and Arvin E. (1995) Inhibition of nitrification by creosote-contaminated water. *Water Research* **29**, 1603-1606.
- Edwards J.S., Covert M. and Palsson B. (2002) Metabolic modelling of microbes: The flux-balance approach. *Environmental Microbiology* **4**, 133-140.
- Egli K., Fanger U., Alvarez P.J.J., Siegrist H., van der Meer J.R. and Zehnder A.J.B. (2001) Enrichment and characterization of an anammox bacterium from a rotating biological contactor treating ammonium-rich leachate. *Archives of Microbiology* **175**, 198-207.
- Fang F., Ni B.-J., Li X.-Y., Sheng G.-P. and Yu H.-Q. (2009) Kinetic analysis on the two-step processes of AOB and NOB in aerobic nitrifying granules. *Applied Microbiology and Biotechnology* **83**, 1159-1169.
- Feelisch M. and Stamler J.S.; Donors of nitrogen oxides. In *Methods in Nitric Oxide Research*; Feelisch M. and Stamler J.S., Eds.; John Wiley and Sons: Chichester, England, 1996; pp 71-115.
- Fernández I., Vázquez-Padín J.R., Mosquera-Corral A., Campos J.L. and Méndez R. (2008) Biofilm and granular systems to improve anammox biomass retention. *Biochemical Engineering Journal* **42**, 308-313.
- Fernández I., Mosquera-Corral A., Campos J.L. and Méndez R. (2009) Operation of an anammox SBR in the presence of two broad-spectrum antibiotics. *Process Biochemistry* **44**, 494-498.
- Fernández I., Dosta J., Fajardo C., Campos J.L., Mosquera-Corral A. and Méndez R. (2012) Short- and long-term effects of ammonium and nitrite on the anammox process. *Journal of Environmental Management* **95**, 170-174.

- Finlay B., Maberly J.S.C. and Cooper J.I. (1997) Microbial diversity and ecosystem function. *Oikos* **80**, 209–213.
- Fisher M.M. and Triplett E.W. (1999) Automated approach for ribosomal intergenic spacer analysis of microbial diversity and its application to freshwater bacterial communities. *Applied and Environmental Microbiology* **65**, 4630–4636.
- Folke C., Carpenter S., Walker B., Scheffer M., Elmqvist T., Gunderson L. and Holling C.S. (2004) Regime shifts, resilience, and biodiversity in ecosystem management. *Annual Review of Ecology, Evolution, and Systematics* **35**, 557–581
- Franz K.J. and Lippard S.J. (1998) Disproportionation of nitric oxide promoted by a Mn tropocoronand. *Journal of the American Chemical Society* **120**, 9034–9040.
- Fux C., Huang D., Monti A. and Siegrist H. (2004) Difficulties in maintaining long-term partial nitrification of ammonium-rich sludge digester liquids in a moving-bed biofilm reactor (MBBR). *Water Science and Technology* **49**, 53–60.
- Fux C., Velten S., Carozzi V., Solley D. and Keller J. (2006) Efficient and stable nitrification and denitrification of ammonium-rich sludge dewatering liquor using an SBR with continuous loading. *Water Research* **40**, 2765–2775.
- Gaval G. and Pernelle J.-J. (2003) Impact of the repetition of oxygen deficiencies on the filamentous bacteria proliferation in activated sludge. *Water Research* **37**, 1991–2000.
- Geets J., Cooman M., Wittebolle L., Heylen K., Vanparys B., Vos P., Verstraete W. and Boon N. (2007) Real-time PCR assay for the simultaneous quantification of nitrifying and denitrifying bacteria in activated sludge. *Applied Microbiology and Biotechnology* **75**, 211–221.
- Ghosh G.C., Okuda T., Yamashita N. and Tanaka H. (2009) Occurrence and elimination of antibiotics at four sewage treatment plants in Japan and their effects on bacterial ammonia oxidation. *Water Science and Technology* **59**, 779–786.
- Giger W., Alder A.C., Golet E.M., Kohler H.P.E., McArdell C.S., Molnar E., Siegrist H. and Suter M.J.F. (2003) Occurrence and fate of antibiotics as trace contaminants in wastewaters, sewage sludges, and surface waters. *Chimia* **57**, 485–491.
- Gilbride K.A., Lee D.Y. and Beaudette L.A. (2006) Molecular techniques in wastewater: understanding microbial communities, detecting pathogens, and real-time process control. *Journal of Microbiological Methods* **66**, 1–20.
- Gomez J., Mendez R. and Lema J.M. (2000) Kinetic study of addition of volatile organic compounds to a nitrifying sludge. *Applied Biochemistry and Biotechnology* **87**, 189–202.
- Guisasola A., Jubany I., Baeza J.A., Carrera J. and Lafuente J. (2005) Respirometric estimation of the oxygen affinity constants for biological ammonium and nitrite oxidation. *Journal of Chemical Technology and Biotechnology* **80**, 388–396.
- Gujer W., Henze M., Mino T. and van Loosdrecht M.C.M. (1999). Activated sludge model no. 3. *Water Science and Technology* **39**, 183–193.
- Gujer W. (2006) Activated sludge modelling: past, present and future. *Water Science and Technology* **53**, 111–119.

- Gundersen J.K., Ramsing N.B. and Glud R.N. (1998) Predicting the signal of O<sub>2</sub> microsensors from physical dimensions, temperature, salinity, and O<sub>2</sub> concentration. *Limnology and Oceanography* **43**, 1932–1937.
- Gustavsson D.J.I. and La Cour Jansen J. (2011) Dynamics of nitrogen oxides emission from a full-scale sludge liquor treatment plant with nitrification. *Water Science and Technology* **63**, 2838–2845.
- Güven D., Dapena A., Kartal B., Schmid M.C., Maas B., van de Pas-Schoonen K., Sozen S., Mendez R., Op den Camp H.J.M., Jetten M.S.M., Strous M. and Schmidt I. (2005) Propionate oxidation by and methanol inhibition of anaerobic ammonium-oxidizing bacteria. *Applied and Environmental Microbiology* **71**, 1066-1071.
- Hao X., Heijnen J.J. and van Loosdrecht M.C.M. (2002) Model-based evaluation of temperature and inflow variations on a partial nitrification–ANAMMOX biofilm process. *Water Research* **36**, 4839-4849.
- Hellinga C., Schellen A., Mulder J., van Loosdrecht M.C.M. and Heijnen J.J. (1998) The Sharon process: an innovative method for nitrogen removal from ammonium-rich waste water. *Water Science and Technology* **37**, 135-142.
- Hellinga C., van Loosdrecht M.C.M. and Heijnen J.J. (1999) Model based design of a novel process for nitrogen removal from concentrated flows. *Mathematical and Computer Modelling of Dynamical Systems* **5**, 351–371.
- Henze M., Gujer W., Mino T. and van Loosdrecht M.C.M. (2000) Scientific and Technical Reports No.9: Activated Sludge Models ASM1, ASM2, ASM2d and ASM3. IWA Publishing, London.
- Hetrick E.M. and Schoenfisch M. H. (2009) Analytical chemistry of nitric oxide. *Annual Review of Analytical Chemistry* **2**, 409–433.
- Hippen A., Rosenwinkel K.-H., Baumgarten G. and Seyfried C.F. (1997) Aerobic deammonification: a new experience in the treatment of wastewaters. *Water Science and Technology* **35**, 111-120.
- Hu A., Zheng P., Mahmood Q., Zhang L., Shen L. and Ding S. (2011) Characteristics of nitrogenous substrate conversion by anammox enrichment. *Bioresource Technology* **102**, 536–542.
- Hulshoff Pol L.W., de Castro Lopes S.I., Lettinga G. and Lens P.N.L. (2004) Anaerobic sludge granulation. *Water Research* **38**, 1376-1389.
- Hunik J.H., Bos C.G., van den Hoogen M.P., De Gooijer C.D. and Tramper J. (1994) Co-immobilized *Nitrosomonas europaea* and *Nitrobacter agilis* cells: validation of a dynamic model for simultaneous substrate conversion and growth in  $\kappa$ -carrageenan gel beads. *Biotechnology and Bioengineering* **43**, 1153-1163.
- ISO 8466-1: Water quality - Calibration and valuation of analytical methods and estimation of performance characteristics. Part 1: Statistical evaluation of the linear calibration function; *International Organization for Standardization*: Geneva, Switzerland, 1990.
- ISO 8466-2: Water quality - Calibration and evaluation of analytical methods and estimation of performance characteristics. Part 2: Calibration strategy for non-linear second order calibration functions; *International Organization for Standardization*: Geneva, Switzerland, 1993.

- Jayamohan S., Ohgaki S. and Hanaki K. (1988) Effect of DO on kinetics in nitrification. *Water Supply* **6**, 141-150.
- Jenni S., Mohn J., Emmenegger L. and Udert K.M. (2012) Temperature dependence and interferences of NO and N<sub>2</sub>O microelectrodes used in wastewater treatment. *Environmental Science and Technology* **46**, 2257-2266.
- Jenni S., Vlaeminck S.E., Morgenroth E. and Udert K.M. (2014) Successful application of nitrification/anammox to wastewater with elevated organic carbon to ammonia ratios. *Water Research* **49**, 316-326.
- Jia L., Guo J.-S., Fang F., Chen Y.-P. and Zhang Q. (2012) Effect of organic carbon on nitrogen conversion and microbial communities in the completely autotrophic nitrogen removal process. *Environmental Technology* **33**, 1141-1149.
- Jin R.-C., Yang G.-F., Yu J.-J. and Zheng P. (2012) The inhibition of the anammox process: A review. *Chemical Engineering Journal* **197**, 67-79.
- Joss A., Zabcynski S., Göbel A., Hoffmann B., Löffler D., McArdell C.S., Ternes T.A., Thomsen A. and Siegrist H. (2006) Biological degradation of pharmaceuticals in municipal wastewater treatment: Proposing a classification scheme. *Water Research* **40**, 1686-1696.
- Joss A., Salzgeber D., Eugster J., König R., Rottermann K., Burger S., Fabijan P., Leumann S., Mohn J. and Siegrist H. (2009) Full-Scale Nitrogen Removal from Digester Liquid with Partial Nitrification and Anammox in One SBR. *Environmental Science and Technology* **43**, 5301-5306.
- Joss A., Derlon N., Cyprien C., Burger S., Szivak I., Traber J., Siegrist H. and Morgenroth E. (2011) Combined nitrification-anammox: Advances in understanding process stability. *Environmental Science and Technology* **45**, 9735-9742.
- Kaelin D., Manser R., Rieger L., Eugster J., Rottermann K. and Siegrist H. (2009) Extension of ASM3 for two-step nitrification and denitrification and its calibration and validation with batch tests and pilot scale data. *Water Research* **43**, 1680-1692.
- Kampschreur M.J., Picioreanu C., Tan N., Kleerebezem R., Jetten M.S.M. and van Loosdrecht M.C.M. (2007) Unraveling the source of nitric oxide emission during nitrification. *Water Environment Research* **79**, 2499-2509.
- Kampschreur M.J., van der Star W.R.L., Wielders H.A., Mulder J.W., Jetten M.S.M. and van Loosdrecht M.C.M. (2008a) Dynamics of nitric oxide and nitrous oxide emission during full-scale reject water treatment. *Water Research* **42**, 812-826.
- Kampschreur M.J., Tan N.C.G., Kleerebezem R., Picioreanu C., Jetten M.S.M. and Loosdrecht M.C.M. (2008b) Effect of dynamic process conditions on nitrogen oxides emission from a nitrifying culture. *Environmental Science and Technology* **42**, 429-435.
- Kampschreur M.J., Poldermans R., Kleerebezem R., van der Star W.R.L., Haarhuis R., Abma W.R., Jetten M.S.M. and van Loosdrecht M.C.M. (2009a) Emission of nitrous oxide and nitric oxide from a full-scale single-stage nitrification-anammox reactor. *Water Science and Technology* **60**, 3211-3217.
- Kampschreur M.J., Temmink H., Kleerebezem R., Jetten M.S.M. and van Loosdrecht M.C.M. (2009b) Nitrous oxide emission during wastewater treatment. *Water Research* 2009, **43**, 4093-4103.

- Kartal B., Rattray J., van Niftrik L.A., van de Vossenberg J., Schmid M.C., Webb R.I., Schouten S., Fuerst, J.A., Damsté J.S., Jetten M.S.M. and Strous M. (2007a) Candidatus "Anammoxoglobus propionicus" a new propionate oxidizing species of anaerobic ammonium oxidizing bacteria. *Systematic and Applied Microbiology* **30**, 39-49.
- Kartal B., Kuypers M.M.M., Lavik G., Schalk J., Op den Camp H.J.M., Jetten M.S.M. and Strous M. (2007b) Anammox bacteria disguised as denitrifiers: nitrate reduction to dinitrogen gas via nitrite and ammonium. *Environmental Microbiology* **9**, 635-642.
- Kartal B., Van Niftrik L., Rattray J., van de Vossenberg J.L.C.M., Schmid M.C., Damsté J.S., Jetten M.S.M. and Strous M. (2008) Candidatus 'Brocadia fulgida': an autofluorescent anaerobic ammonium oxidizing bacterium. *FEMS Microbiology Ecology* **63**, 46-55.
- Kartal B., Tan N.C.G., Van Biezen E.D., Kampschreur M.J., van Loosdrecht M.C.M. and Jetten M.S.M. (2010) Effect of nitric oxide on anammox bacteria. *Applied and Environmental Microbiology* **76**, 6304-6306.
- Kartal B., de Almeida N.M., Maalcke W.J., Op den Camp H.J.M., Jetten M.S.M. and Keltjens J.T. (2013) How to make a living from anaerobic ammonium oxidation. *FEMS Microbiology Reviews* **37**, 428-461.
- Kimura Y., Isaka K. and Kazama F. (2011) Effects of inorganic carbon limitation on anaerobic ammonium oxidation (anammox) activity. *Bioresource Technology* **102**, 4390-4394.
- Kindaichi T., Ito T. and Okabe S. (2004) Ecophysiological interaction between nitrifying bacteria and heterotrophic bacteria in autotrophic nitrifying biofilms as determined by microautoradiography-fluorescence in situ hybridization. *Applied and Environmental Microbiology* **70**, 1641-1650.
- Kindt R. and Coe R. (2005) *Tree diversity analysis: a manual and software for common statistical methods for ecological and biodiversity studies*. World Agroforestry Centre, Nairobi, Kenya. <http://www.worldagroforestry.org/resources/databases/tree-diversity-analysis>.
- Kleikemper J., Schroth M.H., Sigler W.V., Schmucki M., Bernasconi S.M. and Zeyer, J. (2005) Activity and Diversity of Sulfate-Reducing Bacteria in a Petroleum Hydrocarbon-Contaminated Aquifer. *Applied and Environmental Microbiology* **68**, 1516-1523.
- Koch G., Egli K., Van Der Meer J.R., Siegrist H. (2000a). Mathematical modeling of autotrophic denitrification in a nitrifying biofilm of a rotating biological contactor. *Water Science and Technology* **41**, 191-198.
- Koch G., Kühni M., Gujer W. and Siegrist H. (2000b) Calibration and validation of activated sludge model no. 3 for Swiss municipal wastewater. *Water Research* **34**, 3580-3590.
- Kuai L. and Verstraete W. (1998) Ammonium removal by the oxygen-limited autotrophic nitrification-denitrification system. *Applied and Environmental Microbiology* **64**, 4500-4506.
- Lackner S., Terada A. and Smets B.F. (2008) Heterotrophic activity compromises autotrophic nitrogen removal in membrane-aerated biofilms: Results of a modeling study. *Water Research* **42**, 1102-1112.
- Lackner S. and Horn H. (2013) Comparing the performance and operation stability of an SBR and MBBR for single-stage nitrification-anammox treating wastewater with high organic load. *Environmental Technology* **34**, 1319-1328.



- Lackner S., Gilbert E.M., Vlaeminck S.E., Joss A., Horn H. and van Loosdrecht M.C.M. (2014) Full-scale partial nitrification/anammox experiences – An application survey. *Water Research* **55**, 292-303.
- Lan C.-J., Kumar M., Wang C.-C. and Lin J.-G. (2011) Development of simultaneous partial nitrification, anammox and denitrification (SNAD) process in a sequential batch reactor. *Bioresource Technology* **102**, 5514-5519.
- Lane D.J. (1991) 16S/23S rRNA sequencing, p. 115–147. In E. Stackebrandt and M. Goodfellow (ed.), *Nucleic acid techniques in bacterial systematics*. John Wiley & Sons, Chichester, United Kingdom.
- Larsen T.A. and Gujer W. (2001) Waste design and source control lead to flexibility in wastewater management. *Water Science and Technology* **43**, 309-318.
- Larsen T.A., Udert K.M. and Lienert J. (2013) *Source Separation and Decentralization for Wastewater Management*. IWA Publishing, London, UK.
- Lide D.R., Ed. *CRC Handbook of Chemistry and Physics*, 89th, ed.; CRC Press: Boca Raton, FL, 2009.
- Lienert J., Bürki T. and Escher B.I. (2007) Reducing micropollutants with source control: substance flow analysis of 212 pharmaceuticals in faeces and urine. *Water Science and Technology* **5**, 87-96.
- Lienert J. and Larsen T.A. (2007) Soft paths in wastewater management – the pros and cons of urine source separation. *Gaia* **16**, 280-288.
- Liu C., Yamamoto T., Nishiyama T., Fujii T. and Furukawa K. (2009) Effect of salt concentration in anammox treatment using non woven biomass carrier. *Journal of Bioscience and Bioengineering* **107**, 519-523.
- Liu, S.T., Horn, H., Müller, E., 2013. A systematic insight into a single-stage deammonification process operated in granular sludge reactor with high-loaded reject-water: characterization and quantification of microbiological community. *Journal of Applied Microbiology* **114**, 339-351.
- Logue J.B., Bürgmann H. and Robinson C.T. (2008) Progress in the ecological genetics and biodiversity of freshwater bacteria. *Bioscience* **58**, 103–113.
- Lotti T., van der Star W.R.L., Kleerebezem R., Lubello C. and van Loosdrecht M.C.M. (2012) The effect of nitrite inhibition on the anammox process. *Water Research* **46**, 2559-2569.
- Loy A., Horn M. and Wagner M. (2003) probeBase: an online resource for rRNA-targeted oligonucleotide probes. *Nucleic Acids Research* **31**, 514-516.
- Ma C., Jin R.-C., Yang G.-F., Yu J.-J., Xing B.-S. and Zhang Q.-Q. (2012) Impacts of transient salinity shock loads on anammox process performance. *Bioresource Technology* **112**, 124-130.
- Mancinelli R.L. and McKay C.P. (1983) Effects of nitric oxide and nitrogen dioxide on bacterial growth. *Applied and Environmental Microbiology* **46**, 198–202.
- Manser R., Gujer W. and Siegrist H. (2005) Consequences of mass transfer effects on the kinetics of nitrifiers. *Water Research* **39**, 4633-4642.

- Mašić A. and Villez K. (2014) Model-based observers for monitoring of a biological nitrification process for decentralized wastewater treatment - Initial results. Conference proceedings of the 2nd IWA Specialized International Conference "Ecotechnologies for Wastewater Treatment" (EcoSTP2014), Verona, Italy, June 23-25, 2014, 396-399.
- Maurer M., Schwegler P. and Larsen T.A. (2003) Nutrients in urine: energetic aspects of removal and recovery. *Water Science and Technology* **48**, 37-46.
- McCarty P.L. (1975) Stoichiometry of Biological Reactions. *Progress in Water Technology* **7**, 157-172.
- McMahon K.D., Martin H.G. and Hugenholtz P. (2007) Integrating ecology into biotechnology. *Current Opinion in Biotechnology* **18**, 287-292.
- Meijer S.C.F., van der Spoel H., Susanti S., Heijnen, J.J. and van Loosdrecht M.C.M. (2002) Error diagnostics and data reconciliation for activated sludge modelling using mass balances. *Water Science and Technology* **45**, 145-156.
- Meyer R.L., Zeng R.J., Giugliano V. and Blackall L.L. (2005) Challenges for simultaneous nitrification, denitrification, and phosphorus removal in microbial aggregates: mass transfer limitation and nitrous oxide production. *FEMS Microbiology Ecology* **52**, 329-338.
- Meyer R. L., Allen D. E. and Schmidt S. (2008) Nitrification and denitrification as sources of sediment nitrous oxide production: A microsensor approach. *Marine Chemistry* **110**, 68-76.
- Metcalf, Eddy (2003) *Wastewater Engineering, Treatment and Reuse*, McGraw-Hill Companies, New York, USA.
- Mohn J., Zeeman M. J., Werner R. A., Eugster W. and Emmenegger L. (2008) Continuous field measurements of  $\delta^{13}\text{C}-\text{CO}_2$  and trace gases by FTIR spectroscopy. *Isotopes in Environmental and Health Studies* **44**, 241-251.
- Mosquera-Corral A., González F., Campos J.L. and Méndez R. (2005) Partial nitrification in a SHARON reactor in the presence of salts and organic carbon compounds. *Process Biochemistry* **40**, 3109-3118.
- Moussa M.S., Hooijmans C.M., Lubberding H.J., Gijzen H.J. and van Loosdrecht M.C.M. (2005) Modelling nitrification, heterotrophic growth and predation in activated sludge. *Water Research* **39**, 5080-5098.
- Moussa M.S., Sumanasekera D.U., Ibrahim S.H., Lubberding H.J., Hooijmans C.M., Gijzen H.J. and van Loosdrecht M.C.M. (2006) Long term effects of salt on activity, population structure and floc characteristics in enriched bacterial cultures of nitrifiers. *Water Research* **40**, 1377-1388.
- Mulder A., van de Graaf A.A., Robertson L.A. and Kuenen J.G. (1995) Anaerobic ammonium oxidation discovered in a denitrifying fluidized-bed reactor. *FEMS Microbiology Ecology* **16**, 177-183.
- Mutlu A.G., Vangsgaard A.K., Sin G. and Smets B.F. (2013) An operational protocol for facilitating start-up of single-stage autotrophic nitrogen-removing reactors based on process stoichiometry. *Water Science and Technology* **68**, 514-521.
- Narasimhan S. and Jordache C. (1999) Data reconciliation and gross error detection: An intelligent use of process data. Gulf Professional Publishing.

- Nelder J.A. and Mead R. (1965) A simplex method for function minimization. *Computer Journal* **7**, 308–313.
- NIST, National Institute of Standards and Technology, <http://webbook.nist.gov/chemistry/>
- Noorman H.J., Heijnen J.J. and Luyben K.C.A.M. (1991) Linear relations in microbial reaction systems: A general overview of their origin, form, and use. *Biotechnology and Bioengineering* **38**, 603-618.
- Noorman H.J., Romein B., Luyben K.C.A.M. and Heijnen J.J. (1996) Classification, error detection and reconciliation of process information in complex biochemical systems. *Biotechnology and Bioengineering* **49**, 364-376.
- Okabe S., Kandaichi T. and Ito T. (2005) Fate of <sup>14</sup>C-labeled microbial products derived from nitrifying bacteria in autotrophic nitrifying biofilms. *Applied and Environmental Microbiology* **71**, 3987-3994.
- Oksanen J., Blanchet F.G., Kindt R., Legendre P., O'Hara R.B., Simpson G.L., Solymos P., Stevens M.H.H. and Wagner H. (2010) Vegan: community ecology package. R package, version 1.17-3. *The R Project for Statistical Computing*, Vienna, Austria.
- Orth J.D., Thiele I. and Palsson B.O. (2010) What is flux balance analysis? *Nature Biotechnology* **28**, 245-248.
- Pellicer-Nàcher C., Sun S., Lackner S., Terada A., Schreiber F., Zhou Q. and Smets B.F. (2010) Sequential aeration of membrane-aerated biofilm reactors for high-rate autotrophic nitrogen removal: Experimental demonstration. *Environmental Science and Technology* **44**, 7628-7634.
- Philips S., Laanbroek H.J. and Verstraete W. (2002) Origin, causes and effects of increased nitrite concentrations in aquatic environments. *Re/Views in Environmental Science and Bio/Technology* **1**, 115-141.
- Podmirseg S.M., Pümpel T., Markt R., Murthy S., Bott C. and Wett B. (2015) Comparative evaluation of multiple methods to quantify and characterise granular anammox biomass. *Water Research* **68**, 194-205.
- Prosser J.I., Bohannon B.J.M., Curtis T.P., Ellis R.J., Firestone M.K., Freckleton R.P., Green J.L., Green L.E., Killham K., Lennon J.J., Osborn A.M., Solan M., van der Gast C.J. and Young J.P.W. (2007) The role of ecological theory in microbial ecology. *Nature Reviews Microbiology* **5**, 384-392.
- Pynaert K., Smets B.F., Wyffels S., Beheydt D., Siciliano S.D. and Verstraete W. (2003) Characterization of an autotrophic nitrogen-removing biofilm from a highly loaded lab-scale rotating biological contactor. *Applied and Environmental Microbiology* **69**, 3626-3634.
- Ravishankara A.R., Daniel J. S. and Portmann R.W. (2009) Nitrous oxide (N<sub>2</sub>O): The dominant ozone-depleting substance emitted in the 21st century. *Science* **326**, 123–125.
- Reichert P. (1998) AQUASIM 2.1e - Computer program for the identification and simulation of aquatic systems. EAWAG, Dübendorf.
- Rodionov S.N. (2004) A sequential algorithm for testing climate regime shifts. *Geophysical Research Letters* **31**, L09204.

- Sánchez O., Martí M.C., Aspé E. and Roeckel M. (2001) Nitrification rates in a saline medium at different dissolved oxygen concentrations. *Biotechnology Letters* **23**, 1957-1602.
- Schalk J., Oustad H., Kuenen J.G. and Jetten M.S.M. (1998) The anaerobic oxidation of hydrazine: A novel reaction in microbial nitrogen metabolism. *FEMS Microbiology Letters* **158**, 61–67.
- Schaubroeck T., Bagchi S., De Clippeleir H., Carballa M., Verstraete W. and Vlaeminck, S.E. (2012) Successful hydraulic strategies to start up OLAND sequencing batch reactors at lab scale. *Microbial Biotechnology* **5**, 403-414.
- Scheffer M. and Carpenter S.R. (2003) Catastrophic regime shifts in ecosystems: linking theory to observation. *Trends in Ecology and Evolution* **18**, 648–656.
- Schmid M.C., Maas B., Dapena A., van de Pas-Schoonen K., van de Vossenberg J., Kartal B., van Niftrik L., Schmidt I., Cirpus I., Kuenen J.G., Wagner M., Sinninghe Damste J.S., Kuypers M., Revsbech N.P., Mendez R., Jetten M.S.M. and Strous M. (2005) Biomarkers for In Situ Detection of Anaerobic Ammonium-Oxidizing (Anammox) Bacteria. *Applied and Environmental Microbiology* **71**, 1677-1684.
- Schmidt I., Hermelink C., van de Pas-Schoonen K., Strous M., op den Camp H.J., Kuenen J.G. and Jetten M.S.M. (2002). Anaerobic Ammonia Oxidation in the Presence of Nitrogen Oxides (NO<sub>x</sub>) by Two Different Lithotrophs. *Applied and Environmental Microbiology* **68**, 5351-5357.
- Schmidt I., van Spanning R.J.M. and Jetten M.S.M. (2004) Denitrification and ammonia oxidation by *Nitrosomonas europaea* wild-type, and NirK- and NorB-deficient mutants. *Microbiology* **150**, 4107–4114.
- Schreiber F., Polerecky L. and de Beer D. (2008) Nitric oxide microsensor for high spatial resolution measurements in biofilms and sediments. *Analytical Chemistry* **80**, 1152–1158.
- Schreiber F., Loeffler B., Polerecky L., Kuypers M.M. and De Beer D. (2009) Mechanisms of transient nitric oxide and nitrous oxide production in a complex biofilm. *ISME Journal* **3**, 1301–1313.
- Schreiber F., Wunderlin P., Udert K.M. and Wells G.F. (2012) Nitric oxide and nitrous oxide turnover in natural and engineered microbial communities: biological pathways, chemical reactions, and novel technologies. *Frontiers in Microbiology* **3**, 372-372.
- Sears K., Alleman J.E., Barnard J.L. and Oleszkiewicz J.A. (2004) Impacts of reduced sulfur components on active and resting ammonia oxidizers. *Journal of Industrial Microbiology and Biotechnology* **31**, 369-378.
- Siegrist H., Reithaar S., Koch G. and Lais P. (1998) Nitrogen loss in a nitrifying rotating contactor treating ammonium-rich wastewater without organic carbon. *Water Science and Technology* **38**, 241–248.
- Siegrist H., Salzgeber D., Eugster J. and Joss A. (2008) Anammox brings WWTP closer to energy autarky due to increased biogas production and reduced aeration energy for N-removal. *Water Science and Technology* **57**, 383-388.
- Sobeck D.C. and Higgins M.J. (2002) Examination of three theories for mechanisms of cation-induced bioflocculation. *Water Research* **36**, 527-538.

- Spindler A. and Vanrolleghem P.A. (2012) Dynamic mass balancing for wastewater treatment data quality control using CUSUM charts. *Water Science and Technology* **65**, 2148-2153.
- Spindler A. (2014) Structural redundancy of data from wastewater treatment systems. Determination of individual balance equations. *Water Research* **57**, 193-201.
- Strous M., Van Gerven E., Kuenen J.G. and Jetten M. (1997a) Effects of aerobic and microaerobic conditions on anaerobic ammonium-oxidizing (anammox) sludge. *Applied and Environmental Microbiology* **63**, 2446-2448.
- Strous M., Van Gerven E., P Zheng., Kuenen J.G. and Jetten M.S.M (1997b) Ammonium removal from concentrated waste streams with the anaerobic ammonium oxidation (anammox) process in different reactor configurations. *Water Research* **31**, 1955–1962.
- Strous M., Heijnen J.J., Kuenen J. G. and Jetten M.S.M. (1998) The sequencing batch reactor as a powerful tool for the study of slowly growing anaerobic ammonium-oxidizing microorganisms. *Applied Microbiology and Biotechnology* **50**, 589–596.
- Strous M., Kuenen J.G. and Jetten M.S.M. (1999) Key physiology of anaerobic ammonium oxidation. *Applied and Environmental Microbiology* **65**, 3248-3250.
- Strous M., Pelletier E., Mangenot S., Rattei T., Lehner A., Taylor M. W., Horn M., Daims H., Bartol-Mavel D., Wincker P., Barbe V. r., Fonknechten N., Vallenet D., Segurens B. a., Schenowitz-Truong C., Médigue C., Collingro A., Snel B., Dutilh B. E., Op den Camp H. J. M., van der Drift C., Cirpus I., van de Pas-Schoonen K. T., Harhangi H. R., van Niftrik L., Schmid M., Keltjens J., van de Vossenberg J., Kartal B., Meier H., Frishman D., Huynen M. A., Mewes H.-W., Weissenbach J., Jetten M. S. M., Wagner M. and Le Paslier D. (2006) Deciphering the evolution and metabolism of an anammox bacterium from a community genome. *Nature* **440**, 790-794.
- Stubner S. (2002) Enumeration of 16S rDNA of Desulfotomaculum lineage 1 in rice field soil by real-time PCR with SybrGreen(TM) detection. *Journal of Microbiological Methods* **50**, 155–164.
- Stüven R., Vollmer M. and Bock E. (1992) The impact of organic matter on nitric oxide formation by *Nitrosomonas europaea*. *Archives of Microbiology* **158**, 439–443.
- Stumm W. and Morgan J.J. *Aquatic Chemistry*; John Wiley & Sons Inc.: New York, 1996.
- Suneethi S. and Joseph K. (2011) Batch culture enrichment of ANAMMOX populations from anaerobic and aerobic seed cultures. *Bioresource Technology* **102**, 585–591.
- Udert K.M., Fux C., Münster M., Larsen T., Siegrist H. and Gujer W. (2003) Nitrification and autotrophic denitrification of source-separated urine. *Water Science and Technology* **48**, 119–130
- Udert K.M., Larsen T.A. and Gujer W. (2005) Chemical nitrite oxidation in acid solutions as a consequence of microbial ammonium oxidation. *Environmental Science and Technology* **39**, 4066–4075.
- Udert K.M., Larsen T.A. and Gujer, W. (2006) Fate of major compounds in source-separated urine. *Water Science and Technology* **54**, 413-420.

- Udert K.M., Kind E., Teunissen M., Jenni S. and Larsen T.A. (2008) Effect of heterotrophic growth on nitrification/anammox in a single sequencing batch reactor. *Water Science and Technology* **58**, 277–284.
- Udert K.M., Brown-Malker S. and Keller J. (2013) Electrochemical systems. In: *Source Separation and Decentralization for Wastewater Treatment*, T.A. Larsen, K.M. Udert and J. Lienert (eds.), IWA Publishing, London, UK, pp. 321-335.
- Unisense (2010a) *Nitrous Oxide Sensor User Manual*, Version October 2010. Unisense, Aarhus, Denmark.
- Unisense (2010b) *Nitric Oxide Sensor User Manual*, Version October 2010. Unisense, Aarhus, Denmark.
- van de Graaf A., Mulder A., de Bruijn P., Jetten M., Robertson L. and Kuenen J. (1995) Anaerobic oxidation of ammonium is a biologically mediated process. *Applied and Environmental Microbiology* **61**, 1246-1251.
- van de Pas-Schoonen K.T., Schalk-Otte S., Haaijer S., Schmid M., Op Den Camp H., Strous M., Kuenen J.G. and Jetten M.S.M. (2005) Complete conversion of nitrate into dinitrogen gas in co-cultures of denitrifying bacteria. *Biochemical Society Transactions* **33**, 205-209.
- van der Heijden R.T.J.M., Heijnen J.J., Hellinga C., Romein B. and Luyben K.C.A.M. (1994) Linear constraint relations in biochemical reaction systems: I. Classification of the calculability and the balanceability of conversion rates. *Biotechnology and Bioengineering* **43**, 3-10.
- van der Star W.R.L., Abma W.R., Blommers D., Mulder J.-W., Tokutomi T., Strous M., Piciorreanu C. and van Loosdrecht M.C.M. (2007) Startup of reactors for anoxic ammonium oxidation: Experiences from the first full-scale anammox reactor in Rotterdam. *Water Research* **41**, 4149-4163.
- van Dongen U., Jetten M.S.M. and van Loosdrecht M.C.M. (2001) The SHARON–anammox process for treatment of ammonium rich wastewater. *Water Science and Technology* **44**, 153–160.
- Van Drecht G., Bouwman A.F., Harrison J. and Knoop J.M. (2009) Global nitrogen and phosphate in urban wastewater for the period of 1970 to 2050. *Global Biogeochemical Cycles* **23**, issue 4.
- Vangsgaard A.K., Mutlu A.G., Gernaey K.V., Smets B.F. and Sin G. (2013) Calibration and validation of a model describing complete autotrophic nitrogen removal in a granular SBR system. *Journal of Chemical Technology and Biotechnology* **88**, 2007-2015.
- Van Hulle S.W.H., Vandeweyer H.J.P., Meesschaert B.D., Vanrolleghem P.A., Dejans P. and Dumoulin A. (2010) Engineering aspects and practical application of autotrophic nitrogen removal from nitrogen rich streams. *Chemical Engineering Journal* **162**, 1-20.
- van Kempen R., Mulder J.W., Uijterlinde C.A. and van Loosdrecht M.C.M. (2001) Overview: full scale experience of the SHARON<sup>(R)</sup> process for treatment of rejection water of digested sludge dewatering. *Water Science and Technology* **44**, 145-152.
- Vázquez-Padín J.R., Fernández I., Morales N., Campos J.L., Mosquera-Corral A. and Méndez R. (2011) Autotrophic nitrogen removal at low temperature. *Water Science and Technology* **63**, 1282-1288.

- Venables W.N., Smith D.M. and the R Development Core Team; *An Introduction to R*, Version 2.10.1., 2009.
- Villez K., Corominas L. and Vanrolleghem P. A. (2013) Sensor fault detection and diagnosis based on bilinear mass balances in wastewater treatment systems. *Proceedings of the 11th IWA conference on instrumentation control and automation (ICA2013)*, Narbonne, FR, Sept. 18-20, 2013, appeared on USB-stick (IWA-12744).
- Villez K., Corominas L. and Vanrolleghem P. A. (2015) Sensor placement by means of deterministic global optimization. *2nd IWA New Developments in IT & Water conference*, Rotterdam, NL, February 8-10, accepted for oral presentation.
- Vlaeminck S.E., Cloetens L.F.F., Carballa M., Boon N. and Verstraete W. (2008) Granular biomass capable of partial nitrification and anammox. *Water Science and Technology* **58**, 1113-1120.
- Vlaeminck S.E., Terada A., Smets B.F., Linden D.V.D., Boon N., Verstraete W. and Carballa M. (2009) Nitrogen removal from digested black water by one-stage partial nitrification and anammox. *Environmental Science and Technology* **43**, 5035-5041.
- Vlaeminck S.E., Terada A., Smets B.F., De Clippeleir H., Schaubroeck T., Bolea S., De-meestere L., Mast J., Boon N., Carballa M. and Verstraete W. (2010) Aggregate size and architecture determine microbial activity balance for one-stage partial nitrification and anammox. *Applied and Environmental Microbiology* **76**, 900-909.
- Vlaeminck S.E., De Clippeleir H. and Verstraete W. (2012) Microbial resource management of one-stage partial nitrification/anammox. *Microbial Biotechnology* **5**, 433-448.
- Wang C.-C., Lee P.-H., Kumar M., Huang Y.-T., Sung S. and Lin J.-G. (2010) Simultaneous partial nitrification, anaerobic ammonium oxidation and denitrification (SNAD) in a full-scale landfill-leachate treatment plant. *Journal of Hazardous Materials* **175**, 622-628.
- Wang Q., Garrity G.M., Tiedje J.M. and Cole J.R. (2007) Naive Bayesian classifier for rapid assignment of rRNA sequences into the new bacterial taxonomy. *Applied and Environmental Microbiology* **73**, 5261–5267.
- Warnes G. R. (2010) gplots: various R programming tools for plotting data, 2.8.0 ed. *The R Project for Statistical Computing*, Vienna, Austria.
- Weimann J. (2003) Toxicity of nitrous oxide. *Best Practice & Research Clinical Anaesthesiology* **17**, 47-61.
- Weissenbacher N., Takacs I., Murthy S., Fuerhacker M. and Wett B. (2010) Gaseous nitrogen and carbon emissions from a full-scale deammonification plant. *Water Environment Research* **82**, 169–175.
- Welsh D.T. (2000) Ecological significance of compatible solute accumulation by microorganisms: from single cells to global climate. *FEMS Microbiology Reviews* **24**, 263-290.
- Wett B. and Rauch W. (2003) The role of inorganic carbon limitation in biological nitrogen removal of extremely ammonia concentrated wastewater. *Water Research* **37**, 1100-1110.
- Wett B. (2007) Development and implementation of a robust deammonification process. *Water Science and Technology* **56**, 81-88.

- Wett B., Hell M., Hyhuis G., Puempel T., Takacs I. and Murthy S. (2010) Syntrophy of aerobic and anaerobic ammonia oxidisers. *Water Science and Technology* **61**, 1915-1922.
- Whitaker R.J., Grogan D.W. and Taylor J. W. (2003) Geographic barriers isolate endemic populations of hyperthermophilic archaea. *Science* **301**, 976–978.
- Wiesmann U. 1994. Biological nitrogen removal from wastewater. *Advances in Biochemical Engineering / Biotechnology* **51**, 113–154.
- Wilsenach J. and van Loosdrecht M.C.M. (2006) Integration of processes to treat wastewater and source-separated urine. *Journal of Environmental Engineering* **132**, 331-341.
- Winkler M.K.H., Kleerebezem R. and van Loosdrecht M.C.M. (2012a) Integration of anammox into the aerobic granular sludge process for main stream wastewater treatment at ambient temperatures. *Water Research* **46**, 136-144.
- Winkler M.K.H., Yang J., Kleerebezem R., Plaza E., Trela J., Hultman B. and van Loosdrecht M.C.M. (2012b) Nitrate reduction by organotrophic anammox bacteria in a nitrification/anammox granular sludge and a moving bed biofilm reactor. *Bioresource Technology* **114**, 217-223.
- Wittebolle L., Vervaeren H., Verstraete W. and Boon N. (2008) Quantifying community dynamics of nitrifiers in functionally stable reactors. *Applied and Environmental Microbiology* **74**, 286–293.
- Wunderlin P., Mohn J., Joss A., Emmenegger L. and Siegrist H. (2012a) Mechanisms of N<sub>2</sub>O production in biological wastewater treatment under nitrifying and denitrifying conditions. *Water Research* **46**, 1027-1037
- Wunderlin P., Lehmann M.F., Siegrist H., Tuzson B., Joss A., Emmenegger L. and Mohn J. (2012b) Isotope signatures of N<sub>2</sub>O in a mixed microbial population system: constraints on N<sub>2</sub>O producing pathways in wastewater treatment. *Environmental Science and Technology* **47**, 1339-1348.
- Wyffels S., Van Hulle S.W.H., Boeckx O., Volcke E., van Cleemput O., Vanrolleghem P. and Verstraete W. (2004). Modeling and simulation of oxygen-limited partial nitritation in a membrane-assisted bioreactor (MBR). *Biotechnology and Bioengineering* **86**, 531-542.
- Yang G.-F., Guo X.-L., Chen S.-X., Liu J.-H., Guo L.-X. and Jin R.-C. (2013) The evolution of Anammox performance and granular sludge characteristics under the stress of phenol. *Bioresource Technology* **137**, 332-339.
- Yannarell A.C., Kent A.D., Lauster G.H., Kratz T. K. and Triplett E. W. (2003) Temporal patterns in bacterial communities in three temperate lakes of different trophic status. *Microbial Ecology* **46**, 391–405.
- Yu R., Kampschreur M.J., van Loosdrecht M.C.M. and Chandran K. (2010) Mechanisms and specific directionality of autotrophic nitrous oxide and nitric oxide generation during transient anoxia. *Environmental Science and Technology* **44**, 1313–1319.
- Zhu S. and Chen S. (2001) Effects of organic carbon on nitrification rate in fixed film biofilters. *Aquacultural Engineering* **25**, 1-11.
- Zumft W. G. (1993) The biological role of nitric oxide in bacteria. *Archives of Microbiology* **160**, 253–264.



## **CURRICULUM VITAE**

2009 – 2015	PhD student at the Swiss Federal Institute of Aquatic Science and Technology (Eawag), Department of Process Engineering, Dübendorf, Switzerland
2007 – 2009	Scientific assistant at the Swiss Federal Institute of Aquatic Science and Technology (Eawag), Department of Process Engineering, Dübendorf, Switzerland
2002 – 2007	Studies in environmental engineering with a focus on urban water management and water resources management (Dipl. Umwelt.-Ing. ETH), Swiss Federal Institute of Technology (ETH), Zürich
1998 – 2002	High School, Type MN, Dübendorf (ZH)
1995 – 1998	Secondary School, Uster (ZH)
1989 – 1995	Primary School, Uster (ZH)
January 19, 1983	Born in Uster (ZH)

